SCHOOL OF CIVIL ENGINEERING

JOINT HIGHWAY RESEARCH PROJECT

JHRP-81-17

THREE-DIMENSIONAL SLOPE STABILITY ANALYSIS

R. H. Chen

PURDUE UNIVERSITY
INDIANA STATE HIGHWAY COMMISSION

Final Report

THREE-DIMENSIONAL SLOPE STABILITY ANALYSIS

TO: H. L. Michael, Director
Joint Highway Research Project

FROM: J.-L. Chameau, Research Associate
Joint Highway Research Project

September 30, 1981

Project: C-36-36N

File: 6-14-14

Attached is a Final Report on the JHRP study titled "Three-Dimensional Slope Stability Analysis for Indiana Highways". The research and report were performed by Mr. R. H. Chen, Graduate Instructor on our staff, under the direction of J.-L. Chameau and C. W. Lovell of our staff. The report is titled "Three-Dimensional Slope Stability Analysis".

This report presents methods of three-dimensional slope stability analysis using limit equilibrium concepts and the finite element method. Two different computer programs based on the limit equilibrium concept, LEMIX and BLOCK 3, were developed to analyze rotational and translational slides, respectively. In addition a 3-D finite element computer program, FESPON, was also generated to analyze rotational slides. Several slope stability analyses were performed using the three-dimensional programs BLOCK 3, LEMIX, and FESPON, for different slope angles, soil parameters, and pore water conditions. The results obtained with these techniques were compared to those given by conventional two-dimensional methods. The 3-D programs are valuable tools for geotechnical engineers in the evaluation of the stability of highway slopes.

The Report is submitted for review, comment and acceptance as fulfillment of the objectives of the approved Study.

Respectfully submitted,

J.-L. Chameau/ms

J.-L. Chameau
Research Associate

JLC:ms

Attachment

cc: A. G. Altschaeffl
J. M. Bell
W. L. Dolch
R. L. Eskew
J. D. Fricker
G. D. Gibson
W. H. Goetz
M. J. Gutzwiller
G. K. Hallock
J. F. McLaughlin
R. D. Miles
P. L. Owens
B. K. Partridge
G. T. Satterly
C. F. Scholer
R. M. Shanteau
K. C. Sinha
C. A. Venable
L. E. Wood
E. J. Yoder
S. R. Yoder

Final Report

THREE-DIMENSIONAL SLOPE STABILITY ANALYSIS

by

Rong-Her Chen
Graduate Instructor in Research

Joint Highway Research Project

Project No.: C-36-36N

File No.: C-14-14

Prepared as Part of an Investigation

Conducted by

Joint Highway Research Project
Engineering Experiment Station
Purdue University

in cooperation with the

Indiana Department of Highways

The contents of this report reflect the views of the author who is responsible for the facts and the accuracy of the data presented herein.

Purdue University
West Lafayette, Indiana
September 30, 1981

ACKNOWLEDGEMENTS

The author would like to thank his major professor, Dr. J.-L. Chameau, for his counsel and valuable suggestions. Special thanks are extended to Professor C. W. Lovell for his guidance, support, and understanding as the author's former advisor. The kind encouragement provided by Dr. W. D. Kovacs is appreciated.

The author is grateful to Professor E. C. Ting for his helpful suggestions. Thanks are due to Professor J. T. P. Yao for serving in the committee. Thanks are due to my former classmate and colleague, Dr. T. H. Wu, for his information and helpful discussion.

The author appreciates the Indiana State Highway Commission and Federal Highway Administration for their financial sponsorship. The research was administrated through the Joint Highway Research Project, Purdue University, West Lafayette, Indiana.

Miss Cathy Minth and Mrs. Edith Vanderwerp provided secretarial help. Mrs. Ziza Saleeb did part of the drafting work. Thanks are extended to all of them.

Finally, the author would like to thank his wife, Mong-Chu, for her sacrifice, encouragement, and understanding during this study. This work could never have been finished without her.

TABLE OF CONTENTS

LIST OF TABLES

LIST OF FIGURES

LIST OF ABBREVIATIONS AND SYMBOLS

Abbreviations

JHRP - Joint Highway Research Project

OCR - Overconsolidation Ratio

OMC - Ordinary Method of Columns

OMS - Ordinary Method of Slices

TRB - Transportation Research Board

1-D - One-Dimensional

2-D - Two-Dimensional

3-D - Three-Dimensional

Special Symbols

A prime ("'") indicates that the variable is in terms of effective stress.

Δ (Delta) indicates a change or variation in a variable.

Σ (Sigma) used as summation symbol.

C_L Symbol for Center Line.

Symbols

b - The width of the slice.

c,c' - Strength intercept in terms of total (c) and effective (c') stresses, respectively.

c_m - Mobilized cohesion.

D - Depth to a weak layer, measured from the toe.

e_o - Initial void ratio.

E_i, E_t, E_{ur} - Initial, tangent, and unloading modulus, respectively.

F - Factor of safety.

F_2, F_3 - Two-dimensional and three-dimensional factor of safety, respectively.

G - Shear modulus.

G - Poisson's ratio parameter, value of ν_i at $\sigma_3 = P_a$

H - Height of a slope or embankment.

I_p - Plasticity index.

K, K_{ur} - Loading and unloading modulus numbers.

K_o - Coefficient of earth pressure at rest.

ℓ - Length of the base of a slice.

ℓ_c - Length of half of a central cylinder.

ℓ_s - Length of the minor axis of an ellipsoid.

L - Length of a shear surface.

M_d - The driving moment.

M_o - Moment around the center O.

M_r - The resisting moment.

n - Modulus exponent, relate E_i and E_{ur} to σ_3.

N, N' - Total and effective normal forces acting on the base, respectively.

P_a - Atmospheric pressure.

Q - Resultant of all side and end shear forces acting on a slice (or a column).

r - Radial distance from the center to the failure surface.

r_u - Pore water pressure parameter

R - End shear force.

R - Radius of a circular failure surface.

R_f - Failure ratio.

T_a - Allowable shear strength.

u - Pore water pressure.

w - Water content.

w - Subscript designating weak soil layer.

W - Weight of a mass.

x - Horizontal distance from the slice to the center of rotation.

Greek Alphabet

α - Inclination of shear surface with respect to the horizontal.

β - Slope inclination.

β - Inclination of weak soil layer.

ρ - Density of a soil.

θ - The parallel inclination of all side forces.

σ_1, σ_3 - Maximum and minimum principal stresses.

σ_v, σ_h - Vertical and horizontal stresses.

σ_N - Normal stress on a selected plane.

τ - Shear stress.

τ_N - Shear stress on a selected plane.

$\varepsilon_a, \varepsilon_r, \varepsilon_v$ - Axial, radial and volumetric strains.

ϕ, ϕ' - Strength angle in terms of total (ϕ) and effective (ϕ') stresses, respectively.

ϕ_m - Mobilized strength angle.

ν - Poisson's ratio.

ν_i, ν_t - Initial and tangent Poisson's ratio.

HIGHLIGHT SUMMARY

General methods of three-dimensional slope stability analysis using limit equilibrium concepts and the finite element method are proposed.

Two different computer programs based on the limit equilibrium concept, LEMIX and BLOCK 3, are developed to analyze rotational and translational slides, respectively. For rotational slides, the failure mass is assumed symmetrical and divided into many vertical columns. The interslice forces are assumed to have the same inclination throughout the mass, and the inter-column shear forces are assumed to be parallel to the base of the column and a function of their positions. Force and moment equilibrium are satisfied for each column as well as for the total mass. For translational slides, the critical failure surface is defined according to Rankine's theory and the factor of safety is assumed to be uniform along the total failure surface. The analysis is illustrated for several slope angles, soil parameters, and pore water conditions. The results show that for both translational and rotational slides, the 3-D effect is more significant for cohesive soils with smaller failure lengths. However, a wedge type of failure may result in a smaller factor of safety than that of the 2-D condition. A gently inclined weak layer with lower strength may cause a higher 3-D effect. In rotational slides, the steeper the slope, the less the 3-D effect. Pore water pressures generally cause the 3-D effect to be even more significant.

In addition, a 3-D finite element computer program FESPON is also developed. It uses a hyperbolic stress-strain relationship and an incremental technique to simulate the nonlinear behavior of soils. Isoparametric incompatible elements are used to provide good bending characteristics. The

program can calculate the local factors of safety at selected points on the failure surface as well as the mean factor of safety for a chosen failure mass. The comparison between the limit equilibrium and finite element methods is also conducted for embankments with the same soil conditions and failure surfaces. The agreement is quite good, with the finite element method predictably yielding higher factors of safety.

I. INTRODUCTION

Gravitational, seepage and surcharge loads tend to cause instability in natural and man-made slopes. Stability analysis is an important part of the design of embankments, cut slopes, excavations, and dams. In practice, limit equilibrium methods are used in the analysis of slope stability. It is considered that failure is occurring along an assumed or a known failure surface. The shear strength required to maintain equilbrium is compared with the available shear strength of the soil. This gives an average factor of safety along the failure surface. Most of the stability methods available are two-dimensional and assume plane-strain conditions.

The early limit equilibrium methods were developed for simple failure surfaces such as circular or log-spiral surfaces. Since Fellenius proposed a simple approach in 1936, more than a dozen methods of slices have been proposed. These methods differ in the assumptions made to render the problem determinate and in the statics used in deriving the factor of safety equation. The methods of slices can handle complex geometries and variable soil and water conditions. They are the most commonly used methods of slope stability analysis.

Until now, only a few three-dimensional limit equilibrium methods have been proposed to study the end-effects which occur in actual slides. Relatively little work has been done in this area and these methods are limited to rather simple problems with uncomplicated geometry and soil and water conditions. They also suffer from the same limitations as the two-dimensional methods: (1) They do not adequately represent the stress-strain characteristics of the soil materials; and (2) They can not deal with progressive failure in a rational manner.

The work presented in this dissertation is directed at providing the engineers with a general methodology for three-dimensional slope stability analysis. It follows along two lines: (1) Development of general methods of three-dimensional limit equilibrium analysis; and (2) Generation of a finite element computer program to adequately model the stress-strain characteristics of soils.

The most important types of slides which occur in embankments and slopes are rotational and translational slides. Rotational slides occur in slumps which rotate about an axis parallel to the slope. Translational slides are controlled by surfaces of weakness, such as faults, joints, bedding planes, and variations in shear strength between layers of bedded deposits. These different boundary conditions are taken into account in the present study. Two different computer programs based on the limit equilibrium concept, LEMIX and BLOCK3, are developed to analyze rotational and translational slides, respectively.

For rotational slides, a general method is proposed and the simplifying assumptions used by previous investigators are relaxed. The failure mass is assumed symmetrical and divided into many vertical columns. The inclination of the interslice forces are assumed the same throughout the whole failure mass. The intercolumn shear forces (at the two ends of the column) are assumed parallel to the base of the column and to be a function of their positions. Force and moment equilibrium are satisfied for each column as well as for the total mass. For translational slides, the critical failure surface is assumed according to the Rankine's theory and the factor of safety is applied along the total failure surface. Taken together, the computer programs LEMIX and BLOCK3 can cover a wide range of geometric, soil and water conditions. Typical analyses are presented for several combinations of slope angles, soil parameters and pore water conditions.

In addition, a three-dimensional finite element computer program FESPON is also developed. It uses a hyperbolic stress-strain relationship and an incremental technique to simulate the nonlinear behavior of soils. Isoparametric incompatible elements are used to provide good bending characteristics. The hyperbolic stress-strain parameters are obtained from conventional triaxial and 1-D consolidation test data. This program can calculate the local factors of safety at selected points on the failure surface as well as the mean factor of safety for a chosen failure mass.

Several stability analyses of embankments are performed using existing two-dimensional methods and the programs LEMIX, BLOCK3 and FESPON. The results obtained with these different methods are compared extensively and it is hoped that they will provide the engineers with a better reference in the design and control of embankments.

II. METHODS OF SLOPE STABILITY ANALYSIS

2.1 Slides

Gravitational, seepage and surcharge loads tend to cause instability in natural or man-made slopes. Under these loads a sloping earth mass has a tendency to move downward and outward. In stability analysis and design of control methods to avoid instability, distinction is made between rotational and translational slides. These two types of slides are illustrated in Figure 2.1 and are briefly described in the following sections.

2.1.1 Rotational Slides

The most common rotational slides are little-deformed slumps along a surface of rupture curving concavely upward. In many slumps the underlying surface of rupture, together with the exposed scarps, is spoon-shaped (Fig. 2.1.a). If the slides extend for a considerable distance along the slope perpendicular to the direction of movement, much of the rupture surface may approach the shape of a cylinder with axis parallel to the slope. In slumps the movement is more or less rotational about an axis parallel to the slope. Rotational slides occur most frequently in fairly homogeneous materials, e.g., in constructed embankments and fills.

2.1.2 Translational Slides

In translational sliding the mass progresses out or down and out along a more or less planar or gently undulatory surface and has little of the rotary movement. If the moving mass of a translational slide

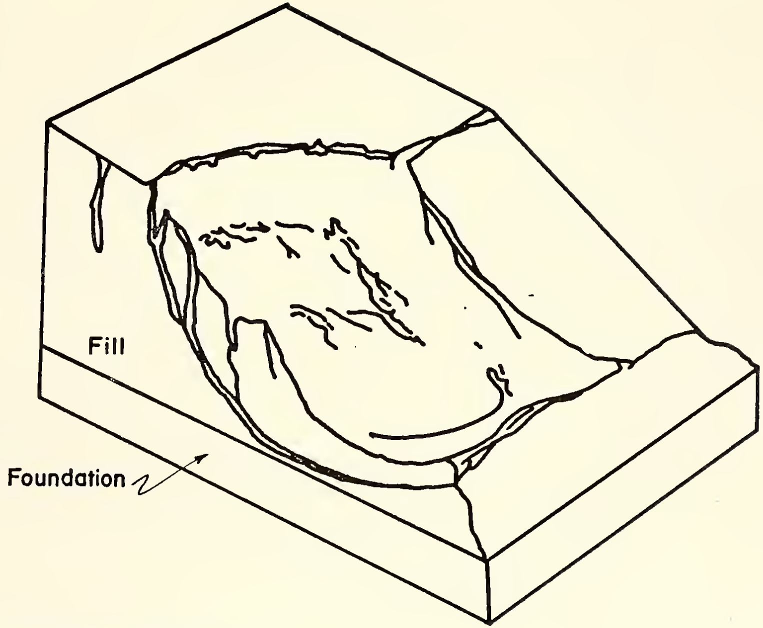

(a) Spoon Shaped Failure

Fig. 2.1 Failure Types

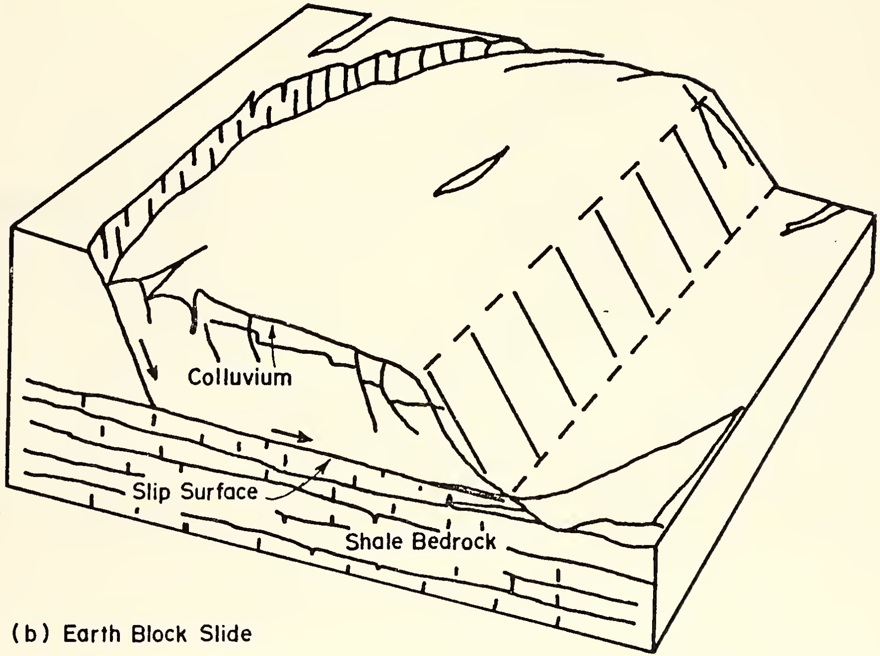

(b) Earth Block Slide

Fig. 2.1 (Cont'd)

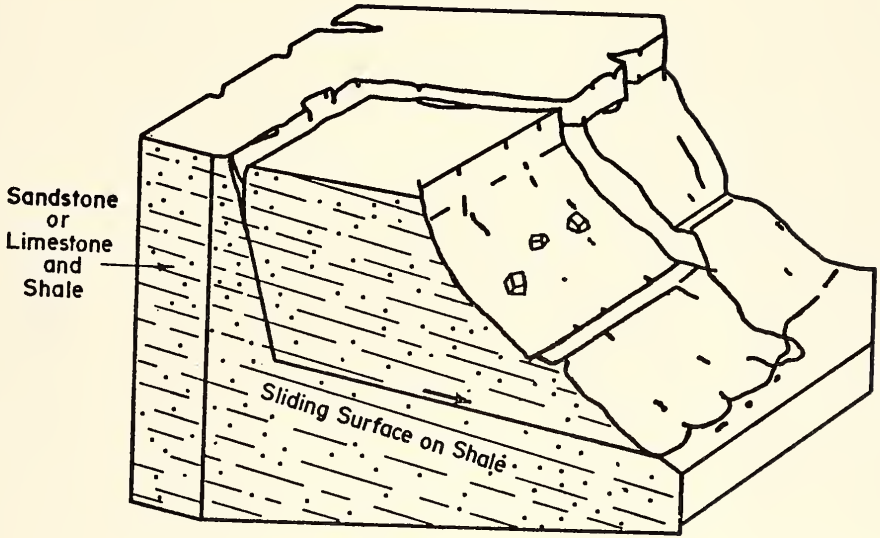

(c) Slab Type Failure

Fig. 2.1 (Cont'd)

consists of a single unit that is not greatly deformed or a few closely related units it may be called a block slide (Fig. 2.1.b and Fig. 2.1.c).

The movement of translational slides is commonly controlled by surfaces of weakness, such as bedding planes and variations in shear strength between layers of bedded deposits.

2.2 Two-Dimensional Slope Stability Analysis by Limit Equilibrium Concept

The stabilities of natural slopes, cut slopes, and fill slopes are commonly analyzed by limit equilibrium methods. These methods take into account the major factors influencing the shearing resistance of a soil.

2.2.1 The $\phi = 0$ Method

Fellenius (1918) proposed what is today commonly known as the '$\phi = 0$' method of stability analysis, a procedure widely used to analyze the short-term stability of slopes.

The shear surface is assumed to be circular. The factor of safety F, defined as the ratio of allowable shear strength to mobilized shear strength, can be obtained by summing moments about the center (Fig. 2.2):

$$Wx - \frac{c_a}{F} \ell_t \, r = 0 \qquad (2.1)$$

in which W is the weight of the soil mass, x the length of the moment arm of W about the center, c_a the undrained strength, ℓ_t the length of the shear surface and r the radius of the circle.

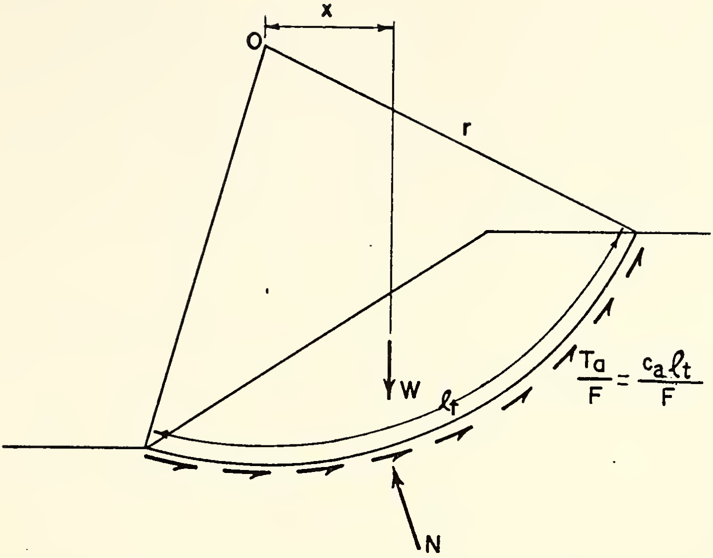

Fig. 2.2 Forces along a Circular Shear Surface

The factor of safety F is derived from equation (2.1):

$$F = \frac{c_a \ell_t \, r}{Wx} \tag{2.2}$$

In this method, the normal stresses all act through the center of the circle regardless of their distribution. The shear stresses all act at the same distance from the center of the circle and therefore their moment arm is constant and independent of their distribution. Thus, the use of a circular shear surface results in statical determinancy with respect to moment equilibrium.

2.2.2 The Log Spiral Procedure

When ϕ is not equal to zero, a circular shear surface is insufficient to achieve statical determinancy. However, it may be achieved by a log spiral shear surface in the form:

$$r = r_o \, e^{\Theta \tan \phi_m} \tag{2.3}$$

where r is the radial distance from the center point to a point on the spiral, r_o the reference radius, Θ the angle between r and r_o, and ϕ_m the mobilized friction angle for the shear surface.

This shape has the property that all the resultants of the normal stresses and frictional components of shear strength (N tan ϕ_m) pass through the center point of the spiral. Consequently, their contributions to the moments cancel out and the moment equation only involves the weight force and the cohesive resistance of the soil.

Since a value of tan ϕ_m must be assumed in equation (2.3) to define a shear surface, the mobilized cohesion which is calculated may result in a different factor of safety with respect to cohesion than was assumed in calculating φ_m. Thus, several trials are necessary to obtain a balanced factor of safety which satisfies

$$F = \frac{c}{c_m} = \frac{\tan \phi}{\tan \phi_m} \tag{2.4}$$

2.2.3 The Friction Circle Procedure

For a circular shear surface the resultants of the normal stresses and frictional component of shear resistance will lie tangent to a circle of radius r sin ϕ', called the friction circle (Fig. 2.3). The magnitude and location of this resultant and the factor of safety may be obtained from the three available equilibrium conditions (Taylor, 1937, 1948).

For a reasonable distribution of normal stresses along the shear surface, the resultant force must be less than the scalar sum of its component (Fig. 2.4). Consequently the resultant force must lie tangent to a circle of greater radius than the friction circle. This method thus underestimates the contributions of the moment from the resultant force and therefore the factor of safety obtained is a lower bound solution.

2.2.4 Methods of Slices

During the past three decades approximately one dozen methods of slices have been developed (Wright, 1969). They differ in: (1) the assumptions used to render the problem determinate; and (2) the statics employed in deriving the factor of safety equation. The methods of slices can handle complex geometric and variable soil and water conditions and therefore they are the most commonly used methods. Some of the most significant methods are presented below.

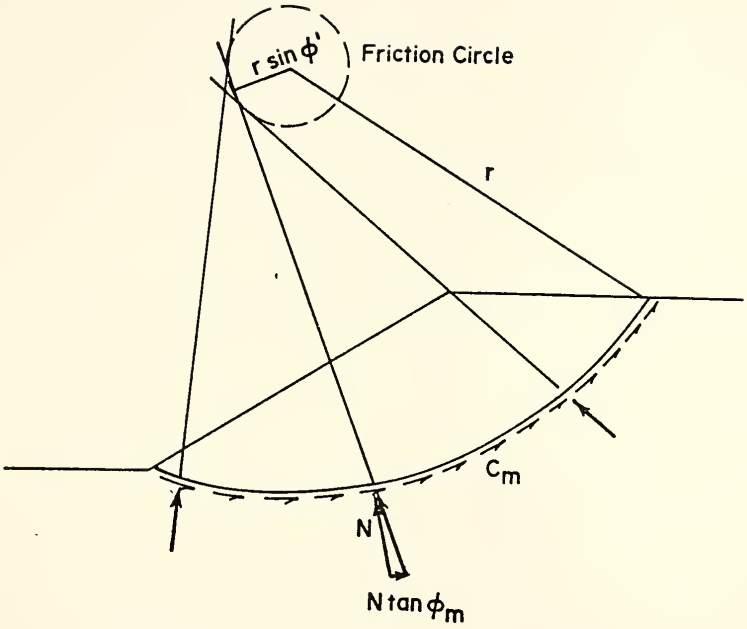

Fig. 2.3 Equivalent Force System for a Circular Shear Surface

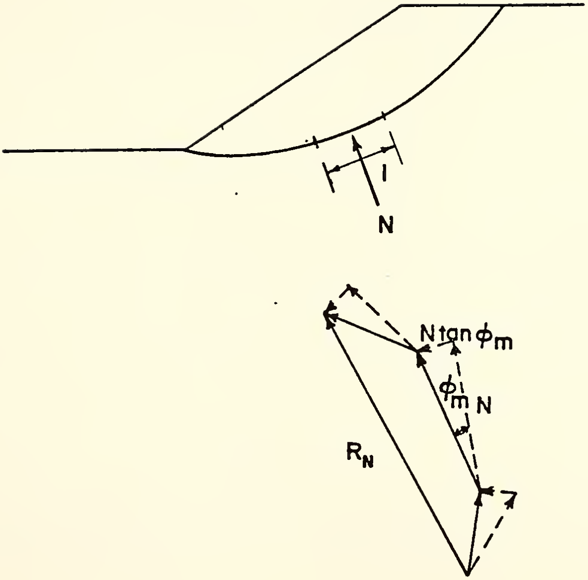

Fig. 2.4 Normal and Frictional Shear Forces Acting on a Shear Surface.

2.2.4.1 Ordinary Method

The ordinary method is the simplest of the methods of slices. In this method the interslice forces are neglected (Fellenius, 1936) and the equilibrium of each slice is obtained by summing forces in the vertical and horizontal directions (Fig. 2.5):

$\Sigma F_V = 0$

$$W - N \cos \alpha - \frac{T_a}{F} \sin \alpha = 0 \tag{2.5}$$

$\Sigma F_H = 0$

$$\frac{T_a}{F} \cos \alpha - N \sin \alpha = 0 \tag{2.6}$$

where W is the weight of the slice, N normal force on the base of the slice, α angle between the tangent to the center of the base of the slice and the horizontal, and T_a the allowable shear strength.

Solving for equation (2.5) and (2.6) gives:

$$N = W \cos \alpha \tag{2.7}$$

The factor of safety is derived from the summation of moments about a common point, $\Sigma M_o = 0$:

$$\Sigma\, Wx - \Sigma \frac{T_a}{F} r - \Sigma\, N f = 0 \tag{2.8}$$

where x, r, and f are the moment arms of W, T_a and N, respectively.

Introducing the Mohr-Coulomb failure criterion the factor of safety can be obtained as a function of the strength parameters:

$$F = \frac{\Sigma\{c' \ell r + (N - u\ell) r \tan \phi'\}}{\Sigma\, Wx - \Sigma\, N f} \tag{2.9}$$

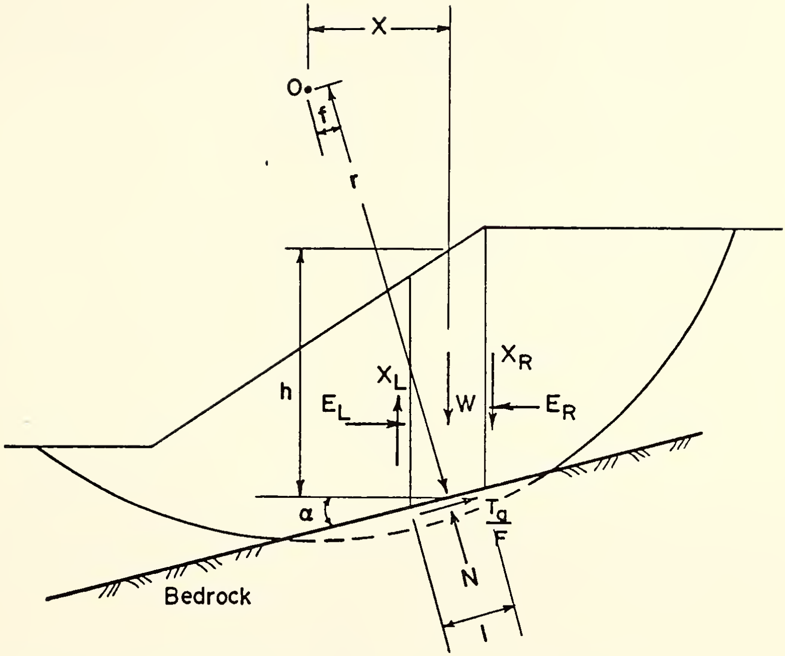

Fig.2.5 Forces System for the Method of Slices

where c' is the effective cohesion intercept, ϕ' the effective friction angle, u the pore water pressure, and ℓ the area of the base.

2.2.4.2 Simplified Bishop Method

The simplified Bishop method assumes the interslice forces to be horizontal. The normal force on the base of each slice is derived by summing forces in a vertical direction (as in equation (2.5)). Introducing the failure criteria and solving for the normal forces give:

$$N = \left(W - \frac{c'\,\ell\,\sin\alpha}{F} + \frac{u\,\ell\,\tan\phi'\,\sin\alpha}{F}\right)/m_\alpha \qquad (2.10)$$

where $m_\alpha = \cos\alpha + (\sin\alpha\,\tan\phi')/F$. The factor of safety is derived from the summation of moments about a common point. This equation is the same as equation (2.8) since the interslice forces cancel out. Therefore, the factor of safety equation is the same as in equation (2.9), with the value of N defined in equation (2.10).

2.2.4.3 Spencer's Method

Spencer's Method assumes there is a constant relationship between the magnitude of the interslice shear and normal forces (Spencer, 1967).

$$\tan\Theta = \frac{X_L}{E_L} = \frac{X_R}{E_R} \qquad (2.11)$$

where Θ is the angle of the resultant interslice force from the horizontal.

Spencer (1967) summed forces perpendicular to the interslice forces to derive the normal force. The same results can be obtained by summing forces in a vertical and horizontal direction (Fig. 2.5):

$\Sigma F_V = 0$

$$W + (X_R - X_L) - N \cos \alpha - \frac{T_a}{F} \sin \alpha = 0 \qquad (2.12)$$

$\Sigma F_H = 0$

$$(E_L - E_R) - N \sin \alpha + \frac{T_a}{F} \cos \alpha = 0 \qquad (2.13)$$

Solving equations (2.12) and (2.13):

$$N = \left\{ W + (E_R - E_L) \tan \Theta - \frac{c'\ell\sin\alpha}{F} + \frac{u\ell\tan\phi'\sin\alpha}{F} \right\} / m_\alpha \qquad (2.14)$$

Spencer (1967) derived two factor of safety equations. One is based on the summation of moments about a common point and the other on the summation of forces in a direction parallel to the interslice forces. The moment equation is the same as equation (2.8). The factor of safety equation is the same as equation (2.9).

Spencer's method yields two factors of safety for each angle of side forces. When the two factors of safety are equal for some angle of the interslice forces, both force and moment equilibriums are satisfied.

2.2.4.4 Janbu's Simplified Method

Janbu's simplified method uses a correction factor f_o to account for the effect of the interslice shear forces. The correction is related to cohesion, angle of internal friction, and the shape of the failure surface (Janbu et al, 1956).

The normal force can be obtained from equation (2.10). The factor of safety equation is derived from the horizontal equilibrium (Fig. 2.5):

$\Sigma F_H = 0$

$$\Sigma(E_L - E_R) - \Sigma\, N \sin\alpha + \Sigma \frac{T_a}{F} \cos\alpha = 0 \qquad (2.15)$$

Since $\Sigma(E_L - E_R) = 0$, the factor of safety is:

$$F_o = \frac{\Sigma\{c'\, \ell \cos\alpha + (N - u\ell) \tan\phi' \cos\alpha\}}{\Sigma\, N \sin\alpha} \qquad (2.16)$$

The corrected factor of safety is

$$F = f_o\, F_o \qquad (2.17)$$

The correction factors F_o have been generated by Janbu (1956) for different failure surfaces. For a long flat slip surface the interslice forces are not significant and consequently the correction factor approaches unity.

2.2.4.5 Janbu's Rigorous Method

Janbu's rigorous method assumes that the point of application of the interslice forces can be defined by a 'line of thrust'.

The normal force has a form similar to equation (2.14):

$$N = \left\{W + (X_R - X_L) - \frac{c'\ell \sin\alpha}{F} + \frac{u\ell \tan\phi' \sin\alpha}{F}\right\} / m_\alpha \qquad (2.18)$$

The factor of safety equation is the same as equation (2.13). The difference between simplified and rigorous methods is that the latter takes into account the shear forces in the derivation of the normal force.

To solve for the factor of safety, the shear forces may be set to zero for initial calculations. The factor of safety is obtained by iterative calculations as in the Bishop's Simplified Method so that an assumed value of F leads to an improved value and so on. The interslice forces then can be computed from the sum of the moments about the mid-point of the base of each slice (Fig. 2.6):

$$\Sigma M_m = 0$$

$$X_L(b/2) + X_R(b/2) + E_L\{t_L - (b/2)\tan\alpha\} \tag{2.19}$$

$$- E_R\{t_R + (b/2)\tan\alpha - b\tan\alpha_t\} = 0$$

where t_L, t_R = vertical distance from the base of the slice to the line of thrust on the left and right sides of the slice, respectively.

α_t = angle between the line of thrust on the left side of a slice and the horizontal.

After rearranging equation (2.19), several terms can be shown to be negligible. After eliminating these terms, equation (2.19) simplifies to:

$$X_L = E_L \tan\alpha_t + (E_R - E_L)\frac{t_R}{b} \tag{2.20}$$

with

$$(E_L - E_R) = \{W + (X_R - X_L)\}\tan\alpha - \frac{T_a}{F\cos\alpha} \tag{2.21}$$

The horizontal interslice forces are obtained by integration from right to left across the slope. The magnitude of the interslice shear forces then can be obtained from equation (2.21). The factor of safety is recalculated with these computed values of interslice forces. Using these new values of F and interslice forces a new position of

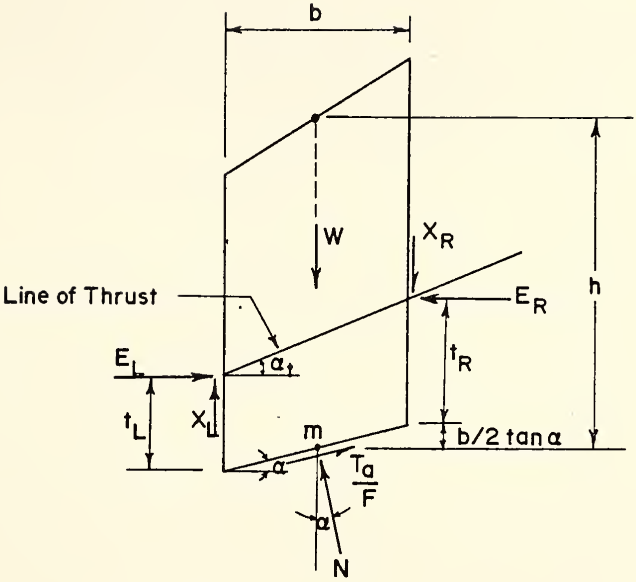

Fig. 2.6 Forces Acting on Each Slice for Janbu's Rigorous Method

the line of thrust is determined. The iterations are stopped when successive values of F are nearly identical.

2.2.4.6 Morgenstern-Price Method

The Morgenstern-Price Method assumes an arbitrary mathematical function to describe the direction of the interslice forces:

$$\frac{X}{E} = \lambda\ f(x) \tag{2.22}$$

where λ is a constant to be evaluated in solving for the factor of safety and $f(x)$ is a functional variation with respect to x. For a constant function, the Morgenstern-Price method is the same as the Spencer's method. The normal force is derived from equation (2.18). Two factor of safety equations are computed, one with respect to moment equilibrium and one with respect to force equilibrium. The moment equilibrium equation is taken with respect to a common point. The factor of safety equation is the same as the one derived for Spencer's method. The computation of interslice shear forces is similar to the derivation presented for Janbu's rigorous method.

2.2.5 Comparison of Factors of Safety for Example Problem

Fredlund and Krahn (1977) used the methods of slices to solve an example problem in order to assess the effects of the interslice forces assumption. The problem is shown in Fig. 2.7 and the results are presented in Table 2.1. The results in Table 2.1 show that the factor of safety with respect to moment of equilibrium is relatively insensitive to the interslice forces assumption (see also Fig. 2.8). Therefore, the

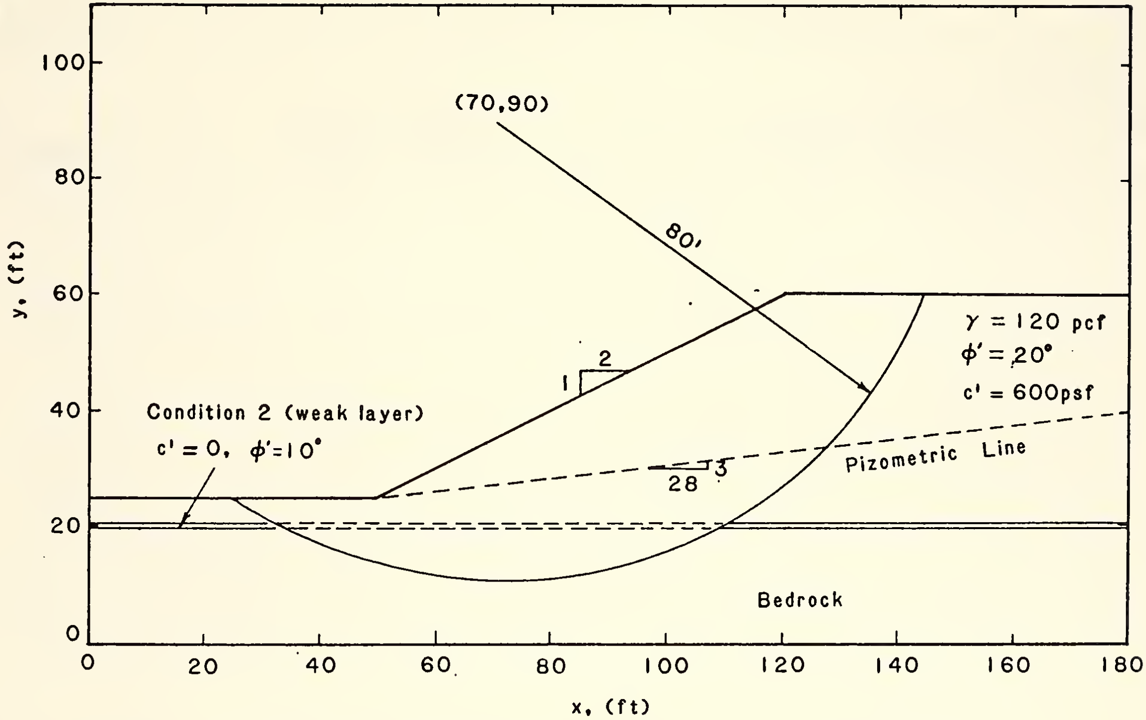

Fig. 2.7 Example Problem (after Fredlund and Krahn, 1977)

TABLE 2.1 COMPARISON OF FACTORS OF SAFETY FOR EXAMPLE PROBLEM (AFTER FREDLUND AND KRAHN, 1977)

Case no.	Example problem	Ordinary method	Simplified Bishop method	Spencer's method			Janbu's simplified method	Janbu's rigorous method*	Morgenstern-Price method $f(x)$ = constant	
				F	θ	λ			F	λ
1	Simple 2:1 slope, 40 ft (12 m) high, $\phi' = 20^{\circ}$, $c' = 600$ psf (29 kPa)	1.928	2.080	2.073	14.81	0.237	2.041	2.008	2.076	0.254
2	Same as 1 with a thin, weak layer with $\phi' = 10^{\circ}$, $c' = 0$	1.288	1.377	1.373	10.49	0.185	1.448	1.432	1.378	0.159
3	Same as 1 except with $r_u = 0.25$	1.607	1.766	1.761	14.33	0.255	1.735	1.708	1.765	0.244
4	Same as 2 except with $r_u = 0.25$ for both materials	1.029	1.124	1.118	7.93	0.139	1.191	1.162	1.124	0.116
5	Same as 1 except with a piezometric line	1.693	1.834	1.830	13.87	0.247	1.827	1.776	1.833	0.234
6	Same as 2 except with a piezometric line for both materials	1.171	1.248	1.245	6.88	0.121	1.333	1.298	1.250	0.097

* The line of thrust is assumed at 0.333 of height of each slice.

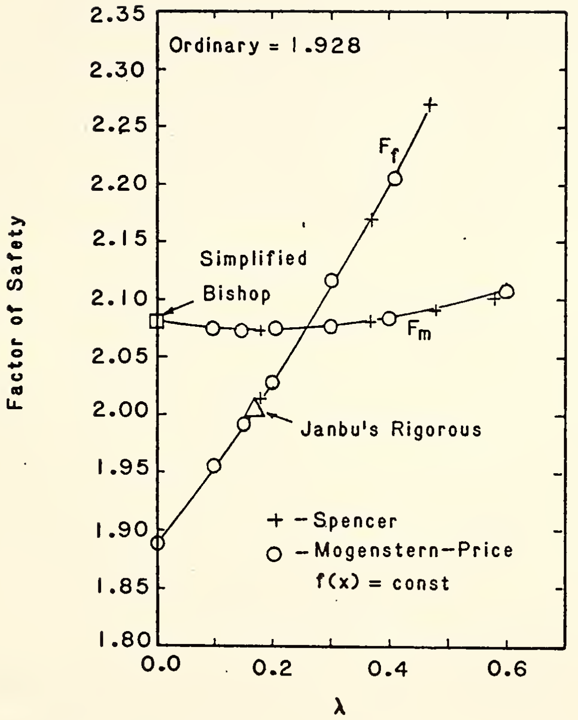

Fig. 2.8 Comparison of Factors of Safety for Case I of Example Problem (after Fredlund and Krahn, 1977)

factors of safety obtained by the Spencer and Morgenstern-Price methods are generally similar to those computed by the simplified Bishop method.

2.3 Three-Dimensional Slope Stability Analysis by Limit Equilibrium Concept

Although there are many two-dimensional methods developed, only a few three-dimensional limit equilibrium methods are available. Until now, the developed 3-D methods are limited to rather simple problems, i.e., simple geometry, uncomplicated soil and water conditions. These methods are summarized below.

2.3.1 Weighted Average Procedure

In Fig. 2.9 consider several parallel cross sections through the slope. For these let A_1, A_2, A_3, etc. be the areas and F_1, F_2, F_3, etc. be the limit equilibrium factors of safety calculated for each cross section, respectively (Fig. 2.10). The overall factor of safety may be defined as follows (Sherard et al. 1963; Lambe and Whitman, 1969):

$$F = \frac{F_1A_1 + F_2A_2 + F_3A_3 + \dots}{A_1 + A_2 + A_3 + \dots} \tag{2.23}$$

This weighted average factor of safety will be less than that by the method considering the end resistance.

2.3.2 Inclusion of End Effects Procedure

When the failure mass is long and the cross-sectional area of the potential failure mass is nearly uniform at various sections along its axis, end effects may be directly included in a 2-D analysis. Consider the $\phi = 0$ type of analysis for example. In Fig. 2.11, let the failure

Weighted Average Procedure

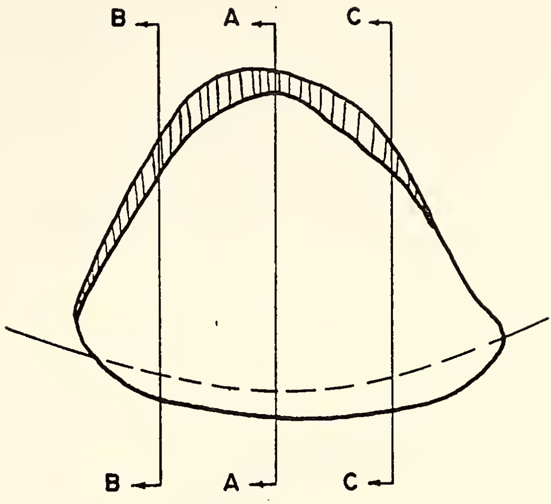

$$F = \frac{F_1 A_1 + F_2 A_2 + F_3 A_3}{A_1 + A_2 + A_3 + \ldots}$$

Figure 2.9 Plan View of Landslide

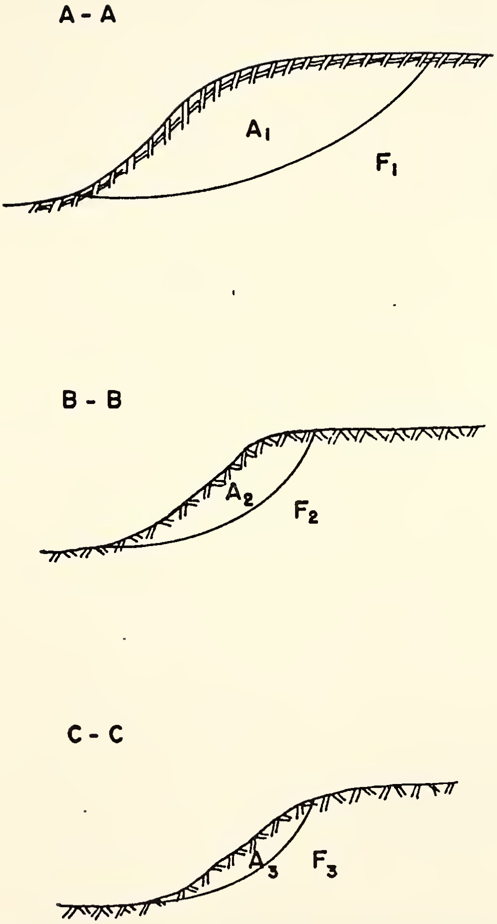

Figure 2.10 Factor of Safety for Different Cross Sections

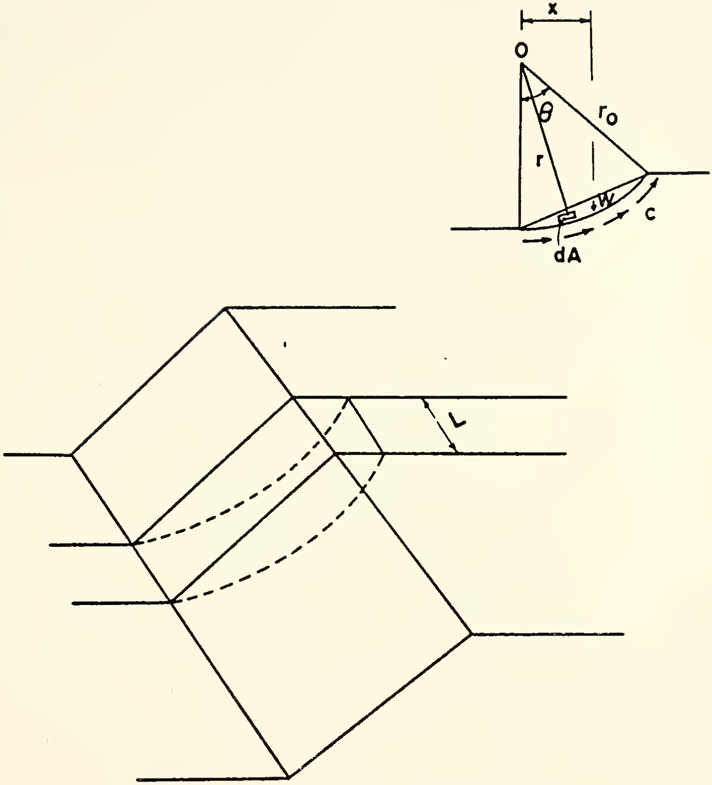

$$F = \frac{c \cdot r_0^2 \theta L + 2\sum\sum c \; dA \cdot r}{W \; x \; L}$$

Figure 2.11 Inclusion of End Effects for $\phi = 0$

length be L. The resistance will include: (1) that along the cylindrical surface of sliding of length L and radius r_o, giving a resisting moment of $c\ r_o^2\ \Theta\ L$; and (2) that at two ends giving a combined resisting moment of $2M_o$. Considering a small element area dA at a distance r from the center of the circle, M_o will be equal to $\Sigma\Sigma$ cdAr, where c is the undrained strength. Therefore the new factor of safety is given by:

$$F = \frac{c\ r_o^2\ \Theta\ L + 2\Sigma\Sigma\ cdAr}{W \times L} \qquad (2.24)$$

When L is very large in comparison to M_o, equation (2.24) reduces to the two-dimensional form. In a similar manner end effects can be taken into account in other problems where c and ϕ are included in the analysis or the slip surface cross section is wedge shaped or of arbitrary shape.

Baligh and Azzouz (1975) studied three-dimensional effects on the stability of slopes in cohesive soils. The failure mass was taken as a surface of revolution extending along the ground surface for a finite length 2L (Fig. 2.12). Different geometries and shapes were considered to analyze the 'end effects' by attaching either an ellipsoid or a cone at each end of the finite cylinder. Consider the surface of revolution shown in Figure 2.12 which is symmetrical with respect to the plane z = 0 and has a generator defined by its radial distance r from the Z-axis according to:

$$r = g(z) \qquad (2.25)$$

The factor of safety is defined as:

$$F = \frac{M_r}{M_d} \qquad (2.26)$$

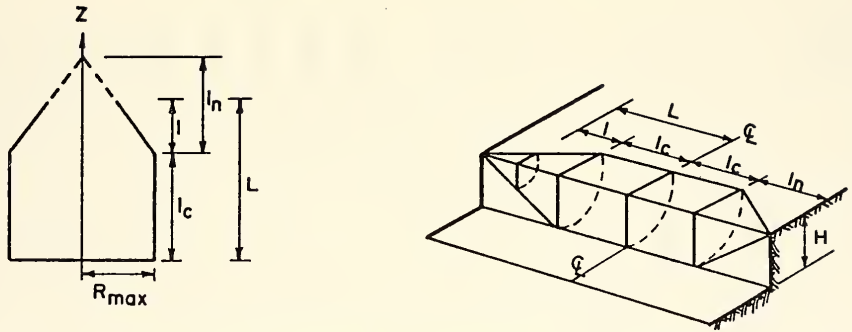

(a) Cone Attached to a Cylinder

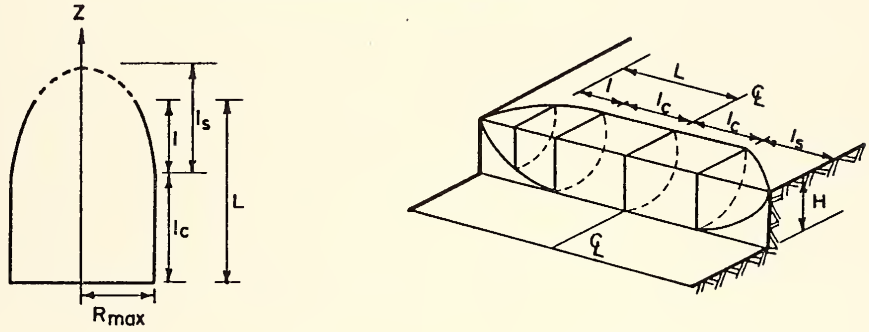

(b) Ellipsoid Attached to a Cylinder

Figure 2.12 Different Geometries of Failure Surfaces and Their Plan Views in which the resisting moment M_r is:

$$M_r = \int_0^L M_r^o \left(\frac{ds}{dz}\right) ds \tag{2.27}$$

with

$$\frac{ds}{dz} = \sqrt{1 + \left(\frac{dg}{dz}\right)^2} \tag{2.28}$$

and the driving moment M_d is:

$$M_d = \int_0^L M_d^o \, dz \tag{2.29}$$

M_r^o and M_d^o are the resisting and driving moments computed in plane strain problems and are functions of the coordinate z.

In general, it is found that F increases from its two-dimensional value. For long shallow failures (in which the ratio of length along axis of slope to depth of failure is greater than eight) the increase is of the order of 5% and can be disregarded. For short deep failures in which this ratio is less than 2 to 4, the increase in factor of safety can exceed 20% ~ 30% and three-dimensional effects must therefore be considered. Baligh and Azzouz also found that the length of failure is difficult to predict since it is very sensitive to slope and material parameters. Finally, the slope angle has little effect on the increase in the factor of safety due to end effects.

2.3.3 General Method

Previous methods are limited to cohesive soils and specific cases. Hovland (1977) proposed a general approach for three-dimensional slope stability analysis by defining the factor of safety as the ratio of the total available resistance along a failure surface to the total mobilized stress along it. In order to simplify the analysis, the ordinary method of slices was used. Thus the inter-column forces can be ignored and both normal and shear stresses on the base of each column are obtained simply as the component of the weight of the column.

In two-dimensional case, the factor of safety is:

$$F_2 = \frac{\Sigma(c\ A_2 + W_2 \cos\alpha \tan\phi)}{\Sigma\ W_2 \sin\alpha}$$

$$= \frac{\Sigma(\frac{c\ \Delta y}{\cos\alpha} + \rho\ z\ \Delta y \cos\alpha \tan\phi)}{\Sigma\ \rho\ z\ \Delta y \sin\alpha} \tag{2.30}$$

If cohesion c, friction angle ϕ, and density ρ are constants, then:

$$F_2 = (\frac{c}{\rho}) \frac{\Sigma \sec\alpha}{\Sigma z \sin\alpha} + (\tan\phi) \frac{\Sigma\ z \cos\alpha}{\Sigma\ z \sin\alpha} \tag{2.31a}$$

or

$$F_2 = (\frac{c}{\rho H})\ G_{c2} + \tan\phi\ G_{\phi 2} \tag{2.31b}$$

The G_{c2} and $G_{\phi 2}$ terms are only functions of geometry and H is the height of the slope.

In three-dimensional case, the factor of safety may be presented in a similar form by dividing the soil mass above the failure surface into a number of vertical soil columns. Assume the XY plane to be horizontal, the Z axis to be vertical, and the Y axis to be in the direction of downslope movement (Fig. 2.13). Let Δx and Δy define the

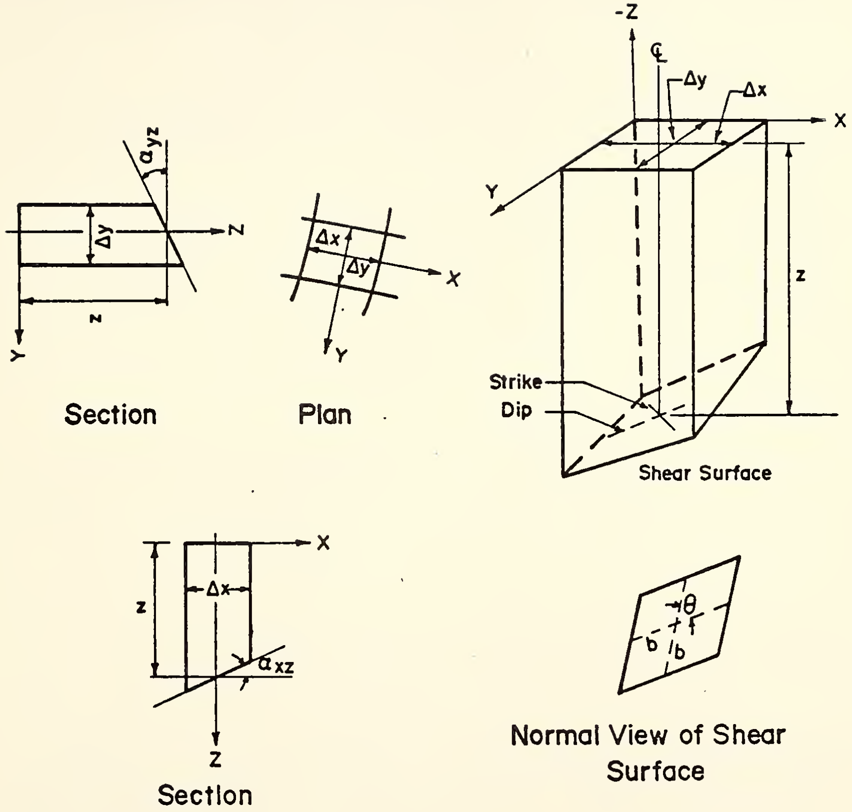

Figure 2.13 Plan, Section, and Three-Dimensional Views of One Soil Column

cross-sectional area of vertical soil columns on the XY plane and assume that both Δx and Δy are constant for all columns. Then:

$$F_3 = \frac{\sum_x \sum_y \left\{ \frac{c\ \Delta x\ \Delta y\ \sin\Theta}{\cos\alpha_{xz}\ \cos\alpha_{yz}} + \rho\ z\ \Delta x\ \Delta y\ \cos(DIP)\ \tan\phi \right\}}{\sum_x \sum_y \rho\ z\ \Delta x \Delta y\ \sin\alpha_{yz}} \tag{2.32}$$

in which α_{xz} and α_{yz} are the dip angles in the XZ and YZ planes respectively, and:

$$\cos\ (DIP) = (1 + \tan^2 \alpha_{xz} + \tan^2 \alpha_{yz})^{-1/2} \tag{2.33}$$

$$\sin\Theta = (1 - \sin^2 \alpha_{xz}\ \sin^2 \alpha_{yz})^{1/2} \tag{2.34}$$

If c, ϕ, ρ, Δx, and Δy are constant:

$$F_3 = \frac{c}{\rho} \frac{\sum_x \sum_y \sec\alpha_{xz}\ \sec\alpha_{yz}\ \sin\Theta}{\sum_x \sum_y z\ \sin\alpha_{yz}} + \tan\phi \frac{\sum_x \sum_y z\ \cos(DIP)}{\sum_x \sum_y z\ \sin\alpha_{yz}}$$

or

$$F_3 = \left(\frac{c}{\rho H}\right) G_{c3} + \tan\phi\ G_{\phi 3} \tag{2.35}$$

Hovland reported that every c - ϕ soil may have its own critical shear surface and geometry. His studies also suggest that the F_3/F_2 ratio is quite sensitive to the soil parameters c and ϕ, and to the basic shape of the shear surface. However, three-dimensional factors of safety are generally much higher than two-dimensional factors of safety, although in some situations it is not so. His studies also indicated that landslides in cohesive soils may follow a wide shear surface geometry, approaching a 2-D case. On the other hand slides in cohesionless soil may follow a 3-D wedge type surface.

2.4 Finite Element Method

Although limit equilibrium methods are widely used, they are subjected to criticism for three main reasons (Wright, 1973): (1) These methods do not consider the stress-strain characteristics of the soil; (2) the factor of safety assumed is the same for every slice, even though there is no reason to expect this to be true except at failure; (3) some of the equilibrium methods do not satisfy all the conditions of equilibrium. However, Wright (1973) concluded that the normal stress distributions determined by linear elastic finite element analyses are very nearly the same as those determined by Bishop's Simplified Method for flat slopes and large values of dimensionless parameters $\lambda_{c\phi}$ $(= \frac{\gamma H \tan\phi}{c})$. The average factors of safety determined by the two methods are very nearly the same, varying only by 0% to 8%. However, the material was assumed to have linear elastic behavior which may not be true. In his discussion Resendiz (1974) used hyperbolic stress-strain relationships proposed by Kondner (1963) to analyze fourteen embankments under end-of-construction conditions. The potential failure line was determined as the locus of ε_{max}, the maximum principal strain, and the factor of safety was determined as the mean value of the ratio σ_{df}/σ_d along the potential failure line:

$$F = \frac{\text{the principal stress difference at failure } (\sigma_{df})}{\text{the acting principal stress difference } (\sigma_d)} \qquad (2.36)$$

It was shown that the conventional factors of safety are always lower than the ones obtained from this method. The difference may be as large as 30% depending on the magnitude of the factor of safety and on the slope angle. In three-dimensional problems, Lefebre & Duncan (1973) used the finite element method to analyze three dams in V-shaped valleys with three different valley wall slopes equal to 1/1, 3/1, and 6/1. The material was assumed linear elastic. They concluded that: (1) for dams in valleys with wall slope as steep as 1/1 the results will be significantly less accurate, as a result of cross-valley arching; and (2) plane stress analysis of the maximum longitudinal section does not provide accurate results.

2.5 Other Methods of Slope Stability Analysis

An alternative method of slope stability analysis is to investigate the shear stresses by using the theory of elasticity (Perloff and Baron (1976), Romani (1970), Romani, Lovell and Harr (1972)). The factor of safety is defined as the shear strength divided by the shear stress at the point where this ratio is the least, hence it gives the safety at the most critical point.

The method may be useful when dealing with soils where progressive failure is likely to occur. However, it does not take into account the redistribution of stress which occurs when the stress level at a point approaches the strength.

2.6 Summary

1. In dealing with a slope stability problem, the choice of suitable methods should be dependent on the type of failure considered. In this chapter, two kinds of slides, rotational and translational, were defined.

2. Several commonly used two-dimensional slope stability analyses were briefly presented. The derivations are similar. Some methods satisfy determinancy, some do not. Of all the rigorous methods Spencer's method is the simplest and can produce quite accurate results.
3. Three-dimensional limit equilibrium methods developed so far are limited to simple geometry of failure mass, simple soil conditions, and cannot take into account the water conditions. More research on 3-D analysis is worthwhile.
4. Finite element methods are superior to limit equilibrium methods because of their power to handle complicated geometry, many soil parameters, water conditions, and to consider the stress-strain relationships of soils. However, they are much more complicated to use than limit equilibrium methods.
5. Although the results from both limit equilibrium and finite element methods have been compared for 2-D cases, comparisons for 3-D cases are not available.

III. LIMIT EQUILIBRIUM METHODS

3.1 Introduction

At a time when sophisticated approaches had yet to be developed and little was known about the mechanical behavior of earth masses, the limit equilibrium concept played an important role to make possible the use of simple theoretical approaches in solving many problems. In recent years, remarkable progress has been made in the area of stress analysis of continua and discontinua. Development of sophisticated numerical techniques and fast computers have facilitated this progress. However, the limit equilibrium concept has survived and is still considered to be reliable by most practitioners.

In Chapter II, two types of slides (rotational and translational) were defined and, as we mentioned previously, most of the equilibrium methods deal with plane strain conditions. In this Chapter, both types of failure mechanism are considered and three-dimensional solutions are derived. The assumptions in solving these problems and the derivations of equations are presented.

3.2 Block Type of Failure

When there is a very soft or loose material beneath a slope, the failure surface usually occurs along this soft or loose layer. The examples may be a slope underlain by a weak contact between colluvium and sloping bedrock, or between sidehill fill and sloping foundation.

The failure is perceived to be that of a relatively intact mass moving above a relatively well defined failure surface.

Mendez (1972) developed a quite general computer program to analyze the stability of a three-plane surface, but the profile was limited to two kinds of soils, i.e., a strong one over a weak one. Mohan (1972) also made simplifying assumptions with respect to the shape of the sliding surface, but his solution is quite versatile with respect to the potential complexity of the subsurface. The 2-D computer program BLOCK or BLOCK2 (Boutrup, 1977) can select the critical surface of very complicated soil conditions and apply the same factor of safety throughout the whole failure surface.

In order to study the 3-D block type of failure, a 3-D computer program BLOCK3 is developed. The assumptions and the derivation of the factor of safety are presented in the following sections.

3.2.1 Assumptions

Fig. 3.1 shows the free body diagram of a block type of failure in three-dimensional sapce. Boutrup (1977) analyzed the block type of failure by using the method of slices and applied the same factor of safety throughout the most critical failure surface. It was found that the most critical failure surface was close to that selected from Rankine theory, i.e., the shear surface makes $(45 + \phi/2)$ and $(45 - \phi/2)$ angles with the horizontal in active and passive zones, respectively. Therefore, in this study the ends of the most critical surface will be chosen as that from Rankine theory just for simplicity and convenience in comparison of results.

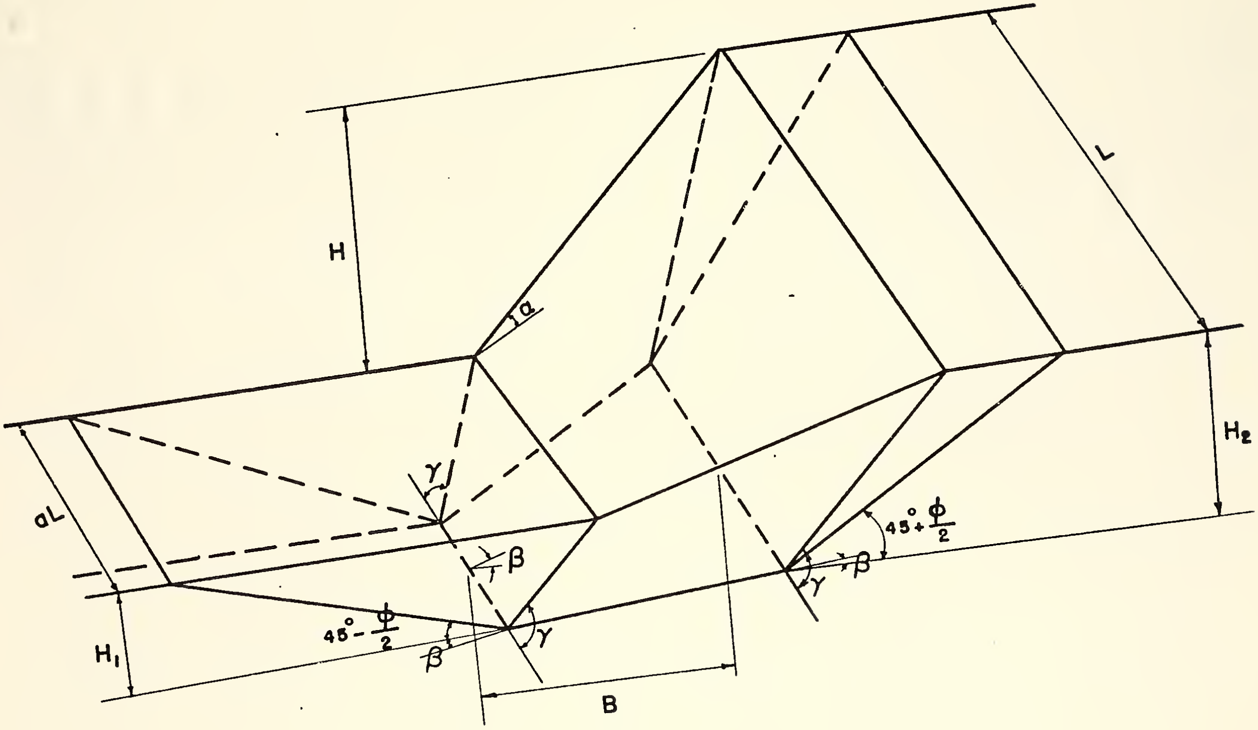

Fig. 3.1 3-D Block Type Failure

The assumptions of the method are listed below.

1. The problem is three-dimensional and symmetrical.
2. The ground surface is defined by three slopes and well-defined toe and crest.
3. The soil strata are laterally continuous.
4. The sliding surfaces are plane.
5. The boundaries between (1) active and central blocks, (2) passive and central blocks are vertical. No shear forces along these boundaries.
6. The bottom surfaces are at $(45 + \phi/2)$ and $(45 - \phi/2)$ angles with the horizontal for active and passive zones, respectively.
7. The factor of safety is the same throughout the whole failure surface.
8. The water surface is far below the ground surface.
9. The forces acting at the ends of blocks may be computed by assuming K_o conditions and linear lateral stress distribution.

3.2.2 Derivation of Equations

The analysis is divided into three parts, namely:

(1) Calculation of the total force acting on the central block from the active block. This force is a function of the factor of safety.

(2) Calculation of the total force acting on the central block from the passive block. This force is also a function of the factor of safety.

(3) Calculation of base, side, and end forces on the central block and of the factor of safety against failure.

3.2.2.1 Active Force

Fig. 3.2 shows the free body diagram of the active block. In Fig. 3.3, consider the force polygon and sum all forces in X and Y coordinate axes:

$$\Sigma F_x = 0$$

$$P_a + 2F_{asm} \sin \phi_m \cos\xi \ \sin (45 - \phi/2) + c_m (A_{ab} + 2A_{as} \cos \xi) \sin (45 - \phi/2) - F_{ab} \cos (45 - \phi/2 + \phi_m) = 0 \qquad (3.1)$$

$$\Sigma F_y = 0$$

$$- W_a + 2F_{asm} \sin \phi_m \cos \xi \cos (45 - \phi/2) + c_m (A_{ab} + 2A_{as} \cos \xi) \cos (45 - \phi/2) + F_{ab} \sin (45 - \phi/2 + \phi_m) = 0 \qquad (3.2)$$

where P_a = the active force

W_a = the weight of the active block

F_{asm} = the mobilized force acting on the end of the active block

ϕ_m = the mobilized frictional angle

ξ = the angle, on the bottom of the active block, of the intersection of the inclined end with the vertical plane

c_m = the mobilized cohesion intercept

A_{ab} = the area of the bottom of the active block

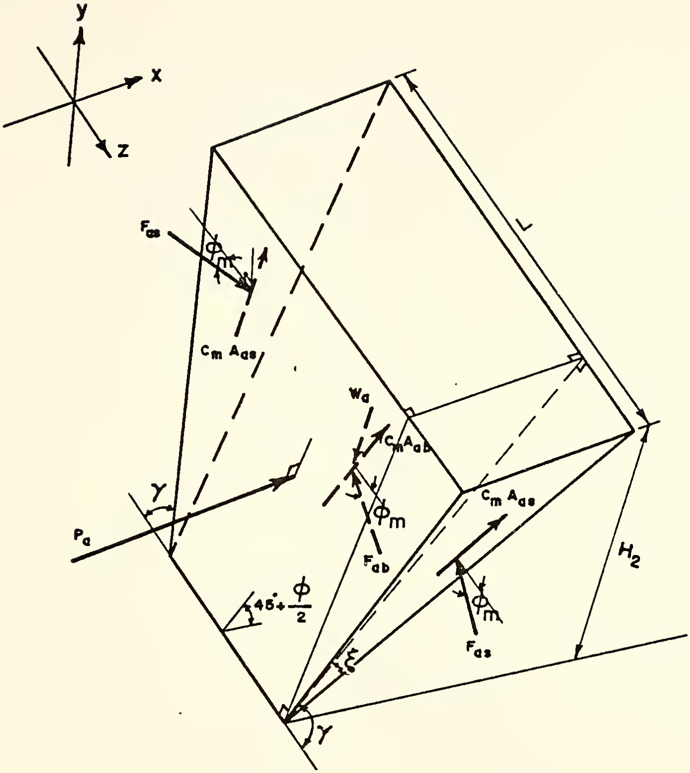

Figure 3.2 Free Body Diagram in Active Case

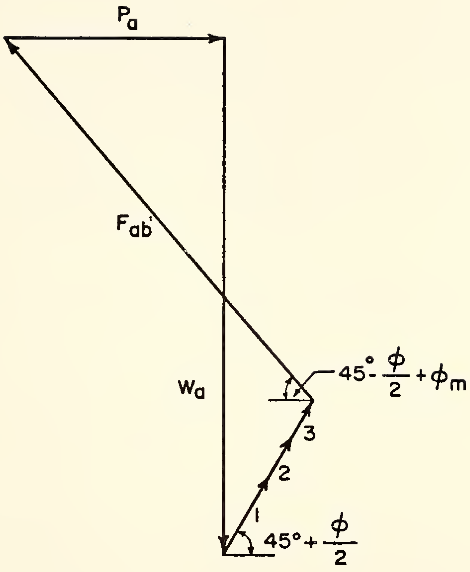

1) $C_m \cdot A_{ab}$ 2) $2 \cdot C_m \cdot A_{as} \cdot \cos \xi$ 3) $2 \cdot F_{asm} \cdot \sin \phi_m \cdot \cos \xi$

Figure 3.3 Force Polygon in Active Case

A_{as} = the area of the end of the active block

F_{ab} = the mobilized force acting on the bottom of the active block

Rearranging equation (3.2):

$$F_{ab} = \csc (45 - \phi/2 + \phi_m) \{W_a - 2F_{asm} \sin \phi_m \cos \xi \cos (45 - \phi/2)$$

$$- c_m (A_{ab} + 2A_{as} \cos \xi) \cos (45 - \phi/2)\} \qquad (3.3)$$

The active force is obtained by substituting equation (3.3) into equation (3.1) and combining the similar terms:

$$P_a = W_a \tan (45 + \phi/2 - \phi_m) - \{c_m (A_{ab} + 2A_{as} \cos \xi)$$

$$+ 2F_{asm} \sin \phi_m \cos \xi\} \cos (45 - \phi/2) \{\tan (45 - \phi/2)$$

$$+ \tan (45 + \phi/2 - \phi_m)\} \qquad (3.4)$$

3.2.2.2 Passive Force

Fig. 3.4 shows the free body diagram of the passive block. In Fig. 3.5, consider the force polygon and sum all forces along X and Y coordinate axes:

$$\Sigma F_x = 0$$

$$- P_P + (2c_m A_{Ps} \cos \eta + c_m A_{pb} + 2F_{psm} \sin \phi_m \cos \eta)$$

$$\cos (45 - \phi/2) + F_{pb} \cos (45 + \phi/2 - \phi_m) = 0 \qquad (3.5)$$

$$\Sigma F_y = 0$$

$$- W_P - (2c_m A_{ps} \cos \eta + c_m A_{pb} + 2F_{psm} \sin \phi_m \cos \eta)$$

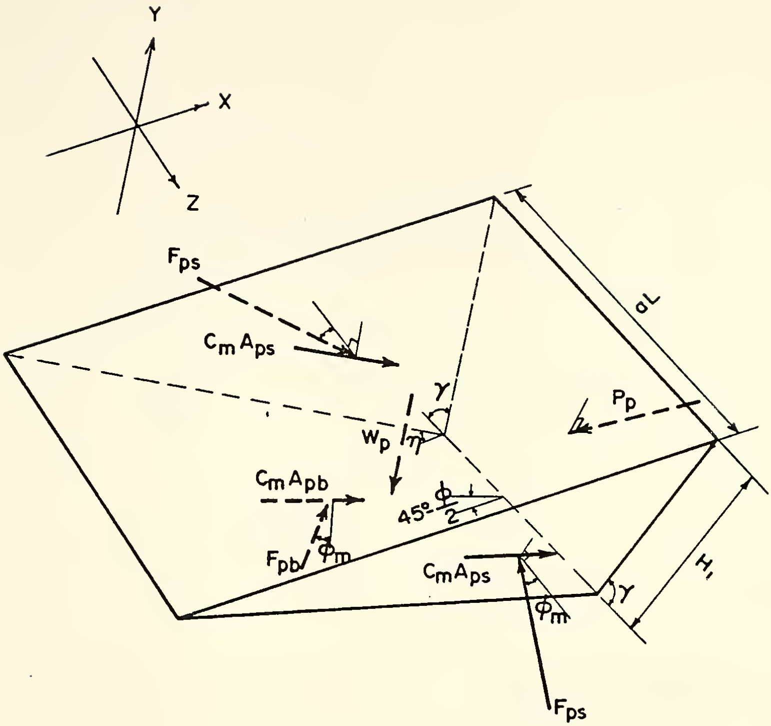

Figure 3.4. Free Body Diagram in Passive Case

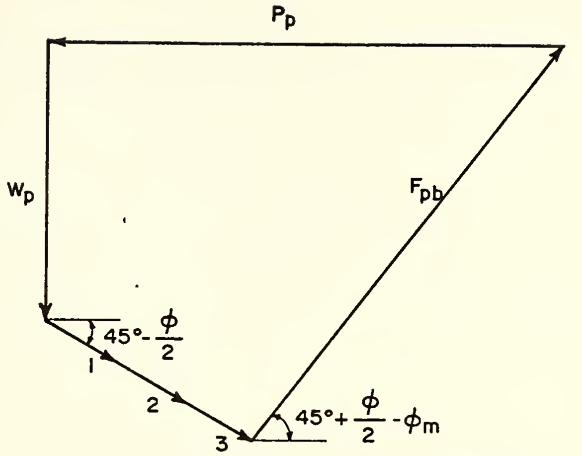

1) $C_m \cdot A_{pb}$ 2) $2 \cdot C_m \cdot A_{ps} \cdot \cos\eta$ 3) $2 \cdot F_{psm} \sin\phi_m \cos\eta$

Figure 3.5 Force Polygon in Passive Case

$$\sin (45 - \phi/2) + F_{pb} \sin (45 + \phi/2 - \phi_m) = 0 \qquad (3.6)$$

where P_p = the passive force

W_p = the weight of passive block

F_{psm} = the mobilized force acting on the end of the passive block

F_{pb} = the mobilized force acting on the bottom of the passive block

A_{pb} = the area of the bottom of the passive block

A_{ps} = the area of the end of the passive block

η = the angle, on the bottom of the active block, of the intersection of the inclined end with vertical plane

Rearranging equation (3.6):

$$F_{pb} = \csc (45 + \phi/2 - \phi_m) \{W_p + (2c_m A_{ps} \cos \eta + c_m A_{pb} + 2F_{psm} \sin \phi_m \cos \eta) \sin (45 - \phi/2)\} \qquad (3.7)$$

The passive force is obtained by substituting equation (3.7) into equation (3.5), and combining the similar terms:

$$P_p = W_p \tan (45 - \phi/2 + \phi_m) + \{c_m (2A_{ps} \cos \eta + A_{pb}) + 2F_{psm} \sin \phi_m \cos \eta\} \cos (45 - \phi/2) \{1 + \tan (45 - \phi/2) \tan (45 - \phi/2 + \phi_m)\} \qquad (3.8)$$

3.2.2.3 Equilibrium of the Central Block and Factor of Safety

Fig. 3.6 shows the free body diagram of the central block. In Fig. 3.7, consider the force polygon and sum all forces along β and η coordinate axes,

$$\Sigma F_{\beta} = 0$$

$$\{(2c_m A_s + 2F_{sm} \sin \phi_m) \cos \alpha + c_{bm} A_b + F_b \sin \phi_m\}$$

$$+ (P_p - P_a) \cos \beta - W \sin \beta = 0 \qquad (3.9)$$

$$\Sigma F_{\eta} = 0$$

$$- W \cos \beta - P_p \sin \beta + F_b \cos \phi_{bm} + P_a \sin \beta = 0 \qquad (3.10)$$

where W = the weight of the central block

F_{sm} = the mobilized force acting on the end of the central block

F_b = the normal force acting on the bottom of the central block

A_s = the area of the end of the central block

A_b = the area of the bottom of the central block

c_{bm} = the mobilized cohesion intercept of the weak soil

α = the angle, on the bottom of central block, of the intersection of the inclined end with vertical plane

β = the angle of inclination of the weak layer

η = the direction normal to β

Rearranging equation (3.10):

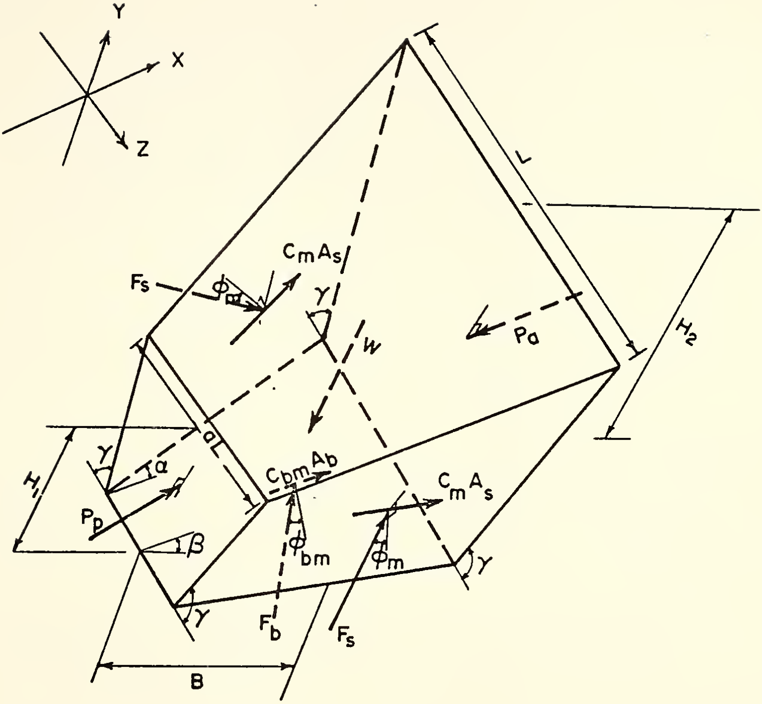

Figure 3.6 Free Body Diagram of Central Block

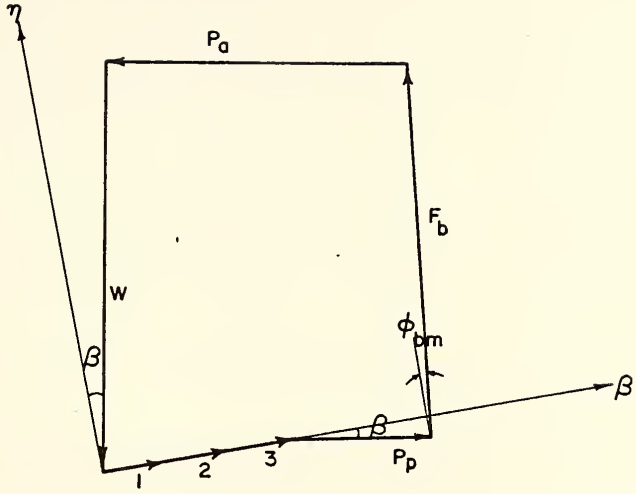

1) $C_{bm} \cdot A_b$ 2) $2 \cdot C_m \cdot A_s \cdot \cos \alpha$ 3) $2 \cdot F_{sm} \cdot \sin \phi_m \cdot \cos \alpha$

Figure 3.7 Force Polygon of Central Block

$$F_b = \sec \phi_{bm} \{W \cos \beta + (P_P - P_a) \sin \beta\} \tag{3.11}$$

Substituting equation (3.11) into equation (3.9), and combining the similar terms leads to:

$$\{(2c_m A_s + 2F_{sm} \sin \phi_m) \cos \alpha + c_{bm} A_b + \tan \phi_{bm}$$

$$(W \cos \beta + (P_P - P_a) \sin \beta)\} + (P_P - P_a) \cos \beta$$

$$- W \sin \beta = 0 \tag{3.12}$$

Equation (3.12) is in terms of the factor of safety F. After substituting the known values listed below, the factor of safety can be calculated by the secant's method (Wolfe, 1959):

$$\tan (45 - \phi/2 + \phi_m) = \frac{\tan (45 - \phi/2) + \tan \phi/F}{1 - \tan (45 - \phi/2) \tan \phi/F}$$

$$\tan (45 + \phi/2 - \phi_m) = \frac{\tan (45 + \phi/2) - \tan \phi/F}{1 + \tan (45 + \phi/2) \tan \phi/F}$$

$$\sin \phi_m = 1/\{1 + (F/\tan \phi)^2\}^{1/2}$$

$$\tan \xi = \sin (45 + \phi/2)/\tan \gamma$$

$$\cos \xi = 1/\{1 + (\sin (45 + \phi/2)/\tan \gamma)^2\}^{1/2}$$

$$\tan \eta = \sin (45 - \phi/2)/\tan \gamma$$

$$\cos \eta = 1/\{1 + (\sin (45 - \phi/2)/\tan \gamma)^2\}^{1/2}$$

$$\tan \alpha = \cos \beta \; \{L (1 - a)/2 - (H_2 - H_1)/\tan \gamma\}/B$$

$$\cos \alpha = 1/\{1 + (\cos \beta \; (L (1 - a)/2 - (H_2 - H_1)/\tan \gamma)/B)^2\}^{1/2}$$

$$W = \rho \; B \; (B_1 + B_2 + \sqrt{B_1 \; B_2})/3$$

where $B_1 = H_2 (L - H_2 \cot \gamma)$

$B_2 = H_1 (a L - H_1 \cot \gamma)$

$A_b = \{0.5 (1 + a) L - \cot \gamma (H_1 + H_2)\} B \sec \beta$

$A_s = B (H_1 + H_2)/(2 \cos \alpha \sin \gamma)$

$F_s \sin \phi = k_o \rho B \tan \phi (H_1^2 + H_2^2 + H_1 H_2)/(6 \sin \gamma \cos \alpha \cos \beta)$

$W_a = \rho H_2^2 \tan (45 - \phi/2) \{0.5 L - H_2/(3 \tan \gamma)\}$

$A_{as} = H_2^2 \tan (45 - \phi/2)/(2 \sin \gamma)$

$A_{ab} = (L - H_2/\tan \gamma) H_2 \sec (45 - \phi/2)$

$F_a \sin \phi = k_o \rho H_2^3 \tan \phi \tan (45 - \phi/2)/(6 \sin \gamma)$

$W_p = \rho H_1^2 \tan (45 + \phi/2) \{0.5 a L - H_1/(3 \tan \gamma)\}$

$A_{ps} = H_1^2 \tan (45 + \phi/2)/(2 \sin \gamma)$

$F_{ps} \sin \phi = k_o \rho H_1^3 \tan \phi \tan (45 + \phi/2)/(6 \sin \gamma)$

$A_{pb} = (a L - H_1/\tan \gamma) H_1 \sec (45 + \phi/2)$

where γ = the inclination of the end of the central block

L = the length on the crest of the central block

a = the ratio between the length of the central block at the toe to that at the crest

B = the width of the central block

H_1 = the vertical height of the passive block

H_2 = the vertical height of the active block

k_o = the ratio of horizontal principal stress to vertical principal stress at rest

ρ = the density of soil in the fill or foundation

3.3 Rotational Type of Failure

The Hovland's method to analyze rotational slides has been presented in Chapter II. In this method the failure mass is divided into many vertical columns and the factor of safety is defined simply as the ratio of total available strength over total mobilized stress. Several important simplifying assumptions were employed: (1) forces on the vertical sides of each soil column were assumed to be zero; (2) direction of movement is along the X-Y plane only; (3) the bottom forces act at the center of the bottom area; and (4) equilibrium of forces and moments in each column are satisfied. The following method will relax some of these assumptions and present a general approach to the analysis of rotational failures.

3.3.1 General Description

Fig. 3.8 shows the free body diagram of a vertical column taken out from the failure mass. The parameters included are the normal and shear forces acting on four vertical sides and the bottom, the points of application of these forces, and the overall factor of safety F. Table 3.1 presents a comparison of the number of parameters needed in the two-dimensional and three-dimensional analyses. Making the necessary assumptions to reduce the number of these parameters and make the problem determinate is not an easy task. For the two-dimensional case, the number of unknowns is relatively limited and many different assumptions have been proposed to solve the problem (Chapter II). But, if a three-dimensional problem is dealt with, many more parameters are included and the task of making the problem determinate is much more complicated.

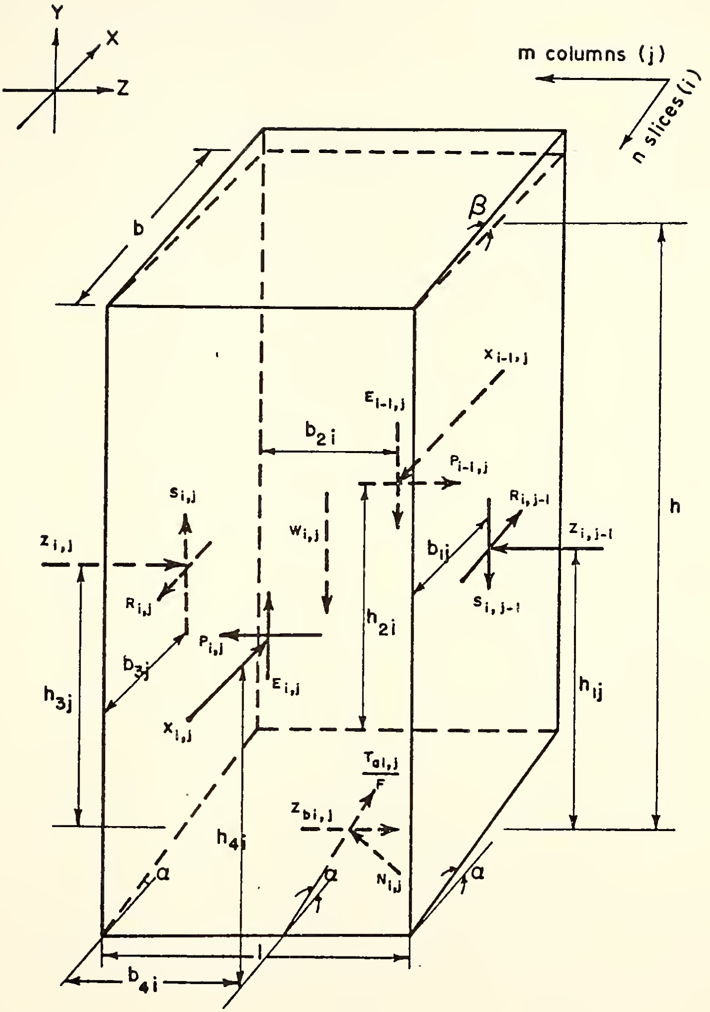

Figure 3.8 Free Body Diagram of a Column

TABLE 3.1 LIST OF UNKNOWNS IN 2-D AND 3-D CASES

Parameters	3-D Unknowns	2-D Unknowns
$Z_{i,j-1}$ $Z_{i,j}$	(m+1)n	0
$X_{i-1,j}$ $X_{i,j}$	(n-1)m	n-1
$R_{i,j-1}$ $R_{i,j}$	(m-1)n	0
$P_{i-1,j}$ $P_{i,j}$	(n-1)m	0
$S_{i,j-1}$ $S_{i,j}$	(m-1)n	0
$E_{i-1,j}$ $E_{i,j}$	(n-1)m	n-1
h_{1j} h_{3j}	(m+1)n	0
h_{2i} h_{4i}	(n-1)m	n-1
b_{1j} b_{3j}	(m+1)n	0
b_{2i} b_{4i}	(n-1)m	n-1
Z_{bij}	mn	0
N_{ij}	mn	n
F	1	1
R_{ext}	2n	0
S_{ext}	2n	0
	12mn-5m+5n+1	5n-3
Reduce to →	(6mn)	→ (3n)

If the mass is divided into 600 vertical columns ($m = 20$, $n = 30$), and the geometry is assumed to be symmetrical, the number of the unknowns remaining are

$$0.5 \cdot 6 \cdot m \cdot n = 0.5 \cdot 6 \cdot 20 \cdot 30 = 1800$$

which is twenty times that in two-dimensional case ($3n = 90$). This large number of equations will not only require tremendous storage in the computer but also long computing times. It is therefore necessary to make more assumptions, as listed below, to simplify the problem.

3.3.2 Assumptions

(1) The failure mass is symmetrical

(2) Direction of movement is along the X-Y plane only (no movement in Z-direction), therefore at the instant of failure the shear stresses along the Y-Z plane are assumed to be zero (Fig. 3.8). This assumption makes:

$$P_{i,j} = P_{i,j-1} = 0$$

$$Z_{bi,j} = 0$$

(3) The length and width of the column is small enough so that it can be assumed that each side force acts along the central vertical line of its side:

$$b_{1j} = b_{3j} = b/2$$

$$b_{2i} = b_{4i} = \ell/2$$

(4) Intercolumn shear forces are assumed to be parallel to the bottom (Fig. 3.9). The cohesion part of the mobilized shear force acts at h/2 from the bottom (resultant of the cohesion acts at the center of the side). The cohesionless part of the mobilized shear force acts at h/3 from the bottom (the intercolumn normal stress distribution is assumed to be linear).

The intercolumn shear forces (at the two ends of the column) are assumed to be a function of their positions; they take the largest value at the outmost point and decrease to zero at the central section because of no relative movement in the middle. The outmost shear forces, R_{ext} and S_{ext}, can be obtained from the following equations, assuming that the K_o condition prevails. These assumptions make:

$$R_{ext} = (0.5\ K_o\ \rho\ h\ \tan\phi + c)\ b\ h\ \cos\alpha$$

$$S_{ext} = R_{ext}\ \tan\alpha$$

$$R_{i,j} = R_{ext}\ f(z) \tag{3.13}$$

$$h_c = h/2$$

$$h_\phi = h/3$$

(5) The interslice forces (on two sides of the column) are assumed to have the same inclination throughout each section (z = constant), then:

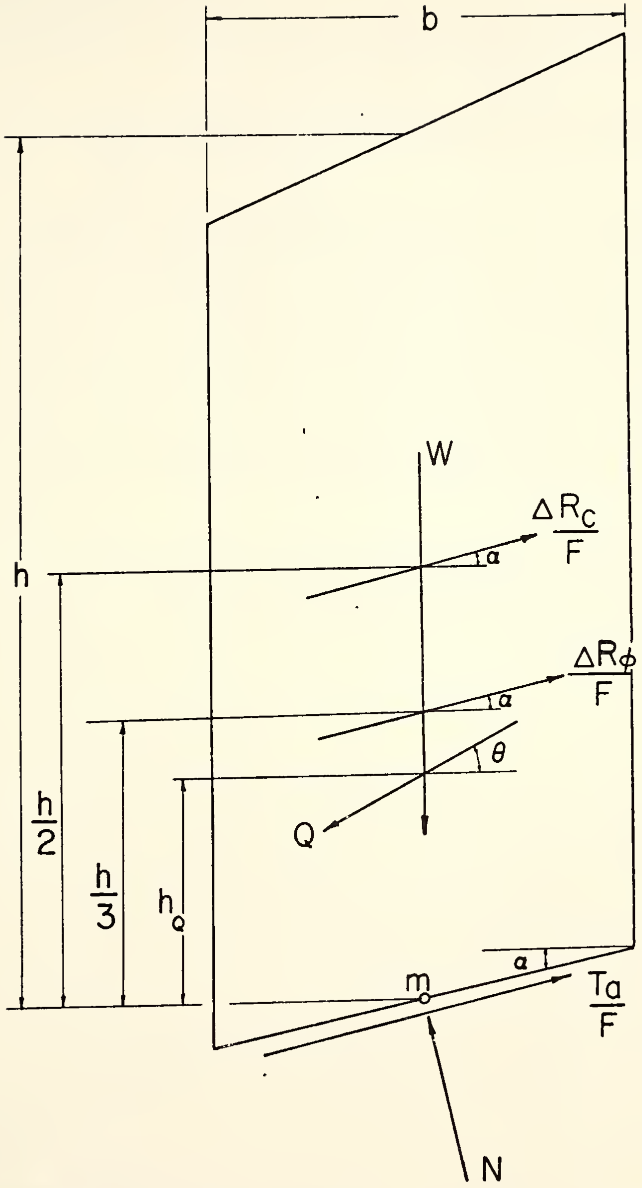

Fig. 3.9 The Force System of a Column in Side View

$$\tan \Theta_i = \frac{E_{ij}}{X_{ij}} = \frac{E_{i-1,j}}{X_{i-1,j}} \qquad (3.14)$$

The resultant of the two interslice forces can be presented as Q.

Table 3.2 lists the unknowns remaining after the above assumptions have been made. The number of the unknowns is reduced from (12mn - 5m + 5n + 1) to (2mn + 1). It is still necessary to have the same number of equations in order to solve for these remaining unknowns. The following procedure will show that the forces, X's and N's (Table 3.2), will not remain in the equations and only the factor of safety F and the inclined angles Θ's are left.

In the following sections, three types of failure geometries are discussed: (1) roller type; (2) spoon shape; and (3) the mixed shape of (1) and (2).

3.3.3 Roller Type Failure

In the roller type of failure, the failure mass is of cylindrical shape with two vertical ends. This problem is very similar to the 2-D problem except that the length of the failure mass is not infinitely long. Consequently the intercolumn shear forces should be taken into consideration.

Fig. 3.10 shows the force polygon of a column. The summation of all forces along the α and η coordinate axes results in:

$$\Sigma F_\alpha = 0$$

$$N' \tan \varphi_m' + \frac{c_b'}{F} \ell\, b \sec \alpha + \frac{\Delta R}{F} - W \sin \alpha - Q \cos (\alpha - \Theta) = 0 \qquad (3.15)$$

TABLE 3.2 LIST OF UNKNOWNS IN 3-D CASE AFTER ASSUMPTIONS

Parameters		3-D Unknowns
$Z_{i,j-1}$ $Z_{i,j}$		0
$X_{i-1,j}$ $X_{i,j}$		$(n-1)m$
$R_{i,j-1}$ $R_{i,j}$		0
$P_{i-1,j}$ $P_{i,j}$		0
$S_{i,j-1}$ $S_{i,j}$		0
$E_{i-1,j}$ $E_{i,j}$		0
h_{1j} h_{3j}		0
h_{2i} h_{4i}		0
b_{ij} b_{3j}		0
b_{2i} b_{4i}		0
Z_{bij}		0
N_{ij}		mn
F		1
R_{ext}		0
S_{ext}		0
Θ_j		m
	Total	$2mn + 1$

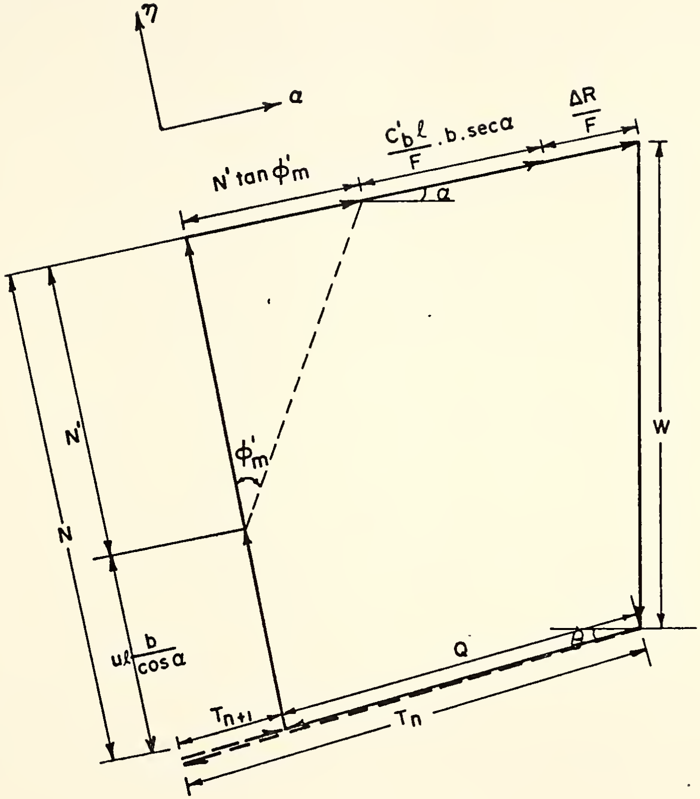

Figure 3.10 Force Polygon of a Column in Roller Type Failure Mass

$\Sigma F_\eta = 0$

$$N' + u\, \ell\, b \sec \alpha - W \cos \alpha + Q \sin (\alpha - \Theta) = 0 \qquad (3.16)$$

where N' = effective normal force acting on the bottom of the column

W = the weight of the column

u = the water pressure acting on the bottom of the column

Q = the resultant of two interslice forces T_n and T_{n+1}

ΔR = the net intercolumn shear force

c_b' = the effective cohesion intercept of the soil beneath the bottom of the column

ϕ_m' = the mobilized effective friction angle

ℓ = the length of the column

b = the width of the column

α = the inclination of the bottom of the column

Θ = the inclination of Q

F = the factor of safety

Rearranging equations (3.15) and (3.16) leads to:

$$Q \cos (\alpha - \Theta) = N' \tan \phi_m' + \frac{c_b'}{F}\, \ell\, b \sec \alpha + \frac{\Delta R}{F} - W \sin \alpha \qquad (3.17)$$

and:

$$N' = - u\, \ell\, b \sec \alpha + W \cos \alpha - Q \sin (\alpha - \Theta) \qquad (3.18)$$

Substituting equation (3.18) into equation (3.17) and combining similar terms result in:

$$Q = \frac{\frac{c'_b}{F}\ \ell\ b\ \sec\alpha + \frac{\tan\phi'}{F}\ (W\cos\alpha - u\ \ell\ b\ \sec\alpha) - W\sin\alpha + \frac{\Delta R}{F}}{\cos(\alpha - \Theta)\ \{1 + \frac{\tan\phi'}{F}\ \tan(\alpha - \Theta)\}} \qquad (3.19)$$

Taking moment at the middle of the base (Fig. 3.9):

$$Q\cos\Theta\ h_Q - \frac{\Delta R_\phi}{F}\cos\alpha\ \frac{h}{3} - \frac{\Delta R_c}{F}\cos\alpha\ \frac{h}{2} = 0 \qquad (3.20)$$

or

$$h_Q = \frac{h\cos\alpha\ (2\ \Delta R_\phi + 3\ \Delta R_c)}{6\ F\ Q\cos\Theta} \qquad (3.21)$$

If the whole failure mass is divided into m sections and if each section is in the state of equilibrium, the sum of all forces in each section must be equal to zero:

$$\Sigma\ Q\cos\Theta = 0 \qquad (3.22)$$

and

$$\Sigma\ Q\sin\Theta = 0 \qquad (3.23)$$

Since Θ is constant, equations (3.22) and (3.23) can be reduced to a unique equation:

$$\Sigma\ Q = 0 \qquad (3.24)$$

The whole system is also in equilibrium with respect to moment equilibrium. Thus the overall moment about any point 0 much be equal to zero (Fig. 3.11):

$$\Sigma\ M_o = 0$$

$$\Sigma\ Q\cos(\Theta - \alpha)\ (r - h_Q\cos\alpha) = 0 \qquad (3.25)$$

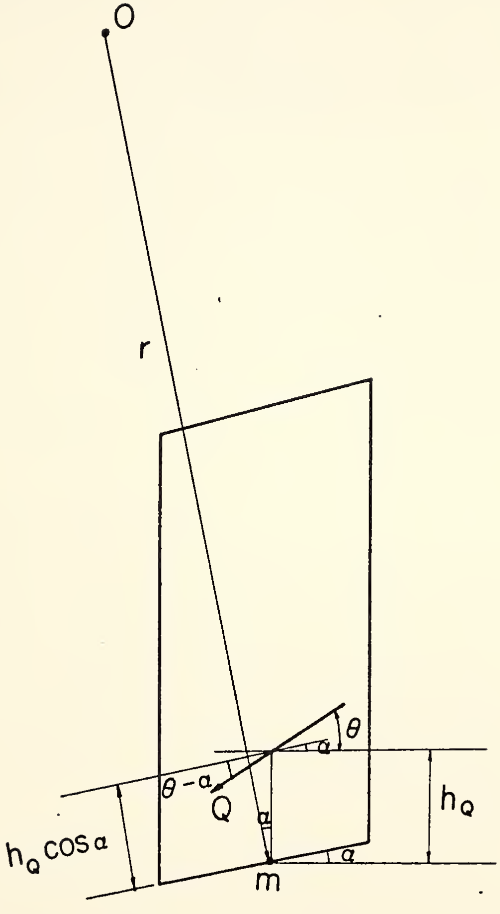

Fig. 3.11 Moment Induced by the Resultant Force about a Point O

Substituting h_Q from equation (3.21):

$$\Sigma\, r \cos(\Theta - \alpha)\,\left(Q - \frac{h \cos^2\alpha\,(2\Delta R_\phi + 3\Delta R_c)}{6r\, F \cos\Theta}\right) = 0 \tag{3.26}$$

If the radius r is constant, then equation (3.26) becomes:

$$\Sigma\,\left\{Q \cos(\Theta - \alpha) - \frac{h \cos^2\alpha \cos(\Theta - \alpha)\,(2\Delta R_\phi + 3\Delta R_c)}{6r\, F \cos\Theta}\right\} = 0 \tag{3.27}$$

For m sections, m equations from the force equilibrium are available (equation (3.24)). One additional equation comes from the overall moment equilibrium (equation (3.26)). The unknowns are Θ_1, Θ_2, ... Θ_m for each section respectively, and the factor of safety F. Because there are (m + 1) equations for (m + 1) unknowns, the problem is rendered determinate and can be solved by using the secant's method for nonlinear equations.

3.3.4 Spoon Shape Failure

In most cases, the shape of the failure mass in the embankment is not a roller type failure, but approaches a spoon shape. In this section, the more realistic spoon shape is discussed. The failure mass is assumed to be symmetrical and has an axis of rotation 0 - 0' (Fig. 3.12). The "spoon" shape is mathematically expressed by an ellipsoid:

$$\frac{x^2}{a^2} + \frac{y^2}{b^2} + \frac{z^2}{c^2} = 1 \tag{3.28}$$

For simplicity, each cross section in the X-Y plane is assumed circular (Fig. 3.13), and:

$$a = b = r_o$$

$$c = r_z$$

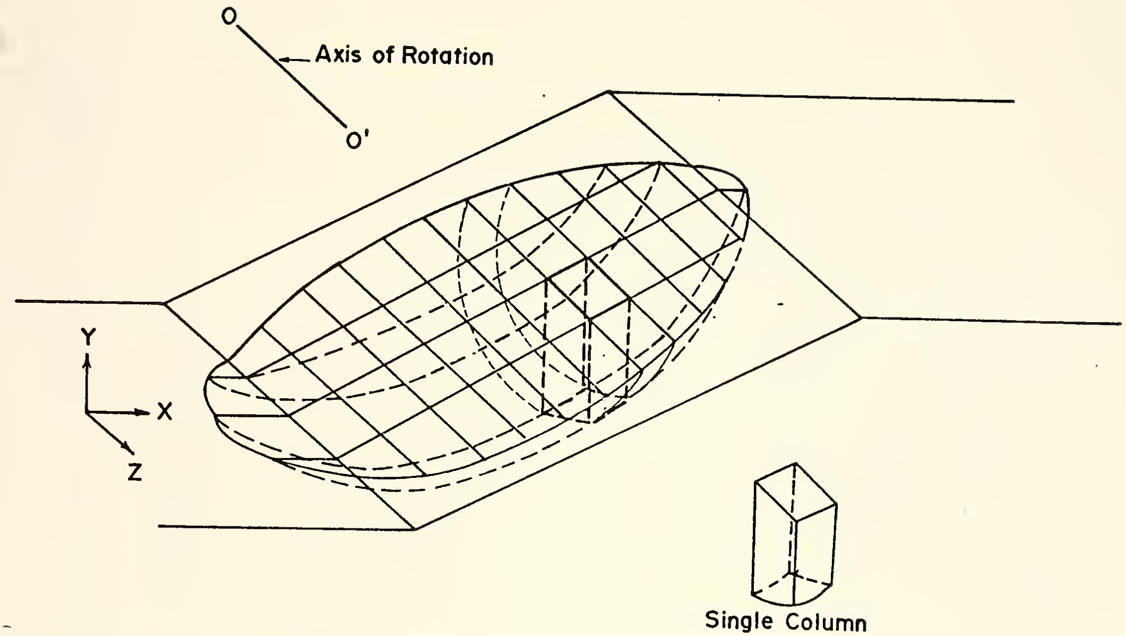

Fig. 3.12 Spoon Shape Failure in the Embankment

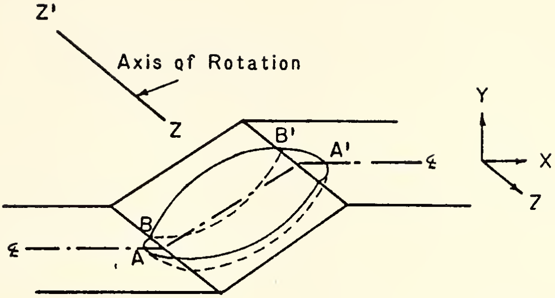

(a) 3-D View of Spoon Shape

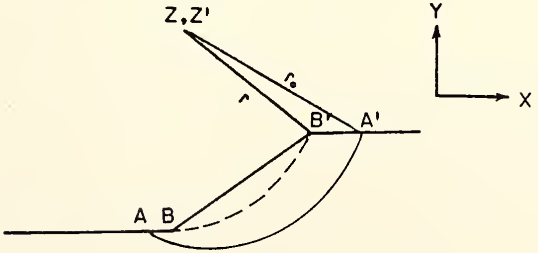

(b) 2-D View of Spoon Shape

Fig. 3.13 2-D and 3-D Views of Spoon Shape

Thus, the equation becomes:

$$\frac{x^2}{r_o^2} + \frac{y^2}{r_o^2} + \frac{z^2}{r_z^2} = 1 \tag{3.29a}$$

or:

$$x^2 + y^2 + m^2z^2 = r_o^2 \tag{3.29b}$$

where: $m = r_o/r_z$

Fig. 3.14 shows the free body diagram of a column. The method allows for different material in the embankment and foundation. The subscript E represent embankment and F represents foundation soil. Fig. 3.15 shows the force system projected on the central plane (X-Y plane) of a column provided that dz is very small. The resultant ΔR_{cE} represents the net sum of two end shear forces R_{cE1} and R_{cE2}, in which the subscripts c, E, 1, 2 stand for cohesion, embankment, end 1, and end 2, respectively.

As previously the failure mass is assumed symmetrical, and there is no movement in the Z-direction. However, all the interslice forces will have the same inclination throughout the whole failure mass. This assumption is different from that assumed in the roller type of failure in which each section had its own inclination of interslice force. Fortunately for the spoon shape of failure, the factor of safety obtained under one Θ assumption makes hardly any difference with that under

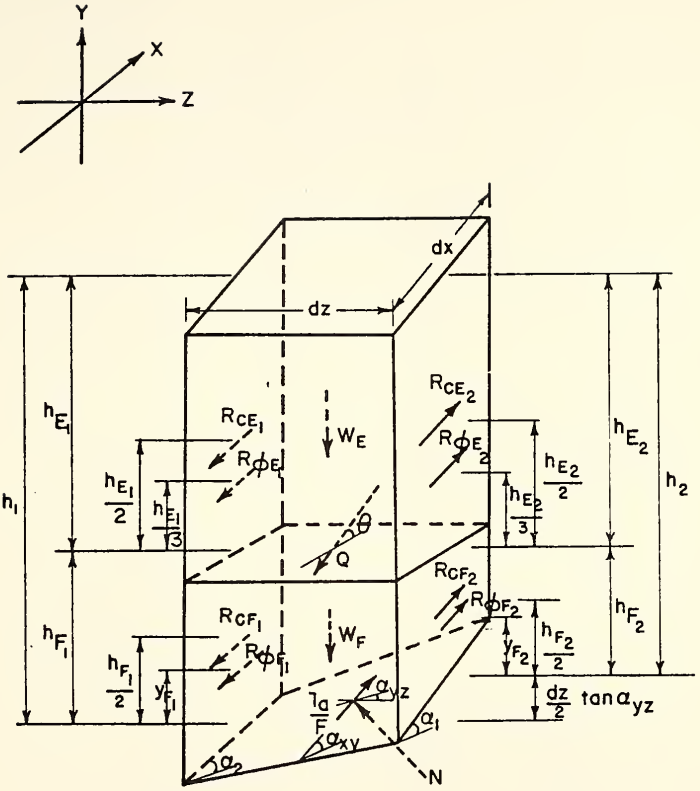

Fig. 3.14. Free Body Diagram of a Column in Spoon Shape Failure

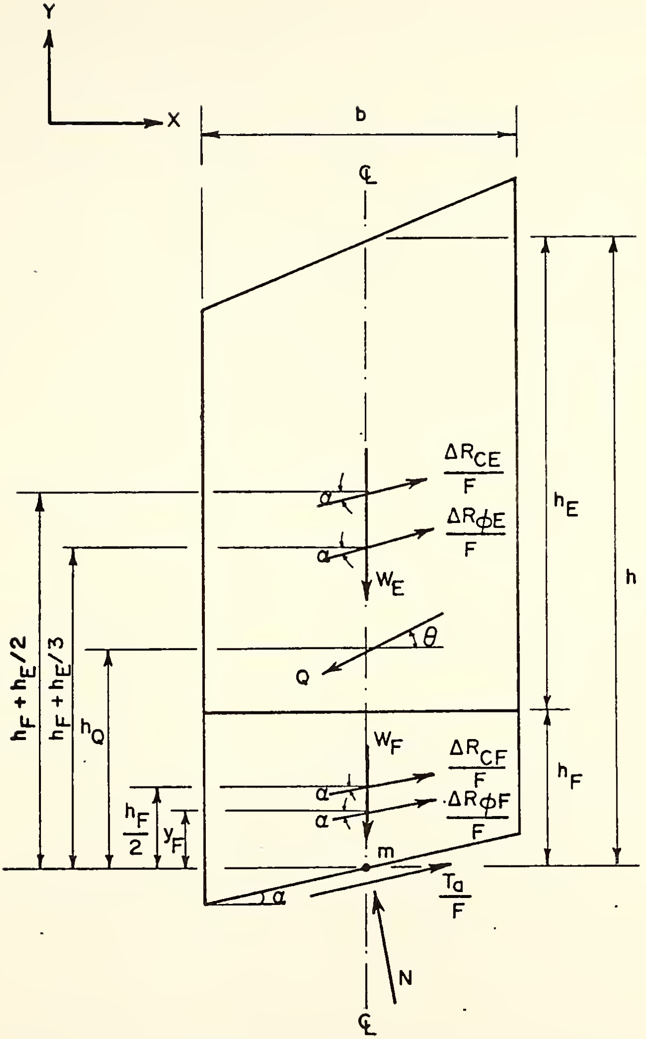

$$y_F = \frac{(m h_E + 1/3\, h_F)\, h_F}{2 m h_E + h_F} \quad \text{in which } m = \frac{\gamma'_E}{\gamma'_F}$$

Fig. 3.15 The Force System of a Column Presented in a 2-D View variable Θ's assumption. Consequently a unique value of Θ can be used throughout the whole failure mass.

Fig. 3.16 shows the force polygon of a column. Considering all forces and summing them in α and η coordinate axes, lead to:

$\Sigma F_\alpha = 0$

$$N' \tan \phi'_m + \frac{c'}{F} A_b - Q \cos(\alpha_{xy} - \Theta) - W \sin \alpha_{xy} + R_2$$

$$\cos(\alpha_2 - \alpha_{xy}) - R_1 \cos(\alpha_{xy} - \alpha_1) - F_w \cos \alpha_{xy} = 0 \quad (3.30)$$

$\Sigma F_\eta = 0$

$$N' + u A_b + Q \sin(\alpha_{xy} - \Theta) - W \cos \alpha_{xy} + R_2 \sin(\alpha_2 - \alpha_{xy})$$

$$+ R_1 \sin(\alpha_{xy} - \alpha_1) + F_w \sin \alpha_{xy} = 0 \quad (3.31)$$

where c' = effective cohesion intercept of soil at the base of the column

A_b = the base area of the column

α_{xy} = the inclination of the intersection between the central section (X-Y plane) and the base

R_1, R_2 = the shear forces acting on two ends 1 and 2

α_1, α_2 = the inclination of the intersection between two ends (end 1 and 2) and the base

F_w = the water force existing (if tension crack is considered)

All other symbols N', ϕ'_m, F, Q, Θ and W have the same definition as before. From equation (3.31):

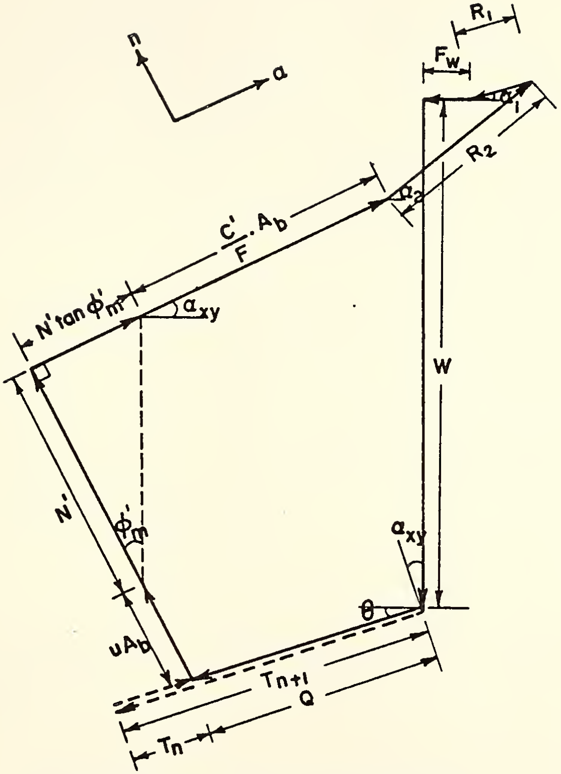

* F_w only appears in the tension zone

Fig. 3.16 Force Polygon of a Column in Spoon Shape Failure

$$N' = - u A_b - Q \sin (\alpha_{xy} - \Theta) + W \cos \alpha_{xy} - R_2 \sin (\alpha_2 - \alpha_{xy})$$

$$- R_1 \sin (\alpha_{xy} - \alpha_1) - F_w \sin \alpha_{xy} \qquad (3.32)$$

After substituting equation (3.32) into equation (3.30):

$$Q = \{\frac{c'}{F} A_b - u A_b \tan \phi_m' + W \cos \alpha_{xy} (\tan \phi_m' - \tan \alpha_{xy})$$

$$+ R_2 \cos (\alpha_2 - \alpha_{xy}) \{1 - \tan \phi_m' \tan (\alpha_2 - \alpha_{xy})\}$$

$$- R_1 \cos (\alpha_{xy} - \alpha_1) \{1 + \tan \phi_m' \tan (\alpha_{xy} - \alpha_1)\}$$

$$- F_w \cos \alpha_{xy} (1 + \tan \phi_m' \tan \alpha_{xy})\}/$$

$$\{\cos (\alpha_{xy} - \Theta) [1 + \frac{\tan \phi'}{F} \tan (\alpha_{xy} - \Theta)]\} \qquad (3.33)$$

If the whole system is in equilibrium, then the sum of all forces in the system must be equal to zero:

$$\Sigma Q = 0 \qquad (3.34)$$

The sum of all moment about any point 0 (Fig. 3.11) must be equal to zero:

$$\Sigma \; Q \cos (\Theta - \alpha) (r - h_Q \cos \alpha) = 0 \qquad (3.34a)$$

or

$$\Sigma \{Q r \cos (\Theta - \alpha) - Q h_Q \cos \alpha \cos (\Theta - \alpha)\} = 0 \qquad (3.34b)$$

where the value of $Q h_Q$ can be obtained by summing all moments in a column at the center of the base of that column (Fig. 3.14). This yields:

$$Q \cos \Theta \, h_Q + \frac{\cos \alpha_1}{F} \{R_{cE1} (h_{F1} + \frac{h_{E1}}{2} - \frac{dz}{2} \tan \alpha_{yz})$$

$$+ R_{cF1} (\frac{h_{F1}}{2} - \frac{dz}{2} \tan \alpha_{yz}) + R_{\phi E1} (h_{F1} + \frac{h_{E1}}{3} - \frac{dz}{2} \tan \alpha_{yz})$$

$$+ R_{\phi F1} (y_{F1} - \frac{dz}{2} \tan \alpha_{yz})\} - \frac{\cos \alpha_2}{F}$$

$$\{R_{cE2} (h_{F2} + \frac{h_{E2}}{2} + \frac{dz}{2} \tan \alpha_{yz}) - R_{cF2} (\frac{h_{F2}}{2} + \frac{dz}{2} \tan \alpha_{yz})$$

$$+ R_{\phi E2} (h_{F2} + \frac{h_{E2}}{3} + \frac{dz}{2} \tan \alpha_{yz}) + R_{\phi F2} (y_{F2} + \frac{dz}{2} \tan \alpha_{yz})\} = 0 \tag{3.35}$$

after rearranging the equation:

$$Q \, h_Q = \frac{1}{6 \cos \Theta \, F} \{\cos \alpha_2 \left[3R_{cE2} (2h_{F2} + h_{E2} + dz \tan \alpha_{yz}) \right.$$

$$+ 3R_{cF2} (h_{F2} + dz \tan \alpha_{yz}) + R_{\phi E2} (6h_{F2} + 2h_{E2} + 3dz \tan \alpha_{yz})$$

$$\left. + 3R_{\phi F2} (2y_{F2} + dz \tan \alpha_{yz}) \right] - \cos \alpha_1 \left[3R_{cE1} (2h_{F1} + h_{E1} \right.$$

$$- dz \tan \alpha_{yz}) + 3R_{cF1} (h_{F1} - dz \tan \alpha_{yz}) + R_{\phi E1}$$

$$\left. (6h_{F1} + 2h_{E1} - 3dz \tan \alpha_{yz}) + 3R_{\phi F1} (2y_{F1} - dz \tan \alpha_{yz}) \right]\} \tag{3.36}$$

The parameters appearing in equation (3.36) are defined in Appendix A.

In these equations the only two unknowns are, (1) the inclination of interslice force Θ and (2) the factor of safety F. Consequently the system of equations can be solved by the secant's method for nonlinear equations.

3.3.5 The Mixed Type Failure

This type of failure is a combination of two kinds of geometry; (1) cylinder in the central portion attached by two cones at two ends (Fig. 2.12a) and (2) cylinder in the central portion attached by two semi-ellipsoids at two ends (Fig. 2.12b). Baligh and Azzouz (1975) examined both cases and found that case (2) is more critical than case (1). In the present study, case (2) is considered and the derivation is the same as those discussed in Sections 3.3.3 and 3.3.4. The computer program is written basically for this mixed type geometry.

3.4 Summary

1. A methodology has been developed to study the block type of failure. The critical failure surface is assumed to make $(45 + \phi/2)$ and $(45 - \phi/2)$ angles with the horizontal in active and passive zones, respectively. The factor of safety is the same along the total failure surface. The active and passive forces are therefore functions of the factor of safety.

2. Similarly a general approach has been proposed to analyze the rotational type of failure. The following assumptions have been made: (1) the failure mass is symmetrical; (2) no movement in the Z-direction; (3) the intercolumn shear forces are parallel to the base; (4) the intercolumn normal stress distribution is linear; (5) the intercolumn shear forces are functions of their positions; and (6) a unique value of Θ, the inclination of the intercolumn shear forces, for the spoon shape of failure or various values of Θ for the roller type of failure.

3. The mixed type of failure is composed of either two semi-ellipsoids or two cones attached at the two ends of the central cylinder. The roller type of failure or spoon shape of failure is just a special case of the mixed type of failure.

IV. FINITE ELEMENT METHOD

4.1 Introduction

The limit equilibrium methods cannot determine strains and deformations within a potential sliding mass. Though it is possible to determine an approximate stress distribution on an assumed slip surface, each method is based on a different set of assumptions and the stress distributions differ considerably from one method to another. Often the limit equilibrium problem is statically indeterminate and different statically admissible solutions may be found for the stress distribution on the failure surface. Consequently, significantly different values of the factor of safety may result from different assumptions of stress distribution on a given slip surface (Lambe and Whitman, 1969). Thus, the factor of safety depends not only on the method of analysis but also on the assumed or implied stress distribution on the failure surface.

Besides, the limit equilibrium methods allow little or no consideration to be given to the history of slope formation, and the consequent initial stresses. In view of these limitations, it is desirable to supplement the conventional stability analyses by stress-deformation studies. In this chapter a three-dimensional finite element computer program is developed to analyze the stability of slopes and embankments. This program, FESPON, uses hyperbolic stress-strain relationship and isoparametric elements with incompatible displacement modes.

4.2 Basis of the Method

Fig. 4.1 shows a continuum divided into discrete parts called 'elements'. These elements are separated from each other by imaginary surfaces and are assumed to be interconnected only at a finite number of nodal points situated on their boundaries. In geotechnical applications the most convenient formulation of the finite element method is for a compatible model in which nodal point displacements are assumed to be the only unknowns. This is generally known as the displacement formulation.

The relationship between generalized displacements $\{f\}$ and nodal displacements $\{\delta\}$ may be expressed as:

$$\{f\} = [N] \; \{\delta\} \qquad (4.1)$$

in which the matrix $[N]$ depends only on the shapes and sizes of elements. The strains $\{\varepsilon\}$ are related to the displacements as follows, assuming deformations to be small:

$$\{\varepsilon\} = [B] \; \{\delta\} \qquad (4.2)$$

in which the matrix $[B]$ depends only on the nodal point coordinates. The stresses are related to the strains by an appropriate matrix $[D]$:

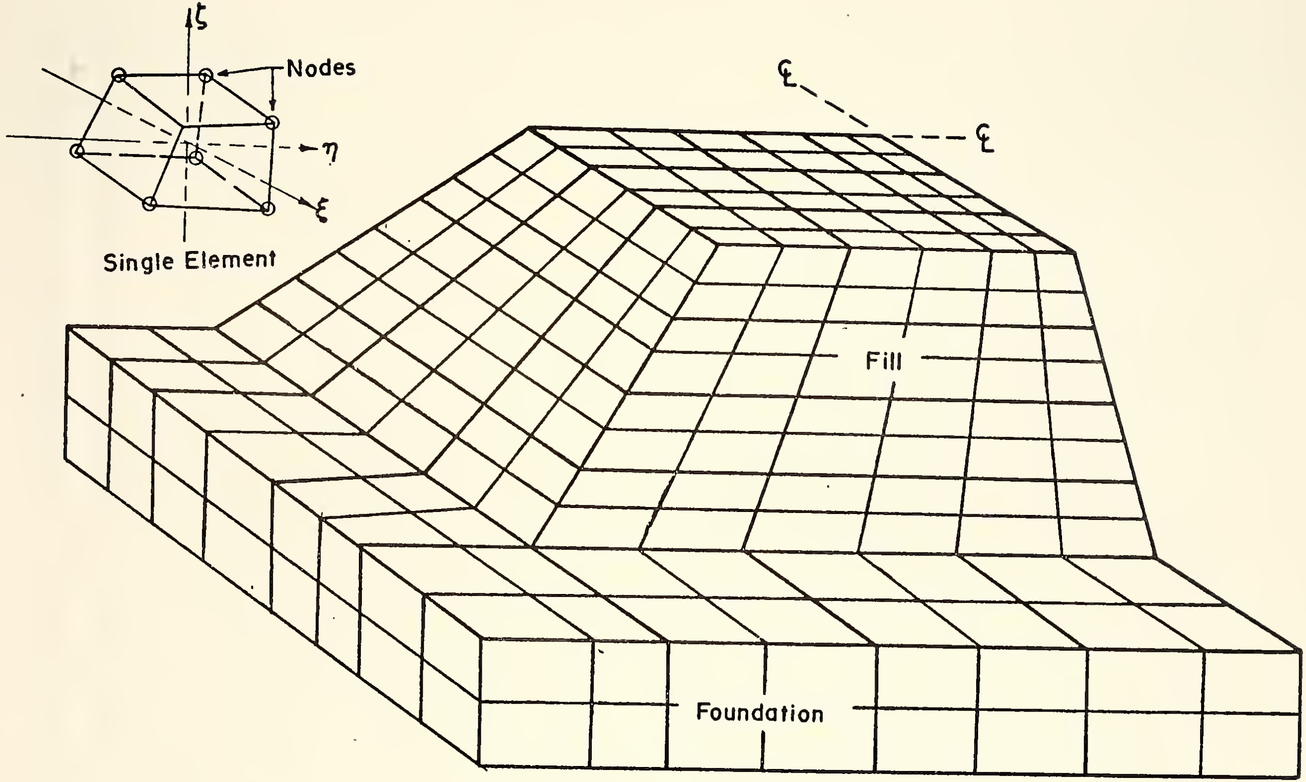

Fig.4.1 3-D Finite Element Mesh

$$\{\sigma\} = [D] \{\varepsilon\} \tag{4.3}$$

For isotropic elastic materials, $[D]$ is dependent only on the modulus of elasticity E and the Poisson's ratio ν. In geotechnical problems it is often desirable to express $[D]$ in terms of shear modulus G and bulk modulus K which are functions of E and ν.

Considering the applied nodal forces and distributed loads, the total potential energy of the system comprising the assemblage of elements and the external loads must be a minimum (from the principle of minimum potential energy).' This requirement leads to a relationship between the nodal forces and displacements for each element. Since each node may be common to several elements, these relationships require assembly in an appropriate manner and the complete system of equations may be written as follows:

$$[k] \{\delta\} = \{F\} \tag{4.4}$$

in which $\{\delta\}$ = the nodal displacement matrix

$\{F\}$ = the resultant nodal forces

$[k]$ = the combined stiffness matrix for the assemblage of elements which approximate the continuum

The stiffness matrix $[k]$ is assembled from individual element stiffness matrices $[k_e]$ which depend on matrices $[B]$ and $[D]$ as follows:

$$[k_e] = \int B^T \, D \, B \, dV \tag{4.5}$$

in which the integration is over the volume of each element in a X, Y, Z-coordinate system. The assemblage and solution of this system of equations is performed by computer. The finite element computer program solves the simultaneous equations to obtain the displacements at each point and subsequently computes the strains and stresses. The details of formulation, assembly, and solution are discussed in many references (Zienkiewicz, 1971; Cook, 1973; and Desai and Abel, 1972).

4.3 Hyperbolic Strain-Strain Relationship

Konder and his co-workers (1963) have shown that the stress-strain curves for a number of remolded cohesive soils, tested in consolidated-undrained triaxial compression, could be approximated by hyperbolas like the one shown in Fig. 4.2. The equation of this hyperbola is:

$$(\sigma_1-\sigma_3) = \frac{\varepsilon}{\frac{1}{E_i} + \frac{\varepsilon}{(\sigma_1-\sigma_3)_{ult}}} \tag{4.6}$$

where E_i is the initial tangent modulus or the initial slope of the stress-strain curve and $(\sigma_1-\sigma_3)_{ult}$ is the asymptotic value of stress difference which is closely related to the strength of the soil. The value of $(\sigma_1-\sigma_3)_{ult}$ is always greater than the stress difference at failure for the soil. When triaxial test data are plotted on the transformed plot as in the lower part of Fig. 4.2, the points frequently are found to deviate from the ideal linear relationship. Experience indicates that a good match is usually achieved by selecting straight lines passing through the points where 70% and 95% of the strength are mobilized (Duncan and Chang, 1970; Kulhawy, Duncan, and Seed, 1969; Hansen, 1963; Daniel and Olson, 1974). Thus, in practice, only two points, the 70% and 95% mobilization points, are plotted on the transformed diagram.

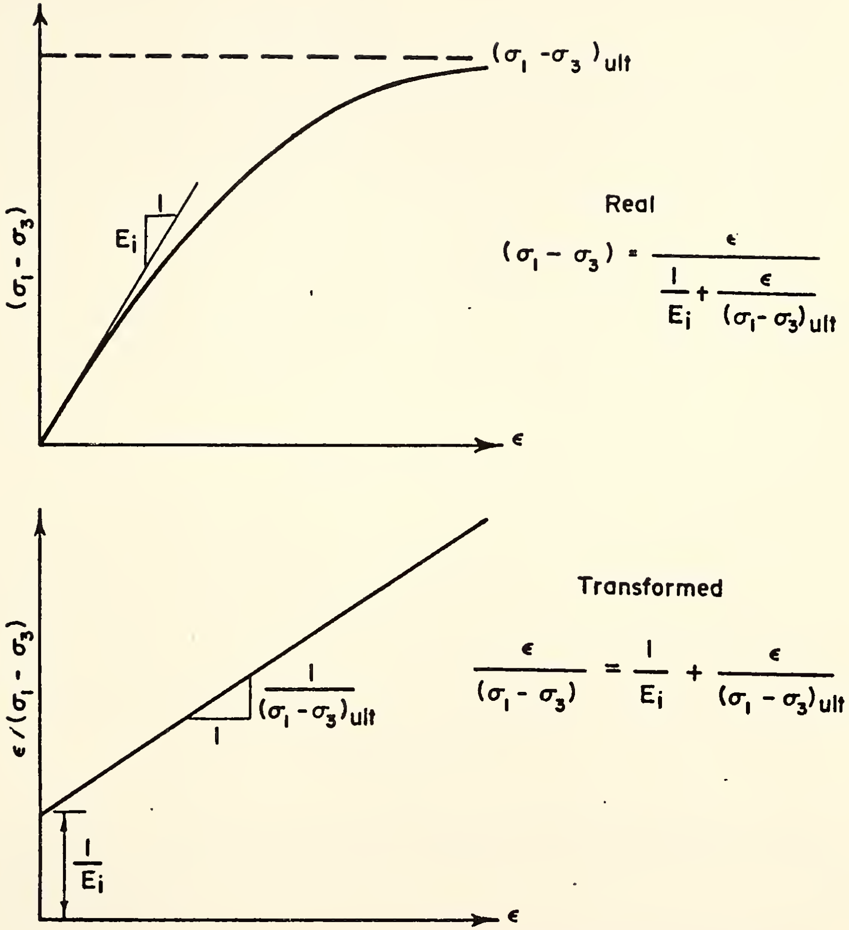

Fig.4.2 Hyperbolic Representation of a Stress-Strain Curve

In order to take into account the increase in strength or a steeper stress-strain curve due to the increase in confining pressure σ_3, Janbu (1970) suggested the following equations (Fig. 4.3):

$$E_i = KP_a(\frac{\sigma_3}{P_a})^n \tag{4.7}$$

in which K is the modulus number, and n is the modulus exponent. Both are dimensionless numbers. P_a is the atmospheric pressure which is introduced to make conversion from one system of units to another more convenient. The variation of $(\sigma_1-\sigma_3)_{ult}$ with σ_3 is accounted for in Fig. 4.4 by relating $(\sigma_1-\sigma_3)_{ult}$ to the stress difference at failure $(\sigma_1-\sigma_3)_f$, and then using the Mohr-Coulomb strength equation to relate $(\sigma_1-\sigma_3)_f$ to σ_3. The values of $(\sigma_1-\sigma_3)_{ult}$ and $(\sigma_1-\sigma_3)_f$ are related by:

$$(\sigma_1-\sigma_3)_f = R_f(\sigma_1-\sigma_3)_{ult} \tag{4.8}$$

in which R_f is the failure ratio. The value of R_f is always smaller than unity, and varies from 0.5 to 0.9 for most soils (Wong and Duncan, 1974). The variation of $(\sigma_1-\sigma_3)_f$ with σ_3 is represented by the Mohr-Coulomb strength relationship, which can be expressed as follows:

$$(\sigma_1-\sigma_3)_f = \frac{2c\cos\phi + 2\sigma_3\sin\phi}{1-\sin\phi} \tag{4.9}$$

in which c and ϕ are the cohesion intercept and the friction angle, as shown in Fig. 4.4.

The tangent modulus E_t is obtained by differentiating equation (4.6) with respect to ε:

$$E_t = \frac{\partial(\sigma_1-\sigma_3)}{\partial\varepsilon} = E_i(1 - \frac{E_i\ \varepsilon}{(\sigma_1-\sigma_3)_{ult} + E_i\ \varepsilon})^2 \tag{4.10}$$

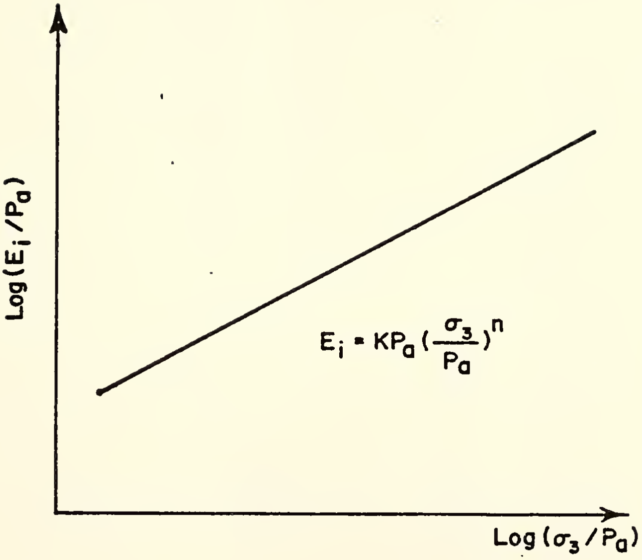

Fig. 4.3 Variation of Initial Tangent Modulus with Confining Pressure

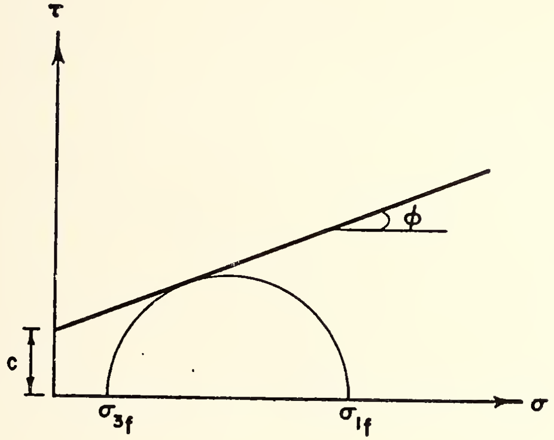

$$(\sigma_1 - \sigma_3)_f = \frac{2\,c \cos\phi + 2\,\sigma_3 \sin\phi}{1 - \sin\phi}$$

$$(\sigma_1 - \sigma_3)_f = R_f\,(\sigma_1 - \sigma_3)_{ult}$$

Fig. 4.4 Variation of Strength with Confining Pressure

Also, after rearranging equation (4.6):

$$E_i\varepsilon = \frac{\sigma_1-\sigma_3}{1-\frac{\sigma_1-\sigma_3}{(\sigma_1-\sigma_3)_{ult}}} \tag{4.11}$$

Substituting equations (4.11), (4.8), (4.9), and (4.7) in equation (4.10) leads to:

$$\begin{aligned} E_t &= E_i\left\{1-\frac{\sigma_1-\sigma_3}{(\sigma_1-\sigma_3)_{ult}}\right\}^2 \\ &= E_i\left\{1-\frac{R_f(\sigma_1-\sigma_3)}{(\sigma_1-\sigma_3)_f}\right\}^2 \\ &= E_i\left\{1-\frac{R_f\ (\sigma_1-\sigma_3)\ (1-\sin\phi)}{2c\ \cos\phi + 2\sigma_3\ \sin\phi}\right\}^2 \\ &= KP_a\left(\frac{\sigma_3}{P_a}\right)^n\left\{1-\frac{R_f\ (\sigma_1-\sigma_3)\ (1-\sin\phi)}{2c\ \cos\phi + 2\sigma_3\ \sin\phi}\right\}^2 \end{aligned} \tag{4.12}$$

If a triaxial specimen is unloaded at some stage during the test, the stress-strain curve followed during unloading is steeper than the curve followed during primary loading, as shown in Fig. 4.5. During subsequent reloading, the stress-strain curve is also steeper than the curve for primary loading and is quite similar in shape to the unloading curve. It is usually reasonably accurate to assume the same value of unloading-reloading modulus E_{ur} for both unloading and reloading. Similar to E_i, E_{ur} is expressed as:

$$E_{ur} = K_{ur}\ P_a\left(\frac{\sigma_3}{P_a}\right)^n \tag{4.13}$$

The unloading-reloading modulus number K_{ur} may be 20% greater than the primary loading modulus number K for stiff soil such as dense sands. For soft soils, such as loose sand, K_{ur} may be three times as

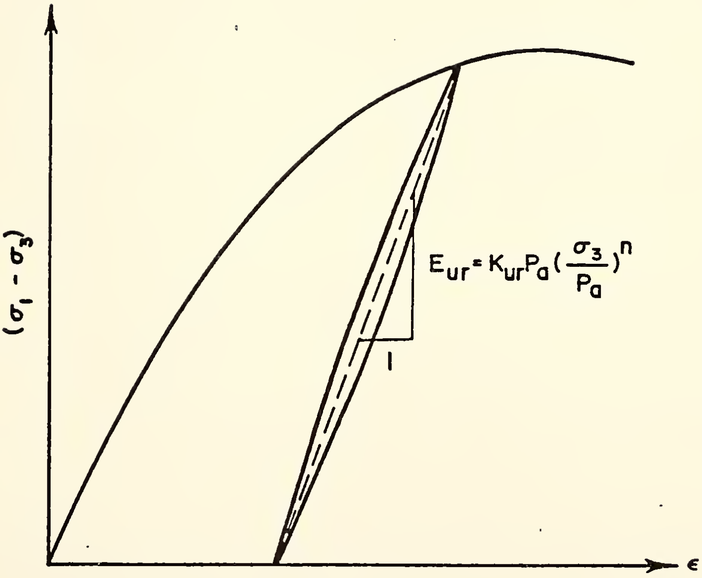

Fig. 4.5 Unloading - Reloading Modulus

large as K. The value of the exponent n is assumed to be the same for both primary loading and unloading.

If the axial and volumetric strains are measured during the triaxial test, it is convenient to calculate the radial strain ε_r using:

$$\varepsilon_r = \frac{1}{2}(\varepsilon_v - \varepsilon_a) \tag{4.14}$$

in which ε_v and ε_a are the volumetric and axial strains, respectively. Taking compressive strains as positive, the value of ε_a is positive and the value of ε_r is negative, the value of ε_v may be either positive or negative.

If the variation of ε_a with ε_r is plotted as shown in Fig. 4.6, the resulting curve can be reasonably represented by a hyperbolic equation of the form:

$$\varepsilon_a = \frac{-\varepsilon_r}{\nu_i - d\,\varepsilon_r}$$

or:

$$-\frac{\varepsilon_r}{\varepsilon_a} = \nu_i - d\,\varepsilon_r \tag{4.15}$$

in which ν_i is the initial Poisson's ratio (at zero strain) and d is a parameter representing the change in the value of Poisson's ratio with radial strain. For saturated soils under undrained conditions, there is no volume change and ν_i is equal to 0.5 for any value of confining pressure. For most other soils the value of ν_i decreases with confining pressures as shown in Fig. 4.7, and this variation of ν_i with σ_3 may be expressed by the equation:

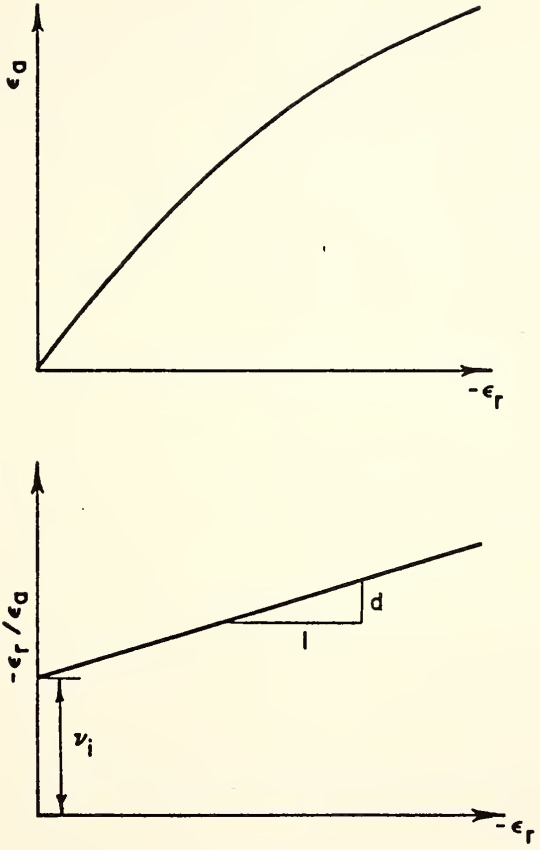

Real

$$\epsilon_a = \frac{-\epsilon_r}{\nu_i - d\epsilon_r}$$

Transformed

$$\frac{-\epsilon_r}{\epsilon_a} = \nu_i - d\epsilon_r$$

Fig.4.6 Hyperbolic Axial Strain-Radial Strain Curves

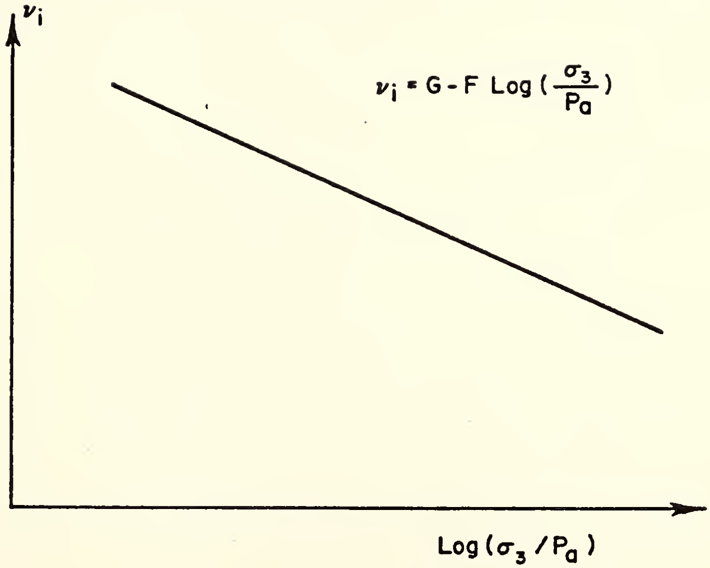

Fig. 4.7 Variation of Initial Tangent Poisson's Ratio with Confining Pressure

$$\nu_i = G - F \log_{10} (\frac{\sigma_3}{P_a}) \tag{4.16}$$

in which G is the value of ν_i at a confining pressure of one atmosphere, and F is the reduction in ν_i for a ten-fold increase in σ_3.

The slope of the curve representing the variation of ε_a with ε_r is $-\nu_t$. This tangent value of Poisson's ratio is expressed in terms of the stresses as follows (Kulhawy, Duncan, and Seed, 1969):

$$\nu_t = \frac{G - F \log (\frac{\sigma_3}{P_a})}{1 - \left\{\frac{d\,(\sigma_1-\sigma_3)}{KP_a(\frac{\sigma_3}{P_a})^n\left[1 - \frac{R_f(\sigma_1-\sigma_3)(1 - \sin\phi)}{2c\cos\phi + 2\sigma_3 \sin\phi}\right]}\right\}^2} \tag{4.17}$$

The nine parameters of the hyperbolic stress-strain relationships and their functions are summarized in Table 4.1.

Frequently, it is impractical to perform drained triaxial tests on soils of low permeability because of the length of time required. In such cases it is possible to determine the values of K and n from consolidation data if the values of c', ϕ', and R_f are known. The effective stress parameters c' and ϕ' may be determined from the results of $\overline{CU}$ tests, and the value of R_f may be estimated on the basis of values determined for similar soils. Values of E_i may be calculated using the following equation (Clough and Duncan, 1969):

Table 4.1 SUMMARY OF THE HYPERBOLIC PARAMETERS

Parameter	Name	Function
K, K_{ur}	Modulus number	Relate E_i and E_{ur} to σ_3
n	Modulus exponent	
c	Cohesion intercept	Relate $(\sigma_1-\sigma_3)_f$ to σ_3
ϕ	Friction angle	
R_f	Failure ratio	Relates $(\sigma_1-\sigma_3)_{ult}$ to $(\sigma_1-\sigma_3)_f$
G	Poisson's ratio parameter	Value of ν_i at $\sigma_3 = p_a$
F	Poisson's ratio parameter	Decrease in ν_i for ten-fold increase in σ_3
d	Poisson's ratio parameter	Rate of increase of ν_t with strain

$$E_i = \frac{\dfrac{\Delta p(1 + e_o)}{\Delta e}\left\{1 - \dfrac{2K_o^{\,2}}{(1 + K_o)}\right\}}{\left\{1 - \dfrac{p(1 - K_o)R_f}{K_o p(\tan^2(45 + \varphi'/2) - 1) + 2c' \tan(45 + \phi'/2)}\right\}^2} \tag{4.18}$$

in which E_i = initial tangent modulus, as defined previously

Δp = increment of pressure in consolidation test

e_o = void ratio at beginning of pressure increment

Δe = decrease in void ratio due to Δp

K_o = coefficient of earth pressure at rest

p = average pressure during increment

c' = cohesion intercept

ϕ' = angle of internal friction

R_f = failure ratio

The value of K_o may be estimated from the test results of Brooker and Ireland (1965), which are shown in Fig. 4.8. When values of E_i have been determined for several different load increments, they are plotted against the corresponding values of σ_3 to determine the value of K and n for the soil. The average value of σ_3 during each increment is calculated using the equation:

$$\sigma_3 = K_o p \tag{4.19}$$

The values of the unloading-reloading modulus number can be determined from the rebound curve in the consolidation test, using the following equation adapted from Clough and Duncan (1969):

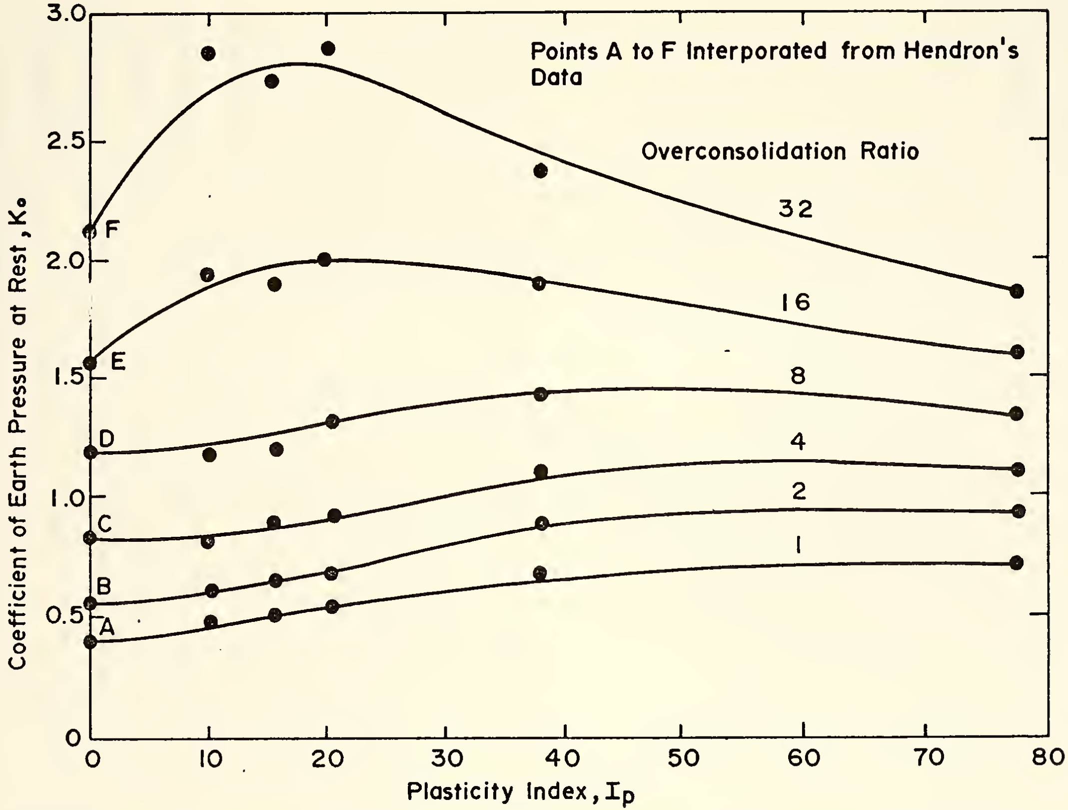

Fig. 4.8 Relation between K_o and I_p for Various Values of Overconsolidation Ratio (after Brooker and Ireland)

$$E_{ur} = \frac{\Delta p(1 + e_o)}{\Delta e} \left\{ 1 - \frac{2(K_o^{\Delta})^2}{(1 + K_o^{\Delta})} \right\} \tag{4.20}$$

in which K_o^{Δ} is the ratio of change in lateral stress to change in vertical stress during unloading in a consolidation test. Values of K_o^{Δ} were derived from the data of Brooker and Ireland (1965), and the variation of K_o^{Δ} with the plasticity index I_p is shown in Fig. 4.9. Clough and Duncan (1969) recommended that E_{ur} be determined at the point on the curve where the pressure has been reduced to half of its value before unloading. Once a value of E_{ur} has been defined, the value of K_{ur} for the soil may be calculated using the equation:

$$K_{ur} = \frac{E_{ur}}{P_a \left(\frac{\sigma_3}{P_a}\right)^n} \tag{4.21}$$

with the value of n determined from the primary loading data, and the value of σ_3 determined from equation (4.19).

4.4 Three-Dimensional Finite Element Computer Program - FESPON

The three-dimensional finite element computer program, FESPON, developed for the present study has been generated from the two-dimensional program ISBILD (Ozawa, 1973). The program ISBILD itself is an improved version of the older program LSBUILD developed by Kulhawy, Duncan, and Seed (1969). These two programs employed the same hyperbolic stress-strain relationship and accommodated the nonlinear behavior of soil by an incremental procedure. The program ISBILD used isoparametric elements with incompatible displacement modes and a more accurate procedure to assign initial stresses to elements. The program

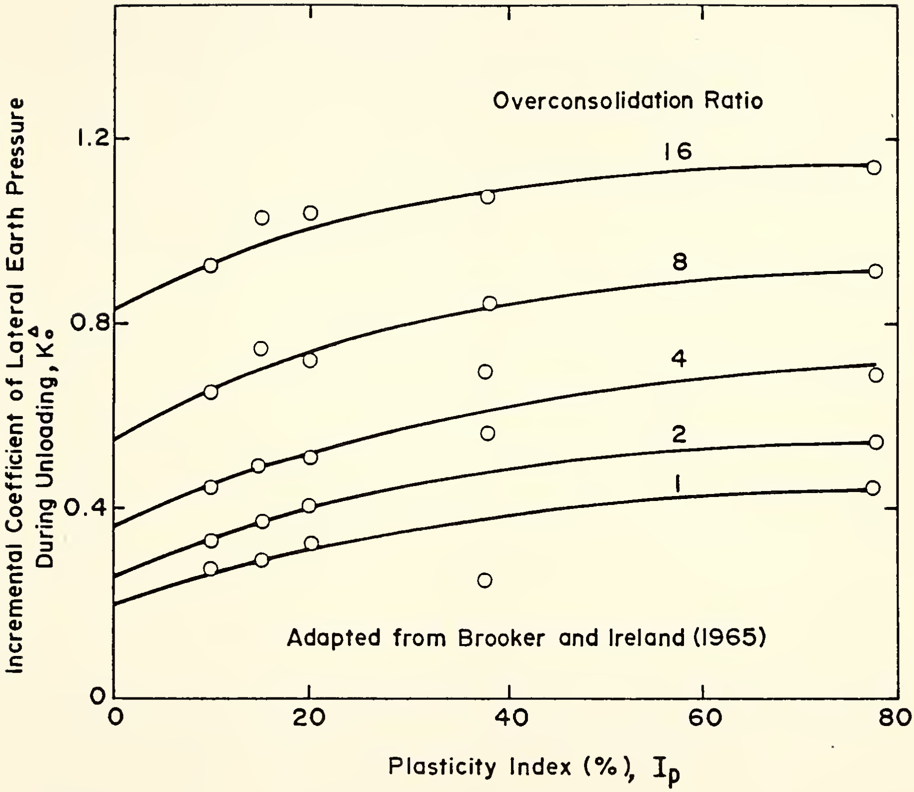

Fig. 4.9 Correlation Between K_o^{Δ} and I_p for Various Values of Overconsolidation Ratios (after Clough and Duncan)

FESPON keeps the main features of these two-dimensional programs but is able to perform three-dimensional analyses.

4.4.1 Nonlinear Incremental Finite Element Method

The nonlinear behavior of soil can be simulated by the successive increments procedure, in which the loading is assumed to be linear within each increment. The modulus values for each element are reevaluated during each increment in accordance with the stresses in the element.

The incremental stress-strain relationship for an isotropic material may be expressed in the form:

$$\begin{Bmatrix} \Delta\sigma_x \\ \Delta\sigma_y \\ \Delta\sigma_z \\ \Delta\tau_{xy} \\ \Delta\tau_{yz} \\ \Delta\tau_{xz} \end{Bmatrix} = \frac{E_t}{(1+\nu_t)(1-2\nu_t)} \begin{bmatrix} (1-\nu_t) & \nu_t & \nu_t & 0 & 0 & 0 \\ \nu_t & (1-\nu_t) & \nu_t & 0 & 0 & 0 \\ \nu_t & \nu_t & (1-\nu_t) & 0 & 0 & 0 \\ 0 & 0 & 0 & \frac{(1-2\nu_t)}{2} & 0 & 0 \\ 0 & 0 & 0 & 0 & \frac{(1-2\nu_t)}{2} & 0 \\ 0 & 0 & 0 & 0 & 0 & \frac{(1-2\nu_t)}{2} \end{bmatrix} \begin{Bmatrix} \Delta\varepsilon_x \\ \Delta\varepsilon_y \\ \Delta\varepsilon_z \\ \Delta\gamma_{xy} \\ \Delta\gamma_{yz} \\ \Delta\gamma_{xz} \end{Bmatrix} \quad (4.22)$$

in which $\Delta\sigma$ and $\Delta\tau$ are stress increments, $\Delta\varepsilon$ and $\Delta\gamma$ strain increments, E_t the tangent modulus, and ν_t the tangent Poisson's ratio. These two parameters are obtained from equations (4.12) and (4.17), respectively. In order to represent post-failure behavior of soils more accurately, Clough and Woodward (1967) suggested the stress-strain relationship in an alternate form:

$$\begin{Bmatrix} \Delta\sigma_x \\ \Delta\sigma_y \\ \Delta\sigma_z \\ \Delta\tau_{xy} \\ \Delta\tau_{yz} \\ \Delta\tau_{xz} \end{Bmatrix} = \begin{bmatrix} M_B+M_D & M_B-M_D & M_B-M_D & 0 & 0 & 0 \\ M_B-M_D & M_B+M_D & M_B-M_D & 0 & 0 & 0 \\ M_B-M_D & M_B-M_D & M_B+M_D & 0 & 0 & 0 \\ 0 & 0 & 0 & M_D & 0 & 0 \\ 0 & 0 & 0 & 0 & M_D & 0 \\ 0 & 0 & 0 & 0 & 0 & M_D \end{bmatrix} \begin{Bmatrix} \Delta\varepsilon_x \\ \Delta\varepsilon_y \\ \Delta\varepsilon_z \\ \Delta\gamma_{xy} \\ \Delta\gamma_{yz} \\ \Delta\gamma_{xz} \end{Bmatrix} \qquad (4.23)$$

in which $M_B = E_t/2(1+\nu_t)(1-2\nu_t)$ and $M_D = E_t/2(1+\nu_t)$. The fact that soils have high resistance to volumetric compression after failure but very low resistance to shearing may be represented by reducing the value of M_D to zero after failure, while M_B is maintained at the value it had in the increment before failure.

It has been found that one of the most effective methods of simulating fill placement is the "average stress" procedure (Ozawa and Duncan, 1973), in which the average stresses during an increment are used for evaluating the modulus and Poisson's ratio. Each increment is analyzed twice, the first time using tangent modulus and Poisson's ratio values based on the stresses at the beginning of the increment, and the second time using tangent modulus and Poisson's ratio values based on the average stresses during the increment. If the stress level decreases during the increment, the unloading-reloading modulus E_{ur} is used in the second evaluation.

4.4.2 Isoparametric Elements

The simplest isoparametric elements are the compatible isoparametric elements which use the same interpolation functions for both the element geometry and the element displacement fields. The geometry and displacement functions are expressed as:

$$\begin{Bmatrix} x \\ y \\ z \end{Bmatrix} = \sum_{i=1}^{N} \phi_i(\xi,\eta,\zeta) \begin{Bmatrix} x_i \\ y_i \\ z_i \end{Bmatrix} \tag{4.24}$$

and

$$\begin{Bmatrix} u_x \\ u_y \\ u_z \end{Bmatrix} = \sum_{i=1}^{N} \phi_i(\xi,\eta,\zeta) \begin{Bmatrix} u_{x_i} \\ u_{y_i} \\ u_{z_i} \end{Bmatrix} \tag{4.25}$$

in which ϕ_i are interpolation functions in terms of local coordinate ξ, η, and ζ, (x_i, y_i, z_i) global nodal point coordinates, and $(u_{x_i}, u_{y_i}, u_{z_i})$ nodal point displacements. It has been shown that compatible isoparametric elements possess poor bending characteristics (Wilson, et al, 1971; Wilson, 1971). Incompatible isoparametric elements use a higher order approximation for the displacements than for the geometry. The additional extra degrees of freedom within the element produce a parabolic incompatibility along the element boundaries. However, the resulting element has good bending characteristics. The displacement functions for the incompatible modes are of the form:

$$\begin{Bmatrix} u_x \\ u_y \\ u_z \end{Bmatrix} = \sum_{i=1}^{N} \phi_i(\xi,\eta,\zeta) \begin{Bmatrix} u_{x_i} \\ u_{y_i} \\ u_{z_i} \end{Bmatrix} + \sum_{j=1}^{M} \psi_j(\xi,\eta,\zeta) \begin{Bmatrix} \alpha_{x_j} \\ \alpha_{y_j} \\ \alpha_{z_j} \end{Bmatrix} \tag{4.26}$$

in which ψ_j are interpolation functions for the displacement amplitudes α_{x_j}, α_{y_j}, and α_{z_j}, which are additional degrees of freedom. For the eight-node element the displacement approximation may be of the following form:

$$u_x = \sum_{i=1}^{8} \phi_i \, u_{x_i} + \psi_1\alpha_{x1} + \psi_2\alpha_{x2} + \psi_3\alpha_{x3}$$

$$u_y = \sum_{i=1}^{8} \phi_i \, u_{y_i} + \psi_1\alpha_{y1} + \psi_2\alpha_{y2} + \psi_3\alpha_{y3} \qquad (4.27)$$

$$u_z = \sum_{i=1}^{8} \phi_i \, u_{z_i} + \psi_1\alpha_{z1} + \psi_2\alpha_{z2} + \psi_3\alpha_{z3}$$

where

$$\phi_1 = \frac{1}{8}(1+\xi)(1+\eta)(1+\zeta) \qquad \phi_5 = \frac{1}{8}(1+\xi)(1+\eta)(1-\zeta)$$

$$\phi_2 = \frac{1}{8}(1-\xi)(1+\eta)(1+\zeta) \qquad \phi_6 = \frac{1}{8}(1-\xi)(1+\eta)(1-\zeta)$$

$$\phi_3 = \frac{1}{8}(1-\xi)(1-\eta)(1+\zeta) \qquad \phi_7 = \frac{1}{8}(1-\xi)(1-\eta)(1-\zeta)$$

$$\phi_4 = \frac{1}{8}(1+\xi)(1-\eta)(1+\zeta) \qquad \phi_8 = \frac{1}{8}(1+\xi)(1-\eta)(1-\zeta)$$

$$\psi_1 = 1-\xi^2$$

$$\psi_2 = 1-\eta^2$$

$$\psi_3 = 1-\zeta^2$$

The functions ψ_1, ψ_2, and ψ_3 must be zero at the eight nodes. Therefore, the resulting element stiffness matrix will be 33x33. However, if the strain energy within the element is minimized with respect to α_i, the additional displacements can be eliminated and a reduced 24x24 stiffness matrix developed. This is identical to the standard static condensation procedure.

4.4.3 Initial Stresses and Procedure of Analysis

For accurate estimation of stresses and displacements, the analyses are performed by dividing the placement of fill into eight or more construction layers. The stresses in each layer due to its own weight immediately after placement are assigned rather than calculated. For elements under a horizontal surface the initial vertical stresses are taken to be equal to the overburden pressure. The initial horizontal stresses are taken as $\nu/(1-\nu)$ times the overburden pressure, where ν is the Poisson's ratio. The shear stresses on horizontal and vertical planes are assumed to be equal to zero. For elements under a sloping surface, estimation of initial stresses is more difficult. The assumptions made by Ozawa and Duncan (1973) in the program ISBILD are used in the present analysis:

$$\sigma_x = \sigma_z = \frac{\nu}{1-\nu} \rho \, h \tag{4.28}$$

$$\sigma_y = \rho \, h \tag{4.29}$$

$$\tau_{xy} = 0.5 \, \rho \, h \sin \alpha_{xy} \tag{4.30}$$

$$\tau_{yz} = 0.5 \, \rho \, h \sin \alpha_{yz} \tag{4.31}$$

$$\tau_{xz} = 0 \tag{4.32}$$

in which ρ h is the overburden pressure at the center of the element, ν the Poisson's ratio, and α the angle of slope of the surface above the element.

The layer being placed is assigned very small modulus values to simulate the fact that a newly added layer of fill on an embankment has very low stiffness. The nodal points at the top of the newly placed layer are assigned zero displacement, i.e., the positions of these nodal points immediately after placement are taken as the reference positions for measuring movements due to subsequent loading. The strains in the newly placed elements are set equal to zero also, thus taking the condition immediately after placement as the reference state for strains.

Each increment of loading is analyzed twice. The changes in stress, strain and displacement during each increment are added to the stresses, strains and displacements existing at the beginning of the increment. These resulting values are then used in the next increment.

The program is capable of handling embankments on rigid or compressible foundations. For a compressible foundation, the initial stresses are set as:

$$\sigma_y = \rho\, h$$

$$\sigma_x = \sigma_z = K_o\, \rho\, h$$

$$\tau_{xy} = \tau_{yz} = \tau_{xz} = 0$$

For more details about the subroutines and their functions, refer to Appendix B.

4.5 Summary

A three-dimensional computer program FESPON is generated from the two-dimensional program ISBILD. The hyperbolic stress-strain relationship is combined with an incremental technique to simulate the nonlinear behavior of soils. Isoparametric incompatible elements are used in order to provide good bending characteristics. The parameters necessary to the analysis can be obtained from triaxial and consolidation test data.

If such data are not available, these parameters can be estimated from values and relationships determined for similar soils by previous investigators. The next chapter will present practical applications of the computer program FESPON.

V. RESULTS AND APPLICATIONS

5.1 Introduction

In the previous chapters, several models were developed to analyze the stability of embankments. In Chapter III, three-dimensional limit equilibrium methods were proposed to study both translational and rotational slides. These methods were implemented in the computer programs BLOCK3 and LEMIX for translational and rotational failures, respectively. In Chapter IV, a three-dimensional finite element computer program FESPON was developed to simulate the construction of embankment. This program makes allowance for the nonlinear stress-strain behavior of soils.

This chapter describes typical applications of these three-dimensional models. The factors of safety obtained with the three-dimensional models are compared with the ones obtained with the two-dimensional models. Results obtained with the three-dimensional finite element computer program are also presented and compared to the results obtained with the limit equilibrium methods.

5.2 Analysis of Translational Slides

In this section the computer program BLOCK3 is used to analyze the stability of highway embankments. This program was developed to study three-dimensional translational slides; the derivation of equilibrium equations and the solution techniques have been discussed in Section 3.2.2.

Translational slides can occur in an embankment when a weak soil layer is present in the foundation soil. This is the problem studied herein. Table 5.1 lists all the geometric and soil parameters necessary to such an analysis. In the following application the ground surface is horizontal and the embankment geometry is assumed as: height of 6.1 m (20 ft), crown width of 12.2 m (40 ft), and slope of 1.5/1. These dimensions are typical for highway embankments in Indiana. The embankment and foundation soils are the same with average density ρ of 1930 kg/m^3 (120 pcf). The frictional angle of the weak soil ϕ_w is taken as equal to zero. These assumptions are not necessary to the program BLOCK3, but they are made to simplify the discussion of the results. The other parameters used in the study are listed in Table 5.2. Several of these parameters are varied in order to assess their effects on the factor of safety against translational sliding. In particular different values were given to: (1) the strength parameters of the embankment and foundation soils; (2) the strength parameters of the weak layer; (3) the inclination of the weak layer; (4) the depth to weak layer; (5) the inclination of the ends of the central block; and (6) the length ratio (a). Factors of safety of the embankment against sliding are computed for several combinations of these parameters, using the program BLOCK3. In all these analyses the stability is investigated to the side of the down-dipping weak seam, which is the most critical case (Boutrup, 1977).

TABLE 5.1 VARIABLES AND SYMBOLS

Variables	Symbols*
Height and width of an embankment	H, B
The upper and lower length at the top of the central block	L, aL
Depth to weak layer, measured from the toe	D
Inclination of ground surface	i
Inclination of weak soil layer	β
Inclination of left and right slope of embankment	β_L, β_R
Inclination of the ends of the block	γ
Strength of embankment soil	$(c, \phi)_E$
Strength of foundation soil	$(c, \phi)_F$
Strength of weak soil	$(c, \phi)_w$

* Refer to Fig. 3.1

TABLE 5.2 SYMBOLS AND RANGE OF VARIABLES FOR AN EMBANKMENT BUILT ON A FOUNDATION SOIL WITH A WEAK SOIL LAYER

	Variables	Symbols	Value or Range
1.	Height of embankment	H	6.1 m (20 ft)
2.	Width of embankment	B	12.2 m (40 ft)
3.	The upper length at the top of the central block	L	6.1 - 97.5 m (20-320 ft)
4.	The ratio of the lower length to upper length at the top of the central block	a	0 - 1.0
5.	Depth to weak layer, measured from the toe	D	1.5 - 12.2 m (5 - 40 ft)
6.	Inclination of ground surface	i	0°
7.	Inclination of weak soil layer	β	0° - 11.3° (0 - 5/1)
8.	Inclination of left and right slope of embankment	β_L/β_R	33.7° (1.5/1)
9.	Inclination of the ends of the block	γ	70° - 90°
10.	Average density of soil	ρ	1930 kg/m^3 (120 pcf)
11.	Strength of embankment soil	c_E, φ_E	47.9 kPa (1000 psf), 0°
			24.0 kPa (500 psf), 10° 0°, 35°
12.	Strength of foundation soil	c_F, ϕ_F	same as 11
13.	Strength of weak soil	c_w	9.6 - 28.7 kPa (200 - 600 psf)

The most significant results of these analyses are presented in Figs. 5.1 to 5.5 and are discussed below. The reader can refer to Appendix C (Tables C.1 to C.9), to obtain a complete description of all the results developed in this study.

In Fig. 5.1 the ratio F_3/F_2 of the 3-D factor of safety to the 2-D factor of safety is plotted versus the length ratio of the embankment L/H, for several values of the depth ratio D/H. The length ratio L/H is the ratio of the length of the embankment L to the height of the embankment H, while the depth ratio D/H is the ratio of the depth to the weak layer D to the height of the embankment H. In these analyses, the weak layer is horizontal ($\beta = 0^{\circ}$) and has a cohesion intercept c_w of 9.6 kPa. This combination of β and c_w gives the highest F_3/F_2 ratios (Tables C.1 to C.3). Two sets of strength parameters are considered for the embankment and foundation soil: (1) c = 47.9 kPa, $\phi = 0^{\circ}$ (solid lines); and (2) c = 0, $\phi = 35^{\circ}$ (dotted lines). The following conclusions can be drawn from Fig. 5.1:

- The ratio F_3/F_2 increases with decreasing length ratio L/H. This three-dimensional effect is more important for cohesive soils than for cohesionless soils.
- For cohesive soils the ratio F_3/F_2 decreases with the depth ratio D/H. On the contrary, for cohesionless soils, the ratio F_3/F_2 increases with decreasing depth ratio D/H.

It is obvious that as the length L gets smaller, the end resistances play a more important role, and consequently a higher factor of safety is obtained with the 3-D method.

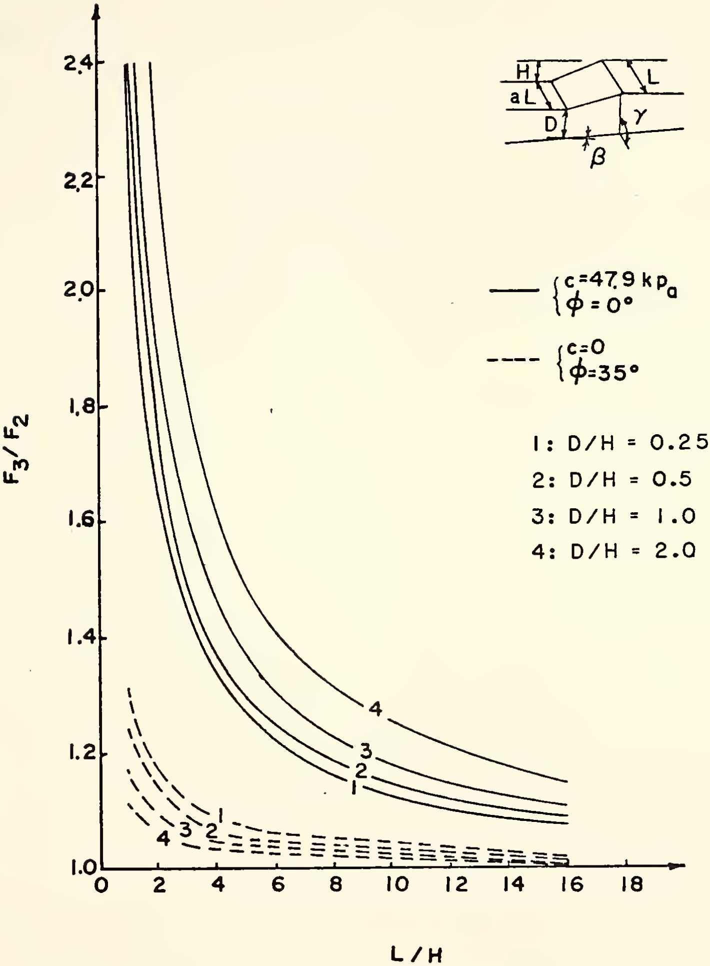

Fig. 5.1 F_3/F_2 vs. L/H for Various D/H and Soil Parameters (at a = 1, β=0°, γ=90°, and $c_{w'}$=9.6kPa)

Fig. 5.2 illustrates the effect of the strength parameter of the weak soil c_w on the F_3/F_2 ratio. The solid lines are for a cohesion intercept c_w of 9.6 kPa and the dotted lines for c_w of 28.8 kPa. For two kinds of foundation soil studied, a lower c_w value results in higher F_3/F_2 ratios.

Fig. 5.3 presents the effect of the inclination of the weak soil layer β on the F_3/F_2 ratio. This figure shows that, for any combinations of depth ratio D/H and soil strength, a steeply inclined weak soil layer always yields smaller F_3/F_2 ratios.

When the end of the block tilts from an angle γ of 90° (vertical ends) to a smaller value (inclined ends), the end area will increase. Hence, the end resistance gets larger and higher F_3/F_2 ratios are obtained. This phenomenon is shown in Fig. 5.4 in which L/H is set to unity. As the ratio L/H increases, this increase in the F_3/F_2 ratio with decreasing inclination γ will certainly be less significant.

It is also predicable that as the front area of the central block gets smaller, which is close to a wedge type of failure, both the passive resistance and the bottom resistance will be reduced. However, the ends area will increase and produce more resistance along the ends of the block. In Fig. 5.5, when L/H ratio is small, the increase of ends resistance may be larger than the decrease of the resistance both from the passive force and the bottom resistance. Therefore, the net resistance is positive and higher F_3/F_2 ratios obtained. As L/H ratio approaches a critical value, the net resistance will be negative, and the 3-D factor of safety F_3 will be less than the 2-D factor of safety F_2, i.e., the F_3/F_2 ratio is less than unity.

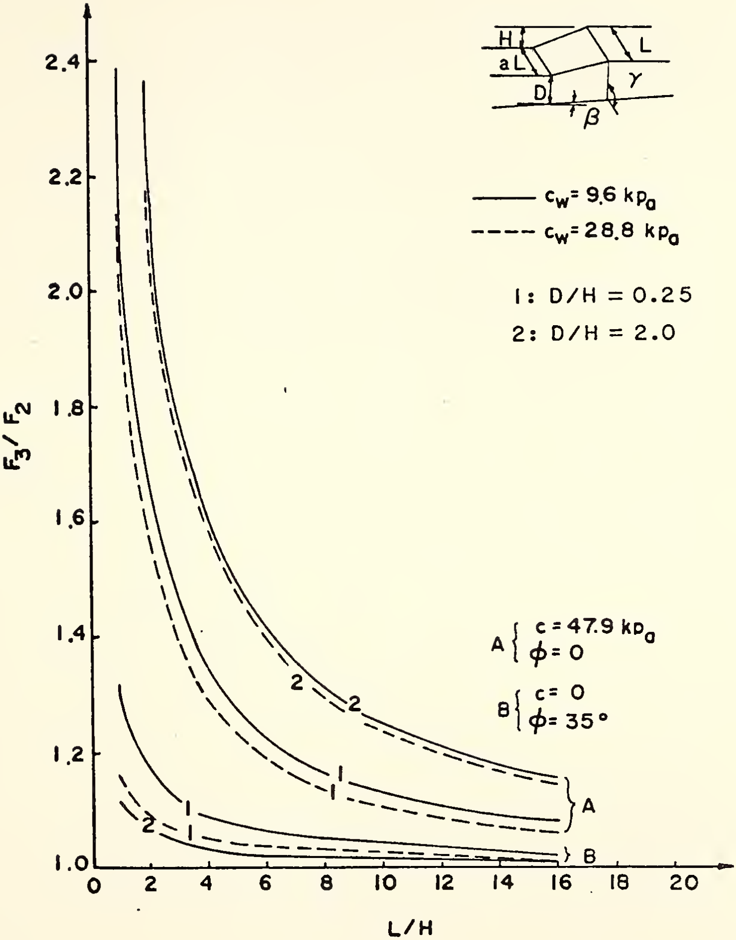

Fig. 5.2 F_3/F_2 vs. L/H for Various c_w and D/H (at a = 1, $\beta = 0°$, and $\gamma = 90°$)

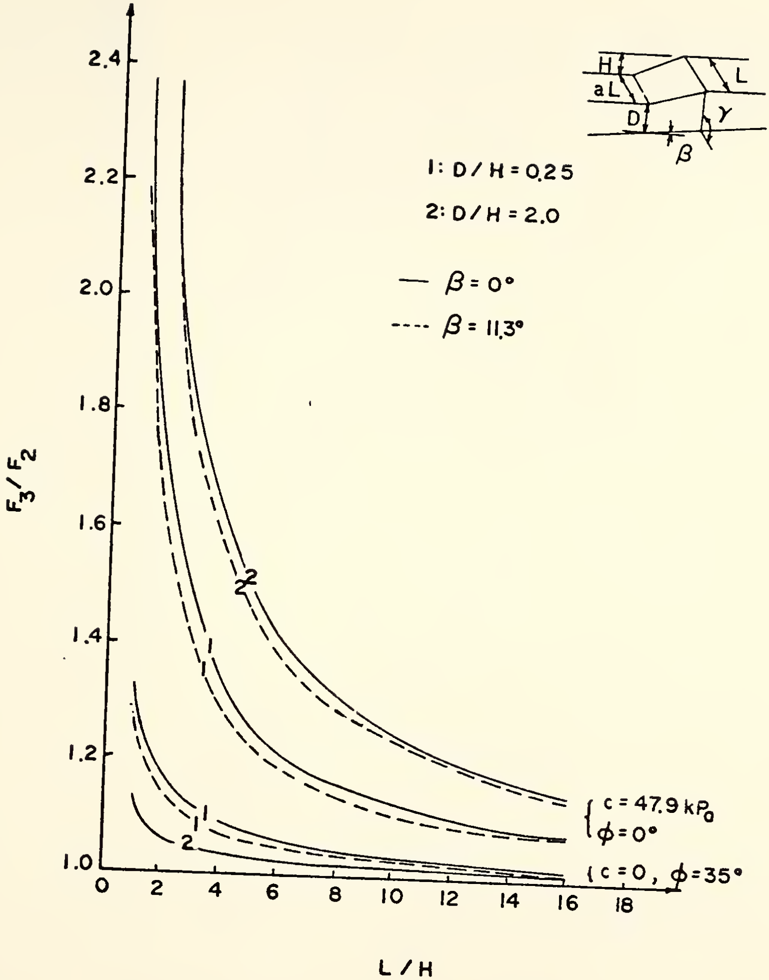

Fig. 5.3 F_3/F_2 vs. L/H for Various β and D/H (at a = 1, γ = 90°, and c_w = 9.6kPa)

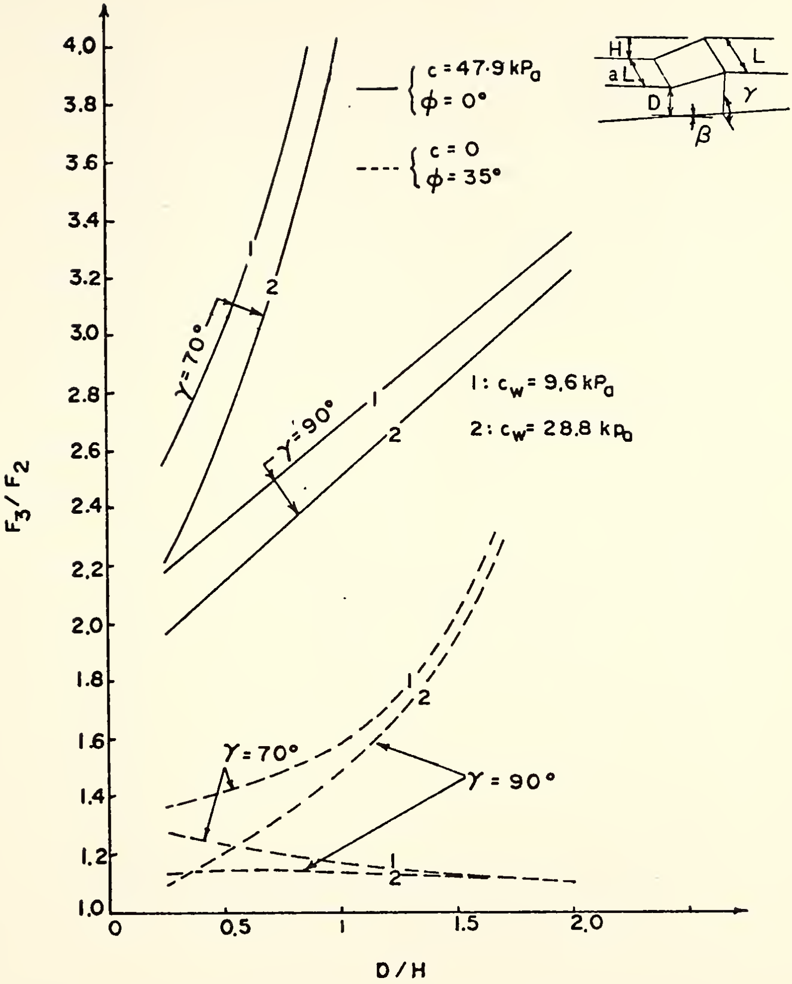

Fig. 5.4 F_3/F_2 vs. D/H for Various γ and c_w
(at L/H = 1, a = 1, and $\beta = 0°$)

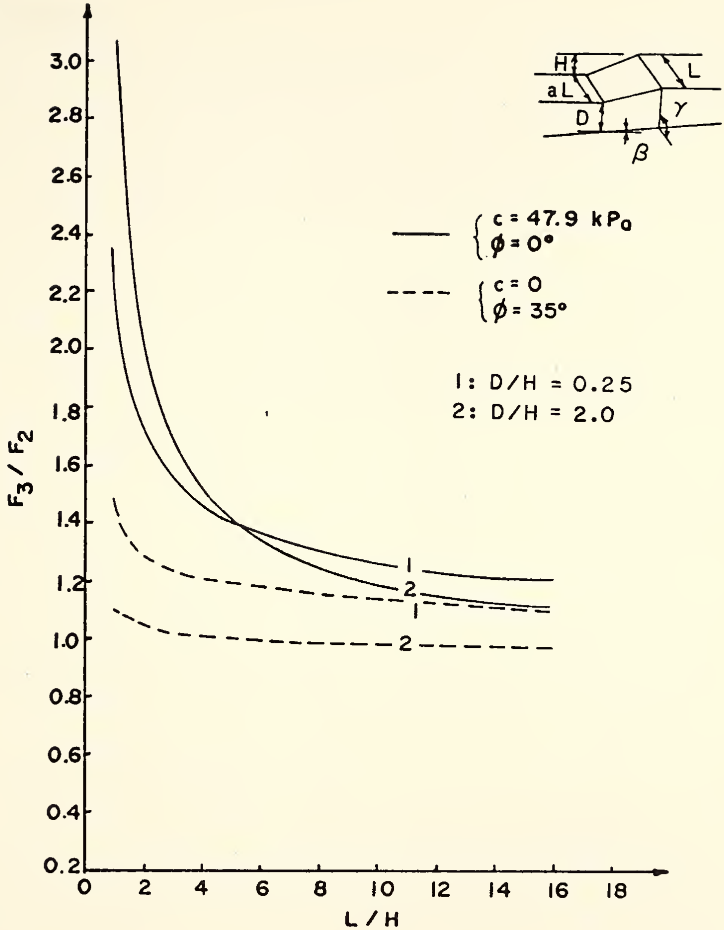

Fig. 5.5 F_3/F_2 vs. L/H for Various D/H and Soil Parameters (at a = 0.8, β = 0°, γ = 90°, and c_w = 9.6kPa)

In summary, the most important results obtained from this study are as follows:

1. For translational sliding, the F_3/F_2 ratio is usually greater than unity. At small values of L/H, this 3-D effect is more significant for cohesive soils than for cohesionless soils.
2. The depth ratio has some effect on the F_3/F_2 ratio as shown in Fig. 5.1.
3. For all soils, cohesive or cohesionless, a lower strength of the weak layer may cause a higher three-dimensional effect.
4. A steep weak soil layer always yields smaller F_3/F_2 ratios than a gently inclined layer.
5. Reducing the inclination of the ends of the central block cause a higher factor of safety due to the increase in end areas.
6. Wedge type of failure will result in the value of F_3/F_2 less than unity, and therefore the stability of a slope needs to be examined carefully when there is potential for such a failure.

5.3 Analysis of Rotational Slides

In this section, the rotational slide will be studied. The soil is assumed to be homogeneous. The 3-D failure surface is composed of a central cylinder attached by two semi-ellipsoids at the two ends. The cross-section of the central cylinder is the most critical circle searched by the 2-D computer program STABL2. After the 2-D critical circle has been determined, the 3-D failure surface then can be generated. The cylinder has a length $2\ell_c$ and the minor axis of the semi-ellipsoids has a length ℓ_s as shown in Fig. 5.6.

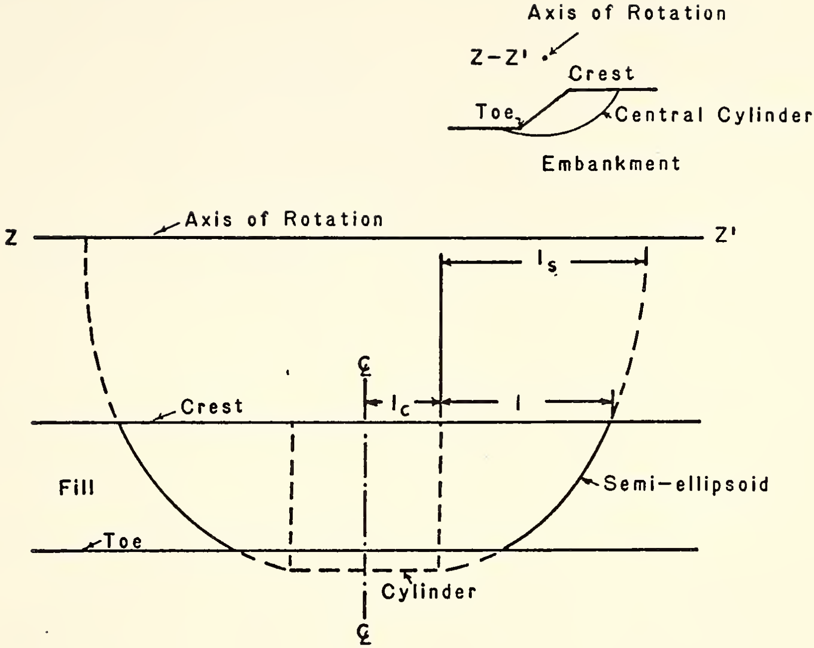

Fig. 5.6 Front View of a Mixed Type of Failure Surface

Five combinations of the strength parameters are considered: (1) $c' = 0$, $\phi' = 40^{\circ}$; (2) $c' = 7.2$ kPa (150 psf), $\phi' = 30^{\circ}$; (3) $c' = 14.4$ kPa (300 psf), $\phi' = 25^{\circ}$; (4) $c' = 21.6$ kPa (450 psf), $\phi' = 20^{\circ}$; and (5) $c' = 28.7$ kPa (600 psf), $\phi' = 15^{\circ}$. The height of the slope is 6.1 m (20 ft) with three different angles, 33.7° (1.5/1), 21.8° (2.5/1), and 16° (3.5/1). Cases with water ($r_u = 0.5$) and without water ($r_u = 0$) conditions are studied. Here, the pore water pressure parameter r_u is defined as:

$$r_u = \frac{u}{\rho h} \tag{5.1}$$

where u is the mean pore water pressure at the base of the column, ρ the density of soil, and h the mean height of the column.

5.3.1 Pore Water Pressure Parameter $r_u = 0$

For each combination of strength parameters and slope angle, the coordinates of the centers and the radii of the critical circles are listed in Table 5.3. The last two columns in the table list the 2-D factors of safety both from STABL2 and Spencer's method. It can be seen from this table that the 2-D factors of safety obtained by STABL2 are always less than those obtained by Spencer's method. STABL2 is generally conservative (Boutrup, 1977). The most critical circles for different combinations of strength parameters and different slopes are plotted in Fig. 5.7. For low cohesion intercept c and high friction angle ϕ , the critical circle tends to be shallow and likely to pass through the toe of the slope. On the other hand, for high cohesion intercept c and low frictional angle ϕ , the critical circle tends to be a deep one and extends beyond the toe.

TABLE 5.3 THE COORDINATES OF THE CENTERS AND RADII OF THE MOST CRITICAL 2-D FAILURE CIRCLES AND THE 2-D FACTORS OF SAFETY (r_u = 0)

Slope Angle	c (kPa)	ϕ (degrees)	X_o (m)	Y_o (m)	Radius (m)	F_2 (STABL2)	F_2 (SPENCER)
	0	40	10.1	6.4	12.9	1.557	1.704
	7.2	30	7.3	1.2	8.3	1.755	1.936
33.7°	14.4	25	7.0	4.6	11.9	2.124	2.301
	21.6	20	7.0	4.6	11.9	2.370	2.537
	28.7	15	5.6	5.0	13.1	2.611	2.776
	0	40	11.3	6.1	12.8	2.334	2.619
	7.2	30	11.3	7.6	14.7	2.315	2.529
21.8°	14.4	25	9.3	4.6	12.7	2.566	2.803
	21.6	20	9.3	4.6	12.7	2.750	2.927
	28.7	15	10.2	4.9	14.5	2.935	3.245
	0	40	19.8	30.5	36.6	3.011	3.075
	7.2	30	15.8	13.7	21.3	2.986	3.224
16°	14.4	25	13.4	7.8	17.2	3.109	3.515
	21.6	20	13.4	7.8	17.2	3.222	3.592
	28.7	15	12.8	7.6	12.7	3.252	3.511

NOTE: X_o is the horizontal distance between the center and the crest; positive value means the center is on the left side of the crest.

Y_o is the vertical distance between the center and the crest; positive value means the center is above the crest.

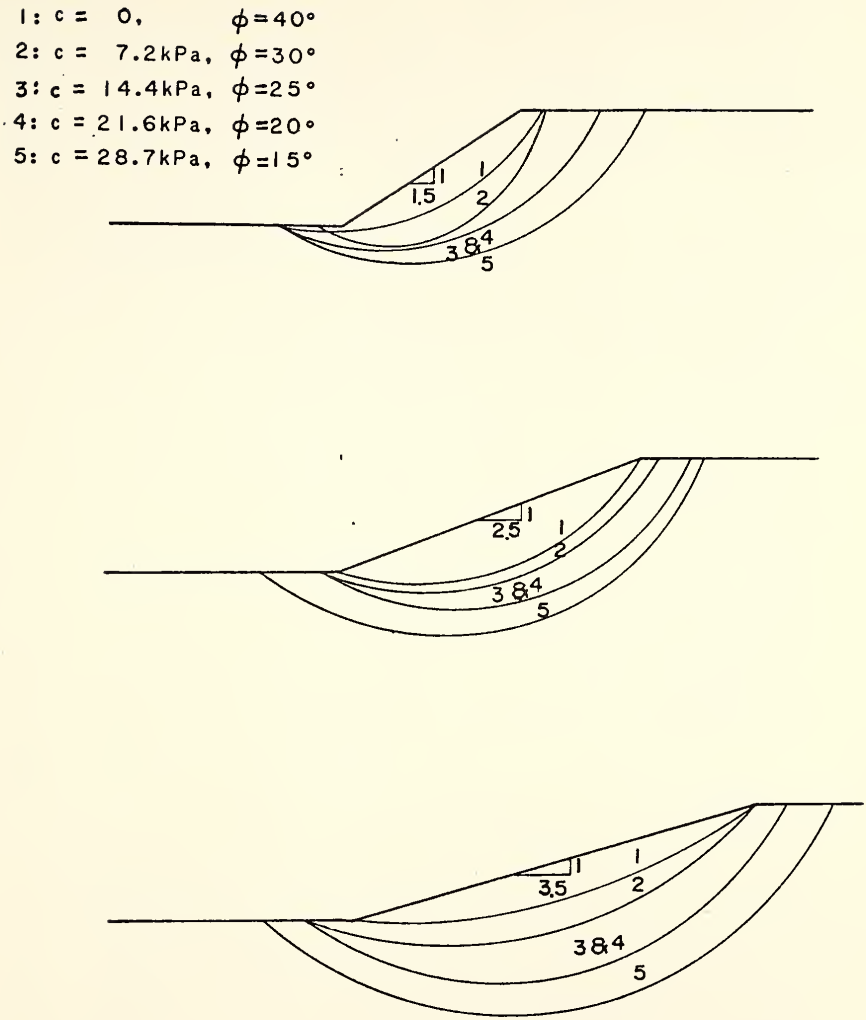

Fig. 5.7 The Most Critical Surfaces for Different Combinations of Strength Parameters in Different Slopes (r_u = 0)

Different ℓ_c/H ratios, 0.5, 1, 2, and 4, with different ℓ_s/H ratios, 0.5, 1, 2, and 4 are studied. Tables D.1 to D.3 show the F_3/F_2 ratios at various ℓ_c/H and ℓ_s/H ratios. The results are obtained by both LEMIX and the Ordinary Method of Columns (OMC). The following conclusions can be drawn from this study:

- As the ℓ_s/H ratio increases, the F_3/F_2 ratio generally decreases as shown in Fig. 5.8. The reason is that when the width of the failure surface increases the end effects are less in general.
- In certain cases (Figs. D.1b, c, d, e, etc.) there is a minimum F_3/F_2 ratio. This means that, theoretically, the failure will most likely occur for the ratio ℓ_s/H corresponding to the minimum F_3/F_2 ratio. However, these curves are very smooth and it is difficult to predict the exact length of the failure mass. This result was also noted by Baligh and Azzouz (1975).
- For cohesive soils, F_3 is always greater than F_2. However, for cohesionless soils, F_3 may be less than F_2 (Fig. 5.8a).
- When the ℓ_c/H ratio increases, F_3 is closer to F_2. A larger ℓ_c/H ratio means that the problem is closer to the plane strain condition. Hence, the curves corresponding to large ℓ_c/H ratio are closer to the line $F_3/F_2 = 1$ (See the difference between Fig. 5.8a and 5.8e).
- The steeper the slope, the less the F_3/F_2 ratio as shown in Fig. 5.9. This is probably because the volume of the failure

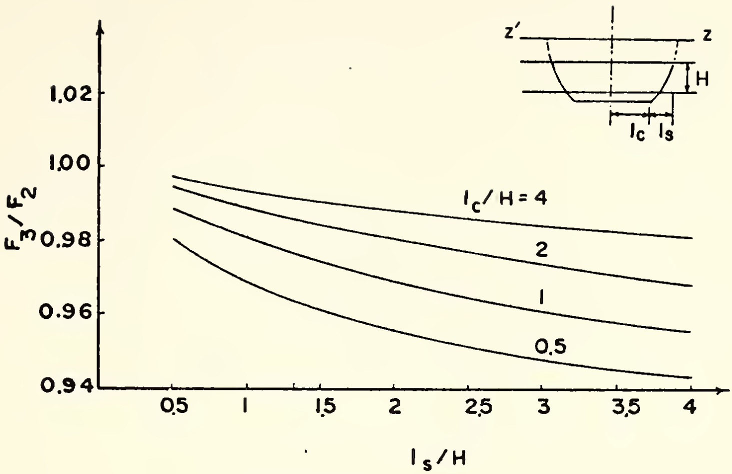

(a) $c = 0$, $\phi = 40°$

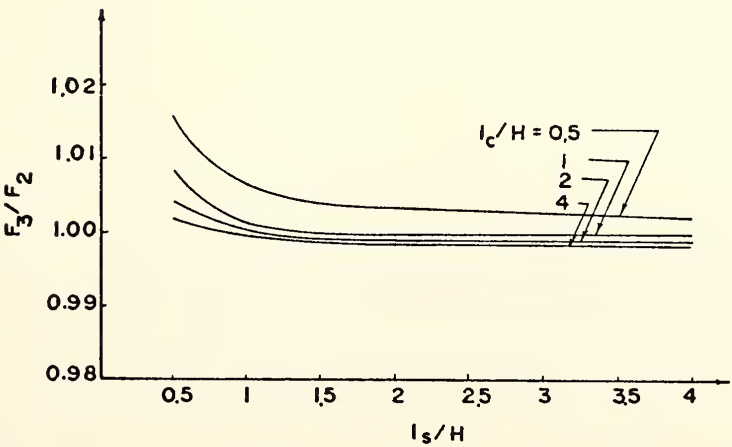

(b) $c = 7.2$ kPa, $\phi = 30°$

Fig. 5.8 Ratio of F_3/F_2 (Slope 1.5/1, $r_u = 0$)

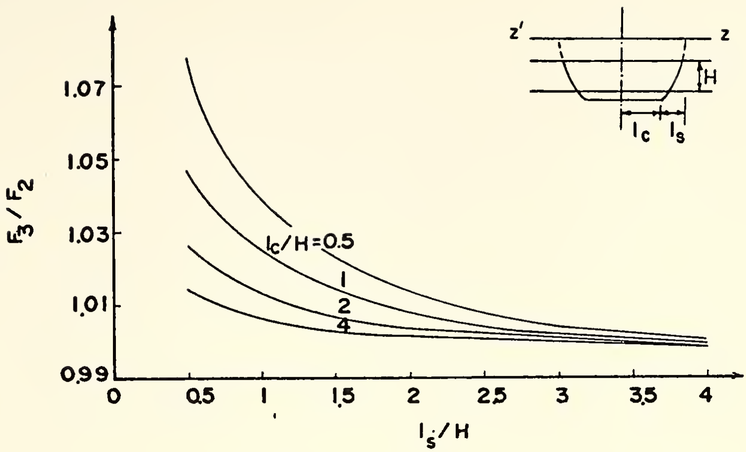

(c) c = 14.4 kPa, $\phi = 25°$

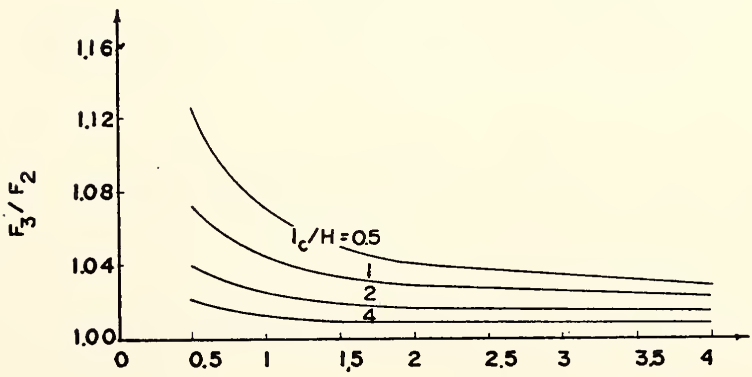

(d) c = 21.6 kPa, $\phi = 20°$

Fig. 5.8 (Cont'd)

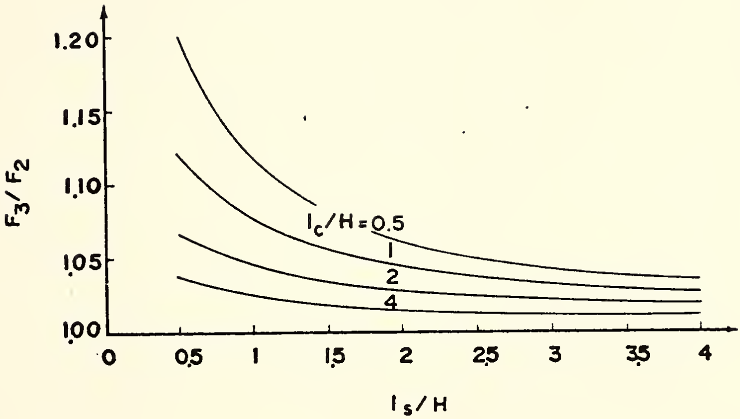

(e) $c = 28.7$ kPa, $\phi = 15°$

Fig. 5.8 (Cont'd)

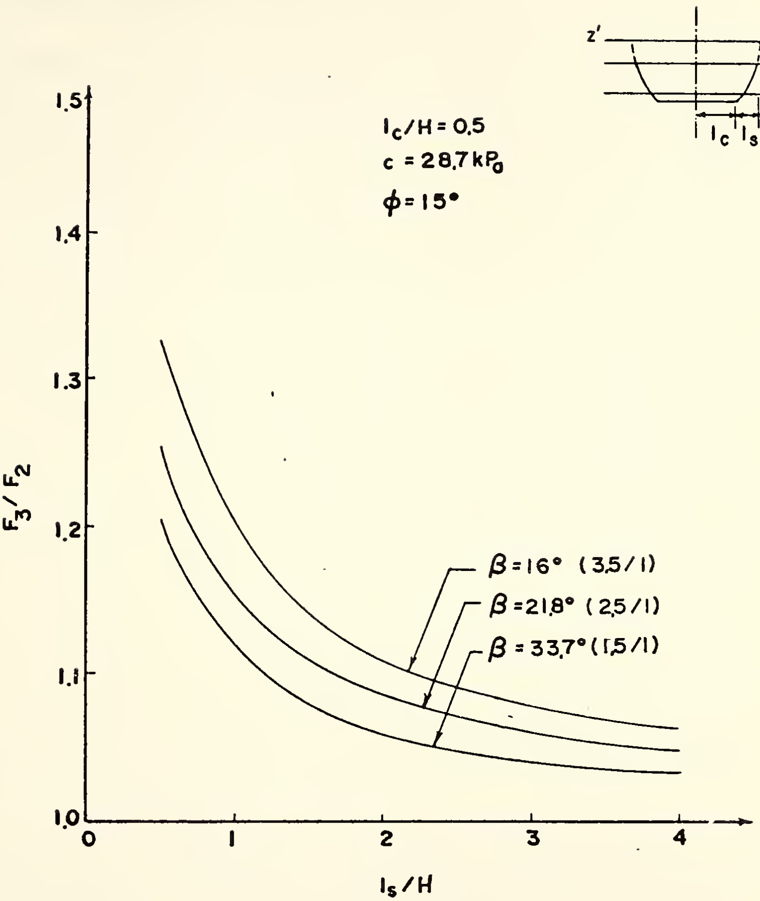

Fig. 5.9 F_3/F_2 vs. l_s/H for Various Slope Angles ($r_u = 0$)

mass is larger in a gentle slope, as shown in Fig. 5.7, and therefore more end effect is produced.

5.3.2 Pore Water Pressure Parameter r_u = 0.5

In order to assess the effect of the pore water condition, the analyses presented in the previous section are repeated with a pore pressure coefficient r_u of 0.5. The combinations of strength parameters and slope angles previously described also apply to the following results.

The coordinates of the centers and the radii of the most critical 2-D circles are listed in Table 5.4. The last two columns show the 2-D factors of safety from both STABL2 and Spencer's methods, respectively. Fig. 5.10 shows the most critical failure surfaces for different combinations of strength parameters and slope angles. As mentioned previously for the case with no pore water pressure, deep failure circles are obtained for cohesive soils. On the contrary, failure surfaces are shallow for cohesionless soils. Comparing Figs. 5.7 and 5.10 indicates that the failure circles go deeper into the foundation when pore water pressures are present.

The results of these studies are plotted in Figs. D3 to D5. The conclusions drawn are the same as those obtained with no pore water pressure. In addition, the comparison between Figs. 5.9 and 5.11 shows that pore water pressure can cause the 3-D effect to be even more significant.

TABLE 5.4 THE COORDINATES OF THE CENTERS AND RADII OF THE MOST CRITICAL 2-D FAILURE CIRCLES AND THE 2-D FACTORS OF SAFETY (r_u = 0.5)

Slope Angle	c' (kPa)	ϕ' (degrees)	X_o (m)	Y_o (m)	Radius (m)	F_2 (STABL2)	F_3 (SPENCER)
	0	40	11.9	15.2	21.6	0.679	1.044
	7.2	30	8.7	6.1	14.5	0.848	1.093
1.5/1	14.4	25	8.7	6.1	14.5	1.227	1.575
	21.6	20	8.7	6.1	14.5	1.657	1.998
	28.7	15	8.7	5.5	17.7	1.999	2.272
	0	40	9.1	18.9	25.0	0.771	1.206
	7.2	30	8.1	5.8	12.1	1.157	1.641
2.5/1	14.4	25	6.4	2.1	9.9	1.505	1.933
	21.6	20	5.3	4.0	13.0	1.877	2.251
	28.7	15	5.3	4.0	13.0	2.163	2.586
	0	40	19.2	28.3	34.5	0.988	1.440
	7.2	30	13.6	8.2	17.5	1.396	1.970
3.5/1	14.4	25	11.3	4.9	14.9	1.749	1.006
	21.6	20	13.3	6.7	18.7	2.053	2.253
	28.7	15	12.2	7.9	21.4	2.316	2.813

Note: X_o is the horizontal distance between the center and the crest; positive value means the center is on the left side of the crest.

Y_o is the vertical distance between the center and the crest; positive values mean the center is above the crest.

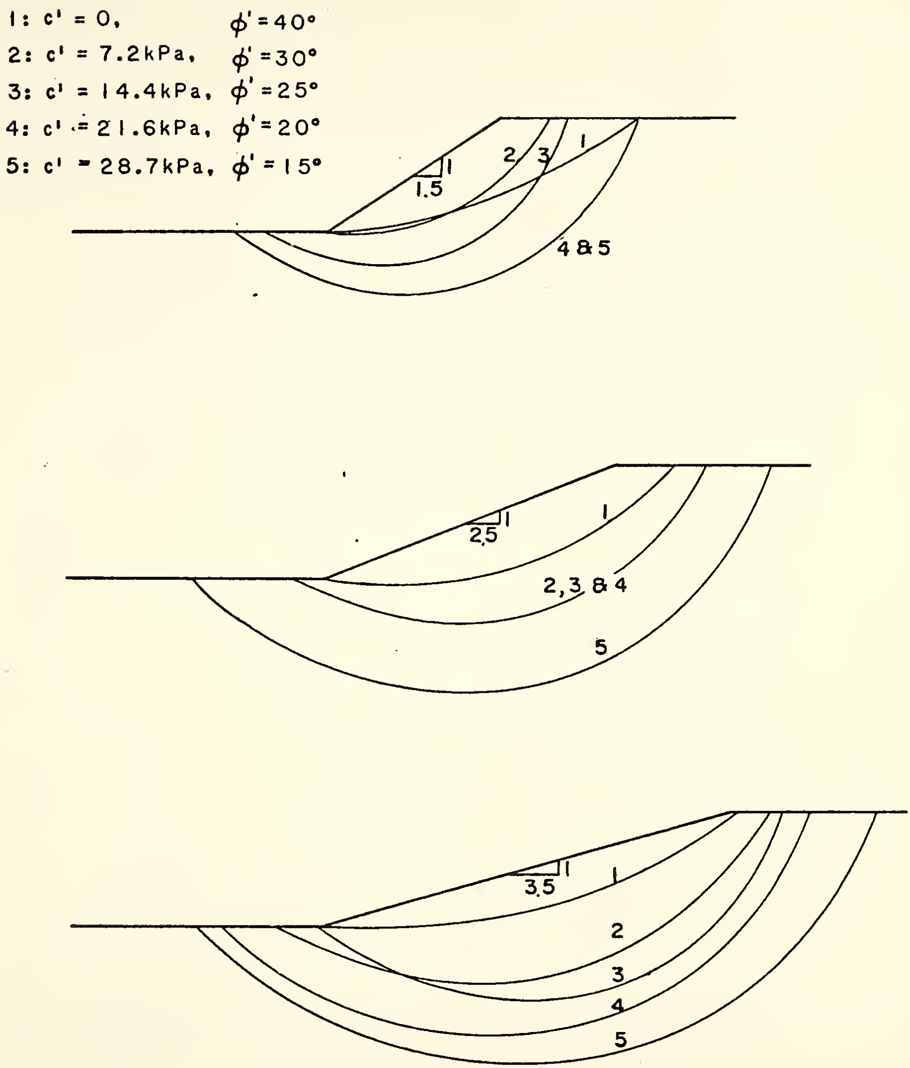

Fig. 5.10 The Most Critical Surfaces for Different Combinations of Strength Parameters in Different Slopes (r_u = 0.5)

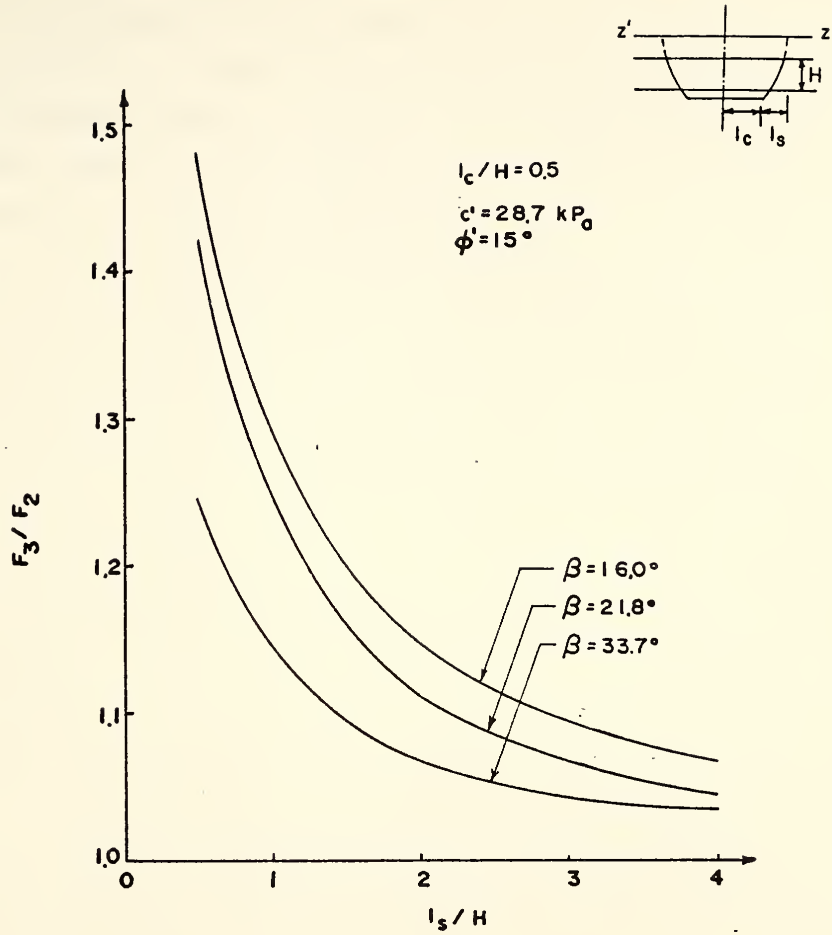

Fig. 5.11 F_3/F_2 vs. l_s/H for Various Slope Angles ($r_u = 0.5$)

5.3.3 Comparison of Interslice Angles between 2-D and 3-D Cases

This section compares the 2-D interslice angle θ_2 with the 3-D interslice angle θ_3. This study is of interest because the interslice angle represents the magnitude of the interslice shear forces which are related to the factor of safety.

The 2-D interslice inclinations corresponding to the critical shear surfaces analyzed by the Spencer's method are shown in Table 5.5 for values of r_u equal to 0 and 0.5, respectively. Although the interslice inclinations are slightly flatter for r_u equal to 0.5, the variations are similar, regardless of the value of r_u. For soils of low cohesion intercept, high frictional angle, and steep slope, the side forces are inclined more steeply.

The comparison between θ_2 and θ_3 is presented in Tables 5.6 and 5.7 and in Fig. 5.12. Several conclusions can be drawn from these results:

- For soil of high cohesion intercept and low frictional angle, θ_3 is less than θ_2. This phenomenon is more significant at smaller ℓ_s/H ratio (See Table 5.6 and the lower part of Fig. 5.12). Therefore, the F_3/F_2 ratio is higher than unity as stated in Sections 5.3.1 and 5.3.2.
- For soil of low cohesion intercept and high frictional angle, θ_3 is larger than θ_2, and consequently F_3 is less than F_2 (See Table 5.7 and the upper part of Fig. 5.12).
- For soils of high cohesion intercept and low friction angle, the interslice angles obtained with a pore pressure parameter of

TABLE 5.5 2-D INTERSLICE ANGLES FOR $r_u = 0$ AND $r_u = 0.5$

Slope Angle	c' (kPa)	φ' (degrees)	Inclination (degrees)	
			$r_u = 0$	$r_u = 0.5$
	0	40	24.4	19.7
	7.2	30	21.0	20.9
1.5/1	14.4	25	15.2	13.2
	21.6	20	13.3	8.7
	28.7	15	9.7	7.2
	0	40	19.3	17.6
	7.2	30	16.4	12.6
2.5/1	14.4	25	14.0	11.3
	21.6	20	12.7	10.1
	28.7	15	8.6	5.5
	0	40	15.5	15.4
	7.2	30	12.6	10.9
3.5/1	14.4	25	10.5	8.9
	21.6	20	9.7	8.9
	28.7	15	7.9	5.3

TABLE 5.6 THE RATIO OF $\tan\theta_3/\tan\theta_2$ FOR SOIL OF $c' = 28.7$ kPa AND $\phi' = 15°$ IN SLOPE OF 1.5/1 ($\theta_2 = 9.7°$ AND $\theta_2' = 7.2°$)

$\tan\theta_3/\tan\theta_2$			ℓ_c/H			
			0.5	1	2	4
ℓ_s/H	0.5	a*	0.811	0.874	0.927	0.958
		b*	0.916	0.956	0.980	0.986
	1	a	0.833	0.906	0.958	0.979
		b	0.888	0.972	1.000	1.014
	2	a	0.885	0.937	0.979	0.989
		b	0.916	0.972	1.014	1.028
	4	a	0.916	0.948	0.979	0.990
		b	0.944	0.972	1.014	1.028

TABLE 5.7 THE RATIO OF $\tan\theta_3/\tan\theta_2$ FOR SOIL OF $c' = 0$ AND $\phi' = 40°$ IN SLOPE OF 1.5/1 ($\theta_2 = 24.4°$ AND $\theta_2' = 19.7°$)

$\tan\theta_3/\tan\theta_2$			ℓ_c/H			
			0.5	1	2	4
ℓ_s/H	0.5	a	1.037	1.023	1.009	1.004
		b	1.033	1.017	1.011	1.006
	1	a	1.056	1.033	1.019	1.009
		b	1.039	1.028	1.017	1.011
	2	a	1.075	1.052	1.033	1.019
		b	1.050	1.033	1.022	1.016
	4	a	1.099	1.075	1.052	1.033
		b	1.055	1.044	1.033	1.022

*a: $r_u = 0$, b: $r_u = 0.5$

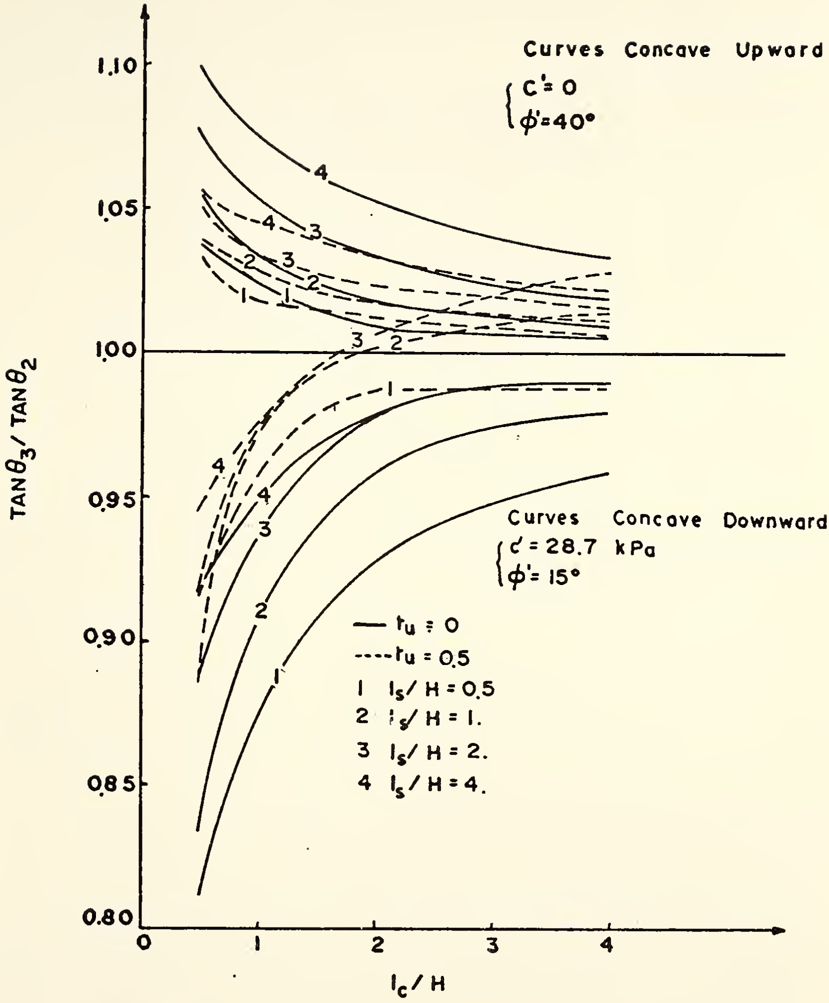

Fig. 5.12 TANθ_3/TANθ_2 vs. l_c/H for Various Soils at Various l_s/H (Slope 1.5/1)

0.5 are larger than those obtained with no pore pressure. The effect is opposite for soil of low cohesion intercept and high friction angle.

- As the ℓ_c/H ratio increases, the $\tan\theta_3/\tan\theta_2$ ratio gets closer to unity (Fig. 5.12). This corresponds to the plane strain condition.
- Steeper slopes show higher $\tan\theta_3/\tan\theta_2$ ratios. This can also be explained by the smaller values of F_3/F_2 for steep slopes (Sections 5.3.1 and 5.3.2).

5.3.4 Comparison of Results (LEMIX and Ordinary Method of Columns)

In the 2-D case, the ordinary method of slices (OMS) usually produces lower values of factor of safety than other more rigorous methods of slices. Therefore, the OMS is generally considered as a more conservative method. In the 3-D case, the results from both LEMIX and the Ordinary Method of Columns (OMC) for no water condition are presented in Tables D.1 to D.3. The results for r_u equal to 0.5 are in Tables D.4 to D.6. The conclusions are as follows:

- For no water condition, the OMC usually produces lower factors of safety. The differences are less than 10% in most cases.
- When pore water pressures exist, the OMC gives higher values of factor of safety for steep slope (Table D.4). For gentle slope, the OMC may produce both higher or lower values of factor of safety (Table D.5 and D.6). Similarly, the difference in results between the two methods is less than 10%.

It is therefore concluded that the OMC also produces satisfactory results for homogeneous soils.

5.4 Finite Element Analysis

In this section the finite element computer program FESPON is used to analyze spoon shape failure surfaces. The results are compared to those obtained with the limit equilibrium method. The hyperbolic parameters used in FESPON are generated from the results of conventional triaxial and consolidation tests on highly plastic Saint Croix clay.

5.4.1 Evaluation of the Values of Hyperbolic Parameters

The values of the hyperbolic parameters can be determined using data from conventional triaxial tests. Weitzel (1979) studied the 'short-term' or as-compacted laboratory strength of a highly plastic Saint Croix clay. The 'short term' refers to the fill material immediately after compaction and before environmental factors have an opportunity to alter the as-compacted condition of the soil. Weitzel measured the as-compacted strength in unconsolidated-undrained triaxial tests. The samples were prepared by kneading compaction to densities that fit on three impact energy curves: low energy, standard, and modified Proctor, with four water contents on each. The samples were then sheared at four levels of confining pressure to simulate a variety of embankment depths.

Johnson (1979) evaluated the effective stress strength parameters for analysis of long term stability. These parameters were evaluated for various compaction conditions through consolidated undrained triaxial tests with pore water pressure measurements. These were run at a constant rate of strain on kneading compacted samples of the same highly plastic clay used by Weitzel. The long term environmental effects were approximated by back pressure saturation and consolidation under states of stress representing the body forces at different positions in the embankment.

The results both from Weitzel's and Johnson's study are used to generate the values of hyperbolic parameters. These hyperbolic parameters then can be used in the computer program FESPON to examine the stability of an embankment of the highly plastic St. Croix clay, both for short-term and long-term conditions.

5.4.1.1 Parameters for Short-Term Condition

The procedure to determine the hyperbolic parameters has been presented in Section 4.3. Wong (1974) developed a computer program SP-1 to evaluate the hyperbolic parameters c, φ, K, n, and R_f using stress-strain data. Value of G, F, and d were obtained using volumetric strain data from conventional triaxial compression tests. Least-square curve-fitting procedures are used in determining the parameters. The data required for the program are confining pressure σ_3, stress difference at failure $(\sigma_1-\sigma_3)_f$, axial strains at 70% and 95% stress levels, and volumetric strains at 70% and 95% stress levels.

These data can be obtained from Appendix C of Weitzel (1979). The hyperbolic parameters are computed for each energy level (or dry density ρ_d) and water content w. Equations of these parameters as functions of energy level and water content can then be generated using regression techniques. The resulting equations are listed below:

$$c = -740 + 0.755\,\rho_d - 14.5\,w \qquad (5.2)$$

$$\phi = 63.4 - 0.00180\,w\,\rho_d + 0.0234\,w^2 \qquad (5.3)$$

$$K = 870 - 0.157\,w\,\rho_d + 4.300\,w^2 + 0.00108\,\rho_d^{\,2} \qquad (5.4)$$

$$n = -4.37 + 0.00226\ \rho_d + 0.0348\ w \tag{5.5}$$

$$G = -1.63 + 0.000798\ \rho_d + 0.0305\ w \tag{5.6}$$

$$d = 14.8 - 0.000384\ w\ \rho_d + 0.00214\ w^2 \tag{5.7}$$

$$F = 0.916 - 0.0000363\ w\ \rho_d + 0.00085\ w^2 \tag{5.8}$$

where c is in kPa, ρ_d in kg/m^3, and w in per cent. The contours of each parameter are plotted in Fig. 5.13. It is necessary to note that these contours may be inappropriate for Modified Proctor energy level because the stress-strain curve of this energy level behaves differently from a hyperbola.

5.4.1.2 Parameters for Long-Term Condition

As we mentioned in Section 4,3, if the long-term stability needs to be examined, the hyperbolic parameters may be obtained from drained triaxial test data. However, it is very often too time consuming to run the drained triaxial tests. Clough and Duncan (1969) developed an approach which used data from ordinary 1-D consolidation tests. The details of this approach was presented in Section 4.3. In the following, the generation of the effective hyperbolic parameters from both Johnson's (1979) $\overline{\mathrm{CU}}$ and DiBernardo's (1979) consolidation data for St. Croix clay is explained.

Johnson (1979) found that the effective stress friction angles ranged only from 18.9 to 21.4 degrees. This measured variation of 2.5 degrees (21.4 - 18.9 = 2.5) was not statistically significant. Therefore, for the range of compaction and consolidation conditions investigated, the effective stress friction angle could be taken as a constant value of 20 degrees. Johnson also generated an equation for the effective stress cohesion intercept c' as follows:

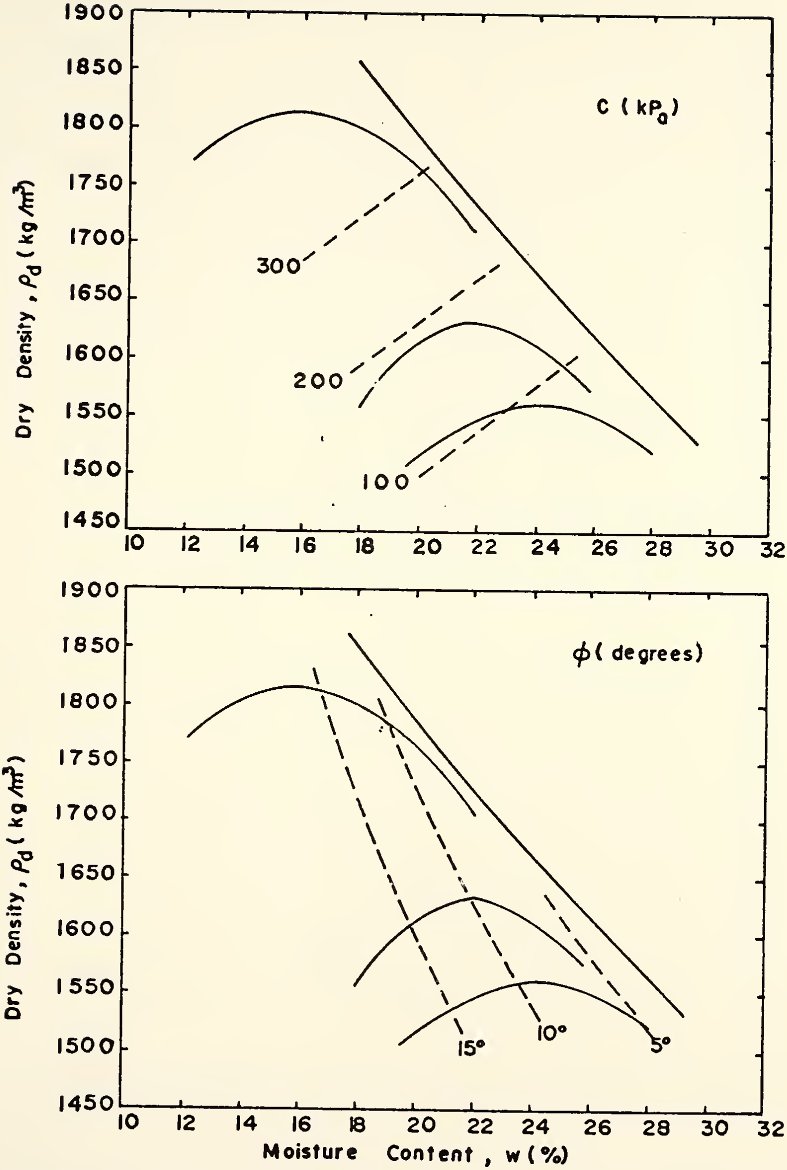

Fig. 5.13 Contours of Hyperbolic Parameters In As-Compacted Condition

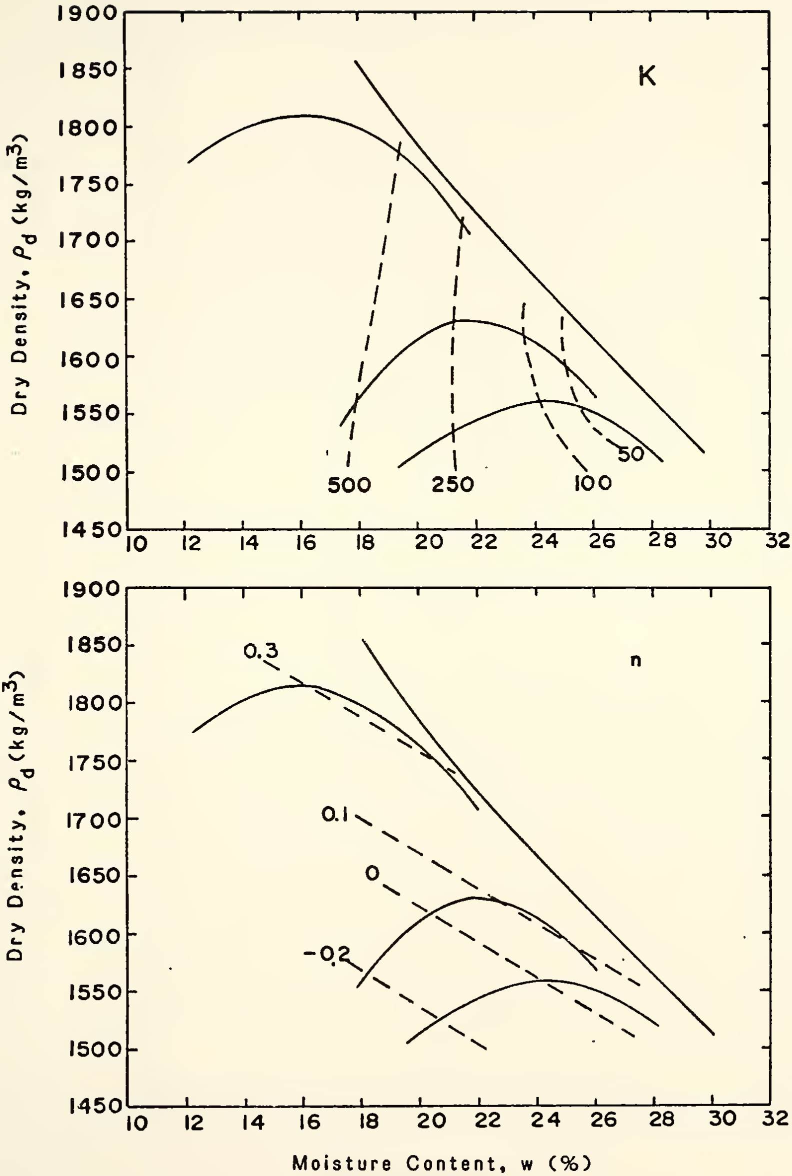

Fig. 5.13 (Cont'd)

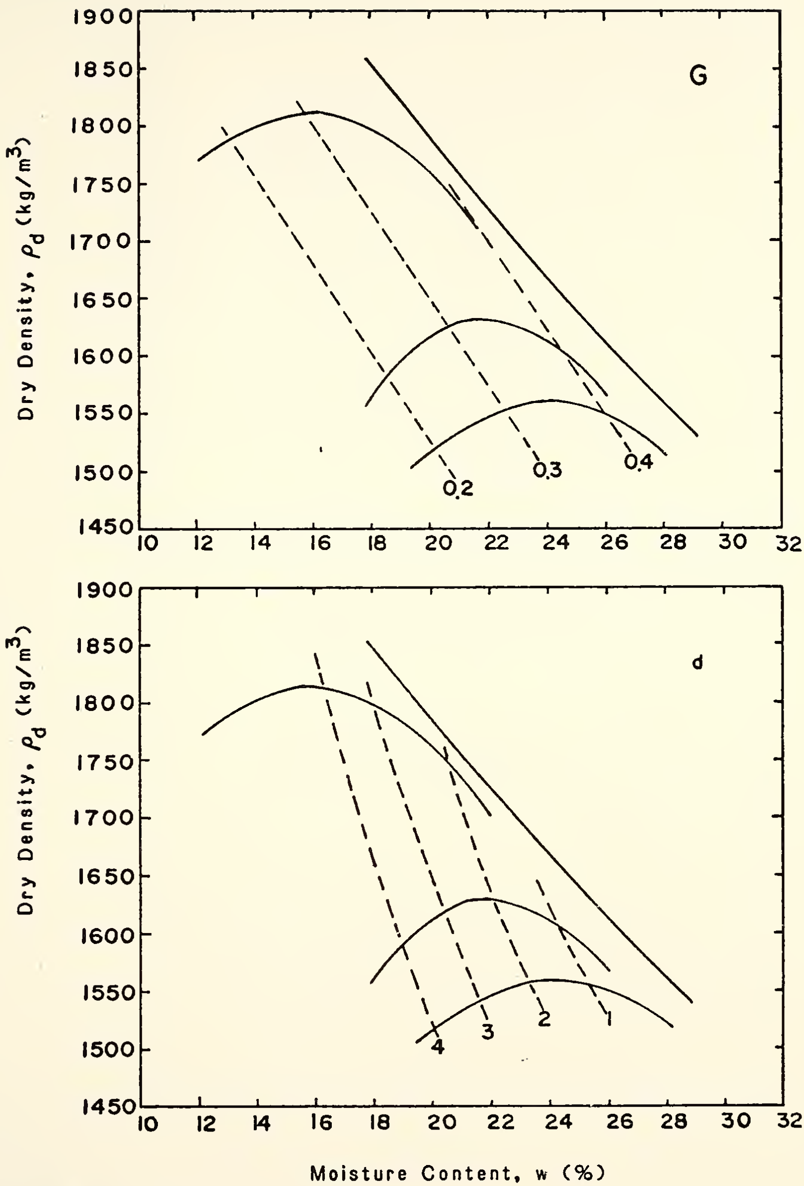

Fig. 5.13 (Cont'd)

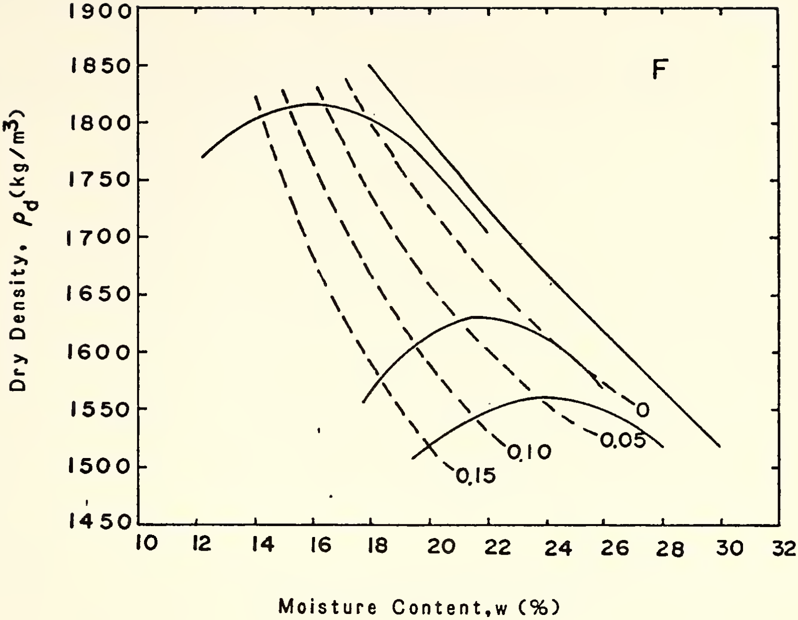

Fig. 5.13 (Cont'd)

$$c' = 1.71 - 3.83\, w \log e_o \qquad (5.9)$$

in which c' = the estimated value of the effective stress intercept (kPa)

w = compaction moisture content (%)

e_o = initial void ratio

With the effective strength parameters c' and ϕ' available, and assuming the failure ratio equal to 0.8 (as obtained from the similar soils), the initial elastic modulus constants, K and n, can be estimated from the consolidation test data. The following example will present the procedure to obtain K and n from the data of DiBernardo's (1979):

<u>Example</u>

For sample number LOA, w = 25.68% and e_o = 0.8206, c' is obtained from equation (5.8) as follows:

$$c' = 1.71 - 3.83\,(0.2568)\log(0.8206) = 10.2 \text{ (kPa)}$$

From Table B2 (DiBernardo, 1979), and considering the normal consolidation range, Table 5.8 is developed.

Let R_f be equal to 0.8, ϕ' equal to 20 degrees, and K_o to 0.6 (as obtained from Fig. 4.8 for OCR equal to one). Take the atmospheric pressure P_a equal to 101.4 kPa, the values in columns 12 and 14 are drawn in the log-log plot of Fig. 5.14. The slope of the curve is n and the intercept at σ_3/P_a equals to one is K. From the figure the values of n = 0.53 and K = 95 are obtained.

If all samples are used to get the mean values of K and n of these samples, the results are as presented in Table 5.9. These data are from

TABLE 5.8 PROCEDURE TO OBTAIN K AND n FOR SAMPLE LOA

1 Applied Load p_i (kPa)	2 e_o	3 Mean Load p (kPa)	4 Increment Δp (kPa)	5 σ_3	6 $\Delta p\,(1 + e_o)\Delta e$
171.52	0.7761	214.41	85.78	0.0228	6682
257.30	0.7533	321.70	128.80	0.0305	7404
386.10	0.7228	482.60	193.0	0.0381	8727
579.10	0.6847				

7 $p(1-K_o)R_f$	8 $K_o p(\tan^2(45 + \phi'/2)-1)$	9 $2c' \tan(45 + \phi'/2)$	10 $1 - \frac{2K_o^2}{(1+K_o)}$
68.6	133.7	29.1	0.55
102.9	200.7	29.1	0.55
154.4	301.0	29.1	0.55

11 E_i (kPa)	12 E_i/P_a	13 σ_3 (kPa)	14 σ_3/P_a
10970	108.2	128.7	1.269
13351	131.7	193.0	1.904
16961	167.3	289.6	2.856

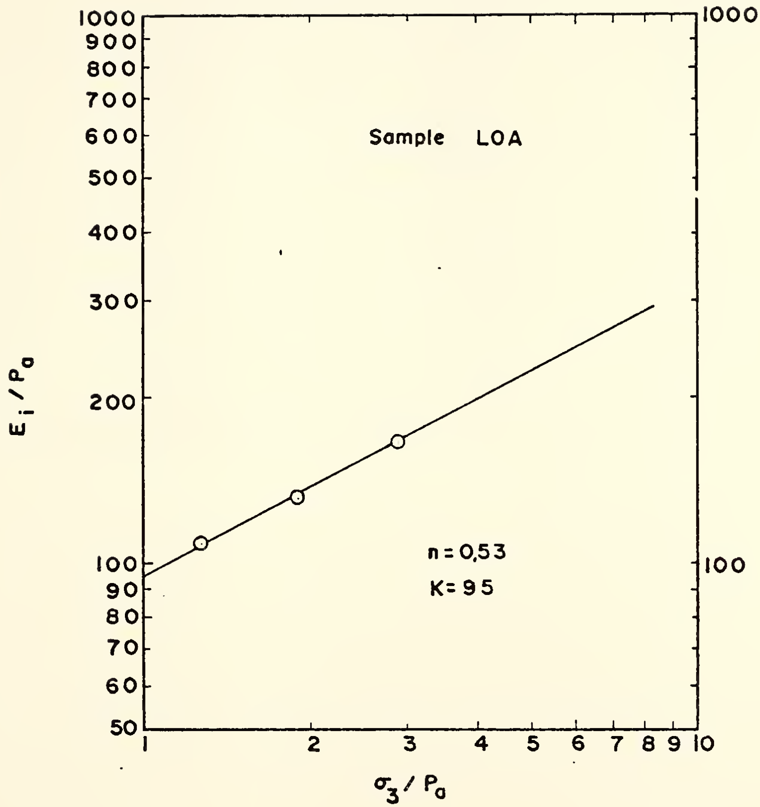

Fig. 5.14 E_i/P_a vs. σ_3/P_a.

TABLE 5.9 VALUES OF κ AND n

Sample Group	Average Water Content w (%)	Average Dry Density ρ_d (kg/m^3)	κ	n
LD	20.51	1456.8	118	0.64
LO	24.24	1513.0	95	0.53
LW	25.68	1540.5	126	0.58
SD	18.74	1532.4	54	1.11
SO	22.45	1636.5	133	0.62
SW	24.54	1603.8	160	0.50
MD	13.96	1796.8	95	0.87
MO	15.66	1845.8	215	0.65
MW	18.86	1776.4	113	0.84

DiBernardo (1979). In this table water content w and dry density ρ_d are mean values; K and n are in terms of these mean values. The results are also plotted in Fig. 5.15, in which the first number in parenthesis is the value of K and the second number is the value of n.

5.4.2 Finite Element Method Results

In Section 5.4.1 the hyperbolic stress-strain parameters were evaluated. These parameters are plotted in Figs. 5.13 and 5.15. They are now introduced in the finite element computer program FESPON to analyze the stability of an embankment under as-compacted and long-term conditions.

5.4.2.1 As-Compacted Condition

The soil parameters for the as-compacted condition are shown in Table 5.10. These parameters are obtained from Fig. 5.13 for a water content w of 26.8% and a dry density ρ_d of 1540 kg/m^3(low energy level). The soil is assumed homogeneous in both embankment and foundation.

The contours of major and minor principal stresses (σ_1 and σ_3) generated by FESPON are presented in Figs. 5.16 and Fig. 5.17. The σ_1 values are related to the overburden pressure (ρh). These contours have similar shape and are parallel to each other. Figs. 5.18 and 5.19 gives the contours of maximum shear stress τ_{max} and stress levels $((\sigma_1 - \sigma_3)/(\sigma_1 - \sigma_3)_f)$. These contours have similar shape; high values of maximum shear stresses correspond to high values of stress levels. These figures can be compared to Fig. 5.20 which shows the critical failure circle as searched by the program STABL2. This critical circle has the

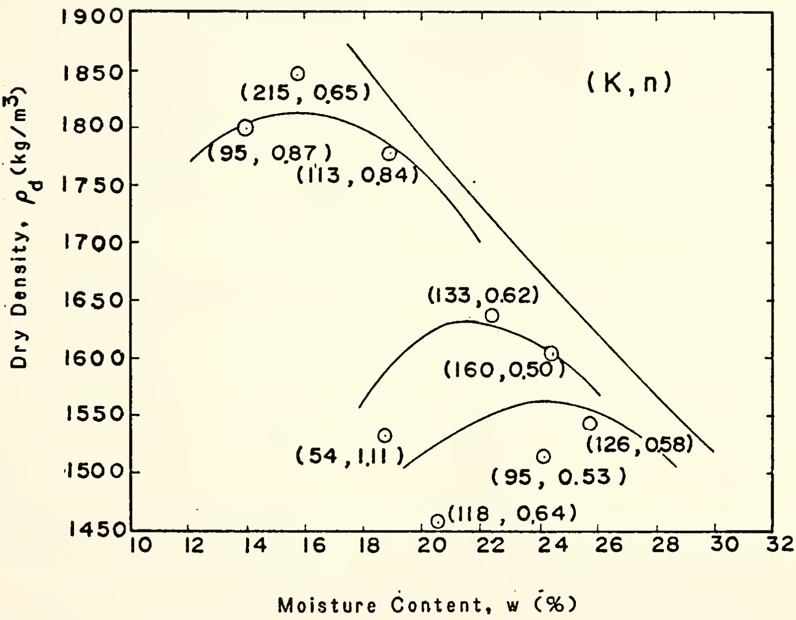

Fig. 5.15 Values of K and n at Various Dry Densities and Water Contents for Long-Term Condition

TABLE 5.10 HYPERBOLIC PARAMETERS FOR AS-COMPACTED CONDITION

c(kPa)	ϕ(degrees)	K	K_{ur}	n	G	d	F	R_f	K_o
34.5	6	36	110	0.048	0.42	0.52	0.028	0.8	0.8

Note: G_s = 2.79, w = 26.8%, ρ_d = 1540 kg/m^3

TABLE 5.11 HYPERBOLIC PARAMETERS FOR LONG-TERM CONDITION

c'(kPa)	ϕ'(degrees)	K	K_{ur}	n	G	d	F	R_f	K_o
10.5	20	125	375	0.55	0.42	0.0	0.0	0.8	0.6

Note: ρ = 1990 kg/m^3

TABLE 5.12 COMPARISON OF F_2 AND F_3 FOR AS-COMPACTED CONDITION (R_z = 12.2 m)

	F_2	F_3	F_3/F_2
LEM	1.59	1.90	1.20
FEM	1.62	2.01	1.24
$\frac{\text{FEM-LEM}}{\text{FEM}}$ x 100%	1.8%	5.5%	

TABLE 5.13 COMPARISON OF F_2 AND F_3 FOR LONG-TERM CONDITION (R_z = 12.2 m)

	F_2	F_3	F_3/F_2
LEM	0.778	0.893	1.15
FEM	0.877	0.981	1.12
$\frac{\text{FEM-LEM}}{\text{FEM}}$ x 100%	11.3%	9.0%	

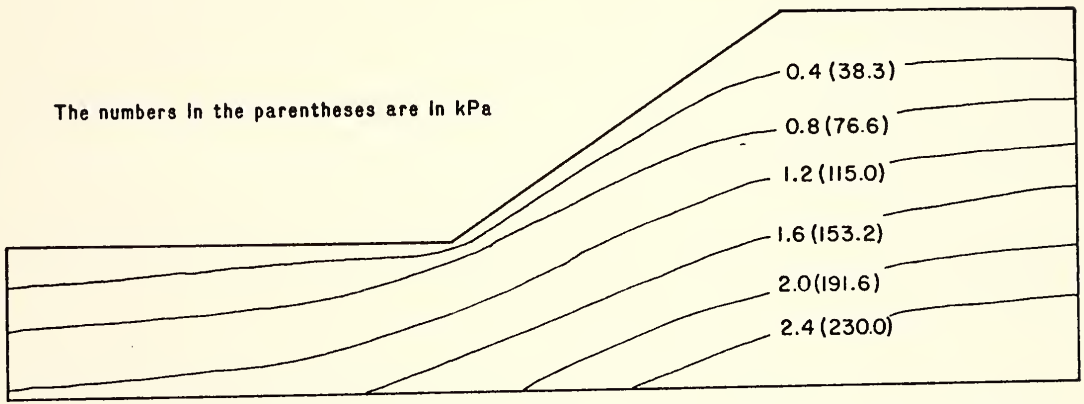

Fig. 5.16 Contours of σ_1 (tsf) (As-Compacted Condition)

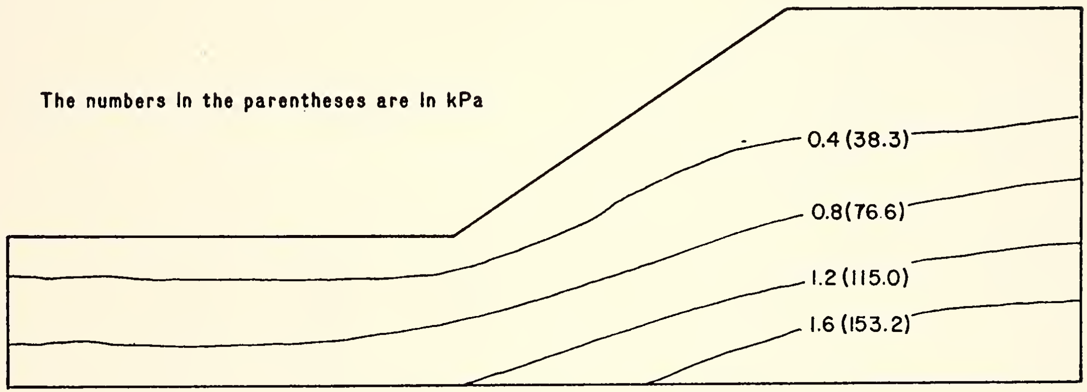

Fig. 5.17 Contours of σ_3 (tsf) (As-Compacted Condition)

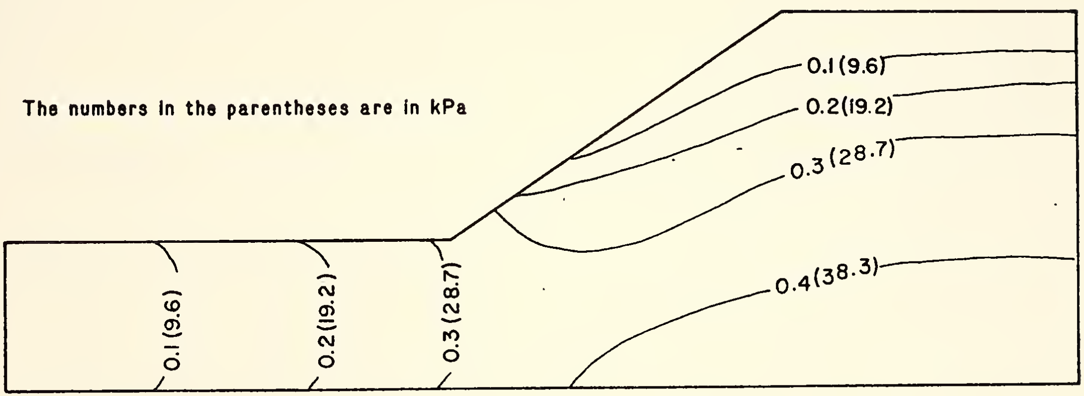

Fig. 5.18 Contours of τ_{max} (tsf) (As–Compacted Condition)

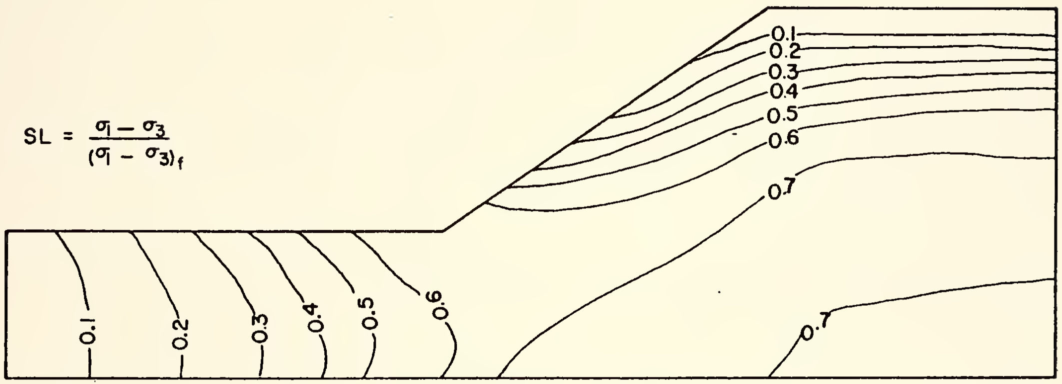

Fig. 5.19. Contours of Stress Level (As–Compacted Condition)

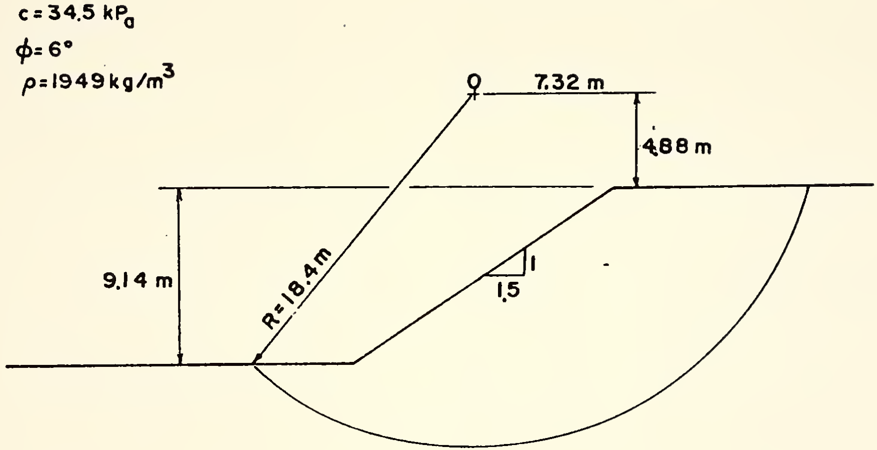

Fig. 5.20 The Critical Failure Surface for Embankment in As-Compacted Condition

maximum value of radius of the spoon shape failure mass (Fig. 3.12). It is obvious that the critical failure surface follows the zone of highest maximum shear stress.

The contours of horizontal (u_x) and vertical (u_y) movements are shown in Figs. 5.21 and 5.22. The maximum horizontal displacements occur close to the toe. The maximum vertical displacements occur about one third of the height (H/3), from the top of the embankment and near the center line. These values of displacements are relative displacements to the top of the embankment. Near the toe, the soil may have positive (or upward) vertical movements.

Local factors of safety are computed along a spoon shape failure surface defined by the critical circle obtained by STABL2 and a minor axis of length 12.2 m (40 ft). The local factor of safety F_N is defined as:

$$F_N = \frac{c + \sigma_N \tan\phi}{\tau_N} = \frac{c}{\tau_N} + \frac{\sigma_N}{\tau_N} \tan \phi \qquad (5.10)$$

where σ_N is normal stress and τ_N the shear stress. The normal stress, shear stress, and local factor of safety are given in Fig. 5.23 for different sections of the failure surface (as a function of the Z-coordinate). The arrow in Fig. 5.23 shows the position of the toe. These figures show that the normal stress is higher in the central portion of the embankment and is very small at the two ends. The shear stress distribution is similar to the normal stress distribution. The maximum shear stresses are only about 20% of the maximum normal stresses. As the section is farther away from the center line, both the normal and shear stresses decrease at the same rate and the local factor of safety increases.

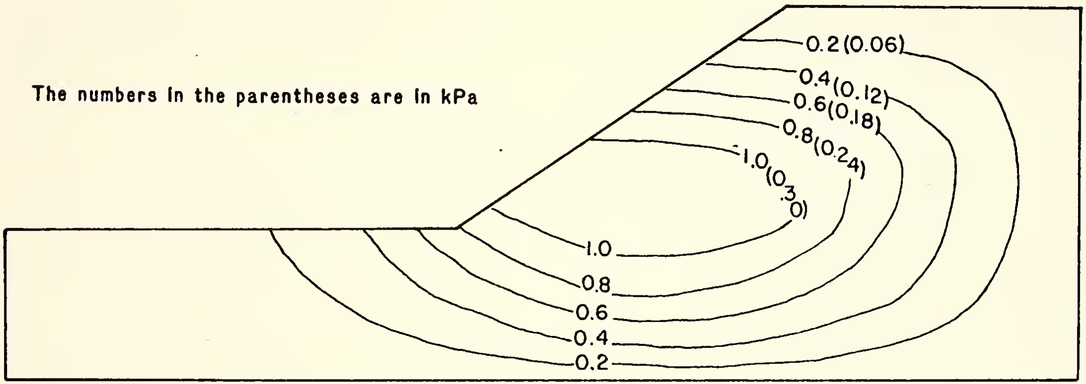

Fig. 5.21 Contours of u_x (ft) (As–Compacted Condition)

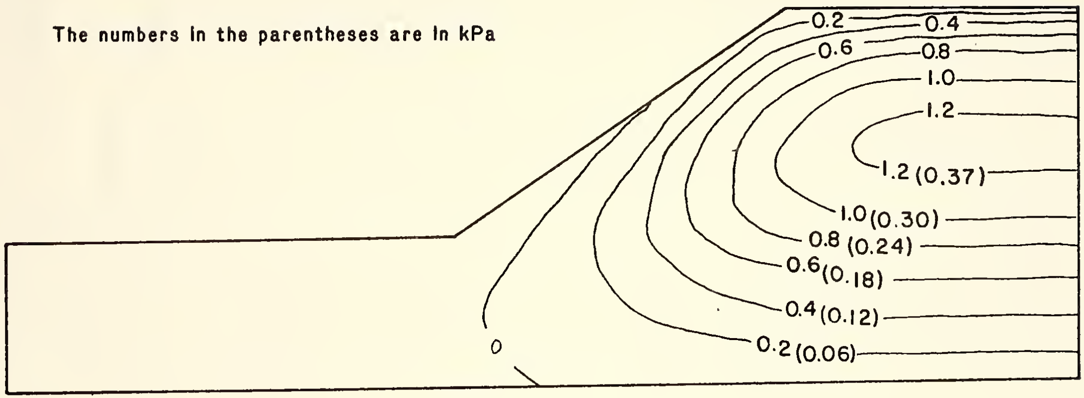

Fig. 5.22 Contours of u_y(ft) (As-Compacted Condition)

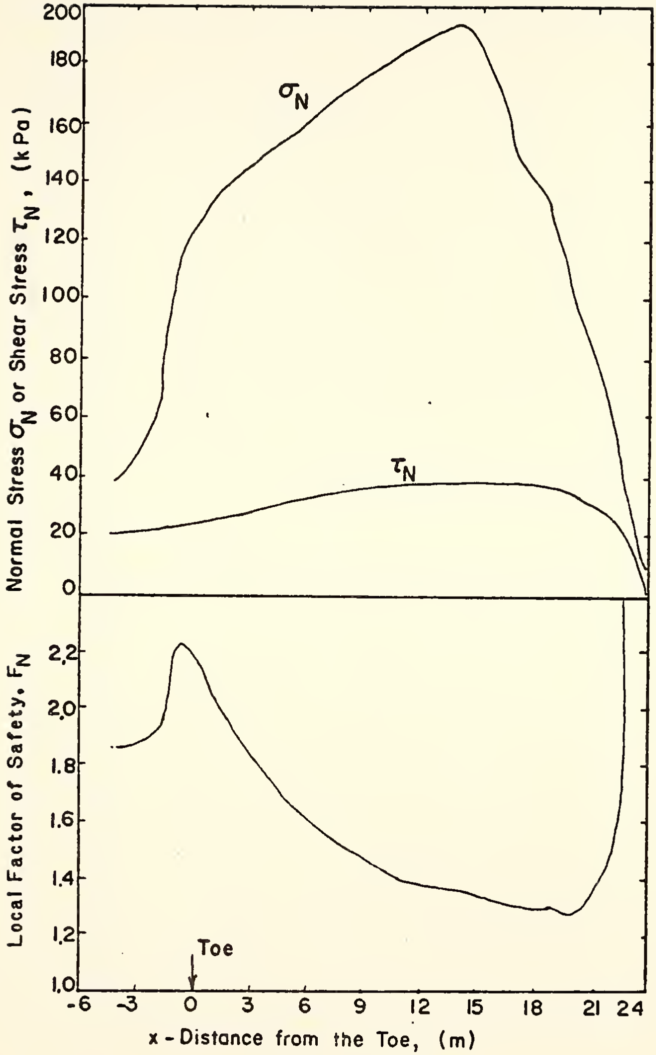

(a) z = 0.76 m

Fig. 5.23 Normal Stress, Shear Stress, and Local Factor of Safety vs. x (As—Compacted)

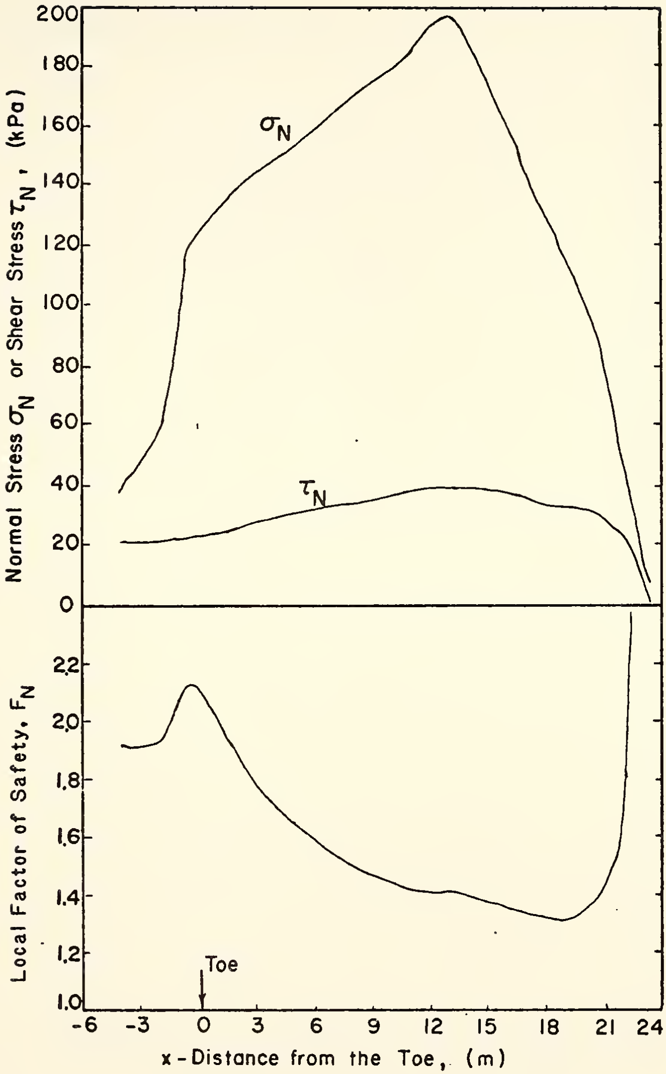

(b) z = 2.3 m

Fig. 5.23 (Cont'd)

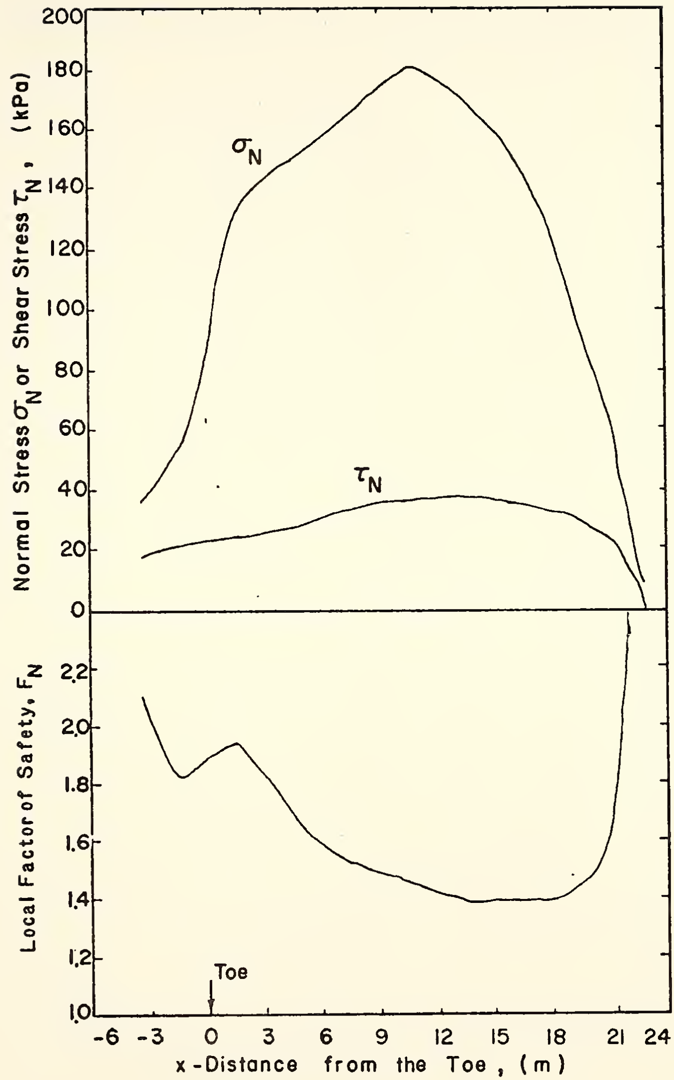

(c) z = 3.8 m

Fig. 5.23 (Cont'd)

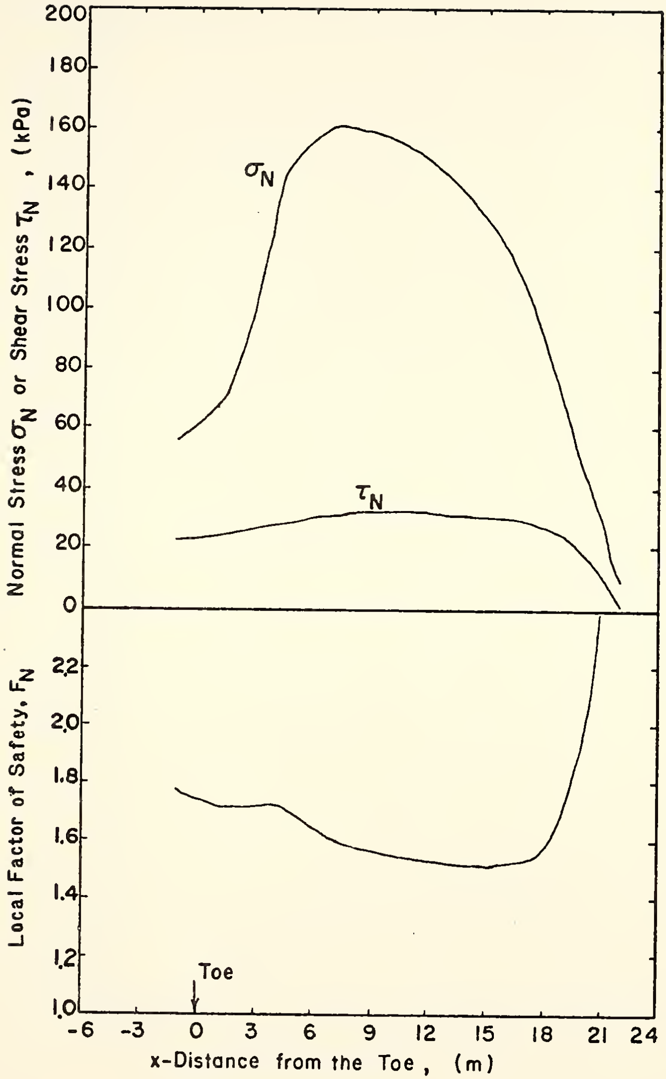

(d) z = 5.3 m

Fig. 5.23 (Cont'd)

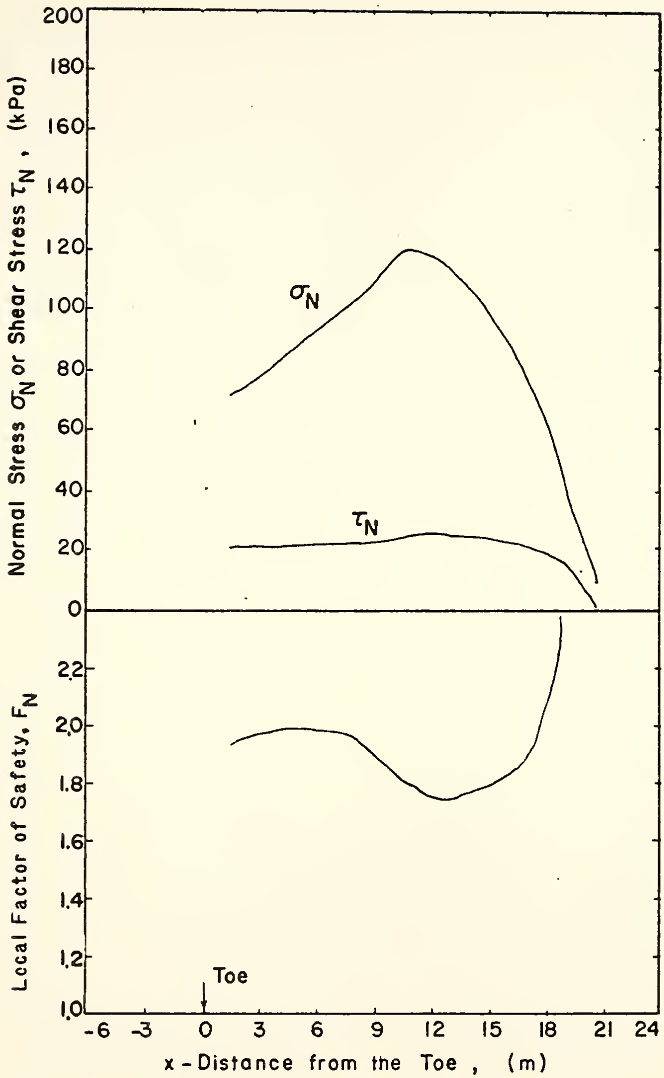

(e) z = 6.9 m

Fig. 5.23 (Cont'd)

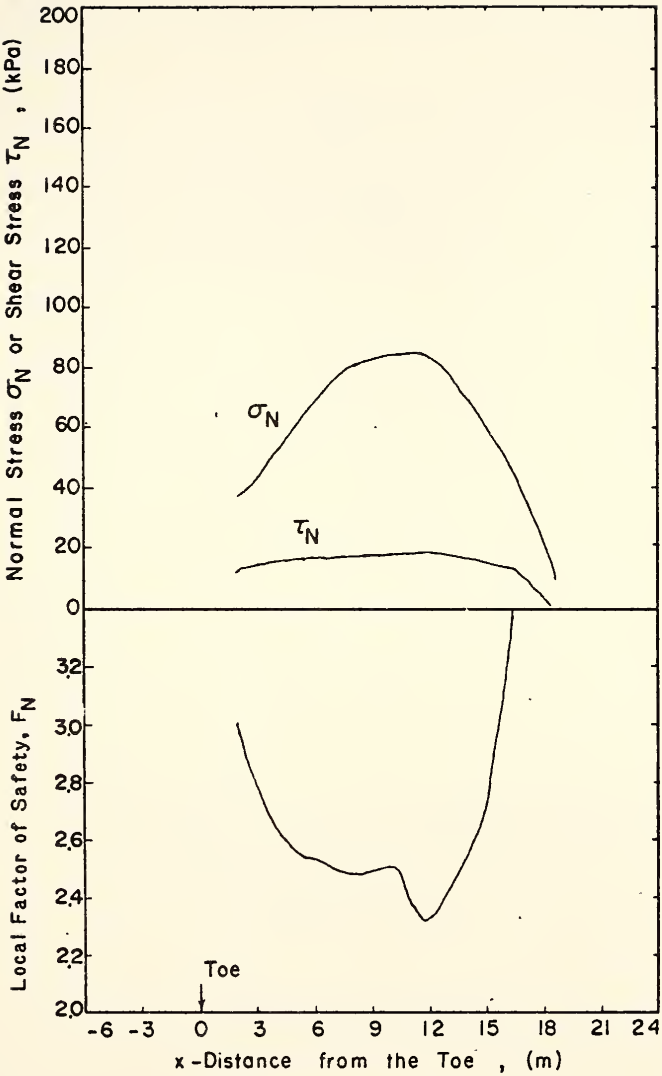

(f) z = 8.4 m

Fig. 5.23 (Cont'd)

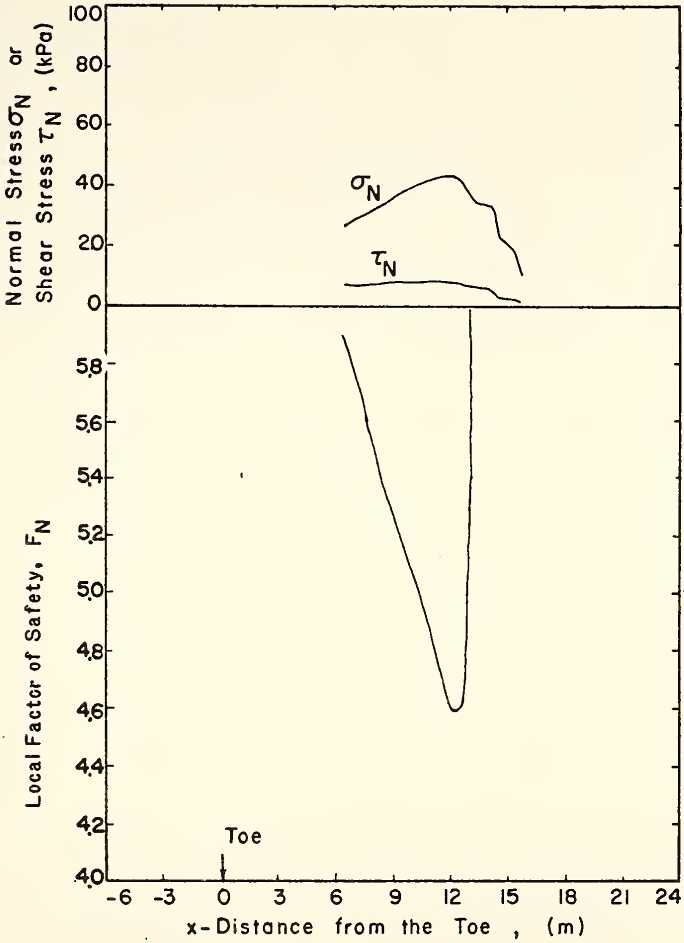

(g) z = 9.9 m

Fig. 5.23 (Cont'd)

5.4.2.2 Long-Term Condition

In this section an effective stress analysis of the embankment is performed for long-term condition. The time effects on the long-term behavior of an embankment are very complex. A more versatile soil model than the one used in the present work would be needed to take into account these effects. Such a model is not available and consequently effects such as change in pore pressure, creep, etc. are disregarded in this analysis.

The soil parameters are listed in Table 5.11. The cohesion intercept is obtained from equation (5.9) with the initial water content and initial void ratio known. The hyperbolic parameters K and n are obtained from consolidation tests on the same soil at the same initial water content (refer to Fig. 5.15). The unloading value of K (K_{ur}) is taken as three times K. The density of soil may change with time due to saturation, settlement, etc. In this example, the final density of soil is taken as 1990 kg/m^3. The pore pressure parameter r_u is equal to 0.5.

Fig. 5.24 shows the contours of stress level obtained with FESPON. The highest stress level is in a zone close to the toe. The critical 2-D circle given by STABL2 is shown in Fig. 5.25. The circle passes through the zone of the highest stress level and indicates that a toe failure may happen in the long-term condition. The curves of normal stress, shear stress, pore water pressure, and local factor of safety along the section of Z-coordinate equal to 2.5 m are shown in Fig. 5.26. The smaller local factors of safety occur in the zone of highest pore water pressure. Conversely, the higher local factors of safety occur near the toe and crest due to low pore water pressure.

$$SL = \frac{\sigma_1' - \sigma_3'}{(\sigma_1' - \sigma_3')_f}$$

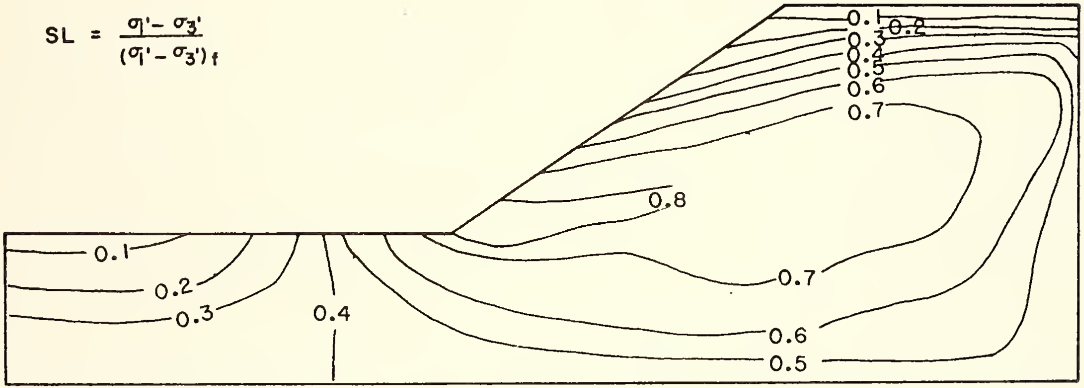

Fig. 5.24 Contours of Stress Level (Long-Term Condition)

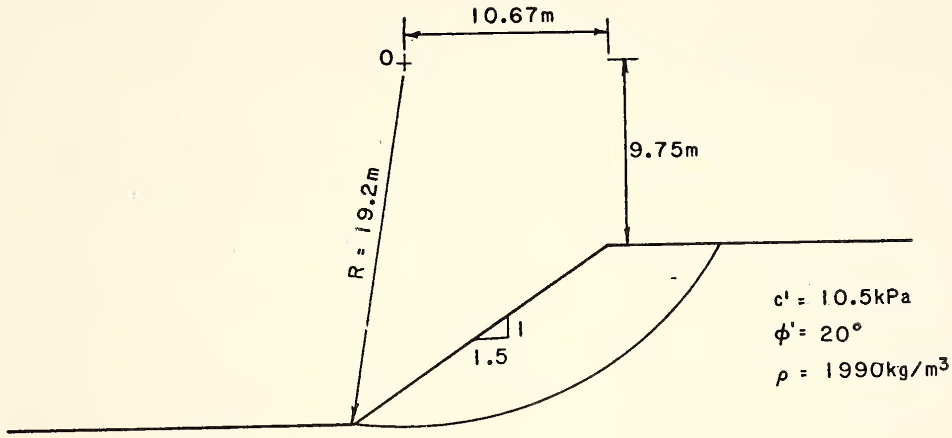

Fig. 5.25 The Critical Failure Surface for Embankment in Long-Term Condition

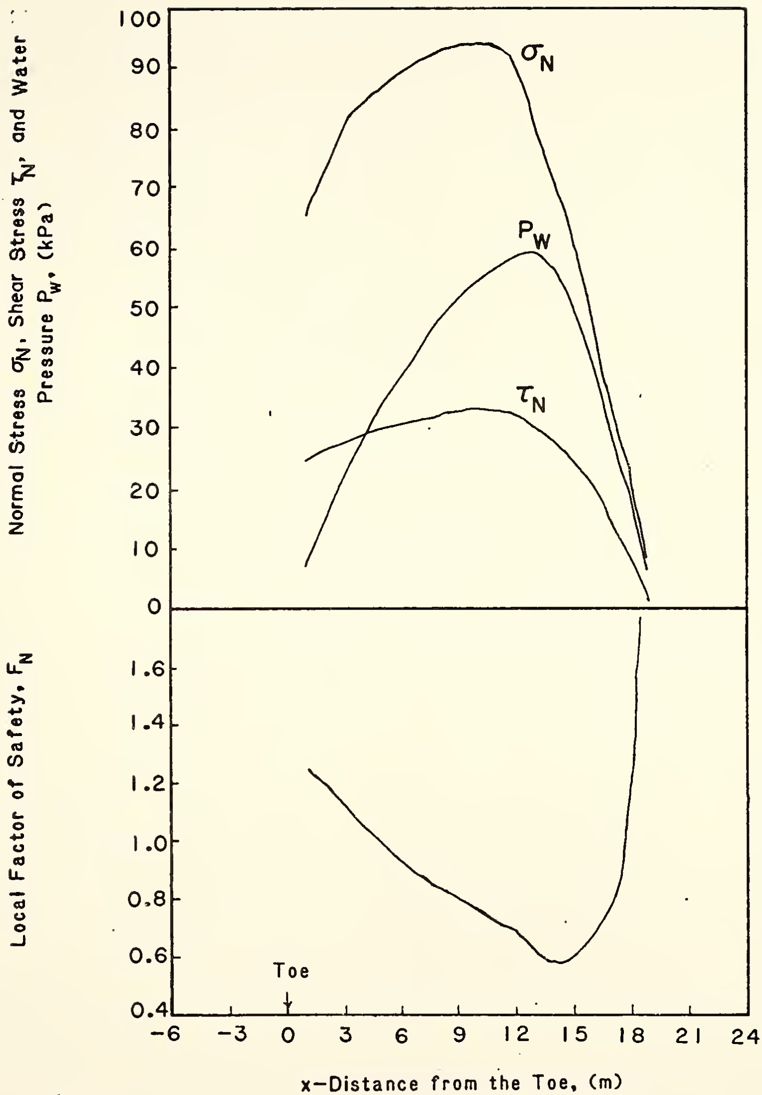

Fig. 5.26 Normal Stress, Shear Stress, Water Pressure, and Local Factor of Safety vs. x at z = 2.5m (Long−Term)

5.4.3 Comparison between Finite Element Method and Limit Equilibrium Method

Although comparisons of the results between finite element and limit equilibrium methods are given in a few papers (Wright, 1973, Résendiz, 1972) for 2-D cases, there is no comparison for 3-D cases. In this section, comparisons of the results for as-compacted and long-term conditions are presented.

The mean factor of safety used in the comparison is defined as

$$\text{Mean } F = \frac{\Sigma(c + \sigma_N \tan\phi)\ dA}{\Sigma\ \tau_N\ dA} \tag{5.11}$$

where the summation Σ is over the whole failure surface and dA is the bottom area of a vertical column.

The results for the as-compacted condition are presented in Table 5.12. The limit equilibrium methods, Spencer's method and LEMIX, yield factors of safety F_2 and F_3 of 1.59 and 1.90, respectively. The two-dimensional finite element computer program ISBILD (Ozawa, 1974) gives a mean factor of safety F_2 of 1.62, while FESPON leads to a mean factor of safety F_3 of 2.01. The ratio F_3/F_2 is 1.20 for the limit equilibrium methods. It is 1.24 for the finite element solutions. The factors of safety obtained from limit equilibrium analysis are smaller than those from finite element analysis. The agreement is quite good in this case with differences of 1.8% and 5.5% in 2-D and 3-D cases, respectively.

Table 5.13 shows the comparison of F_2 and F_3 for the long-term condition. The 3-D factor of safety obtained with the finite element method is 9.0% larger than the one given by the limit equilibrium method. The F_3/F_2 ratios are very close, 1.15 and 1.12 for the limit equilibrium and finite element methods, respectively. Comparing Tables 5.12 and 5.13 indicates that the long-term stability is more critical than the as-compacted stability.

Finally it should be recognized that the strength parameters selected in these examples are for low energy level (wet side). The strength parameters of actual embankments are higher than the ones selected. It is only for the purpose of illustrating that the factors of safety are of the order of 1.5 for the as-compacted condition. This results in low factor of safety for the long-term condition. Actual embankments will show much higher factors of safety than those computed for this example.

5.4.4 Other Applications

The discussion of the results obtained in the previous section was simplified by assuming the embankment and foundation soils to be the same. In fact the finite element computer program FESPON can handle problems with complex soil conditions and/or geometries. This will be illustrated by the following applications.

5.4.4.1 Stability of a Non-homogeneous Embankment

The construction of an embankment in rolled lifts frequently results in non-homogeneous soil properties. The strength characteristics may vary from layer to layer and be different from the foundation soil strength characteristics. Such an embankment is shown in Fig. 5.27. The foundation and compacted fill are composed of two and eight different layers, respectively. The hyperbolic strength parameters of each layer are listed in Table 5.14. Using these data the finite element

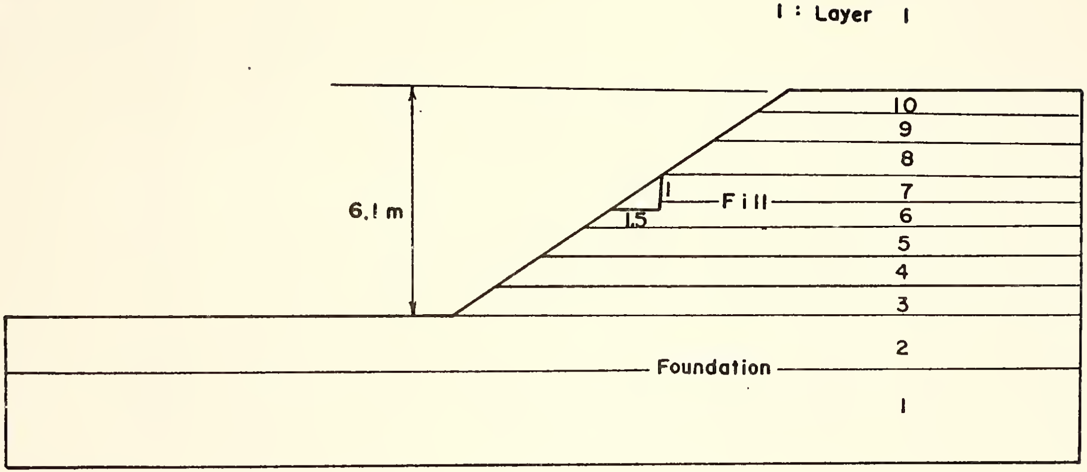

Fig. 5.27 Compacted Fill on a Foundation

TABLE 5.14 HYPERBOLIC PARAMETERS OF COMPACTED FILL ON A FOUNDATION

Layer No.	Density (kg/m^3)	c (kPa)	ϕ (degrees)	K	K_{ur}	n	d	G	F	R_f	k_o
1	1949	39.3	0	80	240	0.2	0.0	0.495	0.0	0.8	0.5
2	1949	39.3	0	80	240	0.2	0.0	0.495	0.0	0.8	0.5
3	1965	41.4	5	40	120	0.03	0.7	0.45	0.035	0.8	
4	1949	41.2	5	40	120	0.03	0.7	0.45	0.035	0.8	
5	1933	41.0	5	40	120	0.03	0.7	0.45	0.035	0.8	
6	1917	40.7	5	40	120	0.03	0.7	0.45	0.035	0.8	
7	1901	40.5	5	40	120	0.03	0.7	0.45	0.035	0.8	
8	1885	40.2	5	40	120	0.03	0.7	0.45	0.035	0.8	
9	1869	40.0	5	40	120	0.03	0.7	0.45	0.035	0.8	
10	1853	39.8	5	40	120	0.03	0.7	0.45	0.035	0.8	

analysis of the embankment is performed similarly to the analyses described in the previous section.

The 3-D limit equilibrium program LEMIX can also be used to analyze the stability of this problem. In this case, since the program LEMIX can only handle one material in the foundation and one in the embankment, it is necessary to use mean values of strength parameters for the foundation and embankment soils. These mean values are given in Fig. 5.28.

The contours of stress level generated by the finite element analysis are shown in Fig. 5.29. Table 5.15 gives the 2-D and 3-D factors of safety obtained with the limit equilibrium and finite element methods. The mean factors of safety obtained by the finite element method on 2-D and 3-D failure surfaces are almost identical to the factor of safety obtained by the limit equilibrium method on the same surfaces (difference of the order of 2%). The methods also result in very consistent F_3/F_2 ratios, 1.31 for the limit equilibrium method and 1.33 for the finite element method.

TABLE 5.15 COMPARISON OF F_2 AND F_3 FOR COMPACTED FILL ON A FOUNDATION IN TOTAL STRESS ANALYSIS (R_z = 12.2 m)

	Mean F_2	Mean F_3	F_3/F_2
LEM	1.527	2.00	1.31
FEM	1.532	2.04	1.33
$\frac{\text{FEM-LEM}}{\text{FEM}}$ x 100%	0.4%	2.0%	

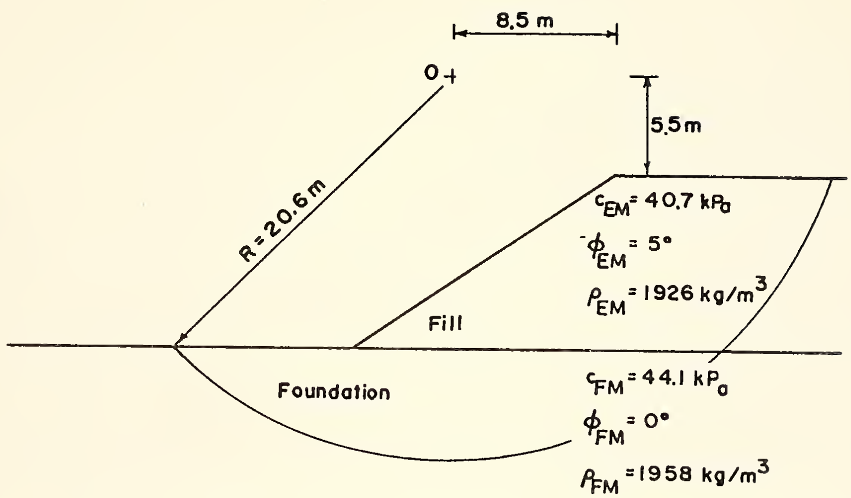

Fig. 5.28 The Critical Failure Surface for Compacted Fill on a Foundation

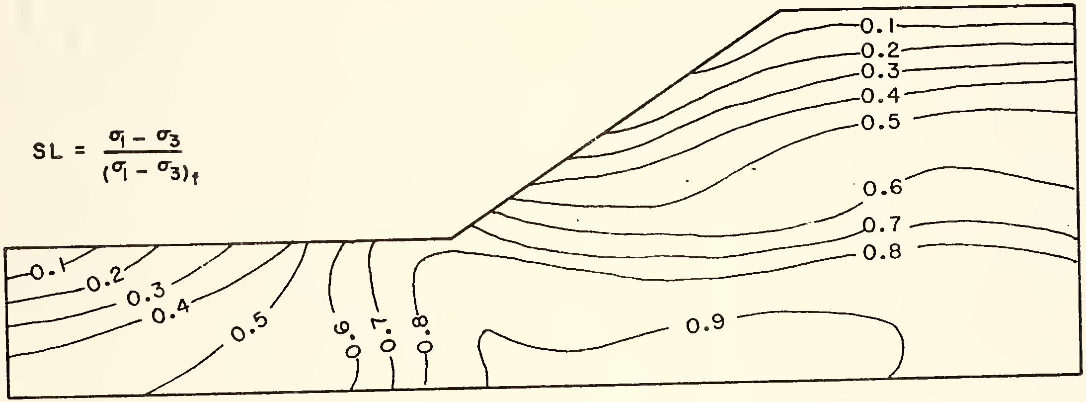

$$SL = \frac{\sigma_1 - \sigma_3}{(\sigma_1 - \sigma_3)_f}$$

Fig. 5.29 Contours of Stress Level (Layered)

5.4.4.2 A Pavement Analysis

Since the program FESPON can simulate the construction of an embankment, it is also capable of analyzing similar problems such as the construction of a pavement. The profile of a pavement section is shown in Fig. 5.30. This problem was studied by Palmerton (1972) who used the 3-D finite element computer program SOLSAP to study the deflection of the pavement. SOLSAP also uses hyperbolic stress-strain relationships, but employs compatible modes for element displacements. This pavement is analyzed using FESPON, and the results are compared to those obtained with the program SOLSAP.

The pavement section is composed of 0.076 m (3 in) of asphaltic pavement, 0.53 m (21 in) of crushed limestone base, and 2.74 m (9 ft) of selected clays. The values of hyperbolic parameters for each layer are given in Figure 5.31. A lateral earth pressure coefficient of 0.5 is assumed. It is also assumed that the stress-strain behavior of the asphaltic pavement is linear; thus the Young's modulus E and Poisson's ratio ν are constant values. This pavement is subjected to a 12-wheel load. Each wheel produces a 113 kN (30 k) vertical force.

The finite element mesh used for the analysis is shown in Fig. 5.32. It is only necessary to grid one-half of the problem since the problem is symmetrical with respect to the center line of the loading. The system is composed of four layers of elements. The wheel loads are applied as point loads, acting at the nodal points. The load is applied in one step for simplicity. Vertical deflections along the section A, B, and C are shown in Figs. 5.33 to 5.35.

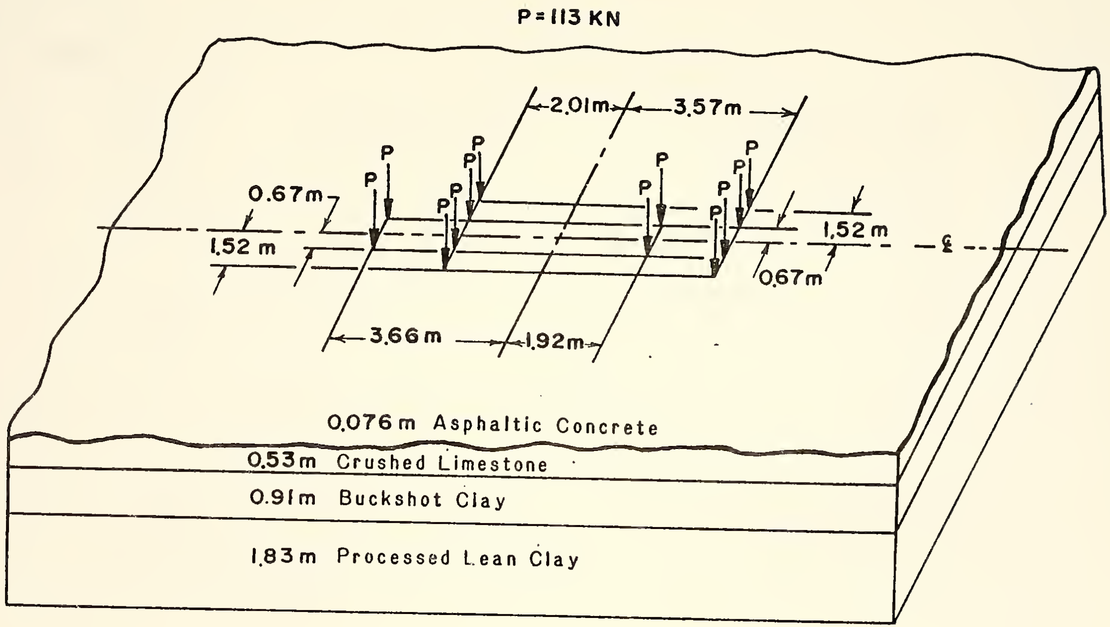

Fig. 5.30 Loading and Foundation Conditions

Depth, (m)	Section Profile	ρ,(kg/m^3)	c,(kN/m)	ϕ	R_f	K	n	d	G	F
0 – 0.076	Asphaltic Concrete	*								
0.076 – 0.61	Crushed Limestone	2077	0	47^o	0.70	2500	0.30	6.4	0.32	0.14
0.61 – 1.52	4 CBR Buckshot Clay	2077	3728	0^o	0.9	500	0.37	0.40	0.43	-0.10
1.52 – 3.35	4 CBR Processed Lean Clay	2077	3728	0^o	0.9	500	0.37	0.40	0.43	-0.10
below 3.35	Natural Loess									

*(Linear Behavior Assumed for Asphaltic Concrete $E = 2.04 \times 10^4 P_a$, $\nu = 0.45$)

Fig. 5.31 Section Profile and Material Properties

128 Elements   225 Nodal Points

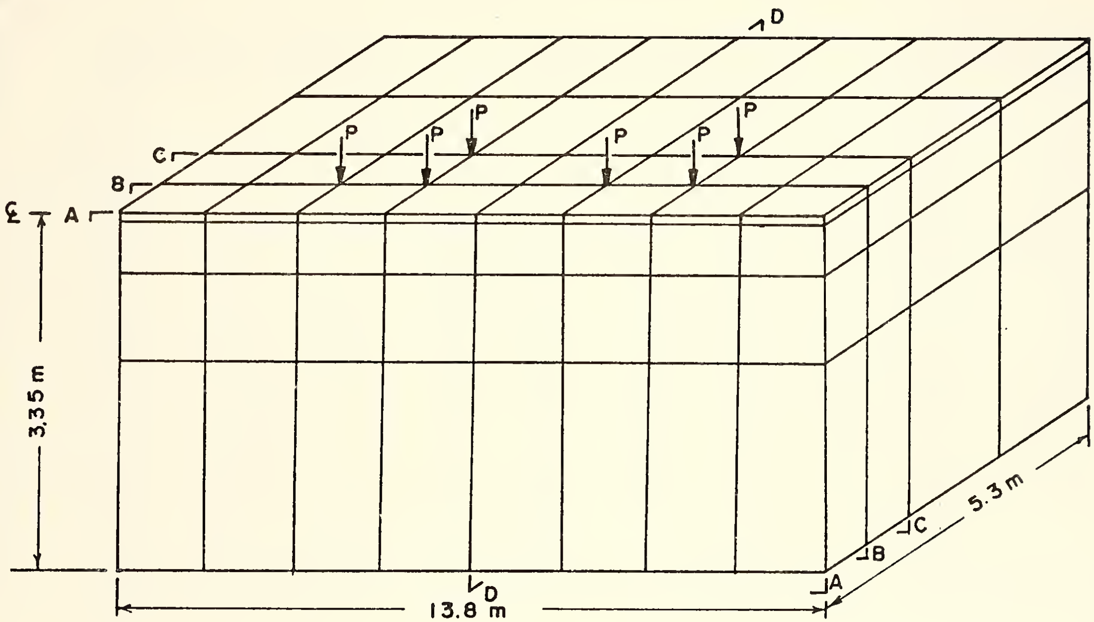

Fig.5.32 Finite Element Mesh

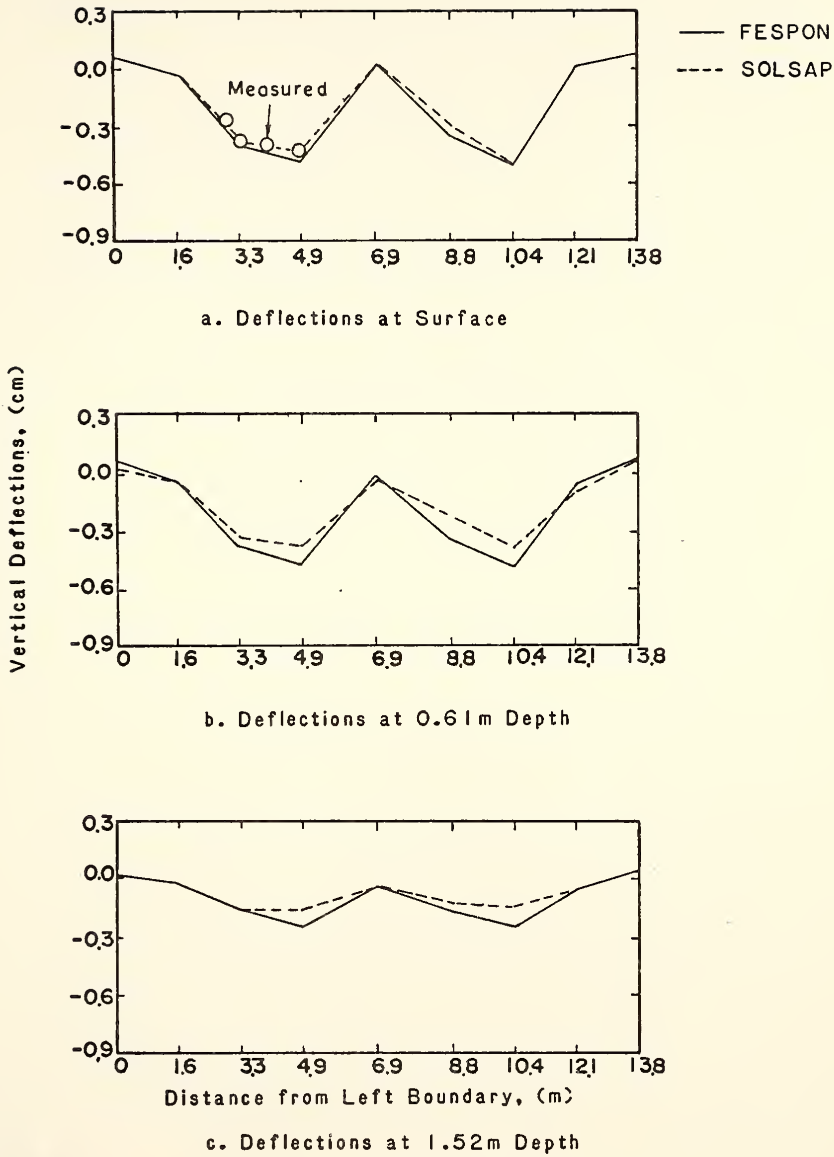

Fig. 5.33 Vertical Deflections—Section A

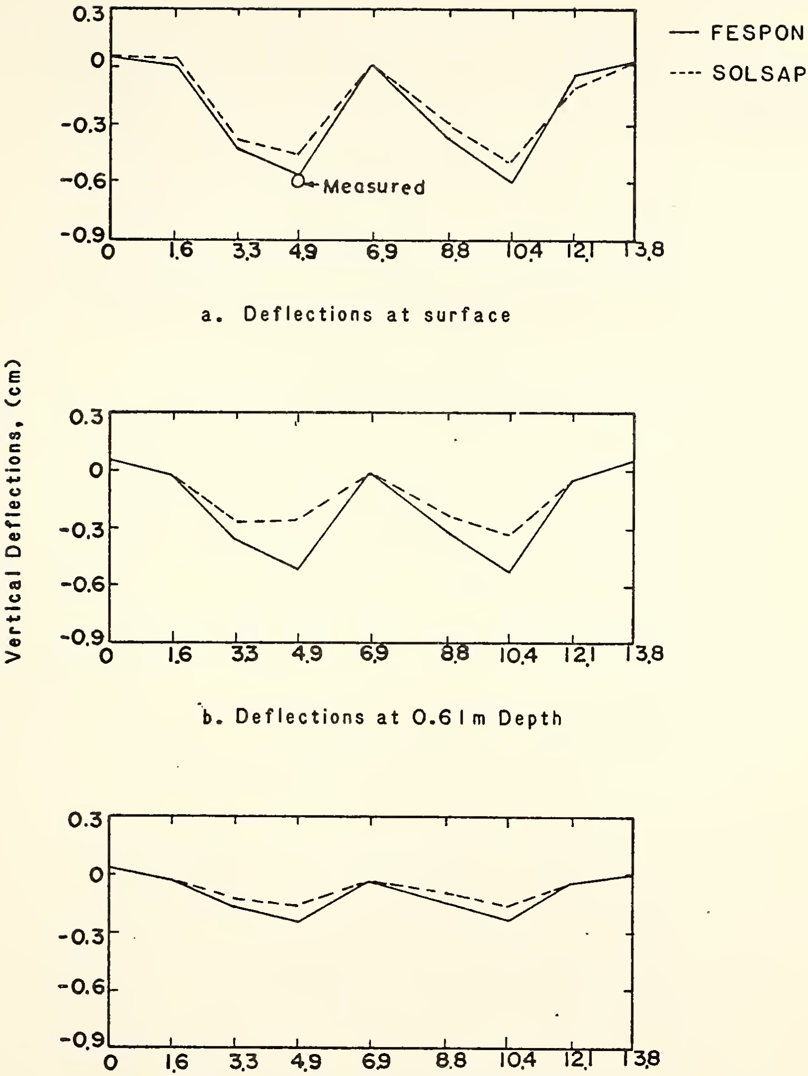

a. Deflections at surface

b. Deflections at 0.61m Depth

Distance from Left Boundary, (m)

c. Deflections at 1.52m Depth

Fig. 5.34 Vertical Deflections—Section B

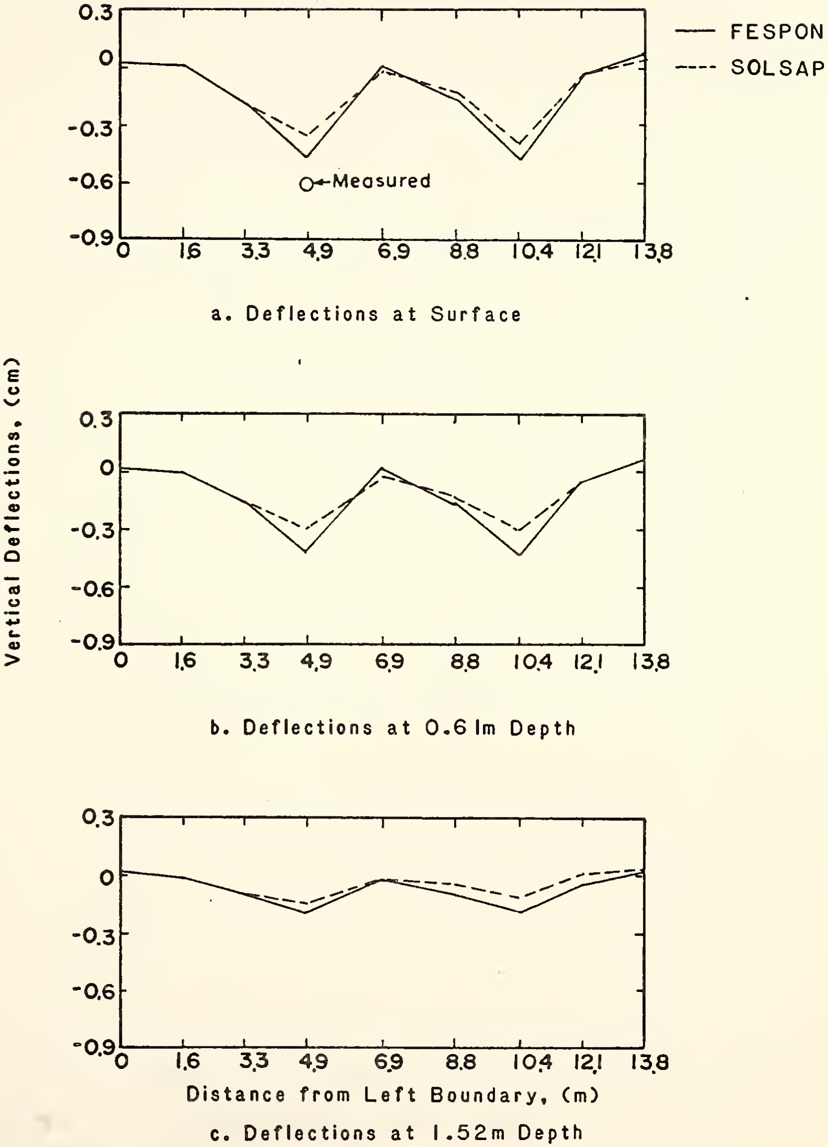

Fig. 5.35 Vertical Deflections—Section C

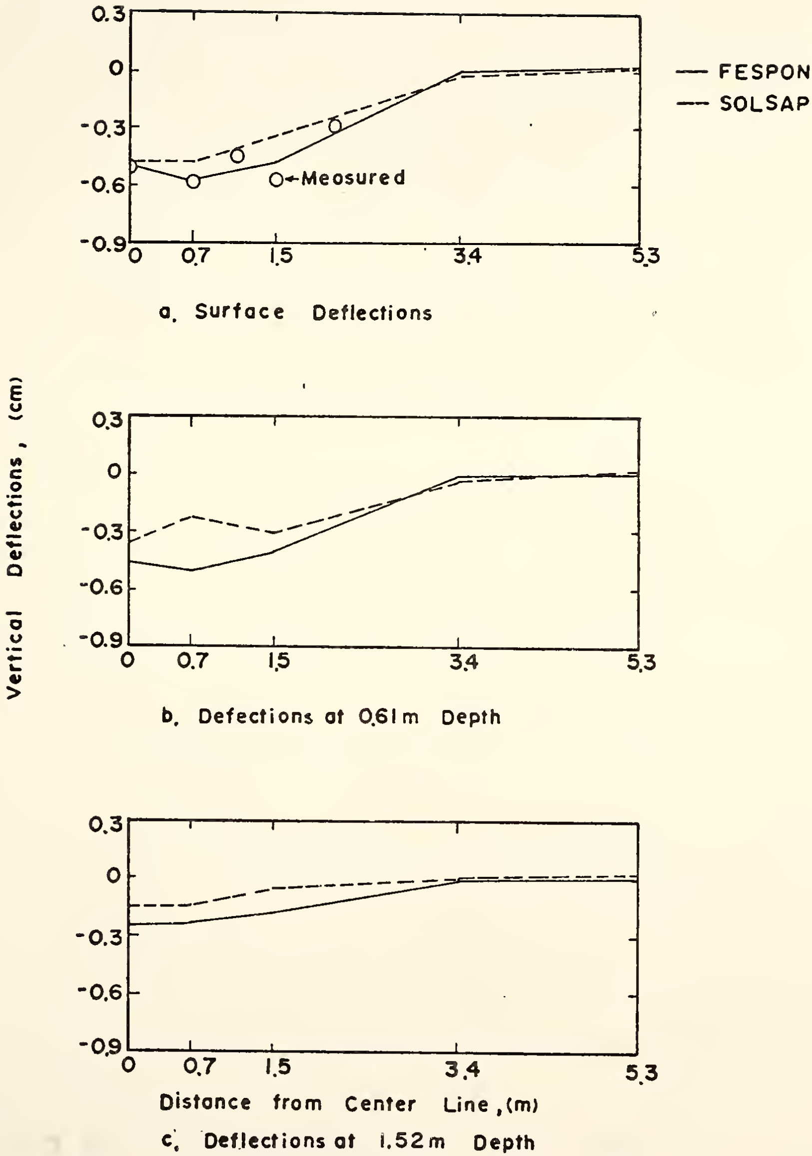

Fig. 5.36 Vertical Deflections—Section D

The dotted lines are results from SOLSAP, while the solid lines are results from FESPON. Field deflections measured at the surface are also given in these figures. Larger deflections are computed by FESPON than by SOLSAP. The comparison between computed values and measured data shows that the program FESPON with incompatible displacement mode produced better agreement with the measured values than the program SOLSAP.

Fig. 5.36 shows similar results in the transverse direction, section D. Again FESPON produces larger vertical deflections and closer agreement with the measured values.

5.5 Summary

Several slope stability analyses were performed using two-dimensional limit equilibrium methods and the three-dimensional programs BLOCK3, LEMIX and FESPON. The main findings of these analyses are as follows:

1. For both translational and rotational slides, the three-dimensional effect is most significant for cohesive soils and small failure lengths.
2. In the case of translational slides, the 3-D effect will increase with decreasing inclination of the weak layer and with lower strength of weak layer.
3. Wedge types of failure should be given particular attention because, in this case, the 3-D factor of safety may be less than the 2-D factor of safety.
4. It is difficult to predict the failure length of a rotational slide.

5. The steeper the slopes, the less important the 3-D effect.
6. Pore water pressures may cause the 3-D effect to be more significant.
7. The agreement between the finite element and limit equilibrium methods is quite good. The average factor of safety given by FESPON on a given failure surface is close to the factor of safety obtained by limit equilibrium on the same failure surface.

VI. CONCLUSIONS

This study is directed at developing techniques of three-dimensional slope stability analysis and comparing the results obtained with these techniques to those given by conventional two-dimensional methods. Computer programs based upon the limit equilibrium method are developed to assess the stability of both translational and rotational slides. A finite element technique is also proposed to perform the analysis of rotational slides.

In studying the stability of translational slides, attention is focused upon the most important controlling factor, the existence of a weak soil layer. The computer program BLOCK3 is generated to perform such an analysis. The ends of the critical surface is assumed according to Rankine's theory and the factory of safety is applied along the total failure surface. The study of translational slides yields several conclusions as follow:

(1) The 3-D factor of safety is usually greater than that of 2-D. However, a wedge type of failure may produce a F_3/F_2 ratio less than unity, and therefore should be examined carefully.

(2) The 3-D effect is more significant for cohesive soils than for cohesionless soils. This is also true for rotational slides.

(3) The lower the strength in the weak soil stratum, the more profound the 3-D effect.

(4) A steeply dipping weak soil always yields smaller ratios of F_3/F_2 than gently dipping layers.

A methodology is developed to study rotational slides, and a computer program LEMIX using the limit equilibrium method is generated. The failure mass is assumed symmetrical and divided into many vertical columns. The inclinations of the interslice forces is assumed the same throughout the whole failure mass. The intercolumn shear forces are assumed parallel to the base of the column and to be a function of their positions. Force and moment equilibrium are satisfied for each column as well as for the total mass. This method can handle different slopes, soil parameters, and pore water conditions and is considered a rather general method. The main conclusions of the analyses of rotational failures are summarized below:

(1) The 3-D effects are more significant at smaller lengths of the failure mass.

(2) For gentle slopes, the 3-D effects are most significant for soils of high cohesion intercept and low friction angle.

(3) For soils of low cohesion intercept and high friction angle, the 3-D factor of safety may be slightly less than that for the 2-D case. Pending more research, the 3-D stability analysis on this type of soil should be examined carefully.

(4) Pore water pressures may cause the 3-D effects to be even greater.

(5) The interslice angle influences the factor of safety. For soils of high cohesion intercept and low friction angle, θ_3 is less than θ_2 and thus F_3 is higher than F_2. The interslice angles θ_3 obtained with a pore pressure parameter of 0.5 are larger than those obtained with no pore pressure ($r_u = 0$). On the contrary, for soils of low cohesion intercept and high friction angle, θ_3 may be higher than θ_2 and hence F_3 is less than F_2. In this case, θ_3 for r_u equal to 0.5 is less than θ_3 for r_u equal to 0.

(6) It is difficult to predict the length of the failure mass.

A finite element computer program FESPON is developed to perform the analysis of spoon shape failures. It uses a hyperbolic stress-strain relationship and an incremental technique to simulate the non-linear behavior of soils. Isoparametric incompatible elements are used to provide good bending characteristics. The comparison of the results from both limit equilibrium method and finite element method are made for highly plastic St. Croix clay for which the stress-strain relationship is assumed to be hyperbolic. The hyperbolic parameters can be generated from conventional traixial test data or consolidation test data. Both the as-compacted condition and long-term condition are studied. The soil conditions and failure surface are assumed to be the same for both limit equilibrium and finite element methods. The results are quite similar, with the finite element method predictably yielding slightly higher factors of safety.

Though the proposed methods provide better techniques to analyze the 3-D slope stability, they still have shortcomings and in particular it is recommended to devote more research to the following points:

1. Development of searching techniques to find 3-D failure surfaces is worthwhile.
2. The assumptions of the angles of inclination and the distribution of the ends shear stress should be carefully studied. This is especially important when the soil conditions are complex.
3. More research on translational slides considering more complicated soil conditions (such as joints, faults, and anisotropy) and water conditions is needed.
4. The 3-D models presented in this dissertation should be applied to actual case studies in order to assess their prediction capabilities.

LIST OF REFERENCES

LIST OF REFERENCES

Baker, R. (1979), "Determination of the Critical Slip Surface in Slope Stability Computations", Publication No. 253, Israel Institute of Technology, Haifa, May, 1979.

Baligh, M. M. and Azzouz, A. S. (1975), "End Effects on Stability of Cohesive Slopes", Journal of the Soil Mechanics and Foundation Engineering Division, ASCE, Vol. 101, No. GT 11, November, 1975, pp. 1105-1117.

Bishop, A. W. (1955), "The Use of the Slip Circle in the Stability Analysis of Slopes", Geotechnique, Vol. 5, No. 1, March, 1955, pp. 7-17.

Boutrup, Eva (1977), "Computerized Slope Stability Analysis for Indiana Highways", JHRP Report No. 77-25 and 77-26, Purdue University, December, 1977. (Also MSCE Thesis, Purdue University, May, 512 pp.).

Brooker, E. W. and Ireland, H. O. (1965), "Earth Pressures at Rest Related to Stress History", Canadian Geotechnical Journal, Vol. 11, No. 1, February, 1965, pp. 1-15.

Chowdhury, R. N. (1978), Slope Analysis, Development in Geotechnical Engineering, Vol. 22, Elsevier, North Holland Inc., 423 pp.

Clough, G. W. and Duncan, J. M. (1969), "Finite Element Analyses of Port Allen and Old River Locks", Report No. TE 69-13, Office of Research Services, University of California, Berkeley, 1969.

Clough, G. W. and Woodward, R. J. (1967), "Analysis of Embankment Stresses and Deformations", Journal of the Soil Mechanics and Foundation Division, ASCE, Vol. 93, No. SM 4, July, 1967, pp. 529-549.

Cook, R. D. (1973), Concepts and Applications of Finite Element Analysis, John Wiley and Sons, Inc., New York, 402 pp.

Daniel, D. E. and Olson, R. E. (1974), "Stress-Strain Properties of Compacted Clays", Journal of the Soil Mechanics and Foundation Engineering Division, ASCE, Vol. 100, No. GT 10, October, 1974, pp. 1123-1136.

Desai, C. S. and Abel, J. F. (1972), Introduction to Finite Element Method, Van Nostrand, Reinhold, New York, 477 pp.

DiBernardo, A. (1979), "The Effect of Laboratory Compaction on the Compressibility of a Compacted Highly Plastic Clay", JHRP Report No. 79-3, Purdue University, May, 1979. (Also MSCE Thesis, Purdue University, West Lafayette, Indiana, May, 187 pp.).

Duncan, J. M. and Chang, C.-Y. (1970), "Nonlinear Analysis of Stress and Strain in Soils", Journal of the Soil Mechanics and Foundation Engineering Division, ASCE, Vol. 96, No. SM 5, September, 1970, pp. 1629-1653.

Fellenius, W. (1918), Discussion of "Kaj-och jordrasen i Göteborg", ("The quay - and landslides in Gothenburg"), Teknisk Tidskrift, V. U., Vol. 46, No. 15, pp. 133-142; Vol. 48, No. 2, pp. 17-19.

Fellenius, W. (1936), "Calculation of the Stability of Earth Dams", Transactions, 2nd Congress on Large Dams, Vol. 4, Washington, D. C., 1936.

Fredlund, D. G. and Krahn, J. (1977), "Comparison of Slope Stability Methods of Analysis", Canadian Geotechnical Journal, Vol. 14, pp. 429-439.

Hansen, J. B. (1963), Discussion of "Hyperbolic Stress-Strain Response: Cohesive Soils", Journal of the Soil Mechanics and Foundation Engineering Division, ASCE, Vol. 89, No. SM 4, July, 1963, pp. 241-242.

Hovland, H. J. (1977), "Three-Dimensional Slope Stability Analysis Method", Journal of the Soil Mechanics and Foundation Engineering Division, ASCE, Vol. 103, No. GT 9, September, 1977, pp. 971-986.

Janbu, N., Bjerrum, L., and Kjaernsli, B. (1956), "Stabilitsberegning for fyllinger skjaeringer og naturlige skraninger. Norwegian Geotechnical Publication No. 16, Oslo, Norway.

Janbu, N. (1963), "Soil Compressibility as Determined by Oedometer and Triaxial Tests", European Conference on Soil Mechanics and Foundation Engineering, Wissbaden, Germany, Vol. 1, pp. 19-25.

Johnson, J. M. (1979), "The Effect of Laboratory Compaction on the Shear Behavior of a Highly Plastic Clay after Saturation and Consolidation", JHRP Report No. 79-7, Purdue University, August, 1979. (Also MSCE Thesis, Purdue University, August, 271 pp.).

Kondner, R. L. (1963), "Hyperbolic Stress-Strain Response: Cohesive Soils", Journal of the Soil Mechanics and Foundations Division, ASCE, Vol. 89, No. SM1, February, 1963, pp. 115-143.

Kulhawy, F. H., Duncan, J. M., and Seed, H. B. (1969), "Finite Element Analysis of Stresses and Movements in Embankments During Construction", Geotechnical Engineering Research Report No. TE-69-4, Department of Civil Engineering, University of California, Berkeley, November, 1969.

Lambe, T. W. and Whitman, R. V. (1969), Soil Mechanics, John Wiley, New York, 533 pp.

Lefebvre, G. and Duncan, J. M. (1973), "Three-Dimensional Finite Element Analysis of Dams", Journal of the Soil Mechanics and Foundation Engineering Division, ASCE, Vol. 99, No. SM 7, July, 1973, pp. 495-507.

Mendez, C. (1972), "Computerized Slope Stability; the Sliding Block Problem", Technical Report No. 21, Purdue University, Water Resources Research Center, February, 1972.

Mohan, A. (1972), "Computerized Slope Stability Analysis: A Sliding Block Model", JHRP Report No. 43, Purdue University, November, 1972.

Morganstern, N. R. and Price, V. W., (1965), "The Analysis of the Stability of General Slip Surfaces," Geotechnique, Vol. 15, No. 1, March, 1965, pp. 79-93.

Ozawa, Y. (1973), "ISBILD: A Computer Program for Analysis of Static Stresses and Movements in Embankments", Geotechnical Engineering Research Report No. TE-73-4, Department of Civil Engineering, University of California, Berkeley, December, 1973.

Palmerton, F. B. (1972), "Application of Three-Dimensional Finite Element Analysis", Proc. Symp. Appl. of Finite Element Method in Geotechnical Engineering, U. S. Waterays Experiment Station, Vicksburg, pp. 155-213.

Perloff, W. H. and Baron, W. (1976), Soil Mechanics Principles and Applications, The Ronald Press Company, New York, 1976, Chapter 12, Stability of Slopes.

Reśendiz, D. (1974), Discussion of "Accuracy Equilibrium Slope Stability Analysis", Journal of the Soil Mechanics and Foundation Engineering Division, ASCE, Vol. 100, No. GT 8, August, 1974, pp. 967-970.

Romani, F. (1970), "Dependence of Stability of Slopes on Initiation and Progression of Failure", Ph.D. Thesis, Purdue University, West Lafayette, Indiana, 1970.

Romani, F., Lovell, C. W. and Harr, M. E. (1972), "Influence of Progressive Failure on Slope Stability", Journal of the Soil Mechanics and Foundations Division, ASCE, Volume 98, No. SM 11, November, 1972, pp. 1209-1223.

Sherard, J. L., Woodward, R. J., Gizienksi, S. G. and Clevenger, W. A. (1963), Earth and Earth Rock Dams, John Wiley, New York.

Siegel, R. A. (1975), "Computer Analysis of General Slope Stability Problems", MSCE Thesis, Purdue University, West Lafayette, Indiana, 1975. (Also JHRP Report No. 75-8, Purdue University, June, 1975).

Spencer, E. (1967), "A Method of Analysis of the Stability of Embankments Assuming Parallel Interslice Forces", Geotechnique, Vol. 17, No. 1, March, 1967, pp. 11-26.

Taylor, D. W. (1937), "Stability of Earth Slopes", Contributions to Soil Mechanics 1925-1940, Boston Society of Civil Engineers, Boston, 1940.

Taylor, D. W. (1948), "Stability of Slopes", Fundamentals of Soil Mechanics, John Wiley and Sons, Inc., New York, 1948, pp. 406-479.

TRB (1978), Landslides - Analysis and Control, Special Report 176, Transportation Research Board, National Academy of Sciences, Washington, D.C.

Weitzel, D. W. (1979), "The Effect of Laboratory Compaction on the Unconsolidated-Undrained Strength Behavior of a Highly Plastic Clay", JHRP Report No. 79-11, Purdue University, August, 1979. (Also MSCE Thesis, Purdue University, August, 218 pp.).

Wilson, E. L. (1971), "Solid SAP, A Static Analysis Program for Three-Dimensional Solid Structures", SESM Report 71-19, Structural Engineering Laboratory, University of California, Berkeley, September 1971.

Wilson, E. L., Taylor, R. L., Doberty, W. P., and Ghaboussai, J. (1971), "Incompatible Displacement Modes", Proceedings of Office of Naval Research Symposium, University of Illinois, Urbana, Illinois, 1971, pp. 43-57.

Wolfe, P. (1959), "The Secant Method for Simultaneous Nonlinear Equations", Communications of the ACM, Vol. 2, pp. 12-13.

Wong, K. S. and Duncan, J. M. (1974), "Hyperbolic Stress-Strain Parameters for Nonlinear Finite Element Analyses of Stresses and Movements in Soil Masses", Report No. TE-74-3, Office of Research Services, University of California, Berkeley, July 1974.

Wright, S. G. (1969), "A Study of Slope Stability and the Undrained Shear Strength of Clay Shales", Ph.D. Thesis, University of California, Berkeley.

Wright, S. G., Kulhawy, F. H., and Duncan, J. M. (1973), "Accuracy of Equilibrium Slope Stability Analysis", Journal of the Soil Mechanics and Foundations Division, ASCE, Vol. 99, No. SM 10, October 1973, pp. 783-791.

Zienkiewicz, O. C. (1971), The Finite Element Method in Engineering Science, McGraw-Hill, London, 521 pp.

APPENDICES

APPENDIX A

End Shear Forces of a Column

The end shear forces can be calculated using the following equations:

$$R_{cE1} = c\ dx\ h_{E1} \tag{A.1}$$

$$R_{cF1} = c_F\ dx\ h_{F1} \tag{A.2}$$

$$R_{\phi E1} = \frac{1}{2} k_o(\rho - \rho_w)\ h_{E1}^{\ 2}\ dx\ \tan\phi_E \tag{A.3}$$

$$R_{\phi F1} = k_o\{(\rho_F - \rho_w)\ h_{E1}h_{F1} + \frac{1}{2}(\rho_F - \rho_w)h_{F1}^{\ 2}\}\ dx\ \tan\phi_F \tag{A.4}$$

Similarly,

$$R_{cE2} = c\ dx\ h_{E2} \tag{A.5}$$

$$R_{cF2} = c_F\ dx\ h_{F2} \tag{A.6}$$

$$R_{\phi E2} = \frac{1}{2} k_o(\rho - \rho_w)\ h_{E2}^{\ 2}\ dx\ \tan\phi_E \tag{A.7}$$

$$R_{\phi F2} = k_o\{(\rho_F - \rho_w)\ h_{E2}\ h_{F2} + \frac{1}{2}(\rho_F - \rho_w)\ h_{F2}^{\ 2}\}\ dx\ \tan\phi_F \tag{A.8}$$

where h_E and h_F are shown in Fig. A.1. The resultant of horizontal forces acting in the foundations part, F_F, and its position, y_F, can be calculated using the following equations,

$$F_F = \rho_E'\ h_E\ h_F + \frac{1}{2}\rho_F'\ h_F^{\ 2} \tag{A.9}$$

$$y_F = \frac{\frac{1}{2}\rho_E'\ h_E\ h_F^{\ 2} + \frac{1}{6}\rho_F'\ h_F^{\ 3}}{\rho_E'\ h_E\ h_F + \frac{1}{2}\rho_F'\ h_F^{\ 2}} = \frac{(mh_E + \frac{1}{3}h_F)\ h_F}{2mh_E + h_F} \tag{A.10}$$

where $m = \rho_E'/\rho_F'$

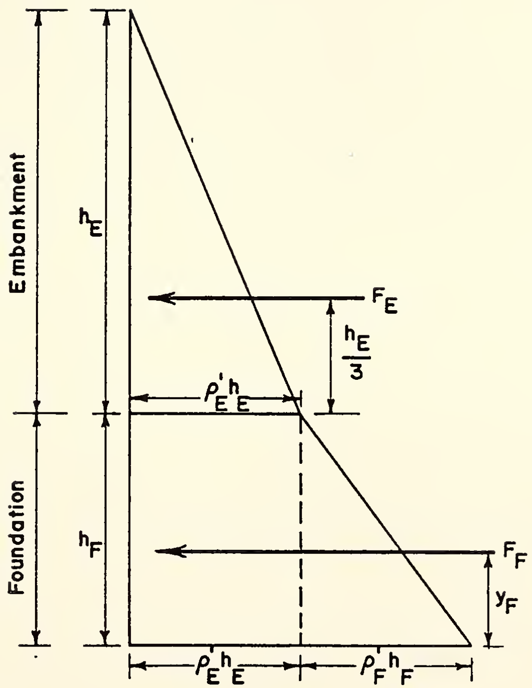

Fig. A.1 Linear Distribution of Horizontal Stress Acting on the End of a Column

APPENDIX B

Program FESPON

This Appendix describes the subroutines of the computer program FESPON and their functions (see Fig. B.1):

(a) Subroutine SETUP reads and prints input data, calculates the equation number according to the nodal points degrees of freedom, calculates the band width, and computes and prints the initial stresses and the initial values of modulus and Poisson's ratio for the elements.

(b) Subroutine RSEIG calculates the principal stresses and their directions in three-dimensional space.

(c) Subroutine COMPAR looks for the major principle stresses and strains, and the minor principal stresses and strains.

(d) Subroutine MODU calculates the modulus values for the elements in accordance with the magnitudes of the stresses in the elements.

(e) Subroutine FOMING calls subroutine RELATE to establish strain-displacement matrices for elements.

(f) Subroutine RELATE forms the strain-displacement matrix.

(g) Subroutine CALNEQ determines the number of elements and nodal points for the problem to be analyzed, the number of equations, the number of equations in each block, and the number of blocks for each construction layer increment or load increment.

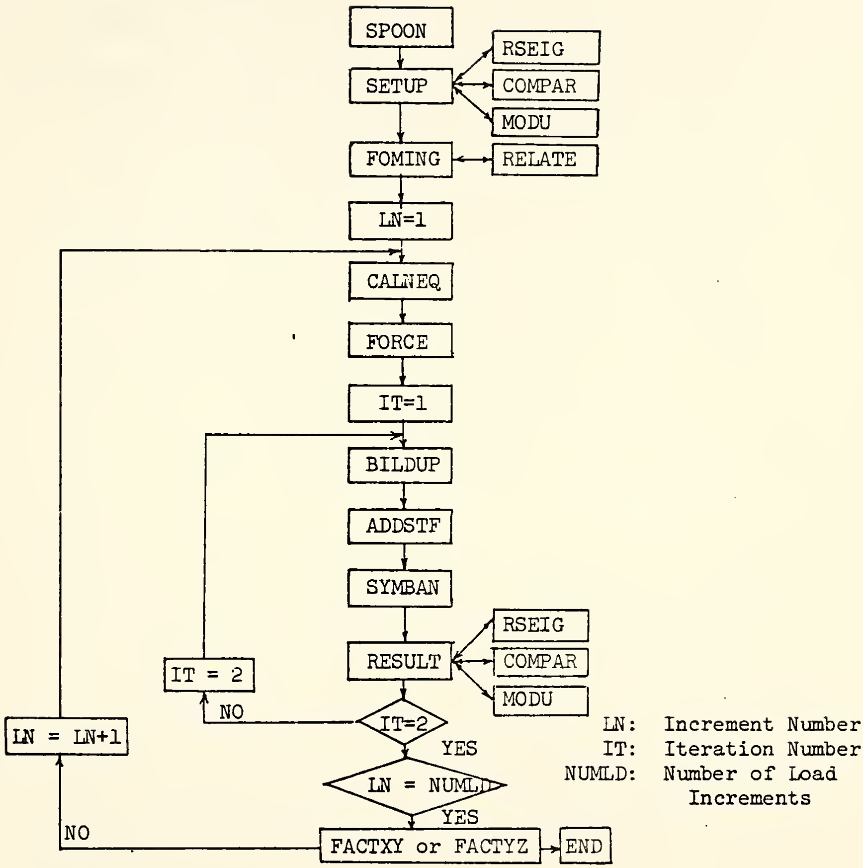

Fig. B.1 The Flow Chart of Computer Program—FESPON

(h) Subroutine FORCE calculates nodal point forces due to weights of added elements (each node takes one-eighth of the weight of the element), reads concentrated load data, prints nodal points forces, sets up a force vector.

(i) Subroutine BILDUP formulates the constitutive equations, forms the element stiffness matrix and the strain-displacement matrix for each element.

(j) Subroutine ADDSTF forms the total stiffness matrix, two blocks at a time, by making a pass through the element stiffness matrices and adding the appropriate coefficients.

(k) Subroutine SYMBAN solves the simultaneous equations representing the structural matrix and the structural load vector for nodal point displacements using the Gaussian elimination technique.

(l) Subroutine RESULT calculates stress increments and average stresses and evaluates the modulus for each element after the first iteration. After the second iteration it calculates the incremental and cumulative displacements for each nodal point, incremental and cumulative stresses and strains for each element, and modulus values for each element to be used in the next increment.

(m) Subroutine FACTXY, assuming the axis of rotation is parallel to the Z-axis and the movement is along the X-Y plane only, selects points on a well defined critical surface, and calculates the six components of stresses at these points. Thus, the local factors of safety can be calculated. After the local factors of safety are obtained, the mean factor of safety may be calculated subsequently.

(n) Subroutine FACTYZ assuming the axis of rotation is parallel to X-axis and the movement is along Y-Z plane only. The functions of FACTXY and FACTYZ are the same.

APPENDIX C

TABLES RELATED TO TRANSLATIONAL SLIDES

TABLE C.1 F_3/F_2 FOR VARIOUS COMBINATIONS OF L, D, c_w, AND β, AT c = 47.9 kPa (1000 psf), $\phi = 0^o$, a = 1 AND $\gamma = 90^o$

Length Ratio $\frac{L}{H}$	Depth Ratio $\frac{D}{H}$	c_w = 9.6 kPa			c_w = 19.2 kPa			c_w = 28.8 kPa		
		0^o	5.7^o	11.3^o	0	5.7^o	11.3^o	0	5.7^o	11.3^o
1	0.25	2.36	2.27	2.18	2.26	2.15	2.06	2.17	2.06	1.96
	0.5	2.51	2.42	2.34	2.42	2.32	2.23	2.33	2.24	2.14
	1.0	2.83	2.74	2.68	2.74	2.66	2.59	2.66	2.59	2.51
	2.0	3.50	3.42	3.36	3.42	3.36	3.29	3.35	3.29	3.22
2	0.25	1.68	1.63	1.59	1.63	1.58	1.53	1.58	1.53	1.48
	0.5	1.75	1.71	1.67	1.71	1.66	1.61	1.66	1.62	1.57
	1.0	1.91	1.86	1.84	1.87	1.83	1.80	1.83	1.79	1.76
	2.0	2.25	2.21	2.18	2.21	2.18	2.14	2.17	2.14	2.11
4	0.25	1.34	1.31	1.29	1.31	1.29	1.26	1.29	1.26	1.24
	0.5	1.37	1.35	1.33	1.36	1.33	1.31	1.33	1.31	1.28
	1.0	1.46	1.43	1.42	1.43	1.41	1.40	1.41	1.40	1.38
	2.0	1.62	1.60	1.54	1.60	1.59	1.60	1.58	1.57	1.55
8	0.25	1.16	1.15	1.14	1.16	1.14	1.13	1.14	1.13	1.12
	0.5	1.19	1.17	1.17	1.18	1.16	1.15	1.16	1.15	1.14
	1.0	1.23	1.22	1.21	1.21	1.20	1.20	1.20	1.20	1.19
	2.0	1.31	1.29	1.29	1.30	1.29	1.28	1.29	1.28	1.28
16	0.25	1.08	1.08	1.08	1.08	1.07	1.07	1.08	1.06	1.06
	0.5	1.09	1.08	1.08	1.09	1.08	1.07	1.08	1.07	1.07
	1.0	1.11	1.10	1.10	1.11	1.10	1.10	1.10	1.10	1.09
	2.0	1.15	1.14	1.14	1.15	1.15	1.14	1.14	1.14	1.14

TABLE C.2 F_3/F_2 FOR VARIOUS COMBINATIONS OF L, D, c_w, AND β, AT $c = 24.0$ kPa (500 psf), $\phi = 10^o$, a = 1 AND $\gamma = 90^o$

Length Ratio $\frac{L}{H}$	Depth Ratio $\frac{D}{H}$	c_w = 9.6 kPa			c_w = 19.2 kPa			c_w = 28.8 kPa		
		0^o	5.7^o	11.3^o	0^o	5.7^o	11.3^o	0^o	5.7^o	11.3^o
1	0.25	1.98	1.94	1.89	1.85	1.79	1.74	1.71	1.70	1.64
	0.5	2.01	1.98	1.95	1.92	1.89	1.84	1.84	1.80	1.75
	1.0	2.08	2.08	2.05	2.03	2.00	1.99	1.98	1.95	1.91
	2.0	2.19	2.19	2.17	2.17	2.15	2.14	2.13	2.11	2.10
2	0.25	1.50	1.47	1.45	1.43	1.40	1.37	1.38	1.35	1.31
	0.5	1.51	1.50	1.48	1.46	1.45	1.42	1.43	1.40	1.38
	1.0	1.55	1.54	1.53	1.52	1.50	1.50	1.49	1.48	1.46
	2.0	1.60	1.60	1.59	1.59	1.58	1.58	1.57	1.56	1.56
4	0.25	1.25	1.24	1.22	1.21	1.20	1.18	1.19	1.18	1.16
	0.5	1.25	1.25	1.24	1.23	1.22	1.21	1.21	1.20	1.19
	1.0	1.28	1.28	1.27	1.26	1.25	1.25	1.25	1.24	1.22
	2.0	1.30	1.30	1.30	1.30	1.29	1.29	1.29	1.28	1.28
8	0.25	1.13	1.12	1.11	1.10	1.10	1.09	1.10	1.09	1.08
	0.5	1.12	1.12	1.12	1.12	1.11	1.10	1.11	1.09	1.09
	1.0	1.14	1.14	1.14	1.13	1.13	1.13	1.12	1.12	1.11
	2.0	1.15	1.15	1.14	1.15	1.14	1.14	1.14	1.14	1.14
16	0.25	1.06	1.06	1.06	1.05	1.04	1.04	1.05	1.04	1.04
	0.5	1.06	1.06	1.06	1.06	1.06	1.05	1.05	1.05	1.05
	1.0	1.07	1.07	1.07	1.06	1.06	1.06	1.06	1.06	1.05
	2.0	1.07	1.07	1.07	1.08	1.07	1.07	1.07	1.07	1.07

TABLE C.3 F_3/F_2 FOR VARIOUS COMBINATIONS OF L, D, c_w, AND β, AT $c = 0$, $\phi = 35°$, $a = 1$ AND $\gamma = 90°$

Length Ratio $\frac{L}{H}$	Depth Ratio $\frac{D}{H}$	c_w = 9.6 kPa			c_w = 19.2 kPa			c_w = 28.8 kPa		
		0°	5.7°	11.3°	0°	5.7°	11.3°	0°	5.7°	11.3°
1	0.25	1.32	1.31	1.28	1.22	1.20	1.19	1.17	1.15	1.13
	0.5	1.24	1.24	1.23	1.20	1.20	1.18	1.17	1.16	1.15
	1.0	1.17	1.17	1.17	1.21	1.15	1.16	1.14	1.14	1.14
	2.0	1.11	1.11	1.12	1.11	1.11	1.12	1.11	1.11	1.12
2	0.25	1.17	1.16	1.14	1.12	1.11	1.10	1.09	1.08	1.07
	0.5	1.13	1.13	1.13	1.10	1.10	1.10	1.09	1.09	1.08
	1.0	1.09	1.09	1.09	1.08	1.08	1.08	1.07	1.07	1.07
	2.0	1.06	1.06	1.06	1.06	1.06	1.06	1.06	1.06	1.06
4	0.25	1.09	1.08	1.07	1.06	1.05	1.04	1.05	1.04	1.04
	0.5	1.06	1.06	1.07	1.05	1.06	1.05	1.05	1.04	1.05
	1.0	1.05	1.05	1.05	1.04	1.04	1.04	1.04	1.04	1.04
	2.0	1.03	1.03	1.03	1.03	1.03	1.03	1.03	1.03	1.03
8	0.25	1.05	1.04	1.04	1.03	1.02	1.02	1.03	1.02	1.01
	0.5	1.04	1.03	1.03	1.02	1.03	1.03	1.02	1.02	1.02
	1.0	1.02	1.02	1.03	1.02	1.02	1.02	1.02	1.02	1.02
	2.0	1.02	1.01	1.02	1.02	1.02	1.02	1.02	1.02	1.02
16	0.25	1.02	1.02	1.01	1.02	1.01	1.01	1.01	1.01	1.01
	0.5	1.01	1.02	1.02	1.01	1.01	1.02	1.01	1.01	1.01
	1.0	1.01	1.02	1.01	1.01	1.01	1.02	1.01	1.01	1.01
	2.0	1.01	1.00	1.01	1.01	1.01	1.01	1.01	1.01	1.01

TABLE C.4 F_3/F_2 FOR VARIOUS COMBINATIONS OF L, D, c_w, AND γ, AT $c = 47.9$ kPa (1000 psf), $\phi = 0^{\circ}$, a = 1, AND $\beta = 11.3^{\circ}$

Length Ratio $\frac{L}{H}$	Depth Ratio $\frac{D}{H}$	c_w = 9.6 kPa			c_w = 19.2 kPa			c_w = 28.8 kPa		
		70°	80°	90°	70°	80°	90°	70°	80°	90°
1	0.25	2.56	2.32	2.18	2.37	2.17	2.06	2.22	2.05	1.96
	0.5	3.02	2.58	2.34	2.82	2.44	2.23	2.66	2.32	2.14
	1.0	4.48	3.23	2.68	4.25	3.09	2.59	4.04	2.97	2.51
	2.0	-	5.09	3.36	-	4.94	3.29	-	4.81	3.22
2	0.25	1.67	1.62	1.59	1.59	1.55	1.53	1.52	1.49	1.48
	0.5	1.82	1.73	1.67	1.73	1.66	1.61	1.66	1.60	1.57
	1.0	2.15	1.96	1.84	2.08	1.90	1.80	2.01	1.84	1.76
	2.0	3.16	2.50	2.18	3.08	2.45	2.14	2.99	2.40	2.11
4	0.25	1.31	1.30	1.29	1.27	1.26	1.26	1.24	1.24	1.24
	0.5	1.37	1.34	1.33	1.33	1.31	1.31	1.30	1.29	1.28
	1.0	1.50	1.45	1.42	1.46	1.42	1.40	1.43	1.40	1.38
	2.0	1.78	1.66	1.54	1.75	1.64	1.60	1.72	1.62	1.55
8	0.25	1.15	1.15	1.14	1.13	1.13	1.13	1.12	1.12	1.12
	0.5	1.18	1.17	1.17	1.15	1.15	1.15	1.14	1.14	1.14
	1.0	1.23	1.21	1.21	1.22	1.20	1.20	1.20	1.19	1.19
	2.0	1.34	1.31	1.29	1.33	1.30	1.28	1.31	1.29	1.28
16	0.25	1.08	1.08	1.08	1.07	1.06	1.07	1.06	1.06	1.06
	0.5	1.09	1.08	1.08	1.07	1.07	1.07	1.07	1.07	1.07
	1.0	1.11	1.10	1.10	1.10	1.10	1.10	1.09	1.09	1.09
	2.0	1.16	1.15	1.14	1.15	1.14	1.14	1.15	1.14	1.14

TABLE C.5 F_3/F_2 FOR VARIOUS COMBINATIONS OF L, D, c_w, AND γ, AT $c = 24.0$ kPa (500 psf), $\phi = 10^\circ$, a = 1, AND $\beta = 11.3^\circ$

Length Ratio $\frac{L}{H}$	Depth Ratio $\frac{D}{H}$	c_w = 9.6 kPa			c_w = 19.2 kPa			c_w = 28.8 kPa		
		70°	80°	90°	70°	80°	90°	70°	80°	90°
1	0.25	2.16	1.98	1.89	1.92	1.80	1.74	1.77	1.68	1.64
	0.5	2.44	2.13	1.95	2.22	1.98	1.84	2.05	1.86	1.75
	1.0	3.23	2.41	2.05	3.03	2.30	1.99	2.83	2.18	1.91
	2.0	-	3.11	2.17	-	3.03	2.14	-	2.95	2.10
2	0.25	1.51	1.47	1.45	1.40	1.38	1.37	1.33	1.32	1.31
	0.5	1.59	1.52	1.48	1.50	1.45	1.42	1.42	1.40	1.38
	1.0	1.75	1.61	1.53	1.69	1.57	1.50	1.62	1.52	1.46
	2.0	2.19	1.79	1.59	2.13	1.76	1.58	2.07	1.73	1.56
4	0.25	1.24	1.22	1.22	1.19	1.18	1.18	1.15	1.15	1.16
	0.5	1.27	1.25	1.24	1.22	1.22	1.21	1.20	1.19	1.19
	1.0	1.33	1.29	1.27	1.30	1.27	1.25	1.26	1.24	1.22
	2.0	1.44	1.35	1.30	1.41	1.33	1.29	1.39	1.33	1.28
8	0.25	1.11	1.11	1.11	1.09	1.09	1.09	1.07	1.08	1.08
	0.5	1.13	1.13	1.12	1.11	1.10	1.10	1.09	1.09	1.09
	1.0	1.15	1.14	1.14	1.14	1.13	1.13	1.12	1.11	1.11
	2.0	1.19	1.16	1.14	1.18	1.16	1.14	1.17	1.15	1.14
16	0.25	1.06	1.05	1.06	1.04	1.04	1.04	1.03	1.03	1.04
	0.5	1.07	1.06	1.06	1.05	1.05	1.05	1.04	1.04	1.05
	1.0	1.08	1.07	1.07	1.07	1.06	1.06	1.05	1.05	1.05
	2.0	1.08	1.08	1.07	1.08	1.08	1.07	1.08	1.07	1.07

TABLE C.6 F_3/F_2 FOR VARIOUS COMBINATIONS OF L, D, c_w, AND γ, AT $c = 0$, $\phi = 35^\circ$, $a = 1$, AND $\beta = 11.3^\circ$

Length Ratio $\frac{L}{H}$	Depth Ratio $\frac{D}{H}$	c_w = 9.6 kPa			c_w = 19.2 kPa			c_w = 28.8 kPa		
		70°	80°	90°	70°	80°	90°	70°	80°	90°
1	0.25	1.36	1.30	1.28	1.19	1.18	1.19	1.09	1.11	1.13
	0.5	1.41	1.30	1.23	1.29	1.22	1.18	1.20	1.17	1.15
	1.0	1.57	1.30	1.17	1.49	1.26	1.16	1.47	1.23	1.14
	2.0	3.42	1.41	1.12	3.30	1.39	1.12	3.18	1.38	1.12
2	0.25	1.16	1.15	1.14	1.09	1.09	1.10	1.04	1.06	1.07
	0.5	1.19	1.14	1.13	1.13	1.11	1.10	1.09	1.09	1.08
	1.0	1.22	1.14	1.09	1.18	1.13	1.08	1.16	1.11	1.07
	2.0	1.35	1.16	1.06	1.33	1.16	1.06	1.32	1.15	1.06
4	0.25	1.08	1.07	1.07	1.04	1.04	1.04	1.02	1.03	1.04
	0.5	1.08	1.08	1.07	1.06	1.06	1.05	1.05	1.04	1.05
	1.0	1.10	1.07	1.05	1.08	1.06	1.04	1.07	1.05	1.04
	2.0	1.13	1.08	1.03	1.13	1.07	1.03	1.12	1.07	1.03
8	0.25	1.04	1.03	1.04	1.02	1.02	1.02	1.01	1.01	1.01
	0.5	1.04	1.04	1.03	1.03	1.03	1.03	1.02	1.02	1.02
	1.0	1.05	1.04	1.03	1.04	1.03	1.02	1.03	1.02	1.02
	2.0	1.06	1.04	1.02	1.06	1.03	1.02	1.05	1.04	1.02
16	0.25	1.01	1.01	1.01	1.01	1.01	1.01	1.01	1.01	1.01
	0.5	1.02	1.02	1.02	1.02	1.02	1.02	1.01	1.01	1.01
	1.0	1.02	1.02	1.01	1.02	1.02	1.02	1.01	1.01	1.01
	2.0	1.03	1.02	1.01	1.03	1.02	1.01	1.03	1.02	1.01

TABLE C.7 F_3/F_2 FOR VARIOUS COMBINATIONS OF L, D, c_w, AND a, AT $c = 47.9$ kPa (1000 psf) $\phi = 0^o$, $\beta = 11.3^o$, AND $\gamma = 90^o$

Length Ratio $\frac{L}{H}$	Depth Ratio $\frac{D}{H}$	c_w = 9.6 kPa			c_w = 19.2 kPa			c_w = 28.8 kPa		
		0.8	0.9	1.0	0.8	0.9	1.0	0.8	0.9	1.0
1	0.25	2.16	2.17	2.18	2.03	2.04	2.06	1.92	1.94	1.96
	0.5	2.27	2.31	2.34	2.15	2.19	2.23	2.07	2.11	2.14
	1.0	2.49	2.58	2.68	2.40	2.49	2.59	2.33	2.42	2.51
	2.0	2.87	3.10	3.36	2.81	3.03	3.29	2.75	2.97	3.22
2	0.25	1.56	1.58	1.59	1.49	1.51	1.53	1.44	1.46	1.48
	0.5	1.60	1.64	1.67	1.54	1.57	1.61	1.49	1.53	1.57
	1.0	1.68	1.76	1.84	1.64	1.72	1.80	1.60	1.67	1.76
	2.0	1.83	1.99	2.18	1.80	1.96	2.14	1.77	1.93	2.11
4	0.25	1.26	1.28	1.29	1.22	1.24	1.26	1.19	1.21	1.24
	0.5	1.26	1.30	1.33	1.23	1.27	1.31	1.21	1.24	1.28
	1.0	1.28	1.35	1.42	1.26	1.33	1.40	1.24	1.30	1.38
	2.0	1.31	1.44	1.54	1.30	1.42	1.60	1.28	1.41	1.55
8	0.25	1.10	1.13	1.14	1.08	1.11	1.13	1.07	1.09	1.12
	0.5	1.09	1.13	1.17	1.07	1.11	1.15	1.06	1.10	1.14
	1.0	1.07	1.14	1.21	1.06	1.13	1.20	1.05	1.12	1.19
	2.0	1.04	1.16	1.29	1.04	1.15	1.28	1.03	1.15	1.28
16	0.25	1.02	1.05	1.08	1.02	1.04	1.07	1.00	1.03	1.06
	0.5	1.01	1.05	1.08	0.99	1.03	1.07	0.98	1.02	1.07
	1.0	0.97	1.04	1.10	0.97	1.03	1.10	0.96	1.02	1.09
	2.0	0.91	1.02	1.14	0.91	1.02	1.14	0.91	1.02	1.14

TABLE C.8 F_3/F_2 FOR VARIOUS COMBINATIONS OF L, D, c_w, AND a, AT $c = 24$ kPa (500 psf), $\phi = 10^o$, $\beta = 11.3^o$, AND $\gamma = 90^o$

Length Ratio $\frac{L}{H}$	Depth Ratio $\frac{D}{H}$	c_w = 9.6 kPa			c_w = 19.2 kPa			c_w = 28.8 kPa		
		0.8	0.9	1.0	0.8	0.9	1.0	0.8	0.9	1.0
1	0.25	1.86	1.87	1.89	1.70	1.72	1.74	1.59	1.62	1.64
	0.5	1.88	1.92	1.95	1.77	1.81	1.84	1.68	1.71	1.75
	1.0	1.89	1.97	2.05	1.82	1.90	1.99	1.75	1.83	1.91
	2.0	1.83	1.99	2.17	1.80	1.96	2.14	1.77	1.93	2.10
2	0.25	1.41	1.43	1.45	1.33	1.35	1.37	1.27	1.30	1.31
	0.5	1.40	1.44	1.48	1.35	1.39	1.42	1.30	1.30	1.38
	1.0	1.39	1.45	1.53	1.36	1.43	1.50	1.31	1.38	1.46
	2.0	1.32	1.44	1.59	1.30	1.43	1.58	1.29	1.41	1.56
4	0.25	1.18	1.21	1.22	1.13	1.16	1.18	1.11	1.13	1.16
	0.5	1.17	1.20	1.24	1.13	1.17	1.21	1.11	1.15	1.19
	1.0	1.13	1.20	1.27	1.11	1.18	1.25	1.09	1.16	1.22
	2.0	1.05	1.17	1.30	1.05	1.16	1.29	1.04	1.15	1.28
8	0.25	1.06	1.09	1.11	1.04	1.06	1.09	1.02	1.05	1.08
	0.5	1.04	1.08	1.12	1.02	1.07	1.10	1.01	1.05	1.09
	1.0	1.00	1.07	1.14	0.99	1.06	1.13	0.97	1.05	1.11
	2.0	0.92	1.02	1.14	0.92	1.02	1.14	0.91	1.02	1.14
16	0.25	1.00	1.03	1.06	0.99	1.01	1.04	0.98	1.01	1.04
	0.5	0.98	1.02	1.06	0.97	1.02	1.05	0.96	1.01	1.05
	1.0	0.93	1.00	1.07	0.93	0.99	1.06	0.92	0.99	1.05
	2.0	0.85	0.95	1.07	0.85	0.95	1.07	0.85	0.95	1.07

TABLE C.9 F_3/F_2 FOR VARIOUS COMBINATIONS OF L, D, c_w, AND a, AT $c = 0$, $\phi = 35^\circ$, $\beta = 11.3^\circ$, AND $\gamma = 90^\circ$

Length Ratio $\frac{L}{H}$	Depth Ratio $\frac{D}{H}$	c_w = 9.6 kPa			c_w = 19.2 kPa			c_w = 28.8 kPa		
		0.8	0.9	1.0	0.8	0.9	1.0	0.8	0.9	1.0
1	0.25	1.29	1.26	1.28	1.14	1.16	1.19	1.08	1.11	1.13
	0.5	1.15	1.19	1.23	1.10	1.15	1.18	1.07	1.11	1.15
	1.0	1.04	1.10	1.17	1.02	1.09	1.16	1.00	1.07	1.14
	2.0	0.90	1.01	1.12	0.90	1.00	1.12	0.90	1.00	1.12
2	0.25	1.09	1.12	1.14	1.04	1.07	1.10	1.01	1.04	1.07
	0.5	1.03	1.08	1.13	1.02	1.06	1.10	0.99	1.04	1.08
	1.0	0.95	1.02	1.09	0.94	1.10	1.08	0.94	1.00	1.07
	2.0	0.84	0.95	1.06	0.84	0.94	1.06	0.84	1.06	1.06
4	0.25	1.01	1.05	1.07	0.99	1.02	1.04	0.98	1.01	1.04
	0.5	0.97	1.02	1.07	0.96	1.01	1.05	0.95	1.00	1.05
	1.0	0.90	0.97	1.05	0.90	0.97	1.04	0.89	0.96	1.04
	2.0	0.81	0.91	1.03	0.81	0.91	1.03	0.81	0.97	1.03
8	0.25	0.96	1.00	1.04	0.96	0.99	1.02	0.96	0.98	1.01
	0.5	0.94	0.99	1.03	1.01	0.98	1.03	0.93	0.98	1.02
	1.0	0.88	0.95	1.03	0.88	0.95	1.02	0.88	0.94	1.02
	2.0	0.79	0.90	1.02	0.79	0.90	1.02	0.79	0.95	1.02
16	0.25	0.95	0.98	1.01	0.95	0.98	1.01	0.95	0.98	1.01
	0.5	0.92	0.97	1.02	0.92	0.97	1.02	0.92	0.97	1.01
	1.0	0.86	0.94	1.01	0.86	0.94	1.02	0.86	0.94	1.01
	2.0	0.78	0.89	1.01	0.78	0.89	1.01	0.78	0.94	1.01

APPENDIX D

FIGURES AND TABLES RELATED TO ROTATIONAL SLIDES

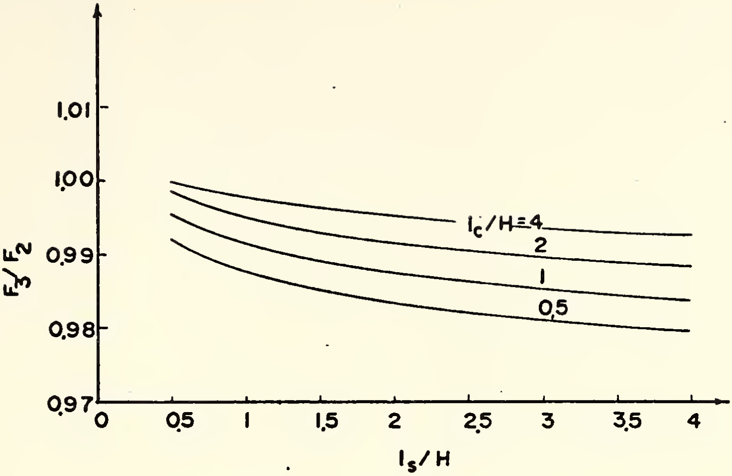

(a) $c'=0$, $\phi'=40°$

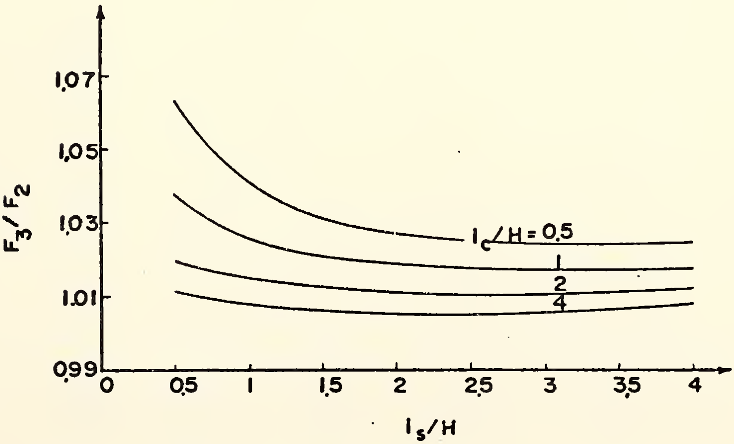

(b) $c'=7.2$ kPa, $\phi'=30°$

Fig. D.1 Ratio of F_3/F_2 (Slope 2.5/1, r_u = 0)

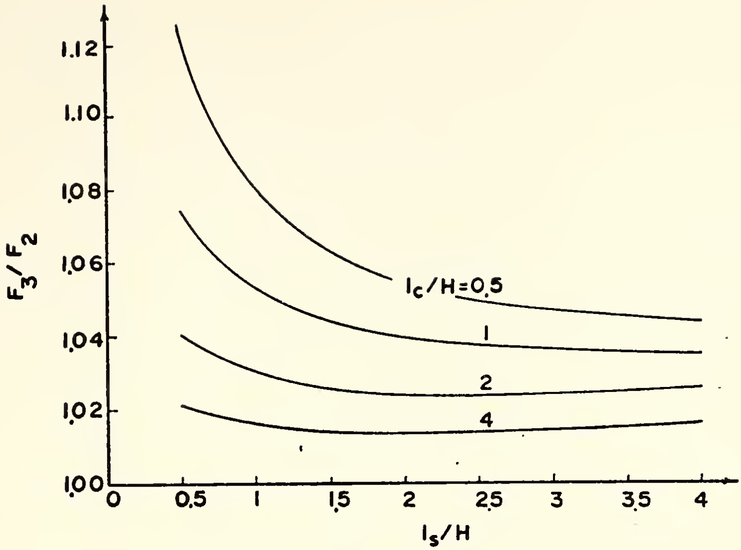

(c) c'=14.4 kPa, φ'=25°

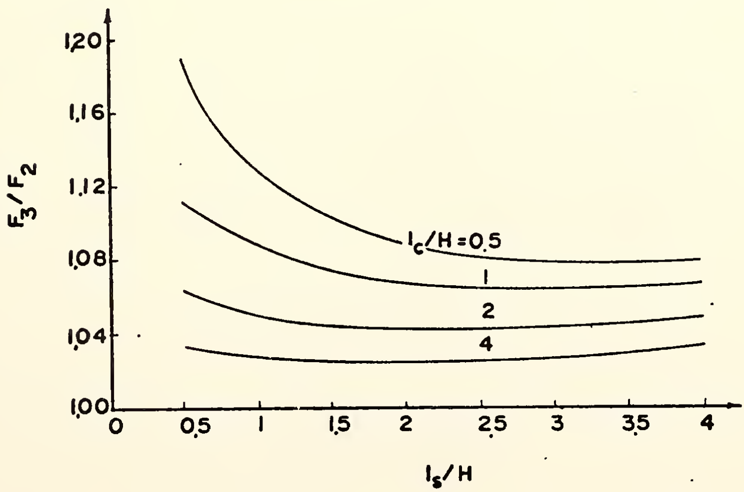

(d) c'=21.6 kPa, φ'=20°

Fig. D.1 (Cont'd)

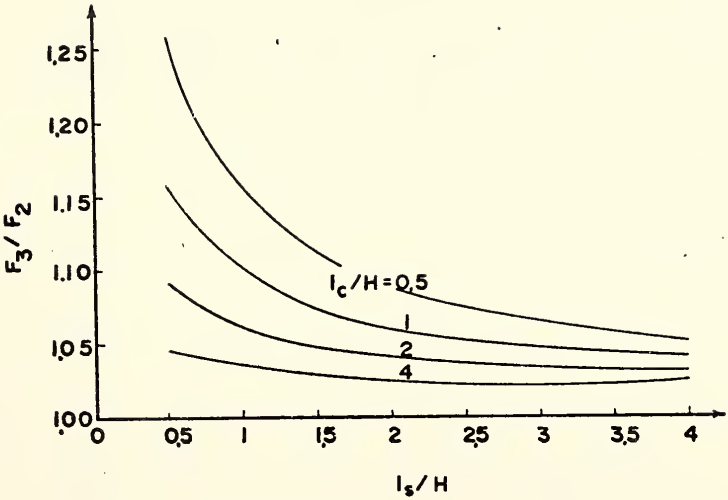

(e) $c'=28.7$ kPa , $\phi'=15°$

Fig. D.1 (Cont'd)

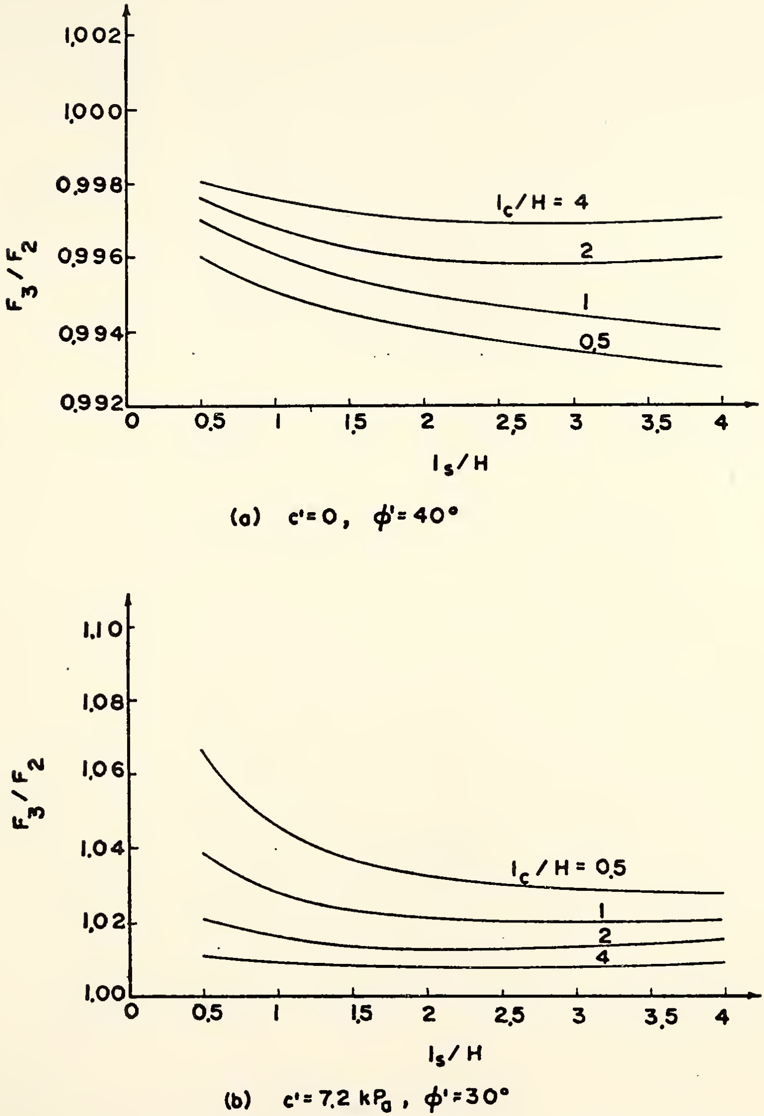

Fig. D.2 Ratio of F_3/F_2 (Slope 3.5/1, $r_u = 0$)

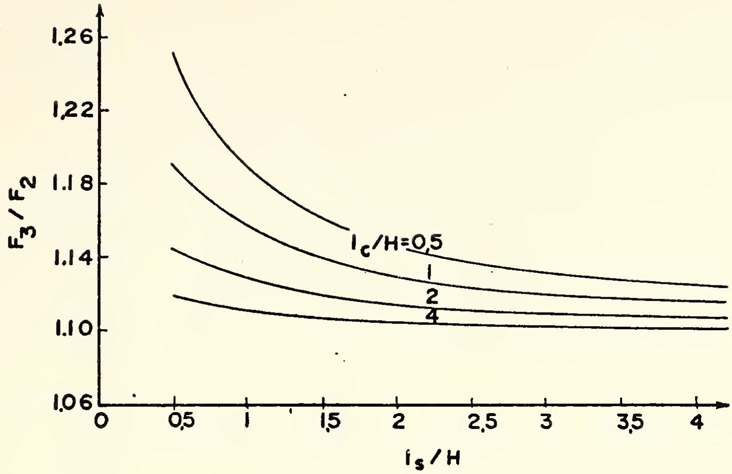

(c) $c' = 14.4$ kPa, $\phi' = 25°$

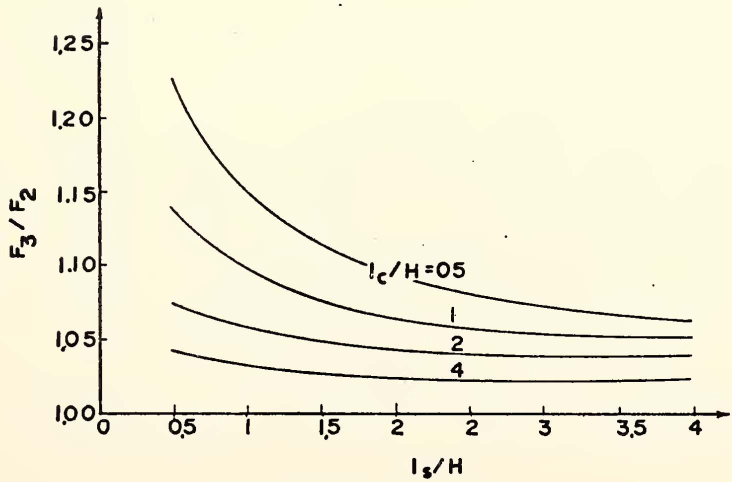

(d) $c' = 21.6$ kPa, $\phi' = 20°$

Fig. D.2 (Cont'd)

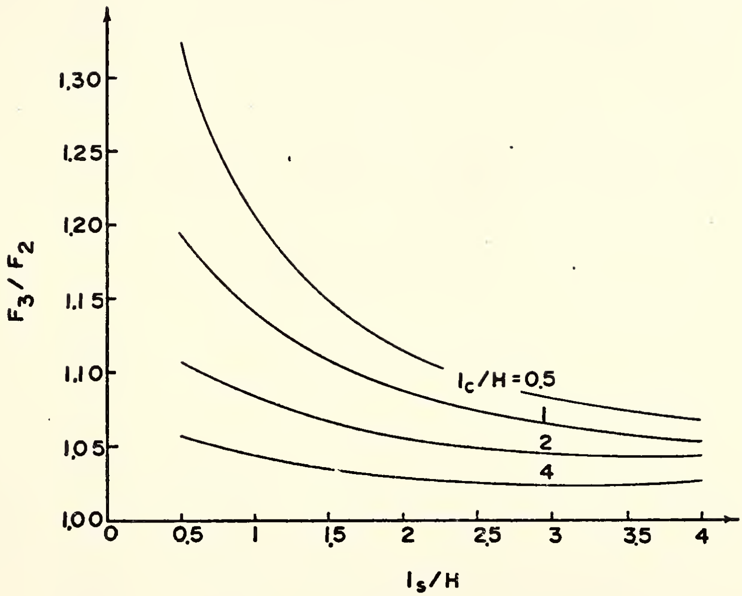

(e) $c' = 28.7$ kPa , $\phi' = 15°$

Fig. D.2 (Cont'd)

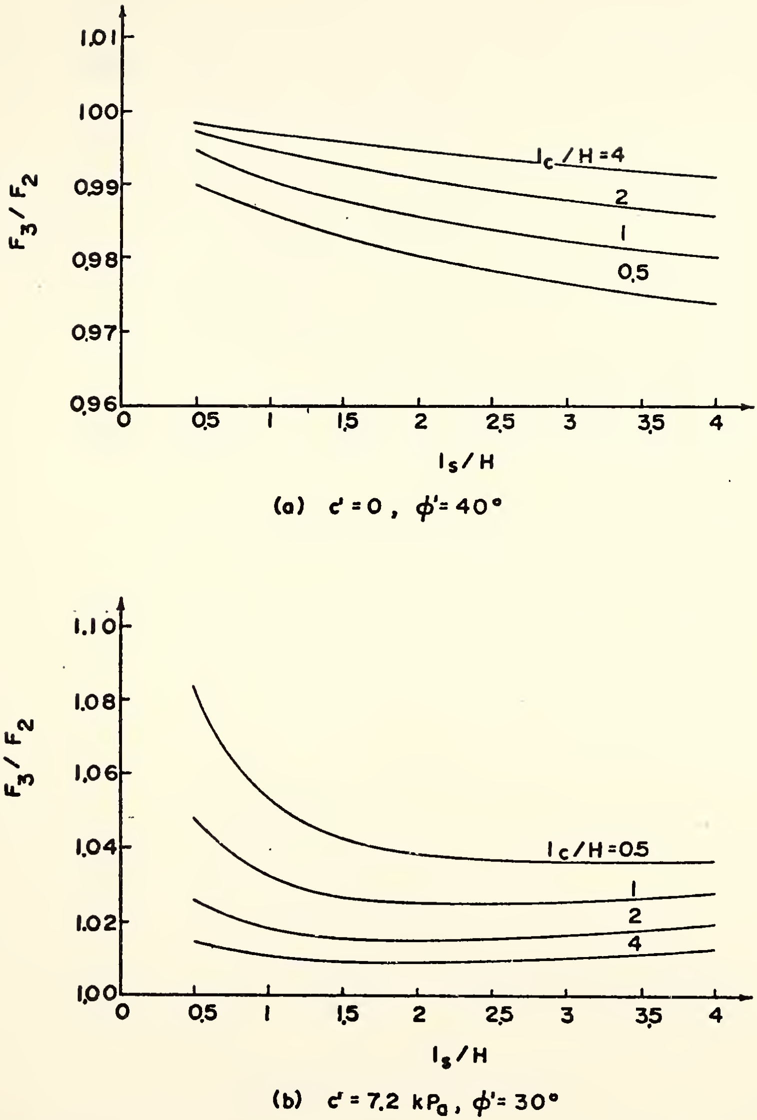

Fig. D.3 Ratio of F_3/F_2 (Slope 1.5/1, $r_u = 0.5$)

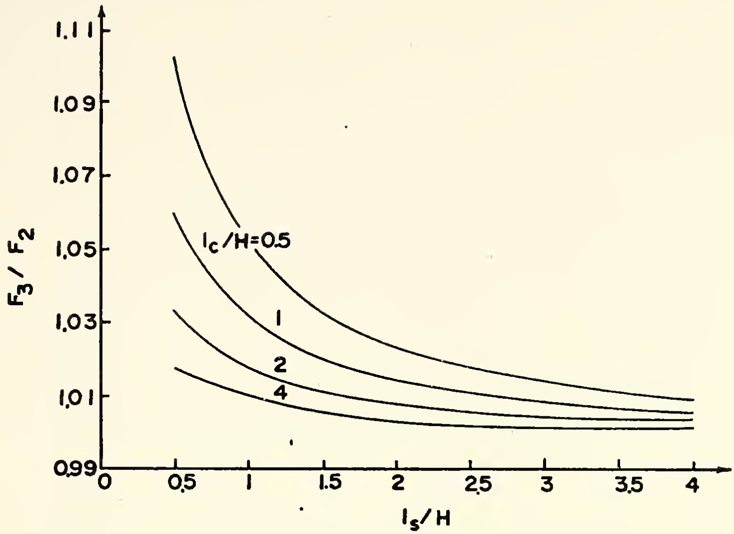

(c) $c' = 14.4$ kPa, $\phi' = 25°$

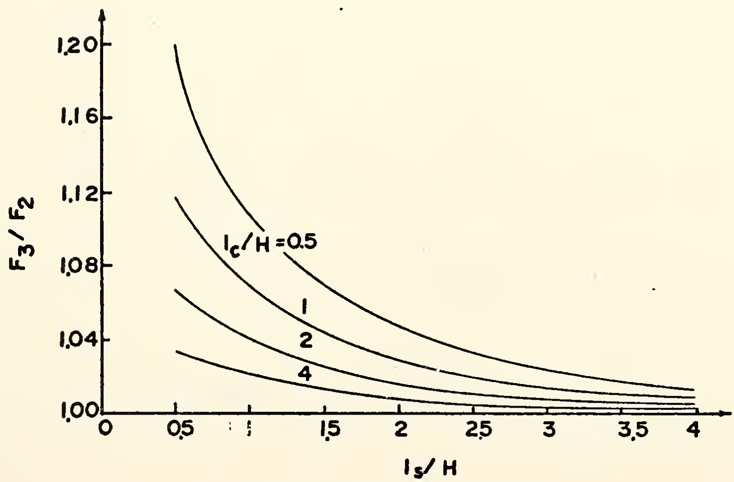

(d) $c' = 21.6$ kPa, $\phi' = 20°$

Fig. D.3 (Cont'd)

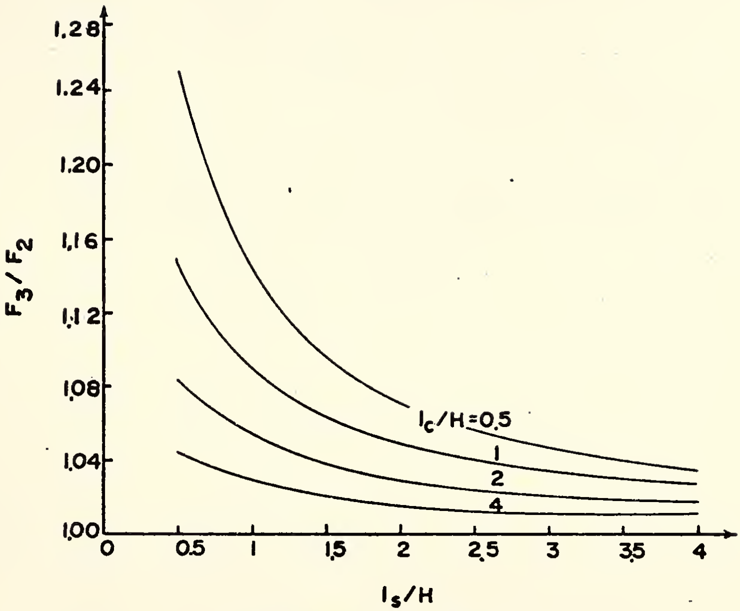

(e) $c' = 28.7$ kPa, $\phi' = 15°$

Fig. D.3 (Cont'd)

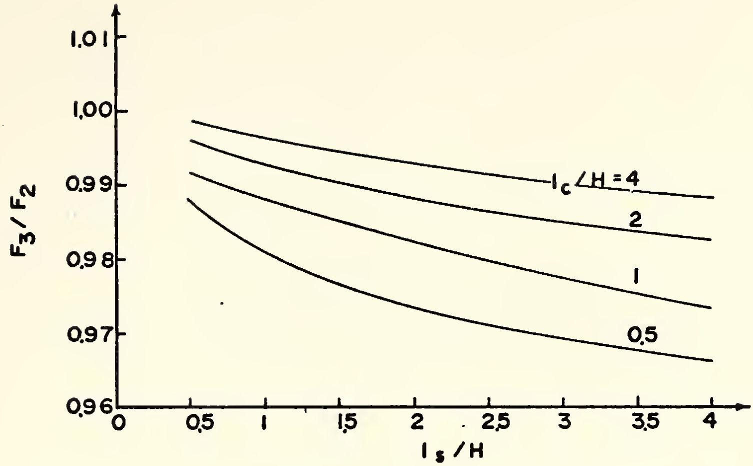

(a) $c'=0$, $\phi'=40°$

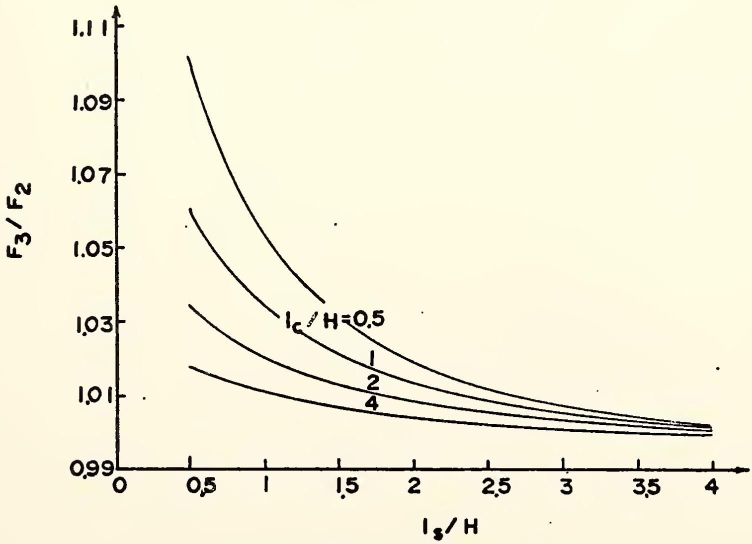

(b) $c'=7.2$ kPa , $\phi'=30°$

Fig. D.4 Ratio of F_3/F_2 (Slope 2.5/1, $r_u=0.5$)

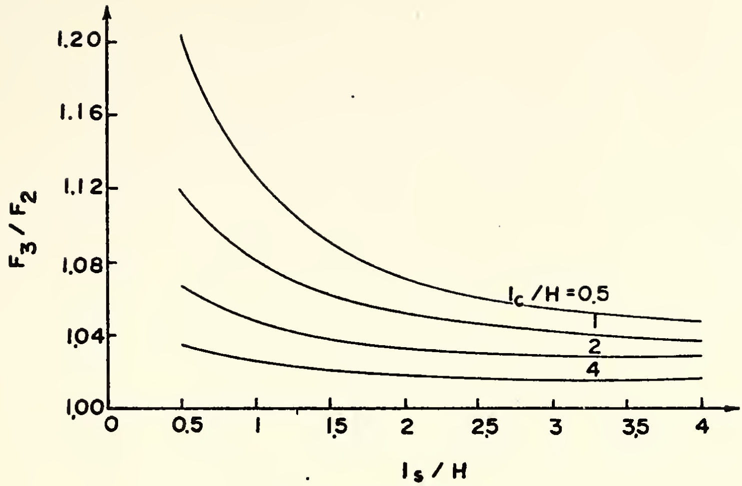

(c) $c' = 14.4$ kPa, $\phi' = 25°$

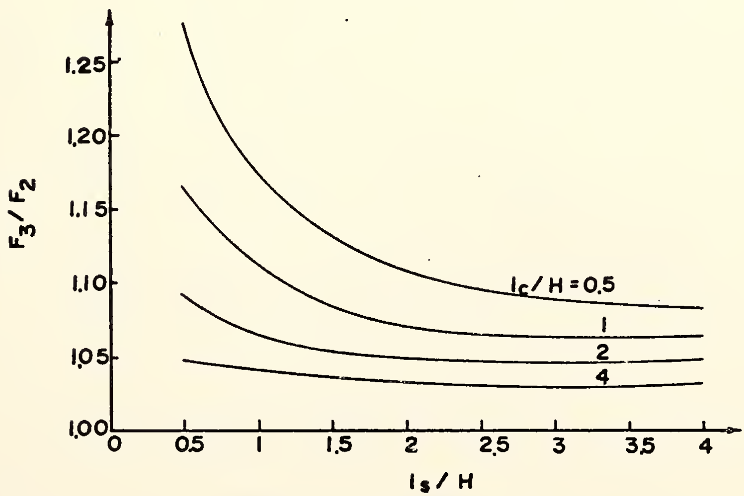

(d) $c' = 21.6$ kPa, $\phi' = 20°$

Fig. D.4 (Cont'd)

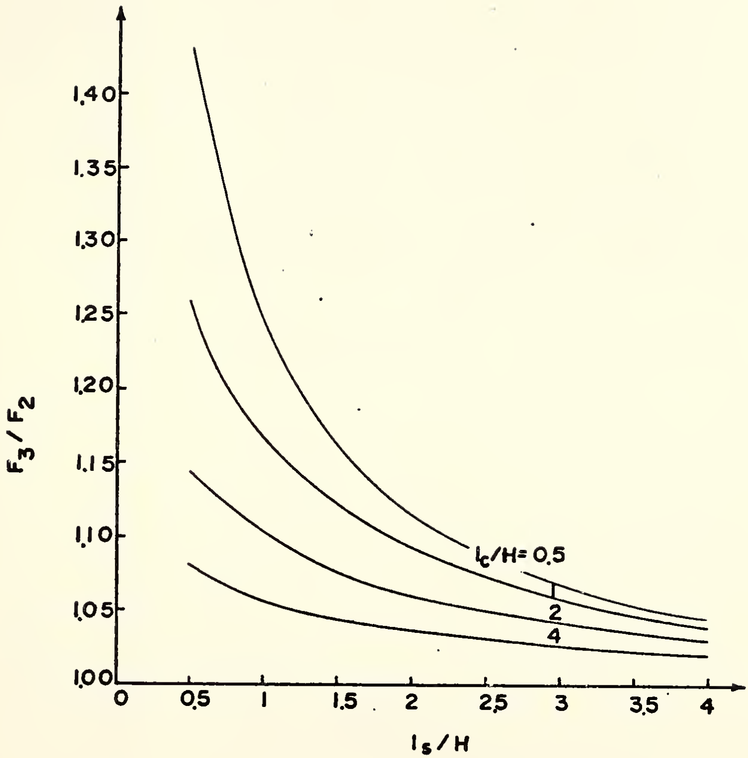

(e) $c' = 28.7$ kP , $\phi' = 15°$

Fig. D.4 (Cont'd)

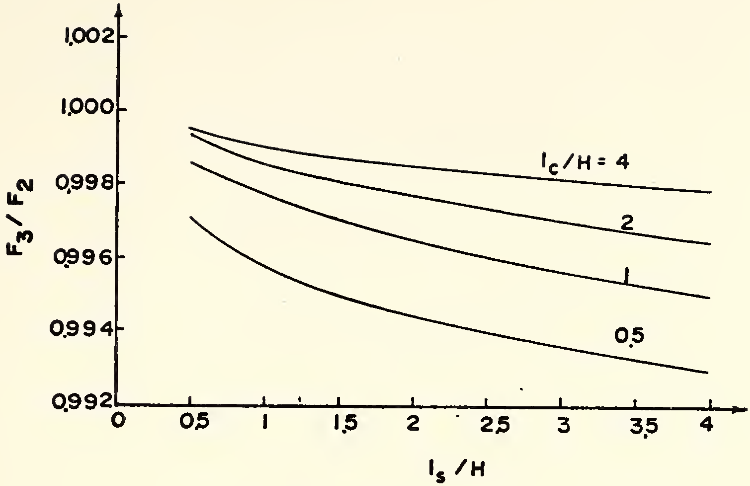

(a) $c' = 0$, $\phi' = 40°$

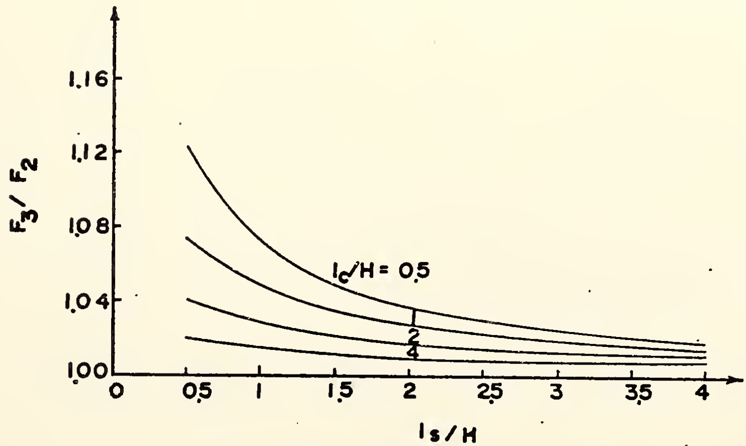

(b) $c' = 7.2$ kPa, $\phi' = 30°$

Fig. D.5 Ratio of F_3/F_2 (Slope 3.5/1, $r_u = 0.5$)

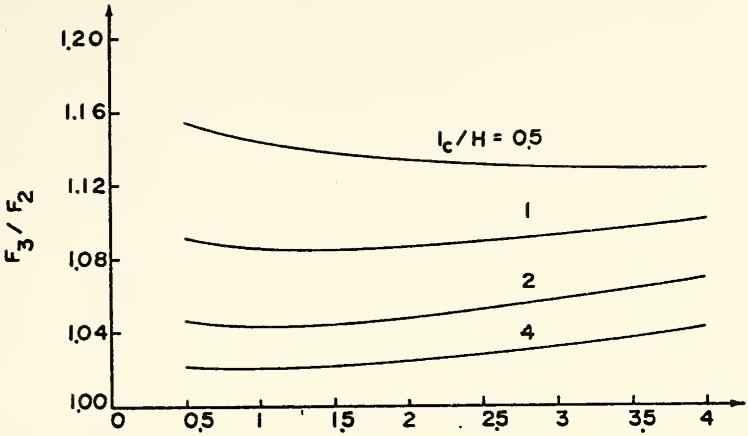

(c) $c' = 14.4$ kPa, $\phi' = 21.6°$

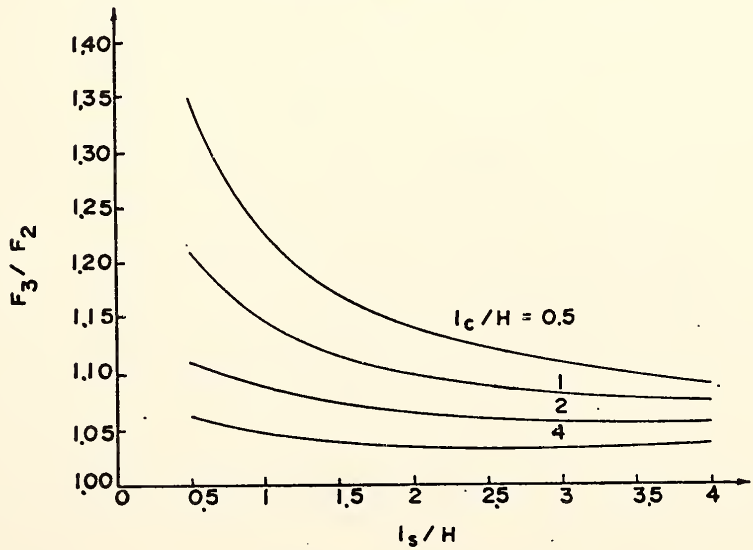

(d) $c' = 21.6$ kPa, $\phi' = 20°$

Fig. D.5 (Cont'd)

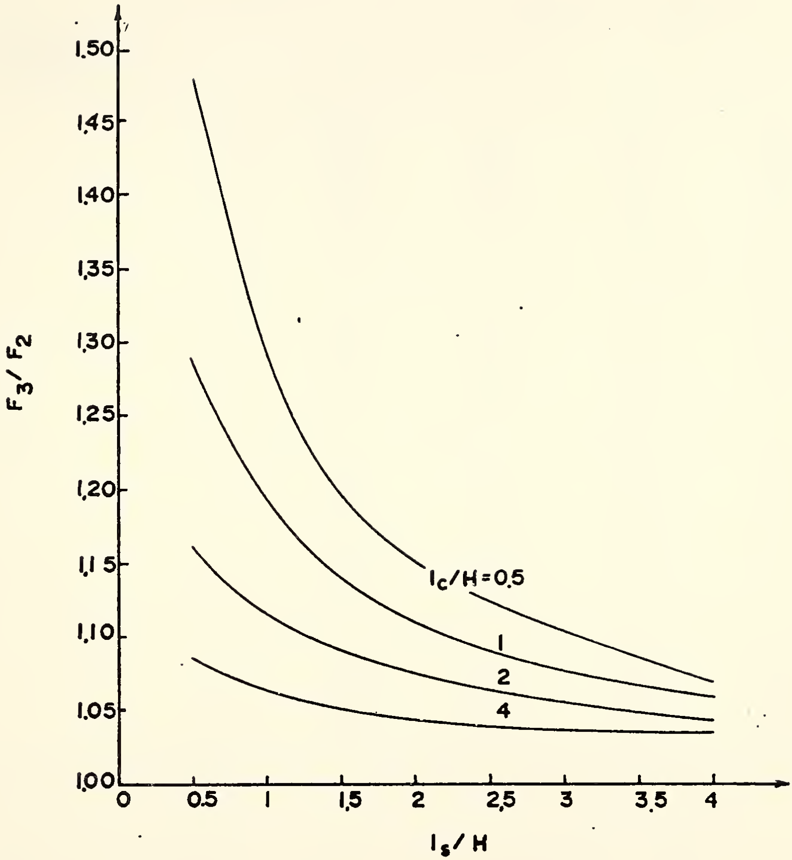

(e) $c' = 28.7$ kPa, $\phi' = 15°$

Fig. D.5 (Cont'd)

TABLE D.1 COMPARISON OF F_3 BETWEEN ORDINARY METHOD OF COLUMNS (OMC) AND LEMIX (Slope 1.5/1, r_u = 0)

$\frac{\text{OMC - LEMIX}}{\text{LEMIX}}$ x 100%			ℓ_c/H			
			0.5	1	2	4
ℓ_s/H	0.5	a*	-13.3	-11.2	-10.1	- 9.5
		b	- 8.8	- 9.2	- 9.7	-10.0
		c	- 4.1	- 4.9	- 5.5	- 6.0
		d	0.5	- 1.2	- 2.5	- 3.4
		e	3.0	1.0	- 0.9	- 2.2
	1	a	-11.4	-10.4	- 9.7	- 9.3
		b	- 9.3	- 9.4	- 9.0	- 9.0
		c	- 5.3	- 5.6	- 5.7	- 6.0
		d	- 1.6	- 2.2	- 2.9	- 3.5
		e	0	- 0.7	- 1.7	- 2.5
	2	a	- 9.6	- 9.3	- 9.2	- 9.9
		b	- 8.9	- 9.1	- 9.3	- 9.6
		c	- 5.2	- 5.4	- 5.6	- 5.9
		d	- 2.3	- 2.7	- 3.1	- 3.6
		e	- 1.5	- 1.7	- 2.2	- 1.7
	4	a	- 8.5	- 8.6	- 8.6	- 8.7
		b	- 8.5	- 8.7	- 9.0	- 9.3
		c	- 4.9	- 5.0	- 5.3	- 5.6
		d	- 2.5	- 2.7	- 3.0	- 3.4
		e	- 1.9	- 2.0	- 2.4	- 2.7

*a: c = 0, $\phi = 40^\circ$; b: c = 7.2 kPa, $\phi = 30^\circ$
c: c = 14.4 kPa, $\phi = 25^\circ$; d: c = 21.6 kPa, $\phi = 20^\circ$
e: c = 28.7 kPa, $\phi = 15^\circ$

TABLE D.2 COMPARISON OF F_3 BETWEEN ORDINARY METHOD OF COLUMNS AND LEMIX (Slope 2.5/1, r_u = 0)

$\frac{OMC - LEMIX}{LEMIX}$ x 100%			ℓ_c/H 0.5	1	2	4
$\frac{\ell_s}{H}$	0.5	a	-16.2	-13.5	-11.8	-10.8
		b	- 9.2	- 8.3	- 7.6	- 7.3
		c	- 7.5	- 7.6	- 7.8	- 8.0
		d	- 2.0	- 3.1	- 4.3	- 4.9
		e	0.1	- 1.7	- 3.3	- 4.5
	1	a	-14.9	-12.5	-11.4	-10.6
		b	- 8.7	- 8.1	- 7.6	- 7.2
		c	- 8.3	- 8.2	- 8.2	- 8.2
		d	- 3.8	- 4.2	- 4.7	- 5.2
		e	- 2.3	- 3.1	- 4.0	- 4.6
	2	a	-11.4	-10.9	-10.5	-10.2
		b	- 7.2	- 7.1	- 6.9	- 6.9
		c	- 7.8	- 7.7	- 7.8	- 8.0
		d	- 4.1	- 4.3	- 4.7	- 5.1
		e	- 3.5	- 3.8	- 4.2	- 4.8
	4	a	- 9.8	- 9.8	- 9.6	- 9.8
		b	- 6.1	- 6.2	- 6.3	- 6.6
		c	- 6.9	- 7.0	- 7.2	- 7.6
		d	- 3.8	- 4.1	- 4.4	- 4.7
		e	- 3.5	- 3.8	- 4.1	- 4.8

TABLE D.3 COMPARISON OF F_3 BETWEEN ORDINARY METHOD OF COLUMNS AND LEMIX (Slope 3.5/1, r_u = 0)

$\frac{\text{OMC - LEMIX}}{\text{LEMIX}}$ x 100%			ℓ_c/H			
			0.5	1	2	4
$\frac{\ell_s}{H}$	0.5	a	- 7.3	- 4.9	- 3.6	- 2.9
		b	- 7.7	- 6.8	- 6.3	- 5.9
		c	- 9.7	- 9.3	- 9.1	- 8.9
		d	- 4.3	- 5.0	- 5.8	- 6.1
		e	- 0.1	- 1.8	- 3.6	- 4.8
	1	a	- 6.5	- 4.6	- 3.5	- 2.8
		b	- 7.9	- 7.0	- 6.4	- 6.0
		c	-10.5	- 9.9	- 9.4	- 9.2
		d	- 5.9	- 5.9	- 6.2	- 6.4
		e	- 3.2	- 3.7	- 4.5	- 5.3
	2	a	- 4.6	- 3.7	- 3.0	- 2.6
		b	- 6.6	- 6.2	- 5.8	- 5.8
		c	- 9.3	- 9.2	- 9.0	- 8.9
		d	- 5.8	- 5.8	- 6.0	- 6.2
		e	- 4.5	- 4.7	- 4.9	- 5.4
	4	a	- 3.0	- 2.7	- 2.6	- 2.4
		b	- 5.2	- 5.2	- 5.2	- 5.2
		c	- 7.9	- 8.1	- 8.2	- 8.3
		d	- 5.1	- 5.2	- 5.5	- 6.0
		e	- 4.5	- 4.6	- 4.9	- 5.3

TABLE D.4 COMPARISON OF F_3 BETWEEN ORDINARY METHOD OF COLUMNS AND LEMIX (Slope 1.5/1, r_u = 0.5)

$\frac{OMC - LEMIX}{LEMIX}$ x 100%			ℓ_c/H			
			0.5	1	2	4
$\frac{\ell_s}{H}$	0.5	a*	0.8	5.0	7.5	8.9
		b	9.2	8.5	8.1	7.7
		c	6.8	4.4	2.4	1.8
		d	7.7	4.6	2.1	0.2
		e	10.6	7.2	4.1	1.8
	1	a	2.2	5.4	7.5	8.8
		b	8.9	8.7	8.2	7.9
		c	4.2	3.1	2.0	0.9
		d	3.3	2.2	0.9	- 0.3
		e	6.0	4.5	3.6	1.4
	2	a	6.0	7.4	8.6	9.3
		b	9.5	9.2	8.6	8.1
		c	3.0	2.5	1.7	0.9
		d	1.0	0.7	0.1	- 0.7
		e	2.8	2.4	1.8	0.9
	4	a	9.2	9.5	9.7	10.1
		b	10.0	9.7	9.1	8.6
		c	2.9	2.5	1.9	1.3
		d	0.4	0.1	- 0.3	- 0.8
		e	1.6	1.4	1.1	0.6

* a: $c' = 0$, $\phi' = 40^\circ$; b: c' = 7.2 kPa, $\phi' = 30^\circ$

c: c' = 14.4 kPa, $\phi' = 25^\circ$; d: c' = 21.6 kPa; $\phi' = 20^\circ$

d: c' = 28.7 kPa, $\phi' = 15^\circ$

TABLE D.5 COMPARISON OF F_3 BETWEEN ORDINARY METHOD OF COLUMNS AND LEMIX (Slope 2.5/1, r_u = 0.5)

$\frac{OMC - LEMIX}{LEMIX}$ x 100%			ℓ_c/H 0.5	1	2	4
$\frac{\ell_s}{H}$	0.5	a	- 3.7	- 0.1	1.9	3.0
		b	- 6.6	- 6.0	- 5.8	- 5.7
		c	0.2	- 0.7	- 1.5	- 2.2
		d	3.8	2.2	0.8	- 0.2
		e	4.5	2.3	0.1	- 1.8
	1	a	- 1.9	0.4	2.1	3.0
		b	- 7.2	- 5.9	- 6.0	- 5.8
		c	- 1.4	- 1.6	- 2.0	- 2.3
		d	0.2	1.1	0.3	- 0.4
		e	1.0	0.1	- 1.1	- 2.3
	2	a	1.4	2.1	3.0	3.6
		b	- 5.7	- 5.6	- 5.6	- 5.4
		c	- 1.9	- 1.7	- 2.0	- 2.3
		d	0.7	1.4	0	- 0.4
		e	- 1.1	- 1.7	- 2.1	- 2.7
	4	a	3.8	4.0	4.1	4.2
		b	- 4.3	- 4.7	- 4.7	- 4.9
		c	- 1.0	- 1.2	- 1.6	- 1.9
		d	0.7	0.6	0.2	- 0.3
		e	- 1.9	- 2.1	- 2.5	- 2.8

TABLE D.6 COMPARISON OF F_3 BETWEEN ORDINARY METHOD OF COLUMNS AND LEMIX (Slope 3.5/1, r_u = 0.5)

$\frac{\text{OMC - LEMIX}}{\text{LEMIX}}$ x 100%			ℓ_c/H			
			0.5	1	2	4
$\frac{\ell_s}{H}$	0.5	a	- 0.9	1.6	3.2	4.0
		b	- 8.5	- 7.7	- 7.3	- 7.0
		c	21.2	18.2	14.5	11.8
		d	4.0	1.7	- 0.6	- 2.3
		e	6.3	3.4	0.5	- 1.7
	1	a	- 0.1	1.9	3.2	4.1
		b	- 9.0	- 8.2	- 7.5	- 7.1
		c	14.0	13.9	12.7	11.1
		d	- 0.2	- 0.9	- 1.8	- 3.0
		e	1.8	0.6	- 1.0	- 2.3
	2	a	2.2	3.0	3.8	4.3
		b	- 7.4	- 7.1	- 6.9	- 6.8
		c	10.6	11.4	11.3	10.6
		d	- 2.5	- 2.4	- 2.7	- 3.2
		e	- 1.2	- 1.5	- 5.0	- 3.0
	4	a	4.0	4.2	4.4	4.6
		b	- 5.6	- 5.8	- 5.9	- 6.2
		c	10.0	10.4	10.5	10.2
		d	- 2.9	- 2.9	- 3.0	- 3.3
		e	- 2.2	- 2.5	- 2.8	- 2.7

APPENDIX E

User's Guide for Computer Programs BLOCK3, LEMIX, and FESPON

User's guide for computer programs BLOCK3, LEMIX, and FESPON is presented in this section. For each program there is an example to show how the input data are prepared and to provide output which can be used to check the operation of the computer programs:

Example Problem 1 - BLOCK3

Example Problem 2 - LEMIX

Example Problem 3 - FESPON

It should be noted that the meshes used in example 3 are too coarse to give accurate results. For accurate values of stress and displacement within an embankment, eight or more layers of elements should be used, and the number of elements should be larger than the ones in this example.

In all three samples, the units are in metric system.

E.1 User's Guide for Program BLOCK3

1. Strength Parameter Card (6F10.0)

1-10	C	- Cohesion of foundation or embankment soil
11-20	FI	- Friction angle of foundation or embankment soil, degrees
21-30	G	- Unit weight or density of foundation or embankment soil
31-40	CB	- Cohesion of weak layer
41-50	FIB	Friction angle of weak layer, degrees
51-60	UK	- Earth pressure coefficient in the foundation or embankment

2. Geometric Data Card (7F10.0)

1-10	TL	- The upper length at the top of the central block
11-20	H	- Height of embankment
21-30	SLOPE	- Slope angle of embankment, degrees
31-40	A	- The ratio of the lower length to upper length at the top of the central block
41-50	D	- Depth ratio; depth (to weak layer) to height of embankment
51-60	BETA	- Inclination of weak soil layer, degrees
61-70	GAMA	- Unit weight or density of weak layer

3. Surcharge Card (2F10.0)

1-10	SURA	- Surcharge on active block
11-20	SURP	- Surcharge on passive block

4. Initial Guess Value Card (F10.0)

1-10 X(1) - Initial guess value of the factor of safety

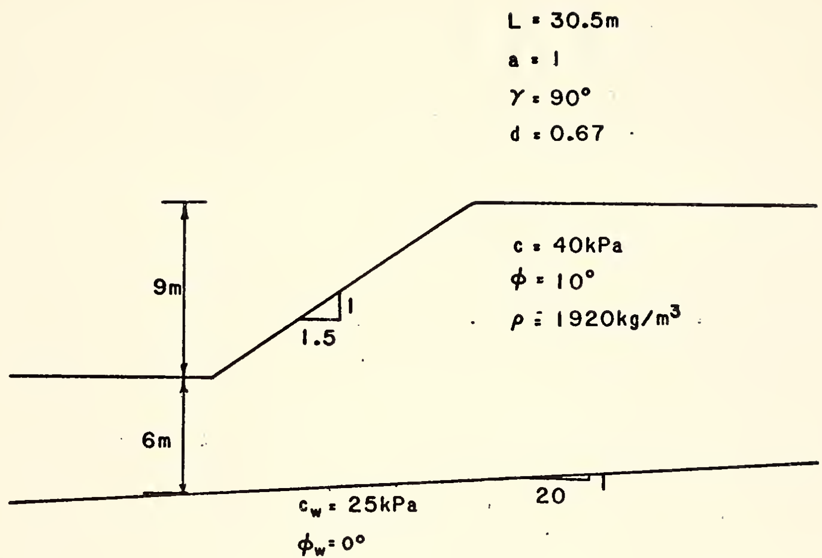

Fig. E.1 Example Problem for Program BLOCK3

UNIT WT	C	FI	CB	FIB
18.81	40.00	10.00	25.00	0

LENGTH	HT	SLOPE	A	D	BETA	GAMA	ALFA	SF
30.50	9.00	33.70	1.00	.67	2.90	90.00	0	2.01

Fig. E.2 Output Data for Program BLOCK3

```
      PROGRAM BLOCK3(INPUT,OUTPUT,TAPE5=INPUT,TAPE6=OUTPUT)
      DIMENSION X(1)
      COMMON/MATL/ TF,TFB,TANA,TANP
      COMMON/FORS/ FAS,FS,FPS,WA,W,WP,CAS,CAB,CCS,CCB,CPS,CPB
      COMMON/GEOM/ COSA,COSB,COSP,SINB,COSKSI,COSETA
      EXTERNAL FCN

C     ******************************************************************

C     READ AND WRITE INPUT DATA

C     ******************************************************************

      READ(5,2000) C,FI,G,CB,FIB,UK
      READ(5,2010) TL,H,SLOPE,A,D,BETA,GAMA
      READ(5,2020) SURA,SURP
      READ(5,2040) XINITI

      PI=3.1415926/180.


      SLOPE=SLOPE*PI
      FI=FI*PI
      TF=TAN(FI)
      FIB=FIB*PI
      TFB=TAN(FIB)
      Q1=45.*PI-FI/2.
      TANP=TAN(Q1)
      COSP=COS(Q1)
      Q2=45.*PI+FI/2.
      TANA=TAN(Q2)
      Q5=FI
      GAMA=GAMA*PI
      BETA=BETA*PI
      Q6=BETA
      COSB=COS(Q6)
      SINB=SIN(Q6)
      Q7=GAMA
      H1=D*H
      B=H/TAN(SLOPE)
      H2=H1+H-B*TAN(Q6)
      COSA=1./SQRT(1.+(COSB*(TL*(1.-A)/2.-(H2-H1)/TAN(GAMA))/B)**2)
      COSETA=1./SQRT(1.+(SIN(PI/4.+FI/2.)/TAN(GAMA))**2)
      COSKSI=1./SQRT(1.+(SIN(PI/4.-FI/2.)/TAN(GAMA))**2)

C     ******************************************************************

C     ACTIVE BLOCK

C     ******************************************************************

      SURA=SURA*TL*H2*TAN(Q1)
      WA=G*H2*H2*TAN(Q1)*(0.5*TL-H2/TAN(Q7)/3.)+SURA
      CAS=0.5*C*H2*H2*TAN(Q1)/SIN(Q7)
      CAB=C*(TL-H2/TAN(Q7))*H2/COS(Q1)
      FAS=UK *G*H2*H2*H2*TAN(Q1)*TAN(Q5)/(6.*SIN(Q7))

C     ******************************************************************

C     PASSIVE BLOCK

C     ******************************************************************

      SURP=SURP*A*TL*H1*TAN(Q2)
```

```
      WA=G*H2*H2*TAN(Q1)*(0.5*TL-H2/TAN(Q7)/3.)+SURA
      CAS=0.5*C*H2*H2*TAN(Q1)/SIN(Q7)
      CAB=C*(TL-H2/TAN(Q7))*H2/COS(Q1)
      FAS=UK *G*H2*H2*H2*TAN(Q1)*TAN(Q5)/(6.*SIN(Q7))
C     ****************************************************************
C     PASSIVE BLOCK
C     ****************************************************************
      SURP=SURP*A*TL*H1*TAN(Q2)
      WP=G*H1*H1*TAN(Q2)*(0.5*A*TL-H1/TAN(Q7)/3.)+SURP
      CPS=0.5*C*H1*H1*TAN(Q2)/SIN(Q7)
      CPB=C*(A*TL-H1/TAN(Q7))*H1/COS(Q2)
      FPS=UK *G*H1*H1*H1*TAN(Q2)*TAN(Q5)/(6.*SIN(Q7))
C     ****************************************************************
C     CENTRAL BLOCK
C     ****************************************************************
      B1=H2*(TL-H2/TAN(Q7))
      B2=H1*(A*TL-H1/TAN(Q7))
      BM=(H1+H2)*((1.+A)*TL-(H1+H2)/TAN(Q7))
      W=G*B*(B1+B2+BM)/6.
      CCS=0.5*C*B*(H1+H2)/(SIN(Q7)*COS(ALFA))
      CCB=CB*(0.5*(1.+A)*TL-(H1+H2)/TAN(Q7))*B/COS(Q6)
      FS=UK *G*B*(H1*H1+H2*H2+H1*H2)*TAN(Q5)/(6.*SIN(Q7)*COS(ALFA)*
     *  COS(Q6))
C     ****************************************************************
C     CALAULATE THE FACTOR OF SAFETY
C     ****************************************************************
      X(1)=XINITI
      N=1
      NDIGIT=7
      RNORM=0.
      CALL SECANT(X,N,FCN,NDIGIT,RNORM)
      SF=X(1)


      PFI=FI/PI
      PFIB=FIB/PI
      PSLOPE=SLOPE/PI
      PBETA=BETA/PI
      PGAMA=GAMA/PI
      PLFA=ALFA/PI
      WRITE(6,1000) G,C,PFI,CB,PFIB,TL,H,PSLOPE,A,D,PBETA,PGAMA,PLFA,SF



10    FORMAT(132H1  UNIT WT        C        FI        CB       FIB   LENGTH
     *      HT     SLOPE        AR        DR       BETA      GAMA      ALFA
     *    SF             //)
1000  FORMAT(8F9.1,2F9.2,2F9.1,F9.2,F10.2)
2000  FORMAT(6F10.0)
2010  FORMAT(7F10.0)
```

```
2020  FORMAT(2F10.0)

2040  FORMAT( F10.0)

      STOP
      END



      SUBROUTINE FCN(X,F,UDF)
      DIMENSION X(1),F(1)
      COMMON/MATL/ TF,TFB,TANA,TANP
      COMMON/FORS/ FAS,FS,FPS,WA,W,WP,CAS,CAB,CCS,CCB,CPS,CPB
      COMMON/GEOM/ COSA,COSB,COSP,SINB,COSKSI,COSETA

      F(1)=(2.*(CCS+FS/SQRT(1.+(X(1)/TF)**2))*COSA+CCB+TFB*W*COSB)/X(1)
     1 -W*SINB+(COSB+TFB*SINB/X(1))*(WP*(TANP+TF/X(1))/(1.-TANP*TF/X(1))
     2 -WA*(TANA-TF/X(1))/(1.+TANA*TF/X(1))+COSP*(1./X(1))*((2.*CPS*
     3 COSKSI+CPB+2.*FPS*COSKSI/SQRT(1.+(X(1)/TF)**2))*(1.+TANP*(
     4 TANP+TF/X(1))/(1.-TANP*TF/X(1)))+(2.*CAS*COSETA+CAB+2.*FAS
     5 *COSETA/SQRT(1.+(X(1)/TF)**2))*(TANP+(TANA-TF/X(1))/
     6 (1.+TANA*TF/X(1)))))

      RETURN
      END
```

E.2 User's Guide for Program LEMIX

1. Embankment Information Card (8F10.2)

1-10	C	- Cohesion of embankment soil
11-20	FI	- Friction angle of embankment soil, degrees
21-30	GAMA	- Unit weight or density of embankment soil
31-40	RU	- Pore water pressure parameter, r_u
41-50	BETA	- Slope angle of embankment, degrees
51-60	H	- Height of embankment
61-70	EK	- Earth pressure coefficient in embankment
71-80	GW	- Unit weight or density of water

2. Foundation Information Card (5F10.2)

1-10	CF	- Cohesion of foundation soil
11-20	FIF	- Friction angle of foundation soil, degrees
21-30	GAMAF	- Unit weight or density of foundation soil
31-40	HTF	- The distance between the crest and foundation
41-50	FK	- Earth pressure coefficient in foundation

3. Critical Circle Information Card (4F10.2, 3I5)

1-10	RXY	- The radius of the 2-D critical circle, R_{xy}
11-20	RZ	- The length of minor axis of the semi-ellipsoid
21-30	CX1	- X-distance, from center to crest
31-40	Y	- Y-distance, from center to crest
41-45	NCOLUM	- Number of columns along Z-direction
46-50	NSLICE	- Number of slices along X-Y plane
51-55	IFTC	- Zero, if tension crack is not considered; otherwise punch one

4. Miscellaneous Card (4F10.2, 4I5)

1-10	TWOD	- The ratio between half of the length of the central cylinder to the height of the slope
11-20	EX	- The exponential number of X-coordinate. One means the shear stress distribution is linear, two means the distribution is hyperbolic, etc.
21-30	FACTS	- The ratio between the subsequent length to former length of the minor axis of the spoon
31-40	FACTR	- The ratio between the subsequent length to former length of the central cylinder
41-45	NSP	- Number of various spoons investigated
46-50	NRL	- Number of various cylinders investigated
51-55	ICOND	- One, if the results from the Ordinary Method of Columns need to be printed out; otherwise, punch zero
56-60	IPRINT	- One, if the information of width, height, area, and weight of the columns need to be printed out; Otherwise, punch zero

5. Initial Guess Value Cards (2F10.2)

1-10	X(1)	- The initial guess value of the factor of safety
11-20	X(2)	- The initial guess value of the angle of inclination, degrees

These cards must be read for as many times as the number of NSP x NRL.

REMARKS:

The value of RNORM in the output indicates

- If RNORM = 0.0, then X is a root of the given system of equations to machine accuracy.
- If RNORM .GT. 0.0 then the relative convergence criterion was satisfied. In this case RNORM = F(1)**2 + ... + F(N)***2 where F contains the function values at X, N the number of nonlinear equations to be solved.

- If RNORM = -1.0, then SECANT was unable to find a better approximation than the current X. If this approximation is not good enough the user may try a new initial guess.
- If RNORM = -2.0 then the maximum number of iterations was exceeded. The user may try a new initial guess value.
- If RNORM = -3.0 then SECANT was forced to stop because it was unable to improve the approximation to the root. The user may try a new initial guess.

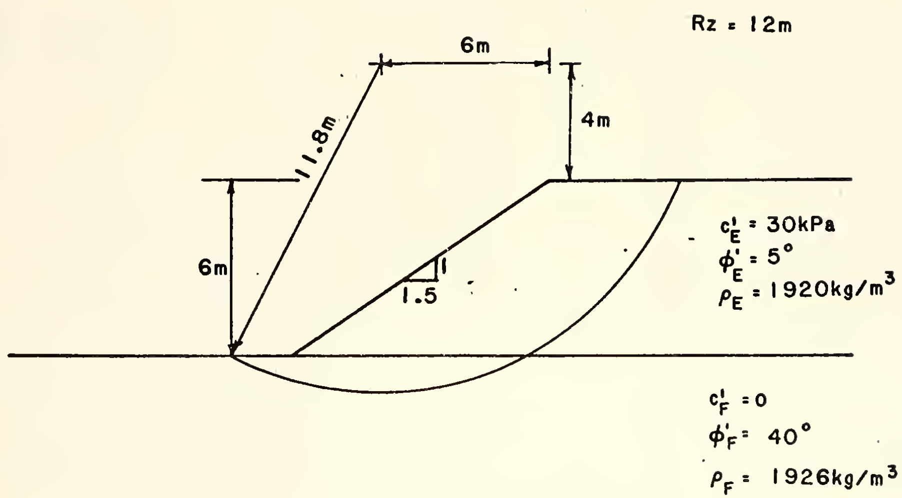

Fig. E.3 Example Problem for Program LEMIX

EMBANKMENT HEIGHT**************************	6.000
SLOPE ANGLE********************************	33.690
NUMBER OF SLICES**************************	30
NUMBER OF COLUMNS*************************	10
BIG RADIUS*********************************	11.180
SMALL RADIUS*******************************	12.000
X-DIST. FROM CENTER TO CREST**************	6.000
Y-DIST. FROM CENTER TO CREST**************	4.000
TENSION CRACK******************************	0
EXPONENTIAL NUMBER************************	1.000

**********EMBANKMENT PARAMETERS*********

C	FI	GAMA	RU
30.00	5.00	18.81	0

**********FOUNDATION PARAMETERS*********

C	FI	GAMA	HTF
0	40.00	18.86	6.00

THE WIDTH OF CURVE SHAPE IS***************	9.641
HALF WIDTH OF UNIFORM CROSS SECTION IS***	.006

	FS	THET	RNORM
2-D (SPENCER)	2.375	14.839	.000
3-D	2.408	11.612	.000
3-D (ORDINARY)	2.420		

Fig. E.4 Output Data for Program LEMIX

```
      PROGRAM LEMIX(INPUT,OUTPUT,TAPE5=INPUT,TAPE6=OUTPUT)
      COMMON/MATL/ GAMA,GAMAF,C,CF,TF,TFF,RU,W2,W3,GW
      COMMON/GEOM1/ AXY,AYZ,SLFA,PLFA,YS,YF,HE,HF,SHE,SHF
      COMMON/GEOM2/ R,RAD,BAREA,DX,DZ,DTL,EK,FK
      COMMON/MISL/ NSLICE,NCOLUM,ITER,FW2,FW3,DISTRI
      DIMENSION AXY(50,20),AYZ(50,20),SLFA(50,20),PLFA(50),ALFA(50)
      DIMENSION BAREA(50,20),THET(20)
      DIMENSION RAD(20),YS(50),YP(50),SHE(50,20),SHF(50,20)
      DIMENSION HE(50,20),HF(50,20),YE(50),YF(50),DISTRI(20)
      DIMENSION X(20),XX(50),YY(50),ZZ(50),DX(50),Z(50,20),DZ(50,20)
      DIMENSION FW2(50),FW3(50,20),WH(50,20),W2(50),W3(50,20)
      EXTERNAL FCN
C     ******************************************************************
C     INPUT PARAMETERS
C     ******************************************************************
      READ 1000, C,FI,GAMA,RU,BETA,H,EK,GW
      READ 1010, CF,FIF,GAMAF,HTF,FK
      READ 1020, RXY,RZ,CX1,Y,NCOLUM,NSLICE,IFTC
      READ 1030, TWOD,EX,FACTS,FACTR,NSP,NRL,ICOND,IPRINT
      TC1=1.33*C*SQRT((1.+SIN(FI/57.29577951))/(1.-SIN(FI/57.29577951)))
     * /GAMA
      IF(IFTC .EQ. 0) TC1=0.
      PRINT 2000, H,BETA,NSLICE,NCOLUM,RXY,RZ,CX1,Y,TC1,EX
      PRINT 2010
      PRINT 2020, C,FI,GAMA,RU
      PRINT 2030
      PRINT 2040, CF,FIF,GAMAF,HTF
      R=RXY
      ENA=R*R/(RZ*RZ)
      FI=FI/57.29577951
      FIF=FIF/57.29577951
      TF=TAN(FI)
      TFF=TAN(FIF)
      BETA=BETA/57.29577951
      TB=TAN(BETA)
      RU=RU*GAMA
C     ******************************************************************
C     GEOMETRY OF THE SLOPE
C     ******************************************************************
      THET1=ASIN(Y/R)
      XC=R*COS(THET1)
      HX=XC-CX1
      THET2=ATAN(Y/(XC-HX))-THET1
      EF=H/SIN(BETA)
      OE=Y/SIN(THET1+THET2)
      OF=SQRT(EF**2+OE**2-2.*EF*OE*COS(THET1+THET2+BETA))
      THET3=ASIN(H*SIN(THET1+THET2+BETA)/(SIN(BETA)*OF))
      TOTHET=THET1+THET2+THET3+BETA
      RSIN=R*SIN(THET1+THET2+THET3)
      IF(RSIN-(Y+H)) 6,5,5
5     THET4=3.1415926-ASIN(OF*SIN(THET1+THET2+THET3)/R)-THET1-THET2
     * -THET3
      GO TO 7
6     THET4=3.1415926-ASIN(OE*SIN(THET1+THET2+BETA)/R)-TOTHET
7     Y0=OE*SIN(3.1415926-THET1-THET2-BETA)/COS(BETA)
```

```
      CX2=XC-HX-H/TB
      CX3=R*COS(THET1+THET2+THET3+THET4)
      TT1=THET1*57.29577951
      TT2=THET2*57.29577951
      TT3=THET3*57.29577951
      TT4=THET4*57.29577951

      ANG1=ASIN(SIN(THET1)+TC1/R)
      ANGLE=THET1+THET2+THET3+THET4-ANG1
      DANGLE=ANGLE/FLOAT(NSLICE)

C     READ INITIAL GUESS VALUES FOR SECANT METHOD

      ITER=1
      TWODI=TWOD
      DO 620 IS=1,NSP
      READ 1040, X(1),X(2)
      X(2)=X(2)/57.29577951

C     CALCULATE THE HEIGHT, THE WIDTH, AND THE DIP FOR EACH SLICE

      ET1=ANG1+0.5*DANGLE

      K=0
10    K=K+1
      I=K
      XX(K)=R*COS(ET1)
      CK=XX(K)-CX1
      IF(CK .LT. 0.) GO TO 50
      ZZ(K)=R*SQRT((SIN(ET1)**2-SIN(THET1)**2)/ENA)
      IF(ITER .EQ. 2) GO TO 40
      YY(K)=R*SIN(ET1)
      YS(K)=YY(K)-Y
      IF(YY(K) .GT. (Y+HTF)) GO TO 20
      YE(K)=YS(K)
      YF(K)=0.
      GO TO 30
20    YF(K)=YY(K)-(Y+HTF)
      YE(K)=YS(K)-YF(K)
30    ALFA(K)=ET1
      DX(K)=R*DANGLE*SIN(ET1)
40    ET1=ET1+DANGLE
      GO TO 10

50    I=I-1
      ET2=ET1
60    I=I+1
      L=I
      XX(I)=R*COS(ET2)
      IF(THET4 .LT. 0. .AND. XX(I) .LE. CX3) GO TO 150
      IF(XX(I) .LT. CX2) GO TO 100
      ZZ(I)=SQRT((R*R-XX(I)**2-(XX(I)*TB-Y0)**2)/ENA)
      IF(ITER .EQ. 2) GO TO 90
      DX(I)=R*DANGLE*SIN(ET2)
      YY(I)=R*SIN(ET2)
      YS(I)=YY(I)-Y-Y*TB/TAN(THET1+THET2)+XX(I)*TB
      IF(YY(I) .GT. (Y+HTF)) GO TO 70
      YE(I)=YS(I)
      YF(I)=0.
      GO TO 80
70    YF(I)=YY(I)-(Y+HTF)
      YE(I)=YS(I)-YF(I)
80    ALFA(I)=ET2
90    ET2=ET2+DANGLE
```

```
      GO TO 60
100   IF(THET4 .LT. DANGLE) GO TO 150
      L=L-1
      ET3=ET2
110   L=L+1
      XX(L)=R*COS(ET3)
      IF(XX(L) .LT. CX3) GO TO 150
      IF(L .GT. NSLICE) GO TO 150
      ZZ(L)=SQRT((R*R-XX(L)**2-(Y+H)**2)/ENA)
      IF(ITER .EQ. 2) GO TO 140
      DX(L)=R*DANGLE*SIN(ET3)
      YY(L)=R*SIN(ET3)
      YS(L)=YY(L)-R*SIN(ANGLE+ANG1)
      IF(YY(L) .GT. (Y+HTF)) GO TO 120
      YE(L)=YS(L)
      YF(L)=0.
      GO TO 130
120   YF(L)=YY(L)-Y-HTF
      YE(L)=YS(L)-YF(L)
130   ALFA(L)=ET3
140   ET3=ET3+DANGLE
      GO TO 110
150   IF(ITER .EQ. 2) GO TO 200
      DO 160 I=1,(NSLICE-1)
      YP(I+1)=(YS(I)+YS(I+1))/2.
160   CONTINUE
      YP(1)=TC1
      DO 170 I=1,NSLICE
      PLFA(I)=1.5707963-ALFA(I)
170   CONTINUE
C     CALCULATE THE WEIGHT OF EACH SLICE AND WATER PRESSURE IN
C     TENSION CRACK
      DTL=1.
      FW2(1)=0.5*TC1**2*GW*DTL
      DO 180 I=2,NSLICE
      FW2(I)=0.
180   CONTINUE
      DO 190 I=1,NSLICE
      W2(I)=(YE(I)*GAMA+YF(I)*GAMAF)*DX(I)*DTL
190   CONTINUE
C     ****************************************************************
C     SOLVE 2-D FACTOR OF SAFETY
C     ****************************************************************
      RNORM=0.
      CALL SECANT(X,2,FCN,7,RNORM)
      FS=X(1)
      SETA=X(2)*57.29577951
      RNOR1=RNORM
C     ****************************************************************
C     GENERATE 3-D COORDINATES
C     ****************************************************************
C     FIND THE MAXIMUM WIDTH OF SPOON SHAPE FAILURE SURFACE
200   BIG=ZZ(1)
```

```
      DO 310 I=2,NSLICE
      AB=ZZ(I)
      IF(BIG-AB) 300,310,310
300   BIG=AB
310   CONTINUE
      DTL=BIG/(FLOAT(NCOLUM)-1.)
      TCX=R*COS(ANG1)
      SENSE=(1.-(COS(ANG1))**2-(SIN(THET1))**2)/ENA
      IF(SENSE .LT. 0.) SENSE=0.
      TCZ=R*SQRT(SENSE)


C     CALCULATE THE HEIGHT, SIDE HEIGHT, WIDTH, DIP, AND BOTTOM AREA FOR
C     EACH COLUMN

      RAD(1)=R
      DO 350 J=2,NCOLUM
      RAD(J)=SQRT(R*R-((J-1.5)*DTL)**2*ENA)

      DO 340 I=1,NSLICE
      IF(ZZ(I) .LT. (J-2.)*DTL) GO TO 330
      IF(J .EQ. NCOLUM) GO TO 320
      IF(ZZ(I) .GT. (J-2.)*DTL .AND. ZZ(I) .LE. (J-1.)*DTL) GO TO 320
      DZ(I,J)=DTL
      Z(I,J)=DZ(I,J)*0.5+(J-2.)*DTL
      YHC=SQRT(R*R-XX(I)**2-ENA*((J-1.5)*DTL)**2)
      HF(I,J)=YHC-Y-HTF
      IF(HF(I,J) .LT. 0.) HF(I,J)=0.
      HE(I,J)=YHC-(YY(I)-YS(I))-HF(I,J)
      IF(HE(I,J) .LE. 0.)  HE(I,J)=0.
      SH=SQRT(R*R-XX(I)**2-ENA*((J-2.)*DTL)**2)
      SHF(I,J)=SH-Y-HTF
      IF(SHF(I,J) .LT. 0.) SHF(I,J)=0.
      SHE(I,J)=SH-(YY(I)-YS(I))-SHF(I,J)
      IF(SHE(I,J) .LE. 0.) SHE(I,J)=0.
      AXY(I,J)=ATAN(XX(I)/SQRT(R*R-XX(I)**2-ENA*Z(I,J)**2))
      SLFA(I,J)=ATAN(XX(I)/SQRT(R*R-XX(I)**2-ENA*((J-2.0)*DTL)**2))
      AYZ(I,J)=ATAN(ENA*Z(I,J)/SQRT(R*R-XX(I)**2-ENA*Z(I,J)**2))
      W3(I,J)=DX(I)*DZ(I,J)*(GAMA*HE(I,J)+GAMAF*HF(I,J))
      BAREA(I,J)= DX(I)*DZ(I,J)*(SQRT(1.-(SIN(AYZ(I,J))*SIN(AXY(I,J)))
     1 **2))/(COS(AYZ(I,J))*COS(AXY(I,J)))
      GO TO 340

320   DZ(I,J)=ZZ(I)-(J-2.)*DTL
      Z(I,J)=DZ(I,J)/2.+(J-2.)*DTL
      YHC=SQRT(R*R-XX(I)**2-ENA*Z(I,J)**2)
      HF(I,J)=YHC-Y-HTF
      IF(HF(I,J) .LT. 0.) HF(I,J)=0.
      HE(I,J)=YHC-(YY(I)-YS(I))-HF(I,J)
      IF(HE(I,J) .LE. 0.)  HE(I,J)=0.
      SH=SQRT(R*R-XX(I)**2-ENA*((J-2.)*DTL)**2)
      SHF(I,J)=SH-Y-HTF
      IF(SHF(I,J) .LT. 0.) SHF(I,J)=0.
      SHE(I,J)=SH-(YY(I)-YS(I))-SHF(I,J)
      IF(SHE(I,J) .LE. 0.) SHE(I,J)=0.
      AXY(I,J)=ATAN(XX(I)/SQRT(R*R-XX(I)**2-ENA*Z(I,J)**2))
      SLFA(I,J)=ATAN(XX(I)/SQRT(R*R-XX(I)**2-ENA*((J-2.0)*DTL)**2))
      AYZ(I,J)=ATAN(ENA*Z(I,J)/SQRT(R*R-XX(I)**2-ENA*Z(I,J)**2))
      W3(I,J)=DX(I)*DZ(I,J)*(GAMA*HE(I,J)+GAMAF*HF(I,J))
      BAREA(I,J)=DX(I)*DZ(I,J)*(SQRT(1.-(SIN(AYZ(I,J))*SIN(AXY(I,J)))
     1 **2))/(COS(AYZ(I,J))*COS(AXY(I,J)))
      IF(HE(I,J) .LE. 0. .AND. HF(I,J) .LE. 0.) BAREA(I,J)=0.
      GO TO 340

330   DZ(I,J)=0.
```

```
      Z(I,J)=0.
      HE(I,J)=0.
      HF(I,J)=0.
      SHE(I,J)=0.
      SHF(I,J)=0.
      AXY(I,J)=0.
      AYZ(I,J)=0.
      SLFA(I,J)=0.
      W3(I,J)=0.
      BAREA(I,J)=0.
340   CONTINUE
350   CONTINUE

C     THIS PART DEALS WITH UNIFORM CROSS SECTIONS


      TWOD=TWODI
      DO 610 IU=1,NRL
      C2D=TWOD*H
      DO 360 I=1,NSLICE
      DZ(I,1)=C2D
      AXY(I,1)=PLFA(I)
      BAREA(I,1)=DX(I)*C2D/COS(AXY(I,1))
      W3(I,1)=W2(I)*C2D
      HF(I,1)=YF(I)
      HE(I,1)=YE(I)
      SHE(I,1)=YE(I)
      SHF(I,1)=YF(I)
      SLFA(I,1)=PLFA(I)

C     CALCULATE WATER PRESSURE IN 3-D TENSION CRACK

360   CONTINUE
      DO 390 J=2,NCOLUM
      IF(TCZ .LE. (J-1.)*DTL) GO TO 380
      IF(TCZ .GT. (J-1.)*DTL .AND. TCZ .LE. J*DTL) GO TO 370
      WH(1,J)=SQRT(R*R-TCX**2.-ENA*((J*DTL)/2.)**2.)-Y
      FW3(1,J)=0.5*GW*DTL*WH(1,J)**2
      GO TO 390
370   WH(1,J)=SQRT(R*R-TCX*TCX-ENA*((TCZ+(J-1.)*DTL)**2./4.))-Y
      FW3(1,J)=0.5*GW*(TCZ-(J-1.)*DTL)*WH(1,J)**2
      GO TO 390
380   FW3(1,J)=0.
390   CONTINUE
      WH(1,1)=TC1
      FW3(1,1)=0.5*GW*C2D*TC1**2.
1000  FORMAT(8F10.2)
1010  FORMAT(5F10.2)
      DO 400 I=1,NSLICE
      SHE(I,NCOLUM+1)=0.
      SHF(I,NCOLUM+1)=0.
      SLFA(I,NCOLUM+1)=0.
400   CONTINUE
      DO 410 I=2,NSLICE
      DO 410 J=1,NCOLUM
      WH(I,J)=0.
      FW3(I,J)=0.
410   CONTINUE

      IF(IPRINT .EQ. 0) GO TO 440
      PRINT 2050
      DO 430 J=1,NCOLUM
      DO 420 I=1,NSLICE
      XYA=AXY(I,J)*57.29577951
      YZA=AYZ(I,J)*57.29577951
```

```
      PRINT 2060, I,J,DX(I),DZ(I,J),HE(I,J),HF(I,J),XYA,YZA,
     * BAREA(I,J),W3(I,J)
      IF(J .EQ. NCOLUM) GO TO 420
      IF(I .EQ. NSLICE) PRINT 2050
420   CONTINUE
430   CONTINUE
440   CONTINUE
C     ******************************************************************
C     SOLVE 3-D FACTOR OF SAFETY
C     ******************************************************************


C     ASSUMING INTER-COLUMN SHEAR STRESSES DISTRIBUTION
      DISTRI(1)=0.
      DO 500 J=2,(NCOLUM+1)
      DISTRI(J)=((C2D+(J-2.))/((NCOLUM-1.)*DTL+C2D))**EX
500   CONTINUE
      ITER=3
      RNORM=0.
      X(1)=FS
      X(2)=SETA/57.29577951
      CALL SECANT(X,2,FCN,7,RNORM)
      DEGREE=X(2)*57.29577951
      RNOR2=RNORM
      PRINT 3020, BIG
      PRINT 3030, C2D
      PRINT 3040
      PRINT 3050, FS,SETA,RNOR1
      PRINT 3060, X(1),DEGREE,RNOR2
      IF(ICOND .EQ. 0) GO TO 610
C     CALCULATE FACTOR OF SAFETY FROM ORDINARY METHOD OF COLUMNS
      FST=0.
      FSB=0.
      DO 550 J=1,NCOLUM
      DO 540 I=1,NSLICE
      IF(HE(I,J) .EQ. 0. .AND. HF(I,J) .EQ. 0.) GO TO 540
      HRE=HE(I,J)/(HE(I,J)+HF(I,J))
      HRF=1.-HRE
      IF(HF(I,J)) 510,510,520
510   PA=C
      PB=TF
      GO TO 530
520   PA=CF
      PB=TFF
530   FST=FST+PA*BAREA(I,J)+W3(I,J)*PB*(1.-RU*(HRE/GAMA+HRF/GAMAF))/(
     * SQRT(1.+TAN(AXY(I,J))**2.+TAN(AYZ(I,J))**2))
      FSB=FSB+W3(I,J)*SIN(AXY(I,J))+FW3(I,J)*(Y+2.*WH(I,J)/3.)/RAD(J)
540   CONTINUE
550   CONTINUE
      FSORD=FST/FSB
      PRINT 3070,FSORD
610   TWOD=TWOD*FACTR
      ITER=2
620   ENA=ENA/(FACTS*FACTS)

1020  FORMAT(4F10.2,3I5)
```

```
1030  FORMAT(4F10.2,4I5)
1040  FORMAT(2F10.2)
2000  FORMAT(44H1 EMBANKMENT HEIGHT***************************,F10.3,//
     1         44H  SLOPE ANGLE*********************************,F10.3,//
     2         44H  NUMBER OF SLICES****************************,I10,//
     3         44H  NUMBER OF COLUMNS***************************,I10,//
     4         44H  BIG RADIUS**********************************,F10.3,//
     5         44H  SMALL RADIUS********************************,F10.3,//
     6         44H  X-DIST. FROM CENTER TO CREST****************,F10.3,//
     7         44H  Y-DIST. FROM CENTER TO CREST****************,F10.3,//
     8         44H  TENSION CRACK*******************************,F10.3,//
     9         44H  EXPONENTIAL NUMBER**************************,F10.3,///)
2010  FORMAT(///,≠**********EMBANKMENT PARAMETERS*********≠,///)
2020  FORMAT(40H          C        FI       GAMA         RU,//,4F10.2)
2030  FORMAT(///,≠**********FOUNDATION PARAMETERS*********≠)
2040  FORMAT(//,40H          C        FI       GAMA        HTF,//,4F10.2///
     *//)
2050  FORMAT(106H1    I    J          DX          DZ          HE          HF
     *  AXY         AYZ          BAREA       WEIGHT                 /)
2060  FORMAT(2I5,6F10.2,2F14.2)


3020  FORMAT(45H1    THE WIDTH OF CURVE SHAPE IS**************   ,F10.3/)
3030  FORMAT(45H     HALF WIDTH OF UNIFORM CROSS SECTION IS***   ,F10.3///
     *//)
3040  FORMAT(17X,≠      FS        THET      RNORM≠,/)
3050  FORMAT( 4X,≠2-D≠/,2X,≠(SPENCER)≠,3X,3F10.3//)
3060  FORMAT(4X,≠3-D≠,7X,3F10.3//)
3070  FORMAT(4X,≠3-D≠/,1X,≠(ORDINARY)≠,3X,F10.3)
      STOP
      END




      SUBROUTINE FCN(X,F,UDF)
      COMMON/MATL/ GAMA,GAMAF,C,CF,TF,TFF,RU,W2,W3,GW
      COMMON/GEOM1/ AXY,AYZ,SLFA,PLFA,YS,YF,HE,HF,SHE,SHF
      COMMON/GEOM2/ R,RAD,BAREA,DX,DZ,DTL,EK,FK
      COMMON/MISL/ NSLICE,NCOLUM,ITER,FW2,FW3,DISTRI
      DIMENSION HE(50,20),HF(50,20),YS(50),YYF(50,20),DX(50)
      DIMENSION AXY(50,20),AYZ(50,20),SLFA(50,20),PLFA(50),YF(50)
      DIMENSION SHE(50,20),SHF(50,20),DISTRI(20)
      DIMENSION FW2(50),W3(50,20),W2(50),FW3(50,20),BAREA(50,20)
      DIMENSION RAD(20),DZ(50,20),X(20),F(20)
      F(1)=0.
      F(2)=0.
      RG=GAMA/GAMAF
      IF(ITER.EQ.3) GO TO 740

      DO 730 I=1,NSLICE

      IF(YF(I)) 700,700,710
700   PA=C
      PB=TF
      GO TO 720
710   PA=CF
      PB=TFF

720   F(1)=F(1)+
     1          (PA*DX(I)*DTL/(X(1)*COS(PLFA(I)))+PB*(W2(I)*COS(PLFA(I))
     2          -RU*YS(I)*DX(I)*DTL/COS(PLFA(I)))/X(1)-W2(I)*
     3          SIN(PLFA(I))-FW2(I)*(COS(PLFA(1))+SIN(PLFA(1))*PB/X(1)))
```

```
     4          /(COS(PLFA(I)-X(2))*(1.+TAN(PLFA(I)-X(2))*PB/X(1)))

      F(2)=F(2)+
     1          (PA*DX(I)*DTL/(X(1)*COS(PLFA(I)))+PB*(W2(I)*COS(PLFA(I))
     2          -RU*YS(I)*DX(I)*DTL/COS(PLFA(I)))/X(1)-W2(I)*
     3          SIN(PLFA(I))-FW2(I)*(COS(PLFA(1))+SIN(PLFA(1))*PB/X(1)))
     4          /(1.+TAN(PLFA(I)-X(2))*PB/X(1))
730   CONTINUE
      GO TO 800

740   DO 790 J=1,NCOLUM
      DO 790 I=1,NSLICE

      WEIGHT=W3(I,J)*COS(AXY(I,J))
      FWC=FW3(I,J)*COS(AXY(I,J))
      DZT=DZ(I,J)*TAN(AYZ(I,J))
      TF1=TAN(AXY(I,J)-SLFA(I,J))
      TF2=TAN(SLFA(I,J+1)-AXY(I,J))
      IF(SHE(I,J) .EQ. 0. .AND. SHF(I,J) .EQ. 0.) GO TO 750
      YYF(I,J)=(RG*SHE(I,J)+SHF(I,J)/3.)*SHF(I,J)/(2.*RG*SHE(I,J)+
     * SHF(I,J))

      RCE1=C*DX(I)*SHE(I,J)
      RCF1=CF*DX(I)*SHF(I,J)
      RSE1=0.5*EK*(GAMA-RU)*SHE(I,J)**2*DX(I)*TF
      RSF1=FK*((GAMA-RU)*SHE(I,J)*SHF(I,J)+0.5*(GAMAF-RU)*SHF(I,J)**2)
     * *DX(I)*TFF
      RCE2=C*DX(I)*SHE(I,J+1)
      RCF2=CF*DX(I)*SHF(I,J+1)
      RSE2=0.5*EK*(GAMA-RU)*SHE(I,J+1)**2*DX(I)*TF
      RSF2=FK*((GAMA-RU)*SHE(I,J+1)*SHF(I,J+1)+0.5*(GAMAF-RU)*SHF(I,J+1)
     * **2)*DX(I)*TFF
      R1=(RCE1+RCF1+RSE1+RSF1)*DISTRI(J)
      R2=(RCE2+RCF2+RSE2+RSF2)*DISTRI(J+1)
      TOTR1=R1*COS(SLFA(I,J)-AXY(I,J))
      TOTR2=R2*COS(AXY(I,J)-SLFA(I,J+1))
      RS1=RCE1*(6.*SHF(I,J)+3.*SHE(I,J)-3.*DZT)+RCF1*(3.*SHF(I,J)-3.*DZT
     * )+RSE1*(6.*SHF(I,J)+2.*SHE(I,J)-3.*DZT)+RSF1*(6.*YYF(I,J)-3.*DZT)
      RS2=RCE2*(6.*SHF(I,J+1)+3.*SHE(I,J+1)+3.*DZT)+RCF2*(3.*SHF(I,J+1)+
     * 3.*DZT)+RSE2*(6.*SHF(I,J+1)+2.*SHE(I,J+1)+3.*DZT)+RSF2*(6.*
     * YYF(I,J+1)+3.*DZT)
      RR1=RS1*DISTRI(J)
      RR2=RS2*DISTRI(J+1)

750   IF(HF(I,J)) 760,760,770

760   PA=C
      PB=TF
      GO TO 780

770   PA=CF
      PB=TFF

780   COHESN=PA*BAREA(I,J)
      PORPRE=RU*BAREA(I,J)*(HE(I,J)+HF(I,J))*PB/(COS(AXY(I,J))*SQRT
     * (1.+TAN(AYZ(I,J))**2+TAN(AXY(I,J))**2))

      F(1)=F(1)+
     1          (COHESN/X(1)-PORPRE/X(1)+WEIGHT*(PB/X(1)-TAN(AXY(I,J)))+
     2          (TOTR2*(1.-PB*TF2/X(1))-TOTR1*(1.+PB*TF1/X(1)))/X(1)-FWC
     3          *(1.+PB*TAN(AXY(I,J))/X(1)))/(COS(AXY(I,J)-X(2))*(1.+PB*
     4          TAN(AXY(I,J)-X(2))/X(1)))
```

```
      F(2)=F(2)+RAD(J)*
     1          (COHESN/X(1)-PORPRE/X(1)+WEIGHT*(PB/X(1)-TAN(AXY(I,J)))+
     2          (TOTR2*(1.-PB*TF2/X(1))-TOTR1*(1.+PB*TF1/X(1)))/X(1)-FWC
     3          *(1.+PB*TAN(AXY(I,J))/X(1)))/(1.+PB*TAN(AXY(I,J)-X(2))
     4          /X(1))
     5          -COS(X(2)-AXY(I,J))*COS(AXY(I,J))*(COS(SLFA(I,J+1))*RR2-
     6          COS(SLFA(I,J))*RR1)/(6.*COS(X(2))*X(1))
790   CONTINUE
800   CONTINUE
      RETURN
      END
```

E.3 User's Guide for Program FESPON

1. Control Cards

a) Heading Card (12A6)

2-72	HED	- Title card for program identification

b) Control Data Card (9I5)

1- 5	NUMELT	- Total number of elements in the complete structure
6-10	NUMNPT	- Total number of nodal points in the complete structure
11-15	NFEL	- Number of elements in the foundation part
16-20	NFNP	- Number of nodal points in the foundation part
21-25	NUMCEL	- Number of elements in the preexisting part
26-30	NUMCNP	- Number of nodal points in the preexisting part
31-35	NUMMAT	- Number of different material types
36-40	NLAY	- Number of construction layer increments
41-45	NFORCE	- Number of load increments after construction

2. Material Property Cards

a) Units Conversion Card (F10.0)

1-10	PATM	- Atmospheric pressure expressed in the system of units used in the problem.

For example:

Length	Unit Weight	Cohesion	Atmospheric Pressure
ft	ton/ft^3	ton/ft^2	1.058
ft	kip/ft^3	kip/ft^2	2.116
ft	lb/ft^3	lb/ft^2	211.62
m	ton/m^3	ton/m^2	10.35
m	kN/m^3	kN/m^2	101.4

b) Material Properties (I5,7F10.0/4F10.0)

The first and second cards must be specified for each material.

First Card

1- 5	M	- Material type number
6-15	EMPR(M, 1)	- Unit weight
16-25	EMPR(M, 2)	- Modulus number K
26-35	EMPR(M, 3)	- Unloading-reloading modulus number K_{ur}
36-45	EMPR(M, 4)	- Modulus exponent n
46-55	EMPR(M, 5)	- Poisson's ratio parameter d
56-65	EMPR(M, 6)	- Poisson's ratio parameter G
66-75	EMPR(M, 7)	- Poisson's ratio parameter F

Second Card

1-10	EMPR(M, 8)	- Cohesion c
11-20	EMPR(M, 9)	- Friction angle (degrees)
21-30	EMPR(M,10)	- Failure ratio R_f
31-40	EMPR(M,11)	- Earth pressure coefficient in the foundation K_o (zero or blank if the material is not in the foundation).

3. <u>Nodal Point and Boundary Condition Cards (I5,3F10.0,3I5)</u>

One card for each nodal point.

1- 5	N	- Nodal point number
6-15	X(N)	- X-coordinate (+ to right)
16-25	Y(N)	- Y-coordinate (+ up)
26-30	Z(N)	- Z-coordinate (left-hand rule)
31-35	ID(N, 1)	- Boundary condition code for X-direction
36-40	ID(N, 2)	- Boundary condition code for Y-direction
41-45	ID(N, 3)	- Boundary condition code for Z-direction

Nodal points must be read in sequence. If nodal points cards are omitted, the nodal point data for a series of nodal points are generated automatically at equal spacing between those specified. The boundary condition codes for the generated nodal point are set equal to the boundary condition codes for the previous nodal point. The first and the last nodal points must be specified.

Boundary condition code:

Zero or blank indicates that the nodal point is free to move in that direction and loads may be applied.

One indicates that the nodal point is fixed in that direction.

4. <u>Element Cards (10I5)</u>

One card for each element.

1- 5	N	- Element number
6-10	INP(N,1)	- Number of nodal point I
11-15	INP(N,2)	- Number of nodal point J
16-20	INP(N,3)	- Number of nodal point K
21-25	INP(N,4)	- Number of nodal point L
26-30	INP(N,5)	- Number of nodal point M
31-35	INP(N,6)	- Number of nodal point N
36-40	INP(N,7)	- Number of nodal point O
41-45	INP(N,8)	- Number of nodal point P
46-50	INP(N,9)	- Material number

Elements must be read in sequence. The nodal point numbers must be specified proceeding counterclockwise around each element in the order I, J, K, L, M, N, O, P as shown in Fig. E.1. If element cards are omitted, the element data for a series of elements are generated automatically by increasing the preceding values of I, J,

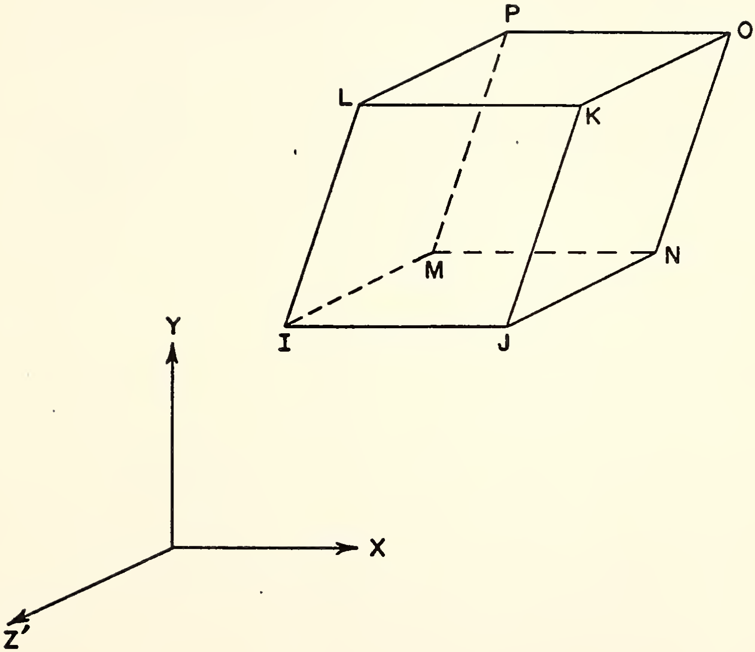

Fig..E.5 Eight Point Three-Dimensional Element

K, L, M, N, O, P by one. The material number for the generated element is set equal to the material number for the previous element. The first and last elements must be specified.

The center of the element is calculated by

$$XCP = \frac{1}{8} \{X(I) + X(J) + X(K) + X(L) + X(M) + X(N) + X(O) + X(P)\}$$

$$YCP = \frac{1}{8} \{Y(I) + Y(J) + Y(K) + Y(L) + Y(M) + Y(N) + Y(O) + Y(P)\}$$

$$ZCP = \frac{1}{8} \{Z(I) + Z(J) + Z(K) + Z(L) + Z(M) + Z(N) + Z(O) + Z(P)\}$$

5. Construction Layer Element and Nodal Point Cards (9I5)

If NLAY = 0, these cards are omitted.

One card for each construction layer.

1- 5	LN	- Number of the construction layer, increasing upward from the bottom
6-10	NOMEL(LN,1)	- Smallest element number of the newly placed elements in this layer
11-15	NOMEL(LN,2)	- Largest element number of the newly placed elements in this layer
16-20	NOMNP(LN,1)	- Smallest nodal point number of the newly placed nodal points in this layer
21-25	NOMNP(LN,2)	- Largest nodal point number of the newly placed nodal points in this layer
26-30	NPHUMP(LN,1)	- The first nodal point on the humped surface
31-35	NPHUMP(LN,2)	- The second nodal point on the humped surface
36-40	NPHUMP(LN,3)	- The third nodal point on the humped surface
41-45	NPHUMP(LN,4)	- The fourth nodal point on the humped surface

For simplicity, the position of the "humped surface" is defined by the coordinates of the four nodal points on the central section (z = 0). To the left of the first nodal point and to the right of the fourth nodal point the surface is assumed to be horizontal.

6. Foundation Cards

If NFEL = 0, these cards are omitted.

a) Control Card (I5,F10.0)

1- 5	NFLAY	- Number of layers of elements in foundation The maximum number of foundation layers is 10.
6-15	HFLEV	- Elevation of rigid base at bottom of foundation.

b) Layer Information Cards (4I5,F10.0)

1- 5	I	- Foundation layer number (Number from bottom upward)
6-10	MATNO(I)	- Material property number for this layer
11-15	NLEL(I)	- The first element number of this layer
16-20	NREL(I)	- The last element number of this layer
21-30	HL(I)	- Elevation of the top of this layer

7. Force Cards

If NFORCE = 0, these cards are omitted.

If NFORCE ≥ 1, NFORCE sets of cards, each set consisting of types (a) through (b) below, are required.

Number of Nodal Point Force Cards to be Used (I5)

1- 5 NUMFC - Number of nodal point force cards for this load case

b) Nodal Point Force Cards (I5,3F10.0)

If NUMFC = 0, these cards are omitted. Otherwise need NUMFC cards.

1- 5 MM - Nodal point number where force is applied

6-15 FX(MM) - X-component of force applied at MM (+ to right)

16-25 FY(MM) - Y-component of force applied at MM (+ up)

26-30 FZ(MM) - Z-component of force applied at MM (right-hand rule)

8. Geometry Cards

a) The Direction of the Movement Card (2I5)

1- 5 IFXY - One, if the movement of the failure mass is along X-Y plane; otherwise zero

6-10 IFYZ - One, if the movement of the failure mass is along Y-Z plane; otherwise zero

b) Number of Layers Card (2I5)

1- 5 LAYSUM - Total number of layers

6-10 MFLAY - Number of layers in the foundation

c) Elevation Information Cards (8F10.0)

1- 5 HEIGHT(1) - Elevation at the top of layer 1

6-10 HEIGHT(2) - Elevation at the top of layer 2

Elevation must be read in sequence from the lowest value to the highest value. They are read in the same card.

d) Foundation Element Number Cards (2I5)

1- 5 MLEL(M) - The first element number of foundation layer M

6-10 MREL(M) - The last element number of foundation layer M

The number must be read from the lowest layer to the highest layer of foundation. The number of these cards are equal to the number of layers in the foundation

e) Embankment Element Number Cards (2I5)

1- 5 MOMEL(LP,1) - The first element number of embankment layer LP

6-10 MOMEL(LP,2) - The last element number of embankment layer LP

The number must be read from the lowest layer to the highest layer of embankment. The number of these cards are equal to the number of layers in the embankments.

9. <u>Factor of Safety Cards</u>

A. If IFXY = 0, these cards are omitted

a) 2-D Critical Circle Information Card (6F10.3,I5)

1-10 XO - X-coordinate of the toe

11-20 YO - Y-coordinate of the toe

21-30 BETA - The angle of the slope on X-Y plane in degrees

31-40 RU - Pore pressure parameter

41-50 GAMAE - Mean unit weight or density of embankment soil

51-60 GAMAF - Mean unit weight or density of foundation soil

61-65 NTIME - Number of critical surfaces selected

b) 3-D Critical Surface Information Cards (7F10.3,2I5/I5)

1-10 RADIUS - The radius of the critical circle, R_{xy}

11-20 RZ - The length of minor axis, R_z, of the semi-ellipsoid

21-30 DANGLE - $\Delta\theta$, the spacing of selecting the points on the failure circles along X-Y plane

31-40 XR - X-coordinate of the center of the ellipsoid

41-50 YR - Y-coordinate of the center of the ellipsoid

51-60 ZR - Z-coordinate of the center of the ellipsoid

61-70 DZ - Δz, the spacing of selecting the points interested along Z-direction

71-75 NUMBER - The number of the sections divided along Z-direction in the embankment

76-80 NUMBF - The number of the sections divided along Z-direction in the foundation

Next Card

1- 5 ISIGN - +1, the semi-ellipsoid on the right side of the central plane is chosen; -1, the left side is chosen. This choice provides the convenience to calculate the factor of safety if the failure mass is not symmetrical

These cards are repeated for as many times as the number of failure surfaces selected.

B. If IFYZ = 0, these cards are omitted

a) 2-D Critical Circle Information Card (6F10.3,I5)

1-10 YO - Y-coordinate of the toe

11-20 ZO - Z-coordinate of the toe

21-30 BETA - The angle of the slope on Y-Z plane, in degrees

31-40 RU - Pore water pressure parameter

41-50 GAMAE - Mean unit weight or density of embankment soil

51-60 GAMAF - Mean unit weight or density of foundation soil

61-65 NTIME - Number of critical surfaces selected

b) 3-D Critical Surface Information Cards (7F10.3,2I5/I5)

1-10 RADIUS - The radius of the critical circle, R_{yz}

11-20 RX - The length of minor axis, R_x, of the semi-ellipsoid

21-30 DANGLE - $\Delta\theta$, the spacing of selecting the points on the failure circles along Y-Z plane

31-40 XR - X-coordinate of the center of the ellipsoid

41-50 YR - Y-coordinate of the center of the ellipsoid

51-60 ZR - Z-coordinate of the center of the ellipsoid

61-70 DX - Δx, the spacing of selecting the points interested along X-direction

71-75 NUMBER - The number of the sections divided along X-direction in the embankment

76-80 NUMBF - The number of the sections divided along X-direction in the embankment

Next Card

1- 5 ISIGN - +1, the semi-ellipsoid on the right side of the central plane is chosen; -1, the left side is chosen. This choice provides the convenience to calculate the factor of safety if the failure mass is not symmetrical.

These cards are repeated for as many times as the number of failure surfaces selected.

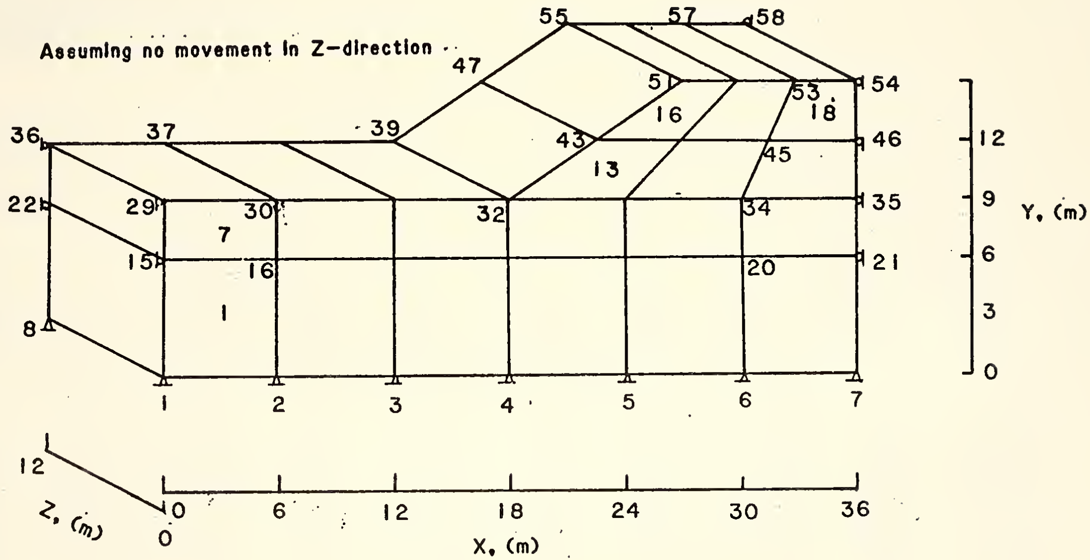

Fig. E.6 Example Problem for Program FESPON

EXAMPLE PROBLEM

```
TOTAL NUMBER OF ELEMENTS*********** 18
TOTAL NUMBER OF NODES************** 58
NUMBER OF ELEMENTS IN FOUNDATION** 12
NUMBER OF NODES IN FOUNDATION***** 42
NUMBER OF PREEXISTING ELEMENTS****  0
NUMBER OF PREEXISTING NODES*******  0
NUMBER OF DIFF. MATERIALS*********  2
NUMBER OF CONSTRUCTION LAYERS*****  2
NUMBER OF LOAD CASES   ************  0
FINAL RESULTS ARE NOT PUNCHED OUT
```

MATERIAL PROPERTY DATA

ATMOSPHERIC PRESSURE= 101.4000

MAT	UNIT WT	K	MODULUS KUR	N	D	POISSON RATIO G	F	C	PHI	FAIL.RATIO	KO
1	18.8600	400.0	600.0	.4000	8.0000	.3000	.1500	0	40.0000	.7500	.5000
2	18.8100	40.0	120.0	.3000	.7000	.4500	.3500	30.0000	5.0000	.8000	-0

STRESSES AND STRESS LEVELS FOR FINAL CONDITION AT END OF INCREMENT

	SIG-X	SIG-Y	SIG-Z	TAU-XY	TAU-YZ	TAU-ZX	SIG-1	SIG-2	SIG-3	SIG1/SIG3	SLMAX
1	69.535	116.178	64.407	2.087	.008	.052	116.271	69.442	64.406	1.805	.278
2	73.872	113.774	65.354	8.198	-.004	.089	115.393	72.254	65.353	1.766	.278
3	92.794	137.879	86.437	20.613	-.015	.068	145.883	86.440	84.788	1.721	.278
4	86.797	155.906	81.365	21.033	-.003	.016	161.804	81.366	80.899	2.000	.278
5	91.128	195.874	96.244	16.102	.000	.004	198.294	96.244	88.708	2.235	.343
6	93.107	213.283	102.552	5.694	-.000	.001	213.552	102.552	92.838	2.300	.361
7	29.522	29.737	21.181	2.008	.016	.396	31.648	27.631	21.161	1.496	.278
8	27.635	27.555	19.531	.014	.023	.350	27.654	27.591	19.516	1.417	.278
9	38.937	33.976	26.517	7.487	-.012	.101	44.344	28.571	26.514	1.672	.278
10	64.933	80.557	54.269	27.655	-.003	.031	101.738	54.270	44.153	2.304	.362
11	51.713	116.271	62.505	17.424	.002	.009	120.674	62.505	47.311	2.551	.431
12	48.965	136.513	68.804	4.521	.000	.002	136.746	68.804	48.732	2.806	.502
13	49.930	49.629	48.779	13.408	.000	.001	63.189	48.779	36.370	1.737	.370
14	84.935	100.985	91.056	11.904	.000	.000	107.316	91.096	78.604	1.365	.357
15	115.635	133.564	122.102	3.064	.000	.000	134.073	122.102	115.126	1.165	.217
16	22.582	23.512	22.582	6.521	0	0	29.585	22.582	16.509	1.792	.191
17	27.098	28.215	27.098	0	0	0	28.215	27.098	27.098	1.041	.016
18	27.098	28.215	27.098	0	0	0	28.215	27.098	27.098	1.041	.016

Fig. E.7 Output Data for Program FESPON

RXY	RYZ	XR	YR	ZR	BETA	DANGLE
11.180	12.000	21.000	19.000	0	33.670	5.000

ELE	X	Y	Z	SIGN	WP	TAUN	AXY	AYZ	AREA	LOCAL FS
17	31.162	14.553	1.500	27.275	0	.408	66.362	16.317	2.924	79.363
17	30.735	13.684	1.500	27.351	0	.468	61.362	13.762	2.924	69.265
17	30.235	12.856	1.500	27.436	0	.513	56.362	11.964	2.924	63.128
17	29.604	12.074	1.500	27.527	0	.543	51.362	10.647	2.924	59.630
14	29.028	11.345	1.500	80.830	0	7.497	46.362	9.653	2.924	4.945
14	28.330	10.675	1.500	82.290	0	9.460	41.362	8.889	2.924	3.932
14	27.577	10.068	1.500	84.073	0	11.152	36.362	8.293	2.924	3.350
14	26.773	9.528	1.500	86.126	0	12.516	31.362	7.827	2.924	2.999
14	25.925	9.061	1.500	88.385	0	13.506	26.362	7.463	2.924	2.794
11	25.041	8.670	1.500	95.428	0	34.681	21.362	7.184	2.924	2.309
11	24.125	8.357	1.500	101.194	0	32.213	16.362	6.975	2.924	2.636
10	23.185	8.125	1.500	69.442	0	28.468	11.362	6.827	2.924	2.047
10	22.229	7.976	1.500	74.391	0	28.646	6.362	6.736	2.924	2.179
10	21.264	7.911	1.500	79.239	0	27.972	1.362	6.697	2.924	2.379
10	20.296	7.930	1.500	83.936	0	26.471	-3.638	6.708	2.924	2.662
10	19.334	8.033	1.500	88.341	0	24.199	-8.638	6.771	2.924	3.063
10	18.385	8.220	1.500	92.219	0	21.240	-13.638	6.887	2.924	3.643
9	17.455	8.489	1.500	38.857	0	7.552	-18.638	7.062	2.924	4.317
9	16.553	8.838	1.500	40.098	0	7.037	-23.638	7.301	2.924	4.782
17	30.378	14.587	4.500	27.275	0	.408	64.798	41.511	2.900	79.323
17	29.957	13.786	4.500	27.345	0	.464	59.798	36.840	2.900	69.814
17	29.469	13.025	4.500	27.423	0	.507	54.798	33.175	2.900	63.849
17	28.916	12.310	4.500	27.505	0	.538	49.798	30.279	2.900	60.259
14	28.303	11.646	4.500	82.355	0	8.272	44.798	27.973	2.900	4.498
14	27.634	11.037	4.500	83.745	0	9.797	39.798	26.129	2.900	3.810
14	26.915	10.489	4.500	85.409	0	11.130	34.798	24.653	2.900	3.367
14	26.150	10.005	4.500	87.295	0	12.199	29.798	23.475	2.900	3.085
14	25.347	9.591	4.500	89.346	0	12.955	24.798	22.546	2.900	2.919
14	24.510	9.248	4.500	91.499	0	13.370	19.798	21.829	2.900	2.842
10	23.647	8.980	4.500	64.760	0	26.513	14.798	21.256	2.900	2.050
10	22.764	8.787	4.500	69.109	0	27.480	9.798	20.553	2.900	2.110
10	21.867	8.672	4.500	73.504	0	27.741	4.798	20.717	2.900	2.223
10	20.963	8.636	4.500	77.811	0	27.315	-.202	20.650	2.900	2.390
10	20.060	8.679	4.500	81.900	0	26.260	-5.202	20.728	2.900	2.617
10	19.164	8.800	4.500	85.646	0	24.666	-10.202	20.953	2.900	2.914
10	18.282	8.999	4.500	83.936	0	22.671	-15.202	21.333	2.900	3.292

OVERALL FACTOR OF SAFETY = 3.453

Fig. E.7 (Cont'd)

```
      PROGRAM FESPON (INPUT,OUTPUT,TAPE1,TAPE2,TAPE3,TAPE4,TAPE7,TAPE8,
     1 TAPE9,TAPE10,TAPE11,PUNCH)
      COMMON /ISOP/ E1,E2,E3,RR(8),ZZ(8),QQ(8),LM(24),P(24),S(33,33),
     1 STR(6,33),STS(6,24),VJAC
      DIMENSION HED(12),T(10)
C
C     PROGRAM CAPACITY CONTROLLED BY THE FOLLOWING TWO STATEMENTS
C
      COMMON A(12000)
      MTOTAL=12000
C
C     PROGRAM CONTROL DATA
C
100   CALL SECOND (T(1))
      READ 1000, HED,NUMELT,NUMNPT,NFEL,NFNP,NUMCEL,NUMCNP,NUMMAT,
     1 NLAY,NFORCE,NPUNCH
      IF (NUMELT .EQ.0) STOP
      PRINT 2000,HED
      PRINT 2010,NUMELT,NUMNPT,NFEL,NFNP, NUMCEL,NUMCNP,NUMMAT,NLAY,
     1 NFORCE
      NUMLD=NLAY+NFORCE
      IF(NPUNCH.EQ.0) GO TO 110
      PRINT 2020
      GO TO 120
110   PRINT 2030
120   CONTINUE
C
C     BLOCK OUT VARIABLES IN A-VECTOR
C
      N1=1
      N2=N1+13*NUMMAT
      N3=N2+3*NUMNPT
      N4=N3+NUMNPT
      N5=N4+NUMNPT
      N6=N5+NUMNPT
      N7=N6+9*NUMELT
      N8=N7+NUMELT
      N9=N8+NUMELT
      N10=N9+NUMELT
      N11=N10+NUMELT
      N12=N11+NUMCEL+1
      N13=N12+NUMCNP+1
      N14=N13+2*NUMLD
      N15=N14+2*NUMLD
      N16=N15+4*NUMLD
      N17=N16+NPUNCH
      N18=N17+NUMNPT
      N19=N18+NUMNPT
      N20=N19+NUMNPT
      N21=N20+6*NUMELT
      N22=N21+6*NUMELT
      N23=N22+6*NUMELT
      NN1=N22+NUMELT
      N31=NN1+NUMELT
      MTMN16=MTOTAL-N17
      NN2=N22+3*NUMNPT
      IF(NN2.GT.N23) N23=NN2
      IF(N23.LT.MTOTAL) GO TO 130
      PRINT 5000
      CALL EXIT
C
C     READ AND PRINT INPUT DATA AND SET UP INITIAL CONDITIONS
C
130   CALL SETUP (A(N1),A(N2),A(N3),A(N4),A(N5),A(N6),A(N7),A(N8),
     1 A(N9),A(N10),A(N11),A(N12),A(N13),A(N14),A(N15),A(N16),A(N17),
```

```
     2 A(N20),A(N21),A(N22),A(NN1),A(N31),NUMELT,NUMNPT,NUMCEL,
     3 NUMCNP,NFEL,NUMMAT,NUMLD,NLAY,NEQ,NEQB,MBAND,PATM,MTMN16,
     4 NMXEQB,NPUNCH)
      CALL SECOND(T (2))
      N24=N23+NEQ
      N25=N24+NEQB
      IF(N25.LT.MTOTAL) GO TO 140
      PRINT 5000
      CALL EXIT
C
C     FORM STRAIN-DISPLACEMENT MATRIX FOR ALL ELEMENTS , STORE ON TAPE 7
C
140   CALL FOMING(A(N3),A(N4),A(N5),A(N6),NUMELT)
      CALL SECOND (T(3))
      T(1)=T(2)-T(1)
      T(2)=T(3)-T(2)
      TIME=T(1)+T(2)
      DO 400 LN=1,NUMLD
      T(10)=0.
      CALL SECOND (T(3))
      PRINT 2000,HED
C
C     DETERMINE CONTROL DATA FOR EACH LAYER
C
      CALL CALNEQ (A(N2),A(N11),A(N12),A(N13),A(N14),A(N15),NUMELT,
     1 NUMNPT,NUMCEL,NUMCNP,NUMLD,NLAY,LN,MBAND,NUMEL,NUMNP,
     2 NELCAL,NNPCAL,NELRED,NNPRED,NEQ,NEQB,NBLOCK,NMXEQB)
      CALL SECOND (T(4))
      NN1=N20+NEQ
C
C     SET UP LOAD VECTOR
C
      CALL FORCE(A(N1),A(N2),A(N3),A(N4),A(N5),A(N6),A(N11),A(N13),
     1 A(N17),A(N18),A(N19),A(N20),A(NN1),NUMELT,NUMNPT,NUMCEL,NUMMAT,
     2 NUMLD,NLAY,LN,NEQ,NEQB,NUMNP)
      CALL SECOND  (T(5))
      T(3)=T(4)-T(3)
      T(4)=T(5)-T(4)
      DO 300 IT=1,2
      CALL SECOND (T(5))
C
C     CALCULATE ELEMENT STIFFNESS MATRIX FOR ALL ELEMENTS,STORE
C                                           ON TAPE 2
C     CALCULATE STRESS-DISPLACEMENT MATRIX FOR ALL ELEMENTS,STORE
C                                            ON TAPE 11
C
      CALL BILDUP (A(N7),A(N8),A(N11),NUMCEL,NUMEL,
     1 NELCAL,NELRED)
      CALL SECOND (T(6))
      NE2B=2*NEQB
      NN1=N17+NE2B*MBAND
      NN2=NN1+NE2B
C
C     FORM TOTAL STIFFNESS MATRIX, STORE ON TAPE4
C
      CALL ADDSTF(A(N17),A(NN1),NUMEL,NEQB,NE2B,NBLOCK,MBAND)
      CALL SECOND (T(7))
      NSB=(MBAND+1)*NEQB
      NNN1=N17+NSB
      NNN2=NNN1+NSB
C
C     SOLVE FOR DISPLACEMENT UNKNOWNS
C
      CALL SYMBAN(A(N17),A(NNN1),A(NNN2),NEQB,MBAND,NBLOCK,NSB,
     1 4,3,1,2,2)
```

```
      CALL SECOND (T(8))
C
C     EVALUATE RESULTS
C
      CALL RESULT(A(N1),A(N2),A(N3),A(N4),A(N5),A(N6),A(N7),A(N8),
     1 A(N9),A(N10),A(N11),A(N12),A(N16),A(N17),A(N20),A(N21),
     2 A(N22),A (N22),A(N23),A(N24),PATM,NUMELT,NUMNPT,NUMCEL,NUMCNP,
     3 NUMMAT,NUMLD,NLAY,LN,IT,NPUNCH,NUMEL,NUMNP,NELCAL,NNPCAL,
     4 NNPRED,NEQ,NEQB,NBLOCK)
      CALL SECOND (T(9))
      PRINT 2100
      DO 250 I=5,8
250   T(I)=T(I+1)-T(I)
      T(9)=T(5)+T (6)+T(7)+T(8)
      PRINT 2110,T(5),T(6),T(7),T (8),T (9)
      IF( IT.LT.2) GO TO 280
      T(10)=T(10)+T(3)+T (4)+T(9)
      PRINT 2120, T(3),T(4),T (10)
      TIME =TIME+T(10)
      GO TO 300
280   T(10)=T(10)+T(9)
300   CONTINUE
400   CONTINUE
      PRINT 2130, T(1),T(2),TIME
      GO TO 100
1000  FORMAT(12A6/10I5)
2000  FORMAT (1H1,12A6)
2010  FORMAT (/,
     135HOTOTAL NUMBER OF ELEMENTS********** I3/
     2 35HOTOTAL NUMBER OF NODES*************  I3/
     335HONUMBER OF ELEMENTS IN FOUNDATION** I3 /
     435HONUMBER OF NODES IN FOUNDATION***** I3 /
     535HONUMBER OF PREEXISTING ELEMENTS**** I3 /
     635HONUMBER OF PREEXISTING NODES******* I3 /
     735HONUMBER OF DIFF. MATERIALS********* I3 /
     835HONUMBER OF CONSTRUCTION LAYERS***** I3 /
     9 35HONUMBER OF LOAD CASES  ************  I3)
2020  FORMAT(49HORESULTS ARE PUNCHED OUT FOR FOLLOWING LOAD CASES /)
2030  FORMAT(34HOFINAL RESULTS ARE NOT PUNCHED OUT /)
5000  FORMAT(// 17H STORAGE EXCEEDED)
2100  FORMAT(14HOSOLUTION TIME /)
2110  FORMAT(/,
     1 35HOFORM ELEMENT STIFFNESSES********** F8.2 /
     2 35HOFORM TOTAL STIFFNESS************** F8.2 /
     3 35HOEQUATION SOLVING***************** F8.2 /
     4 35HOCALCULATE STRESSES AND STRAINS**** F8.2 /
     5 35HOSOLUTION TIME FOR THIS ITERATION** F8.2)
2120  FORMAT(/,
     1 35HODETERMINE CONTROL DATA************ F8.2 /
     2 35HOFORM LOAD VECTOR****************** F8.2 /
     3 35HOTOTAL TIME FOR THIS LOAD CASE***** F8.2)
2130  FORMAT(12HOOVERALL LOG /,
     1 35HODATA INPUT************************ F8.2 /
     2 35HOFORM STRAIN-DISPLACEMENT MATRIX*** F8.2 /
     3 35HOTOTAL SOLUTION TIME***************  F8.2)
      END


      SUBROUTINE SETUP (EMPR,ID,X,Y,Z,INP,BULK,SHEAR,POIS,SLMAX,NCEL,
     1 NCNP,NOMEL,NOMNP,NPHUMP,NLDP,DISP,STRESS,STRAIN,XCP,YCP,ZCP,
     2 NUMELT,NUMNPT,NUMCEL,NUMCNP,NFEL,NUMMAT,NUMLD,NLAY,NEQ,NEQB,
     3 MBAND,PATM,MTMN16,NMXEQB,NPUNCH)
```

```
      DIMENSION EMPR(NUMMAT,13),ID(NUMNPT,3),X(1),Y(1),Z(1)
      DIMENSION BULK(1),SHEAR(1),POIS(1),SLMAX(1),XCP(1),YCP(1),ZCP(1)
      DIMENSION DISP(NUMNPT,3),STRESS(NUMELT,6),STRAIN(NUMELT,6)
      DIMENSION NOMEL(NUMLD,2 ),NOMNP(NUMLD,2 ),INP(NUMELT,9)
      DIMENSION NPHUMP(NUMLD,4    ),NLDP(1),SINITX(10),SINITY(10)
      DIMENSION MATNO(10),NLEL(10    ),NREL(10    ),HL(10)
      DIMENSION SINITZ(10),LM(24),PRS(5),HH(10),SIGAVE(6)
      DIMENSION A(3,3),Z1(3,3),D(3),NCEL(1),NCNP(1)
      REWIND 4
      IF(NPUNCH.EQ.0) GO TO 20
C
C     READ AND PRINT DATA FOR LOAD CASE TO BE PUNCHED OUT
C
      READ 1050, (NLDP(I),I=1,NPUNCH)
      PRINT 1050,(NLDP(I),I=1,NPUNCH)
20    CONTINUE
C
C     READ AND PRINT MATERIAL PROPERTY DATA
C
      READ 1000,PATM
      PRINT 2000, PATM
      PRINT 2010
50    READ 1010, M,(EMPR(M,I),I=1,11)
      PRINT 2020, M,(EMPR(M,I),I=1,11)
      PHI=EMPR(M,9)/57.29577951
      CONST=2.0/(EMPR(M,10)*(1.0-SIN(PHI)))
      EMPR(M,12)=CONST*EMPR(M,8)*COS (PHI)
      EMPR(M,13)=CONST*SIN(PHI)
      IF (M.LT.NUMMAT) GO TO 50
      LL=0
C
C     READ AND PRINT NODAL POINT DATA AND BOUNDARY CONDITIONS
C
100   READ 1020, MM,X(MM),Y(MM),Z(MM),(ID(MM,I),I=1,3)
      IF(LL.LE. 0) GO TO 110
      DIFNP=MM-LL
      DX=(X(MM)-X(LL))/DIFNP
      DY= (Y (MM)-Y(LL))/DIFNP
      DZ=(Z(MM)-Z(LL))/DIFNP
110   LL=LL+1
      IF(MM-LL) 150,140,120
120   X(LL)=X(LL-1)+DX
      Y(LL)=Y(LL-1)+DY
      Z(LL)=Z(LL-1)+DZ
      DO 130 I=1,3
130   ID(LL,I)=ID(LL-1,I)
      GO TO 110
140   IF(NUMNPT-MM)150,160,100
150   PRINT 5000,MM
      CALL EXIT
160   PRINT 2030
      N=0
170   N=N+1
      PRINT 2040, N,X(N),Y(N),Z(N),(ID(N,I),I=1,3)
      IF(N.LT.NUMNPT) GO TO 170
      NN=0
C
C     READ AND PRINT ELEMENT DATA
C
200   READ 1030, N,(INP(N,I),I=1,9)
210   NN=NN+1
      IF(N.LE.NN) GO TO 230
      DO 220 K=1,8
220   INP(NN,K)=INP(NN-1,K)+1
      INP(NN,9)=INP(NN-1,9)
```

```
230   IF(N.GT.NN) GO TO 210
      IF(NUMELT.GT.NN) GO TO 200
      PRINT 2050
      N=0
250   N=N+1
      XCP(N)=0.
      YCP(N)=0.
      ZCP(N)=0.
      DO 255 I=1,8
      II=INP(N,I)
      XCP(N)=XCP(N)+X(II)/8.
      YCP(N)=YCP(N)+Y(II)/8.
255   ZCP(N)=ZCP(N)+Z(II)/8.
      PRINT 2060, N,(INP(N,M),M=1,9),XCP(N),YCP(N),ZCP(N)
      IF (N.LT.NUMELT) GO TO 250
C
C     SET UP EQUATION NUMBERS
C
      NEQ=0
      DO 330 N=1,NUMNPT
      DO 330 I=1,3
      IF(ID(N,I).LE.1000) GO TO 310
      NN=ID(N,I)-1000
      ID(N,I)=ID(NN,I)
      GO TO 330
310   IF(ID(N,I).EQ.1) GO TO 320
      NEQ=NEQ+1
      ID(N,I)=NEQ
      GO TO 330
320   ID(N,I)=0
330   CONTINUE
      PRINT 2070
      PRINT 2080, (N,(ID(N,I),I=1,3),N=1,NUMNPT)
C
C     DETERMINE BAND WIDTH
C
      MBAND=0
      DO 430 N=1,NUMELT
      MIN=100000
      MAX=0
      IJ=0
      DO 410 I=1,8
      II=INP(N,I)
      DO 410 J=1,3
      IJ=IJ+1
410   LM(IJ) =ID(II,J)
      WRITE(4) (LM(I),I=1,24)
      DO 420 L=1,24
      IF(LM(L).EQ.0) GO TO 420
      IF(LM(L).GT.MAX) MAX=LM(L)
      IF(LM(L).LT. MIN) MIN=LM(L)
420   CONTINUE
      NDIF=MAX-MIN+1
      IF(NDIF.GT.MBAND) MBAND=NDIF
430   CONTINUE
      NMXEQB=MTMN16/(MBAND+2)/2
      NEQB=NMXEQB
      IF(NEQB.GT.NEQ) NEQB=NEQ
      PRINT 2085, MBAND,NEQ,NEQB
      IF(NLAY.EQ.0) GO TO 440
C
C     READ AND PRINT CONSTRUCTION SEQUENCE INFORMATION
C
      PRINT 2090
      READ 1040, ((LN,(NOMEL(LN,I),I=1,2),(NOMNP(LN,J),J=1,2),
```

```
     1(NPHUMP(LN,K),K=1,4)),LJ=1,NLAY)
      PRINT 2100, ((LN,(NOMEL(LN,I),I=1,2),(NOMNP(LN,J),J=1,2),
     1(NPHUMP(LN,K),K=1,4)),LN=1,NLAY)
440   CONTINUE
      IF (NUMCEL .EQ. 0) GO TO 450
C
C     READ AND PRINT DATA FOR PREEXISTING ELEMENTS AND NODAL POINTS
C
      PRINT 2110
      READ 1050,(NCEL(N),N=1,NUMCEL)
      PRINT 1050,(NCEL(N),N=1,NUMCEL)
      PRINT 2120
      READ  1050, (NCNP(N),N=1,NUMCNP)
      PRINT 1050, (NCNP(N),N=1,NUMCNP)
450   CONTINUE
C
C     INITIALIZATION OF STRESSES,STRAINS, AND STRESS LEVELS
C     IN ALL ELEMENTS AND DISPLACEMENTS OF ALL NODAL POINTS
C
      DO 500 I=1,NUMELT
      SLMAX(I)=0.
      DO 500 J=1,6
      STRESS(I,J)=0.
500   STRAIN(I,J)=0.
      DO 510 I=1,NUMNPT
      DO 510 J=1,3
510   DISP(I,J)=0.
      IF (NUMCEL .EQ. 0) GO TO 550
C
C     READ STRESSES, STRAINS AND DISPLACEMENTS AND CALCULATE MODULUS
C                 VALUES FOR PREEXISTING PART
C
      READ 1050,NMODL
      READ 1100, (N,(STRESS(N,M),M=1,6),J=1,NUMCEL)
      IF(NMODL .EQ. 0) GO TO 520
      READ 1100, (N,(STRAIN(N,M),M=1,6),J=1,NUMCEL)
      READ 1110,(N,(DISP(N,M),M=1,3),J=1,NUMCNP)
      IF(NMODL .EQ. 1) GO TO 520
      READ 1120, ((N,BULK(N),SHEAR(N),POIS(N),SLMAX(N)),J=1,NUMCEL)
      GO TO 550
520   CONTINUE
      DO 530 I=1,NUMCEL
      N=NCEL(I)
      NN=3
      NM=3
      IND=0
      A(1,1)=STRESS(N,1)
      A(2,2)=STRESS(N,2)
      A(3,3)=STRESS(N,3)
      A(1,2)=STRESS(N,4)
      A(2,3)=STRESS(N,5)
      A(1,3)=STRESS(N,6)
      A(2,1)=A(1,2)
      A(3,2)=A(2,3)
      A(3,1)=A(1,3)
      CALL RSEIG(NM,NN,A,IND,D,Z1)
      CALL COMPAR(D)
      DO 523 JP=1,3
      PRS(JP)=D(JP)
523   CONTINUE
      MTYPE=INP(N,9)
      CALL MODU(EMPR,BULK,SHEAR,POIS,SLMAX,PRS,PATM,NUMMAT,N,
     1 MTYPE,STRLEV,1)
      SLMAX(N)=STRLEV
530   CONTINUE
```

```
550   CONTINUE
      IF(NFEL.EQ.0) GO TO 700
C
C     READ AND PRINT DATA FOR FOUNDATION LAYERS USED IN CALCULATING
C     INITIAL STRESSES
C
      PRINT 2200
      READ 1200,NFLAY,HFLEV
      PRINT 2210, NFLAY,HFLEV
      PRINT 2220
      I=0
600   I=I+1
      READ 1210, I,MATNO(I),NLEL(I),NREL(I),HL(I)
      PRINT 2230,I,MATNO(I),NLEL(I),NREL(I),HL(I)
      IF(I.GT.1) GO TO 610
      HH(I)=HL(I)-HFLEV
      GO TO 620
610   HH(I)=HL(I)-HL(I-1)
620   CONTINUE
      IF(I.LT.NFLAY) GO TO 600
C
C     CALCULATE INITIAL STRESSES AND MODULI FOR FOUNDATION ELEMENTS
C
      DO 670 I=1,NFLAY
      SINITY(I)=0.
      IF( I.EQ.NFLAY) GO TO 640
      NN=I+1
      DO 630 J=NN,NFLAY
      MTYPE=MATNO(J)
630   SINITY(I)=SINITY(I)+EMPR(MTYPE,1)*HH(J)
640   MTYPE=MATNO(I)
      SINITY(I)=SINITY(I)+EMPR(MTYPE,1)*HH(I)/2.
      SINITX(I)=EMPR(MTYPE,11)*SINITY(I)
      SINITZ(I)=SINITX(I)
      NNL=NLEL(I)
      NNR=NREL(I)
      DO 650 N=NNL,NNR
      STRESS(N,1)=SINITX(I)
      STRESS(N,2)=SINITY(I)
650   STRESS(N,3)=SINITZ(I)
      NNL1=NNL+1
      N=NNL
      MTYPE=INP(NNL,9)
      PRS(1)=STRESS(NNL,2)
      PRS(2)=STRESS(NNL,1)
      PRS(3)=STRESS(NNL,3)
      CALL MODU (EMPR,BULK,SHEAR,POIS,SLMAX,PRS,PATM,NUMMAT,N,
     1 MTYPE,STRLEV,1)
      SLMAX(NNL)=STRLEV
      DO 660 N=NNL1,NNR
      BULK(N)=BULK(NNL)
      SHEAR(N)=SHEAR(NNL)
      POIS(N)=POIS(NNL)
660   SLMAX(N)=SLMAX(NNL)
670   CONTINUE
700   CONTINUE
C
C     CALCULATE INITIAL STRESSES AND MODULI FOR LAYERS TO BE ADDED
C
      PRINT 2310
      IF(NLAY.EQ.0) GO TO 790
      DO 780 LN=1,NLAY
      NNL=NOMEL(LN,1)
      NNR=NOMEL(LN,2)
      II1=NPHUMP(LN,1)
```

```
      II2=NPHUMP(LN,2)
      II3=NPHUMP(LN,3)
      II4=NPHUMP(LN,4)
      DO 770 N=NNL,NNR
      IF(NUMCEL .EQ. 0) GO TO 720
      DO 710 M=1,NUMCEL
      IF(N .EQ. NCEL(M)) GO TO 770
710   CONTINUE
720   CONTINUE
      MTYPE=INP(N,9)
      IF(XCP(N).LE.X(II1)) GO TO 731
      IF(XCP(N).LE.X(II2)) GO TO 732
      IF(XCP(N).LE.X(II3)) GO TO 733
      IF(XCP(N).LE.X(II4)) GO TO 734
      SLOPE=0.
      HT=Y(II4)-YCP(N)
      GO TO 740
731   SLOPE=0.
      HT=Y(II1)-YCP(N)
      GO TO 740
732   SLOPE=(Y(II2)-Y(II1))/(X(II2)-X(II1))
      HT=Y(II1)+(XCP(N)-X(II1))*SLOPE-YCP(N)
      GO TO 740
733   SLOPE=(Y(II3)-Y(II2))/(X(II3)-X(II2))
      HT=Y(II2)+(XCP(N)-X(II2))*SLOPE-YCP(N)
      GO TO 740
734   SLOPE=(Y(II4)-Y(II3))/(X(II4)-X(II3))
      HT=Y(II3)+(XCP (N)-X(II3))*SLOPE-YCP(N)
740   BETA=ATAN(SLOPE)
      IF(ZCP(N) .LT. Z(II1) .AND. ZCP(N) .GT. Z(II2)) GO TO 741
      CETA=0.
      GO TO 743
741   CETA=(Y(II2)-Y(II1))/(Z(II1)-Z(II2))
      HT1=Y(II1)+(Z(II1)-ZCP(N))*CETA-YCP(N)
      IF(HT-HT1) 742,743,743
742   HTT=HT1
      GO TO 744
743   HTT=HT
744   STRESS(N,2)=HTT*EMPR(MTYPE,1)
      STRESS(N,4)=0.5*STRESS(N,2)*SIN(BETA)
      STRESS(N,5)=0.5*STRESS(N,2)*SIN(ATAN(CETA))
      STRESS(N,6)=0.
      SIGAVE(2)=STRESS(N,2)/2.
      SIGAVE(4)=STRESS(N,4)/2.
      SIGAVE(5)=STRESS(N,5)/2.
      SIGAVE(6)=0.
      POIS1=EMPR (MTYPE,6)
750   IF(POIS1 .GT.0.49) POIS1=0.49
      STRESS(N,1)=STRESS(N,2)*POIS1/(1.-POIS1)
      SIGAVE(1)=STRESS(N,1)/2.
      STRESS(N,3)=STRESS(N,1)
      SIGAVE(3)=SIGAVE(1)
      NN=3
      NM=3
      IND=0
      A(1,1)=SIGAVE(1)
      A(2,2)=SIGAVE(2)
      A(3,3)=SIGAVE(3)
      A(1,2)=SIGAVE(4)
      A(2,3)=SIGAVE(5)
      A(1,3)=SIGAVE(6)
      A(2,1)=A(1,2)
      A(3,2)=A(2,3)
      A(3,1)=A(1,3)
      CALL RSEIG(NM,NN,A,IND,D,Z1)
```

```
      CALL COMPAR(D)
      DO 753 I=1,3
      PRS(I)=D(I)
753   CONTINUE
      CALL MODU (EMPR,BULK,SHEAR,POIS,SLMAX,PRS,PATM,NUMMAT,N,
     1 MTYPE,STRLEV,1)
      POIST=POIS(N)
      IF (ABS(POIS1 -POIST).LT.0.0001) GO TO 760
      POIS1=POIS1+(POIST-POIS1)/10.
      GO TO 750
760   CONTINUE
      SLMAX(N)=STRLEV
770   CONTINUE
780   CONTINUE
790   CONTINUE
C
C     PRINT INITIAL MODULI AND STRESSES FOR ALL ELEMENTS
C
      DO 800 N=1,NUMELT
      EMOD=2.*SHEAR (N)*(1.+POIS(N))
      PRINT 2320, N,XCP(N),YCP(N),ZCP(N),EMOD,BULK(N),SHEAR(N),POIS(N),
     1 (STRESS(N,M),M=1,6)
800   CONTINUE
      REWIND 8
      REWIND 9
      WRITE(8) ((STRESS(I,J),J=1,6),I=1,NUMELT)
      WRITE(9) ((DISP(N,M),M=1,3),N=1,NUMNPT)
      WRITE(9) ((STRAIN(N,M),M=1,6),N=1,NUMELT)
      RETURN
1000  FORMAT(F10.0)
1010  FORMAT(I5,7F10.0/4F10.0)
1020  FORMAT(I5,3F10.0,3I5)
1030  FORMAT(10I5)
1040  FORMAT(9I5)
1050  FORMAT(15I5)
1100  FORMAT(I5,6F10.0)
1110  FORMAT(I5,3F10.0)
1120  FORMAT(I5,4F10.0)
1200  FORMAT(I5,F10.0)
1210  FORMAT(4I5,F10.0)
2000  FORMAT(///,23H MATERIAL PROPERTY DATA ///,
     1 22H ATMOSPHERIC PRESSURE=,F10.4//)
2010  FORMAT(28X,8H MODULUS,18X,14H POISSON RATIO /
     1 51H  MAT   UNIT WT       K           KUR        N           D,9X,1HG,
     2 9X,1HF,9X,1HC,8X,3HPHI,5X,10HFAIL.RATIO,5X,2HK0 /)
2020  FORMAT(I5,F10.4,2F10.1,8F10.4)
2030  FORMAT(23H1NODAL POINT INPUT DATA//,5H NODE,5X,
     1 23HNODAL POINT COORDINATES,19X,9HB.C. CODE/,7H NUMBER,
     2 56H     X-ORD      Y-ORD      Z-ORD                 XX   YY   ZZ /)
2040  FORMAT(I7,3F10.3,10X,3I5)
2050  FORMAT(31H1EIGHT NODES SOLID ELEMENT DATA//,
     1 5H ELET,5X,15HCONNECTED NODES,21X,5H MATL,4X,
     2 28H  ELEMENT CENTER COORDINATES/
     3 52H  NO.    I    J    K    L    M    N    O    P   NO. ,
     435H     X-ORD        Y-ORD         Z-ORD  /)
2060  FORMAT(10I5,3F12.3)
2070  FORMAT(17H1EQUATION NUMBERS//,20H    N    X    Y    Z/)
2080  FORMAT(4I5)
2085  FORMAT(/,
     1 35H0BAND WIDTH ************************I4 /
     2 35H0NUMBER OF EQUATIONS****************I4 /
     3 35H0NUMBER OF EQUATIONS IN BLOCK******I4)
2090  FORMAT(31H1CONSTRUCTION LAYER INFORMATION // 6H LAYER,
     1 23H   ADDED ELEMENTS          ,12H ADDED NODES,5X,
     2 40H                 NODES OF HUMPED SURFACE       /)
```

```
5000  FORMAT(17H N.P. ERROR ,N = I4)
2100  FORMAT(I5,I9,I6,2X,I10,I6,20X,4I6)
2110  FORMAT(29H0ELEMENTS OF PREEXISTING PART //)
2120  FORMAT(26H0NODES OF PREEXISTING PART //)
2200  FORMAT(28H1FOUNDATION PART INFORMATION)
2210  FORMAT(35H0NUMBER OF LAYER IN FOUNDATION***** I8 /
     1 35H0ELEVATION OF RIGID BOUNDARY******* F8.3 /)
2220  FORMAT(47H0LAYER  MAT. NO.  INCLUSIVE ELEMENTS  ELEVATION /)
2230  FORMAT(I5,3I10,F12.3)
2310  FORMAT(28H1 INITIAL VALUES IN ELEMENTS ///
     1 50H  ELE   X-ORD      Y-ORD      Z-ORD      E        K    ,
     2 74H      G       POISSON      S-XX      S-YY      S-ZZ      S-XY      S-Y
     3Z     S-XZ    //)
2320  FORMAT(I5,3F9.3,3F9.1,7F9.3)
      END


      SUBROUTINE MODU(EMPR,BULK,SHEAR,POIS,SLMAX,PRS,PATM,
     1 NUMMAT,N,MTYPE,STRLEV,KK)
      DIMENSION EMPR(NUMMAT,13),BULK(1),SHEAR(1),POIS(1),SLMAX(1),PRS(3)
C
C     CALCULATE SHEAR MODULUS, BULK MODULUS AND POISSON RATIO VALUES
C
      DEVSTR=PRS(1)-PRS(3)
      DEVFH=EMPR(MTYPE,12)+EMPR(MTYPE,13)*PRS(3)
      IF(DEVFH.GT.0.0) GO TO 100
      STRLEV=0.
      DEVLEV=0.
      GO TO 110
100   DEVLEV=DEVSTR/DEVFH
      STRLEV=DEVLEV/EMPR(MTYPE,10)
110   CONTINUE
      IF(KK.EQ.1) GO TO 140
      IF(PRS(3).GT. 0.0) GO TO 120
      POIS(N)=EMPR(MTYPE,6)
      IF(POIS(N).GT.0.49) POIS(N)=0.49
      GO TO 130
120   IF(STRLEV.LT.1.0.AND.SHEAR(N).GT.0.0001) GO TO 140
130   SHEAR(N)=0.0001
      GO TO 200
140   CONTINUE
      IF(PRS(3).LT. 0.01) PRS(3)=0.01
      IF (KK.EQ.3 .AND. STRLEV. LT. SLMAX(N)) GO TO 150
      EINIT=PATM*EMPR(MTYPE,2)*(PRS(3)/PATM)**EMPR(MTYPE,4)
      EMOD=EINIT*(1.-DEVLEV)**2.
      GO TO 160
150   EMOD=PATM*EMPR(MTYPE,3)*(PRS(3)/PATM)**EMPR(MTYPE,4)
160   CONTINUE
      POIS1=EMPR(MTYPE,6)-EMPR(MTYPE,7)*ALOG10(PRS(3)/PATM)
      EPSAX=DEVSTR/(EINIT*(1.-DEVLEV))
      POIS(N)=POIS1/((1.-EMPR(MTYPE,5)*EPSAX)**2.)
      IF(POIS(N).GT.0.49) POIS(N)=0.49
      SHEAR(N)=EMOD/(2.*(1.+POIS(N)))
      BULK(N)=SHEAR(N)/(1.-2.*POIS(N))
      IF(KK.NE.1) GO TO 200
      IF(STRLEV.GE.1.0.OR.PRS(3).LE.0.0) SHEAR(N)=0.0001
200   CONTINUE
      RETURN
      END
```

```
      SUBROUTINE FOMING(X,Y,Z,INP,NUMELT)
      COMMON /ISOP/ E1,E2,E3,RR(8),ZZ(8),QQ(8),LM(24),P(24),S(33,33),
     1 STR(6,33),STS(6,24),VJAC
      DIMENSION X(1),Y(1),Z(1),INP(NUMELT,9)
      DIMENSION SSS(2),TTT(2),QQQ(2)
      DATA SSS /-0.57735026918963,0.57735026918963/
      DATA TTT /-0.57735026918963,0.57735026918963/
      DATA QQQ /-0.57735026918963,0.57735026918963/
C
C     FORM STRAIN-DISPLACEMENT MATRIX
C
      REWIND 4
      REWIND 7
      DO 300 N=1,NUMELT
      DO 50 I=1,6
      DO 50 J=1,33
50    STR(I,J)=0.
      READ(4) (LM(I),I=1,24)
      WRITE(7) (LM(I),I=1,24)
      DO 100 I=1,8
      II=INP(N,I)
      RR(I)=X (II)
      ZZ(I)=Y(II)
100   QQ(I)=Z(II)
      DO 200 II=1,2
      E1=SSS(II)
      DO 200 JJ=1,2
      E2=TTT(JJ)
      DO 200 KK=1,2
      E3=QQQ(KK)
      CALL RELATE
      WRITE(7) VJAC,((STR(I,J),J=1,33),I=1,6)
200   CONTINUE
      E1=0.
      E2=0.
      E3=0.
      CALL RELATE
      WRITE(7) ((STR(I,J),J=1,24),I=1,6)
300   CONTINUE
      RETURN
      END



      SUBROUTINE RELATE
      COMMON /ISOP/ SX,TY,QZ,RR(8),ZZ(8),QQ(8),LM(24),P(24),S(33,33),
     1 STR(6,33),STS(6,24),VJAC
      DIMENSION HR(11),HZ(11),HQ(11),A(3,11),B(3,3),XX(8,3)
      DIMENSION II(11),JJ(11),KK(11),D(3 ,3 ),IPERM(3)
      DATA II/1,4,7,10,13,16,19,22,25,28,31/
      DATA JJ/2,5,8,11,14,17,20,23,26,29,32/
      DATA IPERM/2,3,1/
      DATA KK/3,6,9,12,15,18,21,24,27,30,33/
C
C     MATRIX OF DERIVATIVES
C
      SP=1.+SX
      SM=1.-SX
      TP=1.+TY
      TM=1.-TY
      QP=1.+QZ
      QM=1.-QZ
C
```

```
      A(1,1)=-TM*QM/8.
      A(1,2)=-A(1,1)
      A(1,3)=TP*QM/8.
      A(1,4)=-A(1,3)
      A(1,5)=-TM*QP/8.
      A(1,6)=-A(1,5)
      A(1,7)=TP*QP/8.
      A(1,8)=-A(1,7)
      A(1,9)=-2.*SX
      A(1,10)=0.
      A(1,11)=0.
C
      A(2,1)=-SM*QM/8.
      A(2,2)=-SP*QM/8.
      A(2,3)=-A(2,2)
      A(2,4)=-A(2,1)
      A(2,5)=-SM*QP/8.
      A(2,6)=-SP*QP/8.
      A(2,7)=-A(2,6)
      A(2,8)=-A(2,5)
      A(2,9)=0.
      A(2,10)=-2.*TY
      A(2,11)=0.

      A(3,1)=-SM*TM/8.
      A(3,2)=-SP*TM/8.
      A(3,3)=-SP*TP/8.
      A(3,4)=-SM*TP/8.
      A(3,5)=-A(3,1)
      A(3,6)=-A(3,2)
      A(3,7)=-A(3,3)
      A(3,8)=-A(3,4)
      A(3,9)=0.
      A(3,10)=0.
      A(3,11)=-2.*QZ
C
C     JACOBIAN
C
      DO 40 I=1,8
      XX(I,1)=RR(I)
      XX(I,2)=ZZ(I)
      XX(I,3)=QQ(I)
40    CONTINUE
      DO 60 I=1,3
      DO 60 J=1,3
      C=0.
      DO 50 L=1,8
50    C=C+A(I,L)*XX(L,J)
60    D(I,J)=C
      VJAC=D(1,1)*D(2,2)*D(3,3)+D(1,2)*D(2,3)*D(3,1)+D(1,3)*D(2,1)*
     1 D(3,2)-D(1,3)*D(2,2)*D(3,1)-D(1,1)*D(2,3)*D(3,2)-D(1,2)*D(2,1)*
     2 D(3,3)
C
      DO 70 I=1,3
      J=IPERM(I)
      K=IPERM(J)
      B(I,I)=(D(J,J)*D(K,K)-D(K,J)*D(J,K))/VJAC
      B(I,J)=(D(K,J)*D(I,K)-D(I,J)*D(K,K))/VJAC
70    B(J,I)=(D(J,K)*D(K,I)-D(J,I)*D(K,K))/VJAC
C
      DO 100 I=1,11
      HR(I)=0.
      HZ(I)=0.
      HQ(I)=0.
      DO 100 J=1,3
```

```
      HR(I)=B(1,J)*A(J,I)+HR(I)
      HZ(I)=B(2,J)*A(J,I)+HZ(I)
100   HQ(I)=B(3,J)*A(J,I)+HQ(I)
C
C     FORM STRIN DISPLACEMENT MATRIX
C
      DO 200 K3=1,11
      I=II(K3)
      J=JJ(K3)
      K=KK(K3)
      STR(1,I)=HR(K3)
      STR(2,J)=HZ(K3)
      STR(3,K)=HQ(K3)
      STR(4,I)=HZ(K3)
      STR(4,J)=HR(K3)
      STR(5,J)=HQ(K3)
      STR(5,K)=HZ(K3)
      STR(6,I)=HQ(K3)
200   STR(6,K)=HR(K3)
C
      RETURN
      END



      SUBROUTINE CALNEQ(ID,NCEL,NCNP,NOMEL,NOMNP,NPHUMP,NUMELT,NUMNPT,
     1 NUMCEL,NUMCNP,NUMLD,NLAY,LN,MBAND,NUMEL,NUMNP,NELCAL
     1 ,NNPCAL,NELRED,NNPRED,NEQ,NEQB,NBLOCK,NMXEQB)
      DIMENSION ID(NUMNPT,3),NCEL(1),NCNP(1)
      DIMENSION NOMEL(NUMLD,2 ),NOMNP(NUMLD,2 ),NPHUMP(NUMLD,4    )
C
C     DETERMINE CONTROL DATA
C
      IF(LN. GT. NLAY) GO TO 10
      PRINT 2000,LN
      PRINT 2010, (NOMEL(LN,N),N=1,2),(NOMNP(LN,M),M=1,2),
     1 (NPHUMP(LN,L),L=1,4)
      GO TO 20
10    LNMLAY=LN-NLAY
      PRINT 2020,LNMLAY
20    CONTINUE
      IF(LN.GT.NLAY) GO TO 80
      IF (NUMCEL .EQ. 0) GO TO 50
      NUMEL=MAX0(NOMEL(LN,2),NCEL(NUMCEL))
      NUMNP=MAX0(NOMNP(LN,2),NCNP(NUMCNP))
      GO TO 60
50    NUMEL=NOMEL(LN,2)
      NUMNP=NOMNP(LN,2)
60    NELCAL=NOMEL(LN,2)
      NELRED=NOMEL(LN,1)
      NNPCAL=NOMNP(LN,2)
      NNPRED=NOMNP(LN,1)
      GO TO 100
80    NUMEL=NUMELT
      NUMNP=NUMNPT
      NELCAL=NUMELT
      NNPCAL=NUMNPT
      NELRED=NUMELT+1
      NNPRED=NUMNPT+1
100   CONTINUE
C
C     DETERMINE NUMBER OF EQUATIONS AND BLOCKS
C
```

```
      NEQB=NMXEQB
      MAX=0
      DO 120 N=1,NUMNP
      DO 120 I=1,3
      IF(ID(N,I) .GT. MAX) MAX=ID(N,I)
120   CONTINUE
      NEQ=MAX
      IF(NEQB .GT. NEQ) NEQB=NEQ
      NBLOCK=(NEQ-1)/NEQB+1
      PRINT 2100,MBAND,NEQ,NEQB,NBLOCK
      RETURN
2000  FORMAT(/,
     1 57H ******************************************************** /
     2 57H ******************************************************** /
     3 57H *                                                      */
     4 45H *  LAYER NUMBER**************************** ,I4,8H      */
     5 57H *                                                     * /
     6 57H ******************************************************** /
     7 57H ******************************************************** /)
2010  FORMAT(/,
     1 35H0ADDED ELEMENTS*******************I5,5H THRU,I5 /
     2 35H0ADDED NODAL POINTS***************I5,5H THRU,I5 /
     3 35H0NODAL POINTS OF HUMPED SURFACE**** 4I5 /)
2020  FORMAT(/,
     1 57H ******************************************************** /
     2 57H ******************************************************** /
     3 57H *                                                     * /
     4 45H *  LOAD CASE AFTER CONSTRUCTION*************,I4,8H     * /
     5 57H *                                                    *  /
     657H********************************************************   /
     757H********************************************************   /)
2100  FORMAT(/,
     1 35H0BAND WIDTH*********************** I4 /
     2 35H0TOTAL NUMBER OF EQUATIONS********* I4 /
     3 35H0NUMBER OF EQUATIONS IN BLOCK****** I4 /
     435H0NUMBER OF BLOCKS*****************  I4 /)
      END



      SUBROUTINE FORCE(EMPR,ID,X,Y,Z,INP,NCEL,NOMEL,FX,FY,FZ,B,R,
     1 NUMELT,NUMNPT,NUMCEL,NUMMAT,NUMLD,NLAY,LN,NEQ,NEQB,NUMNP)
      DIMENSION EMPR(NUMMAT,13),ID(NUMNPT,3),X(1),Y(1),Z(1)
      DIMENSION INP(NUMELT,9),NOMEL(NUMLD,2 ),FX(1),FY(1),FZ(1),B(1)
      DIMENSION R(NEQB),NCEL(1)
C
C     CALCULATE NODAL POINT FORCES DUE TO WEIGHTS OF ADDED ELEMENTS
C
      DO 50 I=1,NUMNP
      FX(I)=0.
      FY(I)=0.
50    FZ(I)=0.
      IF(LN.GT. NLAY) GO TO 400
      NELS=NOMEL(LN,1)
      NELL=NOMEL(LN,2)
      DO 300 N=NELS,NELL
      IF(NUMCEL .EQ. 0) GO TO 100
      DO 80 M=1,NUMCEL
      IF(N.EQ. NCEL(M)) GO TO 300
80    CONTINUE
100   CONTINUE
      FG=0.
      MTYPE=INP(N,9)
```

```
      KK=1
      I=INP(N,1)
      J=INP(N,2)
      K=INP(N,4)
      L=INP(N,5)
120   VOL=((X(J)-X(I))*(Y(K)*Z(L)-Y(L)*Z(K))+(X(L)-X(K))*(Y(I)*Z(J)-
     1 Y(J)*Z(I))+(X(I)-X(K))*(Y(J)*Z(L)-Y(L)*Z(J))+(X(L)-X(I))*
     2(Y(J)*Z(K)-Y(K)*Z(J))+(X(J)-X(L))*(Y(I)*Z(K)-Y(K)*Z(I))+
     3 (X(K)-X(J))*(Y(I)*Z(L)-Y(L)*Z(I)))/6.
      FG=FG-EMPR(MTYPE,1)*VOL
      IF(KK.EQ.5) GO TO 140
      IF(KK.EQ.2) GO TO 137
      IF(KK.EQ.3) GO TO 138
      IF(KK.EQ.4) GO TO 139
      KK=KK+1
      I=INP(N,2)
      J=INP(N,3)
      K=INP(N,4)
      L=INP(N,7)
      GO TO 120
137   KK=KK+1
      I=INP(N,2)
      J=INP(N,5)
      K=INP(N,6)
      L=INP(N,7)
      GO TO 120
138   KK=KK+1
      I=INP(N,2)
      J=INP(N,4)
      K=INP(N,5)
      L=INP(N,7)
      GO TO 120
139   KK=KK+1
      I=INP(N,4)
      J=INP(N,5)
      K=INP(N,7)
      L=INP(N,8)
      GO TO 120
140   CONTINUE
      FG=FG/8.
      KL=8
      DO 250 I=1,KL
      II=INP(N,I)
250   FY(II)=FY(II)+FG
300   CONTINUE
      GO TO 650
400   CONTINUE
C
C     READ NODAL POINT FORCE DATA AND DISTRIBUTED LOAD DATA
C                              FOR LOAD CASE AFTER CONSTRUCTION
C
      READ 1000,NUMFC
      PRINT 2000,NUMFC
      IF(NUMFC.EQ.0) GO TO 550
      DO 520 I=1,NUMFC
520   READ 1010, MM,FX(MM),FY(MM),FZ(MM)
550   CONTINUE
650   CONTINUE
C
C     SET UP FORCE VECTOR
C
      DO 700 I=1,NEQ
700   B(I)=0.
      DO 720 N=1,NUMNP
      DO 720 I=1,3
```

```
      II=ID(N,I)
      IF(II.LT. 1) GO TO 720
      IF(I .EQ. 2) GO TO 710
      IF(I.EQ.3) GO TO 715
      B(II)=B(II)+FX(N)
      GO TO 720
710   B(II)=B(II)+FY(N)
      GO TO 720
715   B(II)=B(II)+FZ(N)
720   CONTINUE
      REWIND 10
      KSHIFT=0
      DO 730 I=1,NEQB
730   R(I)=0.
      DO 750 N=1,NEQ
      II=N-KSHIFT
      R(II)=B(N)
      IF(II .NE. NEQB) GO TO 750
      WRITE(10) R
      KSHIFT=KSHIFT+NEQB
      DO 740 I=1,NEQB
740   R(I)=0.
750   CONTINUE
      WRITE(10) R
C
C     PRINT NODAL POINT FORCES
C
      IF(LN .LE. NLAY) GO TO 760
      PRINT 2030
      GO TO 770
760   PRINT 2035
770   CONTINUE
      DO 800 N=1,NUMNP
800   PRINT 2040, N,FX(N),FY(N),FZ(N)
1000  FORMAT(I5)
1010  FORMAT(I5,3F10.0)
2000  FORMAT(/,
     1 35HONUMBER OF N.P. FORCE CARDS******** ,1X,I3)
2030  FORMAT(19H1NODAL POINT FORCES // 35H    NP     X-FORCE    Y-FORCE    Z-
     1FORCE/)
2035  FORMAT(47H1NODAL POINT FORCES (WEIGHT OF ADDED ELEMENTS ) //,
     1 35H    NP     X-FORCE    Y-FORCE    Z-FORCE/)
2040  FORMAT(I5,3F10.3)
      RETURN
      END
```

```
      SUBROUTINE BILDUP (BULK,SHEAR,NCEL,NUMCEL,NUMEL,NELCAL,NELRED)
      COMMON /ISOP/ E1,E2,E3,RR(8),ZZ(8),QQ(8),LM(24),P(24),S(33,33),
     1 STR(6,33),STS(6,24),VJAC
      DIMENSION BULK(1),SHEAR(1),POIS(1),NCEL(1)
      REWIND 2
      REWIND 11
      REWIND 7
C
C     INITIALIZATION
C
      DO 300 N=1,NUMEL
      KEY=0

      DO 20 I=1,33
      DO 20 J=1,33
```

```
20    S(I,J)=0.
C
C     FORM STIFFNESS MATRIX AND WRITE ON TAPE 2
C
      IF(N .LE. NELCAL .OR. NUMCEL .EQ. 0) GO TO 40
      DO 30 M=1,NUMCEL
      IF (N.EQ. NCEL(M)) GO TO 40
30    CONTINUE
      GO TO 50
40    KEY=1
50    CONTINUE
      IF(KEY .EQ. 0) GO TO 80
      IF(N.GE.NELRED.AND.N.LE.NELCAL) GO TO 60
55    LL=1
      FMAG=1.
      GO TO 80
60    IF (NUMCEL .EQ. 0) GO TO 75
      DO 70 M=1,NUMCEL
      IF(N .EQ. NCEL(M)) GO TO 55
70    CONTINUE
75    LL=0
      FMAG=0.00001
80    CONTINUE
      READ(7) (LM(I),I=1,24)
      C1=FMAG*(BULK(N)+SHEAR(N))
      C2=FMAG*(BULK(N)-SHEAR(N))
      C3=FMAG*SHEAR(N)
      DO 100 LX=1,2
      DO 100 LY=1,2
      DO 100 LZ=1,2
      READ(7) VJAC,((STR(I,J),J=1,33),I=1,6)
      IF(KEY . EQ. 0) GO TO 100
      DO 90 J=1,33
      D1=VJAC*(C1*STR(1,J)+C2*STR(2,J)+C2*STR(3,J))
      D2=VJAC*(C2*STR(1,J)+C1*STR(2,J)+C2*STR(3,J))
      D3=VJAC*(C2*STR(1,J)+C2*STR(2,J)+C1*STR(3,J))
      D4=VJAC*C3*STR(4,J)
      D5=VJAC*C3*STR(5,J)
      D6=VJAC*C3*STR(6,J)
      DO 90 I=J,33
      S(I,J)=S(I,J)+STR(1,I)*D1+STR(2,I)*D2+STR(3,I)*D3+STR(4,I)*D4
     1 +STR(5,I)*D5+STR(6,I)*D6
90    S(J,I)=S(I,J)
100   CONTINUE
      IF(KEY . EQ. 0) GO TO 160
C
C     ELIMINATE EXTRA DEGREES OF FREEDOM
C
      DO 150 NN=1,9
      L=33-NN
      K=L+1
      IF(S(K,K).EQ.0.) GO TO 139
      GO TO 141
139   PRINT 140,K,S(K,K)
140   FORMAT(5X,≠K =≠,I5,≠S(K,K) =≠, F13.3)
141   DO 150 I=1,L
      C=S (I,K)/S (K,K)
      DO 150 J=1,L
150   S(I,J)=S(I,J)-C*S(K,J)
160   CONTINUE
      WRITE(2) (LM(I),I=1,24),((S(I,J),J=1,24),I=1,24)
C
C     FORM STRAIN-DISPLACEMENT MATRIX AND WRITE ON TAPE 11
C
      READ(7) ((STR(I,J),J=1,24),I=1,6)
```

```
      IF(KEY .EQ. 0) GO TO 300
      WRITE(11)(LM(I),I=1,24),((STR(I,J),J=1,24),I=1,6),LL
300   CONTINUE
      RETURN
      END



      SUBROUTINE ADDSTF( A,B,NUMEL,NEQB,NE2B,NBLOCK ,MBAND)
C     FORM GLOBAL EQUILIBRIM EQUATIONS IN BLOCKS
      COMMON /ISOP/ E1,E2,E3,RR(8),ZZ(8),QQ(8),LM(24),P(24),S(33,33),
     1 STR(6,33),STS(6,24),UJAC
      DIMENSION A(NE2B,MBAND),B(NE2B)
      K=NEQB+1
      X=NBLOCK
      MB=SQRT(X)
      MB=MB/2+1
      NEBB=MB*NE2B
      MM=1
C
      NSHIFT=0
      REWIND 10
      REWIND 4
C
C     FORM EQUATIONS IN BLOCKS    (2 BLOCKS AT A TIME)
C
      DO 500 M=1,NBLOCK,2
      DO 100 I=1,NE2B
      DO 100 J=1,MBAND
100   A (I,J)=0.
      READ (10) (B(I),I=1,NEQB)
      IF(M .EQ. NBLOCK) GO TO 120
      READ (10) (B(I),I=K,NE2B)
120   CONTINUE
C
      REWIND 2
      REWIND 3
      NA=3
      NUME=NUM3
      IF(MM .NE. 1) GO TO 150
      NA=2
      NUME=NUMEL
      NUM3=0
150   DO 300 N=1,NUME
      READ(NA) (LM(I),I=1,24),((S(I,J),J=1,24),I=1,24)
      DO 220 I=1,24
      LMN= 1-LM(I)
      II=LM(I)-NSHIFT
      IF(II .LE. 0 .OR.II .GT. NE2B) GO TO 220
      DO 200 J=1,24
      JJ=LM(J)+LMN
      IF(JJ.LE.0) GO TO 200
      A(II,JJ)=A(II,JJ)+S(I,J)
200   CONTINUE
220   CONTINUE
C
C     DETERMINE IF STIFFNESS IS TO BE PLACED ON TAPE 3
C
      IF(MM.GT. 1 )GO TO 300
      DO 250 I=1,24
      II=LM(I)-NSHIFT
      IF(II .GT. NE2B .AND.II .LE. NEBB) GO TO 260
250   CONTINUE
```

```
      GO TO 300
260   WRITE(3) (LM(I),I=1,24),((S(I,J),J=1,24),I=1,24)
      NUM3=NUM3+1
300   CONTINUE
      WRITE(4)  ((A(I,J),I=1,NEQB),J=1,MBAND),(B(I),I=1,NEQB)
      IF(M .EQ. NBLOCK) GO TO 500
      WRITE(4) ((A(I,J),I=K,NE2B),J=1,MBAND),(B(I),I=K,NE2B)
      IF(MM.EQ.MB) MM=0
      MM=MM+1
      NSHIFT=NSHIFT+NE2B
500   CONTINUE
      RETURN
      END



      SUBROUTINE COMPAR(VB)
      DIMENSION PRS(3),VB(3)
      IF(VB(1)-VB(2)) 10,11,11
10    PRS(1)=VB(2)
      PRS(3)=VB(1)
      GO TO 12
11    PRS(1)=VB(1)
      PRS(3)=VB(2)
12    IF(PRS(1)-VB(3)) 13,14,14
13    PRS(2)=PRS(1)
      PRS(1)=VB(3)
      GO TO 18
14    IF(PRS(3)-VB(3)) 16,15,15
15    PRS(2)=PRS(3)
      PRS(3)=VB(3)
      GO TO 18
16    PRS(2)=VB(3)
18    CONTINUE
      VB(1)=PRS(1)
      VB(2)=PRS(2)
      VB(3)=PRS(3)
      RETURN
      END



      SUBROUTINE SYMBAN(A,B,MAXB,NEQB,MB,NBLOCK,NSB,NORG,NBKS,NT1,
     1 NT2,NRST)
      DIMENSION A(NSB),B(NSB),MAXB(NEQB)
C
      NC=MB+1
      NBR=(MB-1)/NEQB+1
      INC=NEQB-1
      NMB=NEQB*MB
      N2=NT2
      N1=NT1
      REWIND NORG
      REWIND NBKS
C
C     REDUCE EQUATIONS BLOCK-BY-BLOCK
C
      DO 900 N=1,NBLOCK
      IF(N.GT.1.AND.NBR.EQ.1) GO TO 110
      IF(NBR.EQ.1) GO TO 105
      REWIND N1
```

```
      REWIND N2
105   NI=N1
      IF(N.EQ.1) NI=NORG
      READ(NI) A
110   DO 300 I=1,NEQB
      D=A(I)
      IF(D)115,300,120
115   M=NEQB*(N-1)+I
      PRINT 116,M,D
116   FORMAT(33H0SET OF EQUATIONS MAY BE SINGULAR    /
     1  26H DIAGONAL TERM OF EQUATION   I8, 8H  EQUALS    1PE12.4)
      STOP
C
120   II=I
      DO 125 J=2,NC
      II=II+NEQB
125   A(II)=A(II)/D
C
      DO 130 J=I,NMB,NEQB
      IF(A(J).NE.0.) MAXB(I)=J
130   CONTINUE
C
      JL=I+1
      IF(JL.GT.NEQB) GO TO 300
      II=I
      DO 200 J=JL,NEQB
      II=II+NEQB
      IF(II.GT.NMB) GO TO 200
      C=A(II)
      IF(C.EQ.0.0) GO TO 200
      C=C*A(I)
C
      KK=J-II
      MAX=MAXB(I)
      DO 150 JJ=II,MAX,NEQB
150   A(JJ+KK)=A(JJ+KK)-C*A(JJ)
C
      KK=J+NMB
      JJ=I+NMB
      A(KK)=A(KK)-C*A(JJ)
200   CONTINUE
300   CONTINUE
      WRITE(NBKS) A,MAXB
C
C     SUBSTITUTE INTO REMAINING EQUATIONS
C
      DO 800 NN=1,NBR
      IF(N+NN.GT.NBLOCK) GO TO 800
      NI=N1
      IF(N.EQ.1) NI=NORG
      IF(NN.EQ.NBR) NI=NORG
      READ(NI) B
      IL=1+NN*NEQB*NEQB
      DO 700 I=1,NEQB
      II=IL
      DO 690 K=1,NEQB
      IF(II.GT.NMB) GO TO 690
      C=A(II)
      IF(C.EQ.0.0) GO TO 690
      C=C*A(K)
      MAX=MAXB(K)
C
      KK=I-II
      DO 640 JJ=II,MAX,NEQB
640   B(JJ+KK)=B(JJ+KK)-C*A(JJ)
```

```
C
      KK=I+NMB
      JJ=K+NMB
      B(KK)=B(KK)-C*A(JJ)
C
690   II=II-INC
700   IL=IL+NEQB
C
      IF(NBR.NE.1) GO TO 750
      DO 740 I=1,NSB
740   A(I)=B(I)
      GO TO 800
750   WRITE(N2) B
800   CONTINUE
C
      M=N1
      N1=N2
900   N2=M
C
C     BACKSUBSTITUTION- RESULTS ON TAPE NRST
C
      NEB=NEQB*(NBR+1)
      NUM=NBR*NEQB
      DO 905 I=1,NEB
905   B(I)=0.
      REWIND NRST
C
      DO 1000 N=1,NBLOCK
      BACKSPACE NBKS
      READ(NBKS) A,MAXB
      BACKSPACE NBKS
      K=NEB
      DO 910 J=1,NUM
      I=K-NEQB
      B(K)=B(I)
910   K=K-1
C
      I=NMB
      K=0
      DO 920 J=1,NEQB
      I=I+1
      K=K+1
920   B(K)=A(I)
C
      DO 950 I=1,NEQB
      J=NEQB+1-I
      MAX=MAXB(J)
      IF(A(J).EQ.0.0) GO TO 950
      KK=J
      JJ=KK+1
      IL=J+NEQB
      C=B(KK)
      DO 940 II=IL,MAX,NEQB
      C=C-A(II)*B(JJ)
940   JJ=JJ+1
      B(KK)=C
950   CONTINUE
C
      I=0
      K=0
      DO 960 J=1,NEQB
      K=K+1
      I=I+1
960   A(I)=B(K)
C
```

```
      WRITE(NRST) (A(I),I=1,NEQB)
 1000 CONTINUE
C
      RETURN
      END




      SUBROUTINE RESULT(EMPR,ID,X,Y,Z,INP,BULK,SHEAR,POIS,SLMAX,NCEL,
     1 NCNP,NLDP,DISP,STRESS,STRAIN,SNEW,DELD,B,R,PATM,NUMELT,
     2 NUMNPT,NUMCEL,NUMCNP,NUMMAT,NUMLD,NLAY,LN,IT,NPUNCH,NUMEL,
     3 NUMNP,NELCAL,NNPCAL,NNPRED,NEQ,NEQB,NBLOCK)
      COMMON /ISOP/ E1,E2,E3,RR(8),ZZ(8),QQ(8),LM(24),P(24),S(33,33),
     1 STR(6,33),STS(6,24),UJAC
      COMMON/JSOP/ LAYSUM,MFLAY,MLEL,MREL,MOMEL,HEIGHT
      DIMENSION EMPR(NUMMAT,13),ID(NUMNPT,3),BULK(1),SHEAR(1),POIS(1)
      DIMENSION INP(NUMELT,9),SLMAX(1),NLDP(1),NCEL(1),NCNP(1)
      DIMENSION DISP(NUMNPT,3),STRESS(NUMELT,6),STRAIN(NUMELT,6)
      DIMENSION SNEW(NUMELT,6),DELD(NUMNPT,3),B(1),R(1)
      DIMENSION SIG(6),EPS(6),PRS(14),A(3,3),Z1(3,3),D(3)
      DIMENSION X(1),Y(1),Z(1)
      DIMENSION HEIGHT(20),MLEL(20),MREL(20),MOMEL(20,2)
      REWIND 2
      REWIND 8
      REWIND 11
C
C     MOVE DISPLACEMENTS INTO CORE
C
      NQ=NEQB*NBLOCK
      DO 10 NN=1,NBLOCK
      READ(2) (R(I),I=1,NEQB)
      N=NEQB
      IF(NN.EQ.1) N=NEQ-NQ+NEQB
      NQ=NQ-NEQB
      DO 10 J=1,N
      I=NQ+J
   10 B(I)=R(J)
      IF(LN.GT.NLAY) GO TO 15
      PRINT 2000,LN,IT
      GO TO 16
   15 LNMLAY=LN-NLAY
      PRINT 2005,LNMLAY,IT
   16 CONTINUE
      IF(IT.LT.2) GO TO 110
C
C     ADD INCREMENTAL DISPLACEMENTS AND PRINT INCREMENTAL AND TOTAL
C                   DISPLACEMENTS
C
      PRINT 2010
      REWIND 9
      READ(9) ((DISP(N,M),M=1,3),N=1,NUMNPT)
      READ(9) ((STRAIN(N,M),M=1,6),N=1,NUMELT)
      DO 20 N=1,NUMNP
      DO 20 I=1,3
   20 DELD(N,I)=0.
      DO 70 N=1,NUMNP
      IF(N .LE. NNPCAL .OR. NUMCNP .EQ. 0) GO TO 40
      DO 30 M=1,NUMCNP
      IF (N.EQ. NCNP(M)) GO TO 40
   30 CONTINUE
      GO TO 70
   40 CONTINUE
      IF(N.LT.NNPRED.OR.N.GT.NNPCAL) GO TO 45
```

```
      IF(NUMCNP .EQ. 0) GO TO 70
      DO 42 M=1,NUMCNP
      IF(N .EQ. NCNP(M)) GO TO 45
42    CONTINUE
      GO TO 70
45    CONTINUE
      DO 50 I=1,3
      II=ID(N,I)
      IF(II.LT.1) GO TO 50
      DELD(N,I)=B(II)
50    CONTINUE
      DO 60 J=1,3
60    DISP(N,J)=DISP(N,J)+DELD(N,J)
70    CONTINUE
      DO 100 N=1,NUMNP
      IF(N .LE. NNPCAL .OR. NUMCNP .EQ. 0) GO TO 90
      DO 80 M=1,NUMCNP
      IF(N .EQ. NCNP(M)) GO TO 90
80    CONTINUE
      GO TO 100
90    CONTINUE
      TD=SQRT(DISP(N,1)**2+DISP(N,2)**2+DISP(N,3)**2)
      PRINT 2050, N,(DELD(N,I),I=1,3),(DISP(N,M),M=1,3),TD,N
100   CONTINUE
110   CONTINUE
C
C     CALCULATE INCREMENTAL STRESSES AND STRAINS, ADD INCREMENTAL
C     STRESSES AND STRAINS AND PRINT STRAINS AND MODULUS VALUES
C
      READ(8) ((STRESS(I,J),J=1,6),I=1,NUMELT)
      DO 120 N=1,NUMEL
      DO 120 I=1,6
120   SNEW(N,I)=STRESS(N,I)
      DO 300 N=1,NUMEL
      IF(N .LE. NELCAL .OR. NUMCEL .EQ. 0) GO TO 160
      DO 140 M=1,NUMCEL
      IF(N .EQ. NCEL(M)) GO TO 160
140   CONTINUE
      GO TO 300
160   CONTINUE
      READ(11) (LM(I),I=1,24),((STR(I,J),J=1,24),I=1,6),LL
      IF(LL.EQ.0) GO TO 222
C
C     FORM STRESS-DISPLACEMENT MATRIX
C
      C1=BULK(N)+SHEAR(N)
      C2=BULK(N)-SHEAR(N)
      C3=SHEAR(N)
      DO 200 K=1,24
      STS(1,K)=C1*STR(1,K)+C2*STR(2,K)+C2*STR(3,K)
      STS(2,K)=C2*STR(1,K)+C1*STR(2,K)+C2*STR(3,K)
      STS(3,K)=C2*STR(1,K)+C2*STR(2,K)+C1*STR(3,K)
      STS(4,K)=C3*STR(4,K)
      STS(5,K)=C3*STR(5,K)
      STS(6,K)=C3*STR(6,K)
      KK=LM(K)
      IF(KK.EQ.0) GO TO 180
      P(K)=B(KK)
      GO TO 200
180   P(K)=0.
200   CONTINUE
      DO 220 I=1,6
      SIG(I)=0.
      DO 220 K=1,24
220   SIG(I)=SIG(I)+STS(I,K)*P(K)
```

```
      GO TO 228
222   CONTINUE
      IF(IT.EQ.1) GO TO 225
      DO 224 I=1,6
224   SIG(I)=0.
      GO TO 228
225   CONTINUE
      DO 226 I=1,6
226   SIG(I)=STRESS(N,I)
228   CONTINUE
      IF(IT.EQ.2) GO TO 240
      DO 230 I=1,6
230   SNEW(N,I)=STRESS(N,I)-0.5*SIG(I)
      GO TO 300
240   CONTINUE
      DO 250 I=1,6
      SNEW(N,I)=STRESS(N,I)-SIG(I)
250   STRESS(N,I)=SNEW(N,I)
      DO 270 I=1,6
      EPS(I)=0.
      IF(LL.EQ.0) GO TO 270
      DO 260 K=1,24
260   EPS(I)=EPS(I)+STR(I,K)*P(K)
270   STRAIN(N,I)=STRAIN(N,I)-EPS(I)*100.
300   CONTINUE
      IF(IT.LT.2) GO TO 400
      PRINT 2100
      DO 360 N=1,NUMEL
      IF(N .LE. NELCAL .OR. NUMCEL .EQ. 0) GO TO 340
      DO 320 M=1,NUMCEL
      IF(N .EQ. NCEL(M)) GO TO 340
320   CONTINUE
      GO TO 360
340   CONTINUE
C
C     CALCULATE PRINCIPAL STRAINS
C
      IND=0
      NM=3
      N1=3
      A(1,1)=STRAIN(N,1)
      A(2,2)=STRAIN(N,2)
      A(3,3)=STRAIN(N,3)
      A(1,2)=STRAIN(N,4)
      A(2,3)=STRAIN(N,5)
      A(1,3)=STRAIN(N,6)
      A(2,1)=A(1,2)
      A(3,2)=A(2,3)
      A(3,1)=A(1,3)
      CALL RSEIG(NM,N1,A,IND,D,Z1)
      CALL COMPAR(D)
      PRS(1)=D(1)
      PRS(2)=D(3)
      PRS(3)=(PRS(1)-PRS(2))/2.
      EMOD=2.*BULK(N)*(1.+POIS(N))*(1.-2.*POIS(N))
      PRINT 2150, N,EMOD,BULK(N),SHEAR(N),POIS(N),(STRAIN(N,M),M=1,6),
     1 PRS(3),N
360   CONTINUE
      PRINT 2200
      PRINT 2160
400   CONTINUE
C
C     CALCULATE PRINCIPAL STRESSES AND NEW MODULUS VALUES
C
      DO 500 N=1,NUMEL
```

```
      IF(N .LE. NELCAL .OR. NUMCEL .EQ. 0) GO TO 440
      DO 420 M=1,NUMCEL
      IF (N .EQ. NCEL(M)) GO TO 440
420   CONTINUE
      GO TO 500
440   CONTINUE
      IND=0
      NM=3
      N1=3
      A(1,1)=SNEW(N,1)
      A(2,2)=SNEW(N,2)
      A(3,3)=SNEW(N,3)
      A(1,2)=SNEW(N,4)
      A(2,3)=SNEW(N,5)
      A(1,3)=SNEW(N,6)
      A(2,1)=A(1,2)
      A(3,2)=A(2,3)
      A(3,1)=A(1,3)
      CALL RSEIG(NM,N1,A,IND,D,Z1)
      CALL COMPAR(D)
      DO 443 I=1,3
      PRS(I)=D(I)
443   CONTINUE
      MTYPE=INP(N,9)
      KL=2
      IF(IT.EQ.1) KL=3
      CALL MODU (EMPR,BULK,SHEAR,POIS,SLMAX,PRS,PATM,NUMMAT,N,
     1  MTYPE,STRLEV,KL)
      IF(IT.LT.2) GO TO 500
      IF(STRLEV.GT.SLMAX(N)) SLMAX(N)=STRLEV
      PRS(4)=(PRS(1)-PRS(3))/2.
C     CALCULATE THREE DIRECTIONS OF STRESSES
      JJ1=1
      DO 451 I=1,3
      PRS(5+(JJ1-1)*I)=57.29577951*Z1(I,1)
      PRS(6+(JJ1-1)*I)=57.29577951*Z1(I,2)
      PRS(7+(JJ1-1)*I)=57.29577951*Z1(I,3)
      JJ1=JJ1+1
451   CONTINUE
      IF(PRS(3).NE.0.) GO TO 460
      PRS(14)=999.99
      GO TO 470
460   PRS(14)=PRS(1)/PRS(3)
470   CONTINUE
C
C     PRINT STRESSES
C
      PRINT 2250, N,(STRESS(N,M),M=1,6),(PRS(I),I=1,3),PRS(14),
     1SLMAX(N),STRLEV
500   CONTINUE
      IF(IT.LT.2) GO TO 530
      REWIND 9
      WRITE(9) ((DISP(N,M),M=1,3),N=1,NUMNPT)
      WRITE(9) ((STRAIN(N,M),M=1,6),N=1,NUMELT)
      IF(LN .EQ. NUMLD) GO TO 501
      GO TO 508
501   READ 2203, IFXY,IFYZ
      IF(IFXY .EQ. 0 .AND. IFYZ .EQ. 0) GO TO 504
      READ 1000, LAYSUM,MFLAY
      READ 1010, ((HEIGHT(I)),I=1,LAYSUM)
      READ 1020, ((MLEL(I),MREL(I)),I=1,MFLAY)
      MELAY=LAYSUM-MFLAY
      READ 1020, ((MOMEL(I,1),MOMEL(I,2)),I=1,MELAY)
      IF(IFXY .EQ. 0) GO TO 502
      CALL FACTXY(EMPR,X,Y,Z,INP,SHEAR,STRESS,NUMELT,NUMMAT)
```

```
502   IF(IFYZ .EQ. 0) GO TO 504
      CALL FACTYZ(EMPR,X,Y,Z,INP,SHEAR,STRESS,NUMELT,NUMMAT)
504   CONTINUE
508   CONTINUE
      REWIND 8
      WRITE(8) ((STRESS(N,M),M=1,6),N=1,NUMELT)
      IF(NPUNCH.EQ.0) GO TO 530
      DO 510 I=1,NPUNCH
      IF(LN.EQ.NLDP(I)) GO TO 520
510   CONTINUE
      GO TO 530
520   CONTINUE
      PUNCH 2500,(N,(STRESS(N,M),M=1,6),N=1,NUMEL)
      PUNCH 2500,(N,(STRAIN(N,M),M=1,6),N=1,NUMEL)
      PUNCH 2550,(N,(DISP(N,M),M=1,3),N=1,NUMNP)
      PUNCH 2600, (N,(BULK(N),SHEAR(N),POIS(N),SLMAX(N)),N=1,NUMEL)
530   CONTINUE
      RETURN
1000  FORMAT(2I5)
1010  FORMAT(8F10.2)
1020  FORMAT(2I5)
2000  FORMAT(15H1LAYER NUMBER =,I3,15H    ITERATION =,I3/
     1 60H************************************************************ /)
2005  FORMAT(12H1LOAD CASE =,I3,15H    ITERATION =,I3/
     1 60H ************************************************************ /)
2010  FORMAT(65H0  NP     DELTA-X   DELTA-Y   DELTA-Z    X-DISP    Y-DISP
     1    Z-DISP ,15H     TOTAL   NP/)
2050  FORMAT(I5,7F10.4,I5)
2100  FORMAT(53H1 MODULUS AND POISSON S RATIO VALUES BASED ON AVERAGE,
     1 30H STRESSES DURING THE INCREMENT,/,
     2 49H  STRAINS FOR FINAL CONDITION AT END OF INCREMENT,//,
     3 51H  ELE  ELAS MOD  BULK MOD  SHEAR MOD   POIS   EPS-X,
     4 56H   EPS-Y  EPS-Z  GAM-XY  GAM-YZ  GAM-ZX    GAMMAX    ELE  /)
2150  FORMAT(I5,3F10.1, 8F8.3,I5)
2160  FORMAT(
     1 132H          SIG-X     SIG-Y     SIG-Z     TAU-XY     TAU-YZ
     2 TAU-ZX     SIG-1     SIG-2     SIG-3     SIG1/SIG3    SLMAX     S
     3LPRES/)
2200  FORMAT(51H1 STRESSES AND STRESS LEVELS FOR FINAL CONDITION AT,
     1 17H END OF INCREMENT,//)
2201  FORMAT(108H              TAUMX     T1-12     T1-23     T1-13      T2-1
     12       T2-23      T2-13     T3-12     T3-23     T3-13 )
2202  FORMAT(5X,6F10.3,2X,4F10.3,////)
2203  FORMAT(2I5)
2250  FORMAT(I5,6F10.3,2X,4F10.3,4X,2F10.3 )
2500  FORMAT(I5,6F10.4)
2550  FORMAT(I5,3F10.4)
2600  FORMAT(I5,4F10.4)
      END
```

```
      SUBROUTINE FACTXY(EMPR,X,Y,Z,INP,SHEAR,STRESS,NUMELT,NUMMAT)
      COMMON/JSOP/ LAYSUM,NFLAY,NLEL,NREL,NOMEL,HEIGHT
      DIMENSION EMPR(NUMMAT,13),X(1),Y(1),Z(1),INP(NUMELT,9)
      DIMENSION STRESS(NUMELT,6),SHEAR(1)
      DIMENSION HEIGHT(20),NLEL(20),NREL(20),NOMEL(20,2)
      READ 2000, XO,YO,BETA,RJ,GAMAE,GAMAF,NTIME
      TB=TAN(BETA/57.29577951)
      YT=HEIGHT(LAYSUM)
      XT=XO+(YT-YO)/TB
      DO 280 INUM=1,NTIME
      READ 2001, RADIUS,RZ,DANGLE,XR,YR,ZR,DZ,NUMBER,NUMBF,ISIGN
```

```
      PRINT 3000
      PRINT 3001, RADIUS,RZ,XR,YR,ZR,BETA,DANGLE
      PRINT 2002
      RTOP=SQRT((XR-XT)**2.+(YR-YT)**2.)
      DIST=ABS(XR*TB-YR+YO-XO*TB)/SQRT(1.+TB*TB)
      TSIGN=0.
      TTAUN=0.
      TCOHES=0.

      I=1
50    ZP=ZR+(FLOAT(I)-0.5)*DZ*ISIGN
      DET=1.-((FLOAT(I)-0.5)*DZ/RZ)**2.
      IF(DET .LT. 0.) GO TO 280
      RXY=RADIUS*SQRT(DET)
      IF(RXY .LE. DIST) GO TO 275
      ALFAO=ASIN((YR-YT)/RXY)
      ANGLE=ALFAO+DANGLE/(2.*57.29577951)
      IF(RXY .GE. RTOP) GO TO 80
60    YL=YR-YO-RXY*SIN(ANGLE)
      YU=(XR-XO+RXY*COS(ANGLE))*TB
      IF(YL .GE. YU) GO TO 70
      GO TO 80
70    ANGLE=ANGLE+DANGLE/(2.*57.29577951)
      GO TO 60

80    YP=YR-RXY*SIN(ANGLE)
      ITER=1
      NI=LAYSUM
90    IF(NI .EQ. 1) GO TO 100
      GO TO 110
100   IF(YP .LE. HEIGHT(1) .AND. YP. GE. 0.) GO TO 120
      GO TO 300
110   IF(YP .LE. HEIGHT(NI) .AND. YP .GT. HEIGHT(NI-1)) GO TO 120
      NI=NI-1
      GO TO 90

120   XP=XR+RXY*COS(ANGLE)
      CKX=XP-XO
      CKY=YP-YO
      IF(CKX .LE. 0. .AND. CKY .GE. 0.) GO TO 270
      IF(CKX .GT. 0. .AND. CKY .GT. 0.) GO TO 130
      GO TO 140
130   SXY=CKY/CKX
      IF(SXY .GE. TB) GO TO 270
140   IF(NI .LE. NFLAY) GO TO 150
      NF=NI-NFLAY
      NS=NOMEL(NF,1)
      GO TO 160
150   NS=NLEL(NI)
160   N1=INP(NS,1)
      N2=INP(NS,2)
      N3=INP(NS,3)
      N4=INP(NS,4)
      N5=INP(NS,5)
      N8=INP(NS,8)

      IF(ITER .EQ. 2) GO TO 210
      IF(X(N1) .EQ. X(N4)) GO TO 170
      CK1=X(N1)+((X(N4)-X(N1))/(Y(N4)-Y(N1)))*(YP-Y(N1))
      GO TO 180
170   CK1=X(N1)
180   IF(X(N2) .EQ. X(N3)) GO TO 190
      CK2=X(N2)+((X(N3)-X(N2))/(Y(N3)-Y(N2)))*(YP-Y(N2))
      GO TO 200
190   CK2=X(N2)
```

```
200   IF(XP .GE. CK1 .AND. XP .LT. CK2) GO TO 210
      NS=NS+1
      GO TO 160

210   IF(Z(N1) .EQ. Z(N4)) GO TO 220
      CK3=Z(N1)-(Z(N1)-Z(N4))*(YP-Y(N1))/(Y(N4)-Y(N1))
      GO TO 230
220   CK3=Z(N1)
230   IF(Z(N5) .EQ. Z(N8)) GO TO 240
      CK4=Z(N5)-(Z(N5)-Z(N8))*(YP-Y(N5))/(Y(N8)-Y(N5))
      GO TO 250
240   CK4=Z(N5)
250   IF(ZP .GE. CK3 .AND. ZP .LT. CK4) GO TO 260
      IF(NI .GT. NFLAY .AND. NS .GE. NOMEL(NF,2)) GO TO 290
      IF(NI .LE. NFLAY .AND. NS. GE. NREL(NI)) GO TO 290
      IF(NI-NFLAY) 252,252,254
252   NS=NS+NUMBF
      GO TO 256
254   NS=NS+NUMBER
256   ITER=2
      GO TO 160

260   AXY=1.5707963-ANGLE
      DX=RXY*(DANGLE/57.29577951)*COS(AXY)
      AYZ=ATAN((RADIUS/RZ)**2.*ABS(ZP-ZR)/(YR-YP))
      AAXY=AXY*57.29577951
      AAYZ=AYZ*57.29577951
      AREA=DX*DZ*SQRT(1.-(SIN(AYZ)*SIN(AXY))**2.)/(COS(AXY)*COS(AYZ))
      VT=SQRT(1.+TAN(AXY)**2.+TAN(AYZ)**2.)
      V1=TAN(AXY)/VT
      V2=1./VT
      V3=TAN(AYZ)/VT
      T1=STRESS(NS,1)*V1-STRESS(NS,4)*V2-STRESS(NS,6)*V3
      T2=-STRESS(NS,4)*V1+STRESS(NS,2)*V2-STRESS(NS,5)*V3
      T3=-STRESS(NS,6)*V1-STRESS(NS,5)*V2+STRESS(NS,3)*V3
      SIGN=T1*V1+T2*V2+T3*V3
      IF(SIGN .LE. 0.) SIGN=0.
      TAUN=SQRT(ABS(T1*T1+T2*T2+T3*T3-SIGN*SIGN))
      MTYPE=INP(NS,9)
      IF(SHEAR(NS) .LE. 0.0001) GO TO 261
      TANFI=TAN(EMPR(MTYPE,9)/57.29577951)
      COHES=EMPR(MTYPE,8)
      GO TO 262
261   TANFI=0.
      COHES=0.
262   IF(XP .GE. XT) GO TO 265
      IF(XP .GT. XO) GO TO 263
      WP=RU*GAMAF*(YO-YP)
      GO TO 267

263   IF(YP .GE. YO) GO TO 264
      WP=RU*(GAMAE*(XP-XO)*TB+GAMAF*(YO-YP))
      GO TO 267

264   WP=RU*GAMAE*(YO+(XP-XO)*TB-YP)
      GO TO 267

265   IF(YP .GE. YO) GO TO 266
      WP=RU*(GAMAE*(YT-YO)+GAMAF*(YO-YP))
      GO TO 267

266   WP=RU*GAMAE*(YT-YP)

267   FS=((SIGN-WP)*TANFI+COHES)/TAUN
      PRINT 2003,NS,XP,YP,ZP,SIGN,WP,TAUN,AAXY,AAYZ,AREA,FS
```

```
      TSIGN=TSIGN+(SIGN-WP)*TANFI*AREA
      TTAUN=TTAUN+TAUN*AREA
      TCOHES=TCOHES+COHES*AREA
      ANGLE=ANGLE+DANGLE/57.29577951
      GO TO 80
270   I=I+1
      GO TO 50
275   TFS=(TSIGN+TCOHES)/TTAUN
      PRINT 2004, TFS
280   CONTINUE
      GO TO 310
290   PRINT 2005
      GO TO 310
300   PRINT 2006
310   CONTINUE
      RETURN
2000  FORMAT(6F10.3,I5)
2001  FORMAT(7F10.3,2I5/I5)
2002  FORMAT(//,110H      ELE         X          Y          Z       SIGN
     1      WP       TAUN       AXY        AYZ       AREA  LOCAL FS)
2003  FORMAT(I10,10F10.3)
2004  FORMAT(//,5X,≠OVERALL FACTOR OF SAFETY = ≠,F10.3)
2005  FORMAT(5X,≠***WARING*** THE FAILURE SURFACE OUTSIDE THE EMBANKMENT
     1 ≠,/)
2006  FORMAT(5X,≠***WARING*** THE FAILURE SURFACE BELOW THE RIGID FOUNDA
     1TION≠,/)
3000  FORMAT(50H1        RXY        RYZ         XR         YR         ZR,
     1 33H      BETA    DANGLE              )
3001  FORMAT(7F10.3)
      END



      SUBROUTINE FACTYZ(EMPR,X,Y,Z,INP,SHEAR,STRESS,NUMELT,NUMMAT)
      COMMON/JSOP/ LAYSUM,NFLAY,NLEL,NREL,NOMEL,HEIGHT
      DIMENSION EMPR(NUMMAT,13),X(1),Y(1),Z(1),INP(NUMELT,9)
      DIMENSION STRESS(NUMELT,6),SHEAR(1)
      DIMENSION HEIGHT(20),NLEL(20),NREL(20),NOMEL(20,2)
      READ 2000, YO,ZO,BETA,RU,GAMAE,GAMAF,NTIME
      TB=TAN(BETA/57.29577951)
      YT=HEIGHT(LAYSUM)
      ZT=ZO-(YT-YO)/TB
      DO 280 INUM=1,NTIME
      READ 2001, RADIUS,RX,DANGLE,XR,YR,ZR,DX,NUMBER,NUMBF,ISIGN
      PRINT 3000
      PRINT 3001,RX,RADIUS,XR,YR,ZR,BETA,DANGLE
      PRINT 2002
      RTOP=SQRT((ZR-ZT)**2.+(YR-YT)**2.)
      DIST=ABS(-ZR*TB-YR+YO+ZO*TB)/SQRT(1.+TB*TB)
      TSIGN=0.
      TTAUN=0.
      TCOHES=0.

      I=1
50    XP=XR+(FLOAT(I)-0.5)*DX*ISIGN
      DET=1.-((FLOAT(I)-0.5)*DX/RX)**2.
      IF(DET .LT. 0.) GO TO 280
      RYZ=RADIUS*SQRT(DET)
      IF(RYZ .LE. DIST) GO TO 275
      ALFAO=ASIN((YR-YT)/RYZ)
      ANGLE=ALFAO+DANGLE/(2.*57.29577951)
      IF(RYZ .GE. RTOP) GO TO 80
```

```
60     YL=YR-YO-RYZ*SIN(ANGLE)
       YU=(ZO-ZR+RYZ*COS(ANGLE))*TB
       IF(YL .GE. YU) GO TO 70
       GO TO 80
70     ANGLE=ANGLE+DANGLE/(2.*57.29577951)
       GO TO 60

80     YP=YR-RYZ*SIN(ANGLE)
       ITER=1
       NI=LAYSUM
90     IF(NI .EQ. 1) GO TO 100
       GO TO 110
100    IF(YP .LE. HEIGHT(1) .AND. YP. GE. 0.) GO TO 120
       GO TO 300
110    IF(YP .LE. HEIGHT(NI) .AND. YP .GT. HEIGHT(NI-1)) GO TO 120
       NI=NI-1
       GO TO 90

120    ZP=ZR-RYZ*COS(ANGLE)
       CKZ=ZO-ZP
       CKY=YP-YO
       IF(CKZ .LE. 0. .AND. CKY .GE. 0.) GO TO 270
       IF(CKZ .GT. 0. .AND. CKY .GT. 0.) GO TO 130
       GO TO 140
130    SYZ=CKY/CKZ
       IF(SYZ .GE. TB) GO TO 270
140    IF(NI .LE. NFLAY) GO TO 150
       NF=NI-NFLAY
       NS=NOMEL(NF,1)
       GO TO 160
150    NS=NLEL(NI)
160    N1=INP(NS,1)
       N2=INP(NS,2)
       N3=INP(NS,3)
       N4=INP(NS,4)
       N5=INP(NS,5)
       N8=INP(NS,8)

       IF(ITER .EQ. 2) GO TO 210
       IF(X(N1) .EQ. X(N4)) GO TO 170
       CK1=X(N1)+((X(N4)-X(N1))/(Y(N4)-Y(N1)))*(YP-Y(N1))
       GO TO 180
170    CK1=X(N1)
180    IF(X(N2) .EQ. X(N3)) GO TO 190
       CK2=X(N2)+((X(N3)-X(N2))/(Y(N3)-Y(N2)))*(YP-Y(N2))
       GO TO 200
190    CK2=X(N2)
200    IF(XP .GE. CK1 .AND. XP .LT. CK2) GO TO 210
       NS=NS+1
       GO TO 160

210    IF(Z(N1) .EQ. Z(N4)) GO TO 220
       CK3=Z(N1)-(Z(N1)-Z(N4))*(YP-Y(N1))/(Y(N4)-Y(N1))
       GO TO 230
220    CK3=Z(N1)
230    IF(Z(N5) .EQ. Z(N8)) GO TO 240
       CK4=Z(N5)-(Z(N5)-Z(N8))*(YP-Y(N5))/(Y(N8)-Y(N5))
       GO TO 250
240    CK4=Z(N5)
250    IF(ZP .GE. CK3 .AND. ZP .LT. CK4) GO TO 260
       IF(NI .GT. NFLAY .AND. NS .GE. NOMEL(NF,2)) GO TO 290
       IF(NI .LE. NFLAY .AND. NS. GE. NREL(NI)) GO TO 290
       IF(NI-NFLAY) 252,252,254
252    NS=NS+NUMBF
       GO TO 256
```

```
254    NS=NS+NUMBER
256    ITER=2
       GO TO 160

260    AYZ=1.5707963-ANGLE
       DZ=RYZ*(DANGLE/57.29577951)*COS(AYZ)
       AXY=ATAN((RADIUS/RX)**2.*ABS(XP-XR)/(YR-YP))
       AAXY=AXY*57.29577951
       AAYZ=AYZ*57.29577951
       AREA=DX*DZ*SQRT(1.-(SIN(AYZ)*SIN(AXY))**2.)/(COS(AXY)*COS(AYZ))
       VT=SQRT(1.+TAN(AXY)**2.+TAN(AYZ)**2.)
       V1=TAN(AXY)/VT
       V2=1./VT
       V3=TAN(AYZ)/VT
       T1=STRESS(NS,1)*V1-STRESS(NS,4)*V2-STRESS(NS,6)*V3
       T2=-STRESS(NS,4)*V1+STRESS(NS,2)*V2-STRESS(NS,5)*V3
       T3=-STRESS(NS,6)*V1-STRESS(NS,5)*V2+STRESS(NS,3)*V3
       SIGN=T1*V1+T2*V2+T3*V3
       IF(SIGN .LE. 0.) SIGN=0.
       TAUN=SQRT(ABS(T1*T1+T2*T2+T3*T3-SIGN*SIGN))
       MTYPE=INP(NS,9)
       IF(SHEAR(NS) .LE. 0.0001) GO TO 261
       TANFI=TAN(EMPR(MTYPE,9)/57.29577951)
       COHES=EMPR(MTYPE,8)
       GO TO 262
261    TANFI=0.
       COHES=0.
262    IF(ZP .GE. ZT) GO TO 265
       IF(ZP .GT. ZO) GO TO 263
       WP=RU*GAMAF*(YO-YP)
       GO TO 267

263    IF(YP .GE. YO) GO TO 264
       WP=RU*(GAMAE*(ZP-ZO)*TB+GAMAF*(YO-YP))
       GO TO 267

264    WP=RU*GAMAE*(YO+(ZP-ZO)*TB-YP)
       GO TO 267

265    IF(YP .GE. YO) GO TO 266
       WP=RU*(GAMAE*(YT-YO)+GAMAF*(YO-YP))
       GO TO 267

266    WP=RU*GAMAE*(YT-YP)

267    FS=((SIGN-WP)*TANFI+COHES)/TAUN
       PRINT 2003,NS,XP,YP,ZP,SIGN,WP,TAUN,AAXY,AAYZ,AREA,FS
       TSIGN=TSIGN+(SIGN-WP)*TANFI*AREA
       TTAUN=TTAUN+TAUN*AREA
       TCOHES=TCOHES+COHES*AREA
       ANGLE=ANGLE+DANGLE/57.29577951
       GO TO 80
270    I=I+1
       GO TO 50
275    TFS=(TSIGN+TCOHES)/TTAUN
       PRINT 2004, TFS
280    CONTINUE
       GO TO 310
290    PRINT 2005
       GO TO 310
300    PRINT 2006
310    CONTINUE
       RETURN
2000   FORMAT(6F10.3,I5)
2001   FORMAT(7F10.3,2I5/I5)
```

```
2002  FORMAT(//,110H        ELE          X          Y          Z       SIGN
     1      WP      TAUN       AXY       AYZ      AREA  LOCAL FS)
2003  FORMAT(I10,10F10.3)
2004  FORMAT(//,5X,≠OVERALL FACTOR OF SAFETY = ≠,F10.3)
2005  FORMAT(5X,≠***WARING*** THE FAILURE SURFACE OUTSIDE THE EMBANKMENT
     1 ≠,/)
2006  FORMAT(5X,≠***WARING*** THE FAILURE SURFACE BELOW THE RIGID FOUNDA
     1TION≠,/)
3000  FORMAT(50H1      RXY       RYZ        XR        YR        ZR,
     1 33H      BETA    DANGLE             )
3001  FORMAT(7F10.3)
      END
```

COVER DESIGN BY ALDO GIORGINI